Bridging the Gap:
Elusive Explosions in the Local Universe

Thesis by
Mansi M. Kasliwal

Advisor
Professor Shri R. Kulkarni

In Partial Fulfillment of the Requirements
for the Degree of
Doctor of Philosophy

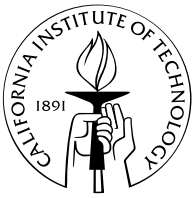

California Institute of Technology
Pasadena, California

2011

(Defended April 26, 2011)

Acknowledgements

The first word that comes to my mind to describe my learning experience at Caltech is exhilarating. I have no words to thank my "Guru", Professor Shri Kulkarni. Shri taught me the "Ps" necessary to Pursue the Profession of a Professor in astroPhysics. In addition to Passion & Perseverance, I am now Prepared for Papers, Proposals, Physics, Presentations, Politics, Priorities, oPPortunity, People-skills, Patience and PJs.

Thanks to the awesomely fantastic Palomar Transient Factory team, especially Peter Nugent, Robert Quimby, Eran Ofek and Nick Law for sharing the pains and joys of getting a factory off-the-ground. Thanks to Brad Cenko and Richard Walters for the many hours spent taming the robot on mimir2:9. Thanks to Avishay Gal-Yam and Lars Bildsten for illuminating discussions on different observational and theoretical aspects of transients in the gap. The journey from idea to first light to a factory churning out thousands of transients has been so much fun that I would not trade this experience for any other.

Thanks to Marten van Kerkwijk for supporting my "fishing in new waters" project with the Canada France Hawaii Telescope. Thanks to Dale Frail for supporting a "kissing frogs" radio program. Thanks to Sterl Phinney, Linqing Wen and Samaya Nissanke for great discussions on the challenge of finding the light in the gravitational sound wave.

Thanks to my thesis committee, Richard Ellis, Sterl Phinney, Fiona Harrison and Tony Readhead for approving a somewhat risky candidacy proposal and for their advice to make it a success.

Thanks to the staff of Palomar Observatory, Keck Observatory, Gemini Observatory, CFHT Observatory, Swift Observatory and EVLA for their utmost co-operation with my rapid response campaigns. Thanks to Patrick Shopbell and Anu Mahabal for supporting the large computational needs of this project.

Friends are what made Caltech home away from home. Thanks to fellow desi junta, Prabha-Krishna, Uday-Shweta, Sushree-Jayakrishnan, Arundhati-Samir, Mayank, Varun and Anti. Thanks to fellow astronomy grads, Ann Marie, Varun, Anti, Tucker, Laura, Walter, Swarnima, Brian and David. Thanks to my carpool buddy, Beth Harnick-Shapiro, Anaheim Public Library's audiobook collection and Sarkis for making the 55,000 mile journey between candidacy and defense manageable. Thanks to my housemate, Nok, for delectable desserts and inspiring Alice demos. Special thanks to Ann Marie, who has been my of-

ficemate since I came here, from the dungeon to the fridge to the half-window to the rap. Special thanks to Uday for Shweta. Special thanks to Prabha, for being a housemate for the first half and always being there for baatein-chai-khana-neenee during the second half. Special thanks to Varun for patiently listening to many excruciating details of this thesis.

And finally, my family, to whom I dedicate this thesis.

Dedication

This thesis is dedicated to my family.

My grandmother Kaki, Ms. Maltibala Kasliwal, who I miss dearly since she left us on the day Caltech called me to offer admission,

My grandfather Kaka, Dr. Sumatikumar Kasliwal, who will always be the sturdy backbone of our family,

All my grandparents, Ms. Maltibala and Dr. Sumatikumar Kasliwal, Ms. Pushpa and Mr. Lalit Bagla, Ms. Rajkumari and Prabhu Narayan Mohta, Ms. Santosh and Bhagirath Prasad Maheshwari, whose blessings are much cherished,

My parents, Ms. Sharda Kasliwal and Mr. Manoj Kasliwal, who (in addition to genes) gave me the strength, wisdom and courage to tirelessly pursue my dreams,

My parents, Ms. Sudha Maheshwari and Mr. Bhanu Mohta, who have supported my academic pursuits wholeheartedly,

My sister and brother-in-law Ji^{3}Ju, Ms. Puja Kasliwal and Mr. Aditya Maheshwari, who helped me survive the transition to a foreign land so far away from home,

My brother, Mr. Parth Kasliwal, who always makes me smile and held my hand as we walked to my shaadi-ka-mandap,

My niece, Ms. Ananya Maheshwari, who is as old as my thesis and with twinkling eyes taught me the five steps in the scientific method via a raisins in club soda experiment,

My nephew, Mr. Aayan Maheshwari, who is an adorable little bundle of joy,

and of course,

My husband, Mr. Setu Mohta, who discovered the first supernova of the Palomar Transient Factory and has quite literally been the steadfast bridge behind the bridging of the gap between novae and supernovae.

Prologue

I vividly remember the drive to Palomar Mountain on October 5, 2006. Professor Shri Kulkarni was driving his bottlegreen van and bragging about how he knew the mountain roads so well that there was no need to bother using brakes.

I had recently passed my qualifying exam in the astrophysics Ph.D. program at Caltech. I had also completed several small research projects exploring the optical, infrared and X-ray wavelengths. I was in search of a thesis topic – something fun, something challenging, something simple enough whose jist I could convey to my parents in a few minutes. To me, this was the beauty of astronomy. Even in the 21st century, scientists were seeking answers to very simple questions.

Caltech is a fun place and so this was a "problem of choice". I had talked to several professors about several different ideas. I had walked into their offices with a blank slate and possible questions and walked out with a well-defined plan of which telescopes could answer these and what would be a list of papers suitable for background reading. This evening though was somehow different.

We were discussing a rather simple yet age-old conundrum in the venerable field of cosmic explosions – the brightest nova was a thousand times fainter than the faintest supernova leaving a wide gap in-between. Nature abhors gaps, then why hadn't astronomers found things in-between? It turned out that novae and supernovae were simply the easiest things to find; novae because they are so abundant and supernovae because they are so bright and long-lived.

So, what could we do differently to bridge the gap? How could we find these elusive transients that were fainter, faster and rarer than supernovae? Shri told me to suspend all practical concerns and just let my imagination run wild. We discussed a Plan A, B and C. But it was really Plan D that was the most compelling. Plan D was also the craziest to imagine implementing on a graduate thesis timescale. It involved taking over all the telescopes on Palomar mountain and running it like a "factory" systematically churning out transients.

I enjoyed thinking about how to find an answer to this simple question. It was definitely something that kept me awake at night. Theoretically, there were several predictions of fundamental stellar physics that should result in transients in the gap. Observationally,

there appeared to be an opportunity to work on a story from the very beginning and chart unexplored territory. As with roads not taken, one could expect a lot of hard work and the most likely outcome of an upper limit. We should be able to better quantify how hard these transients were to find but the odds of finding anything were very small. As we were driving back, Shri said, "There is no question that this is a high-risk high-gain thesis topic. The decision is now yours."

Abstract

For centuries, we have known that our dynamic universe is adorned by cosmic fireworks: energetic and ephemeral beacons of light from a single star that are a million (nova) to a billion (supernova) times brighter than our sun. However, it had been an age-old conundrum that the brightest nova is approximately 1000 times fainter than than the faintest supernova; why should nature leave such a wide "gap"?

In search of an answer, I undertook three systematic surveys for my thesis. Since I was looking for transients fainter, faster and rarer than supernovae, I focussed my search on galaxies in the local universe. We now have convincing evidence of multiple, distinct populations of rare transients bridging this "gap". Perhaps, we are witnessing new stellar physics — shell detonations in ultra-compact white dwarf binaries, electron-capture supernovae, white dwarfs collapsing into neutron stars and birth of black-holes.

A small number of intensively followed-up discoveries of elusive transients sets the stage for population studies with the upcoming "Large Synoptic Survey Telescope". This effort works towards building a complete inventory of transients in the local universe ($d < 200$ Mpc). It better prepares us for the search for potential electromagnetic counterparts to events in the emerging fields of gravitational wave, neutrino and ultra high energy cosmic ray astronomy as these experiments are also limited to the local universe.

Contents

List of Figures

List of Tables

Chapter 1

Introduction

1.1 Framework of Explosions: 2005

The venerable field of cosmic explosions has a rich history. Since the discovery of the first supernova in A. D. 185 and the first nova in A. D. 1670, we have discovered $\approx$6600 supernovae and $\approx$1000 novae. In the past century, explosions have unveiled the synthesis of elements heavier than iron, the acceleration of the universe's expansion and dark energy. However, our studies have been limited to thermonuclear supernovae (white dwarf detonation), core-collapse supernovae (massive star death) and classical novae (accretion-driven burning on a white dwarf).

Two fundamental parameters that describe an explosion are the peak luminosity and the duration. Using these two parameters to characterize transient events, we present a graphical summary of the framework of cosmic explosions in the year 2005 in Figure 1.1. Thousands of supernovae and novae can be neatly squared away into the three gray regions. As is evident, this framework is plagued with gaping white-spaces. Specifically, there is a wide "gap" spanning three orders of magnitude in luminosity between novae and supernovae. The regime of short-duration transients more luminous than novae is also virtually unpopulated.

"Nature abhors gaps" and so it is no surprise that the above-mentioned framework is a product of observational bias towards finding the most luminous (supernovae) and most populous (novae) events first. My thesis effort comprised three systematic surveys for elusive transients that bridge the aforementioned gap.

My motivation, beyond an insatiable curiosity and an intriguing opportunity to navigate

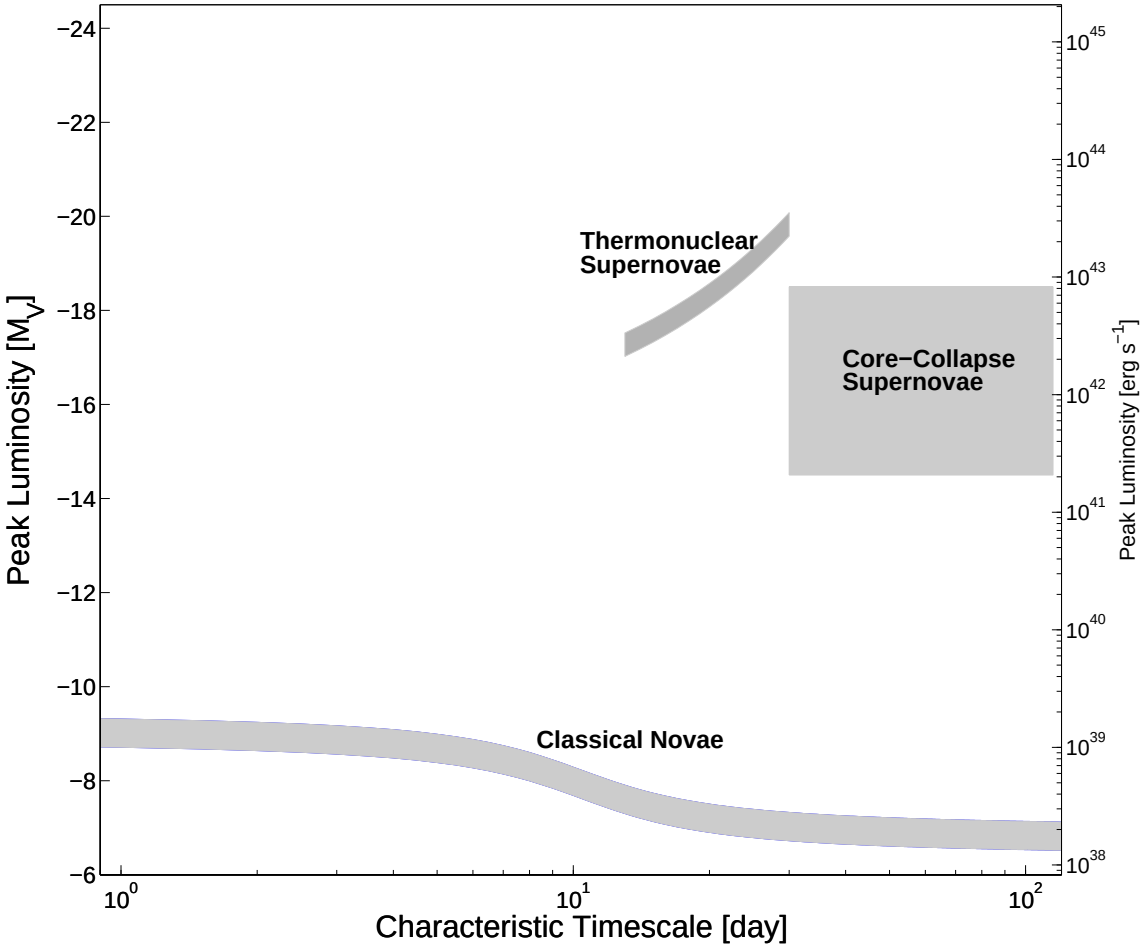

Figure 1.1 Framework of cosmic explosions in the year 2005. Note the wide "gap" in luminosity spanning three orders of magnitude. Also, note the emptiness on timescales shorter than 10 days. This thesis concludes with the framework in the year 2011, presented in Figure 8.1.

uncharted territory, is twofold: the stellar physics one can hope to learn from finding elusive explosions, and the timeliness of a complete inventory in the context of upcoming frontiers in physics.

1.2 The Physics

Theoretically, a wide variety of fundamental stellar outcomes are expected to result in transients in the gap. Recent discoveries have motivated detailed modelling to predict the

explosion signature of several of these outcomes.

1.2.1 Compact Binaries

First, let us take a closer look at accretion-powered thermonuclear runaways on surfaces of white dwarfs. Both classical novae and supernovae of Type Ia (SN Ia) are outcomes of this process. A key difference between them is that classical novae have an ejecta mass of only 10^{-4}–10^{-5} $M_\odot$ and SN Ia undergo a complete detonation with an ejecta mass of 10^{-1}–1 $M_\odot$.

Naturally, the question arises of whether there are explosions where the ejecta mass is intermediate. One scenario that gives ejecta between 10^{-2}–10^{-1} $M_\odot$ is a ".Ia" explosion (Bildsten et al. 2007a; Shen et al. 2010). In an ultra-compact white-dwarf white-dwarf system, with a period shorter than an hour, suppose that mass is transferred from the lower mass Helium white dwarf to the higher mass Carbon-Oxygen white dwarf. A series of novae will result. If the final Helium flash is such that the nuclear timescale is shorter than the hydrodynamical, then the entire shell could detonate, resulting in a ".Ia" explosion. The name ".Ia" is drawn from characteristics that are a tenth of that seen in SN Ia, specifically the explosion mass, the characteristic timescale and the peak luminosity. Whether or not the shock wave also detonates the core is an open question (Waldman et al. 2010).

Next, we consider a scenario involving a total ejecta mass between 10^{-3}–10^{-2} $M_\odot$: accretion induced collapse (AIC) of a rapidly rotating O-Ne-Mg white dwarf into a neutron star before ignition in the core (Metzger et al. 2009; Darbha et al. 2010). O-Ne-Mg white dwarfs require a relatively lower density for electron captures than C-O white dwarfs and thus are more likely to undergo AIC. As the white dwarf accretes mass, it also accretes angular momentum, leading to rapid rotation. After AIC, to conserve angular momentum, the proto-neutron star is expected to have a centrifugally supported disk. As this disk spreads to larger radii and cools, heavy nucleons form, causing the disk to become unbound. Although initially neutron rich ($Y_e \equiv \frac{n_p}{n_p+n_n} \approx 0.1$), the irradiation of electron neutrinos by the protoneutron star evens out the neutron-to-proton ratio ($Y_e \approx 0.5$). Thus, Nickel-56 is synthesized and a radioactivity-powered explosion follows. The characteristics of this explosion are short lifetime, low luminosity, very high ejecta velocities approaching 0.1c and absence of intermediate mass elements.

Next, consider another situation where the powerhouse of a radioactivity-powered explosion is not Nickel-56. Specifically, in the case of neutron-star neutron-star coalescence, the abundance of free neutrons allows significant quantities of very neutron-rich material (e.g. Iodine-135, Antimony-129, Tellurium-129, Xenon-135, Tin-127) to be built up by the r-process (Li & Paczyński 1998; Kulkarni 2005; Metzger et al. 2010). The half-life of these elements is only a few hours and consequently, the explosion is also ephemeral. The peak luminosity is predicted to be in the range of 10^{40}–10^{42} erg s^{-1}. This class of objects have been referred to as mini-supernovae (Li & Paczyński 1998) or macronovae (Kulkarni 2005) or kilonovae (Metzger et al. 2010).

1.2.2 Massive Stars

Let us first review the current understanding of the core-collapse of massive stars. The detailed underpinning of how the gravitational potential energy of the collapsing iron core is converted into a shock-induced explosion is still being ironed out. Several mechanisms, including neutrino-heating-driven, magnetohydrodynamic, acoustic and phase-transition-induced explosions, are being simulated. Recent three-dimensional simulations have finally been able to reproduce an explosion (Nordhaus et al. 2010).

Observationally, the different flavors of core-collapse appear to be related to the envelope mass. The more massive the envelope, the lower the peak luminosity and slower the evolution (hence, the sub-classes of Type IIB, Type IIL and Type IIP from least massive to most massive envelope). Core-collapse supernovae which have expelled their hydrogen shell are called Type Ib and those with neither hydrogen nor helium are called Type Ic.

Unambiguous identification of eight progenitor stars in deep imaging prior to the explosions has directly shown that Type IIP supernovae come from red supergiants in the mass range of 8.5–16.5 $\pm$ 1.5 $M_\odot$ (see recent review by Smartt 2009 and references therein). It is expected that red supergiants in the mass range 15–25 $M_\odot$ result in Type IIL supernovae but this hasn't yet been observationally demonstrated. Two peculiar Type II supernovae have been seen from blue supergiants (SN1987A; SN2000cb, Kleiser et al. 2011).

We currently have very little direct evidence for the fate of more massive progenitors. The three cases where we have seen $> 25\,M_\odot$ progenitor star (or precursor eruption) resulted in three different types of supernovae (Type Ic SN2005gl, Gal-Yam & Leonard 2009; Type

IIn SN2006jc, Pastorello et al. 2007; Type IIB SN2008ax, Crockett et al. 2008). Thus, the fate of stars more massive than $> 25\,M_\odot$ and stars in the transition range of 8–10 $M_\odot$ are open questions.

Stars $> 25\,M_\odot$ may undergo black hole formation at the time of collapse. More massive stars have larger regions in the mantle that have increasing $\rho\, r^3$ such that the shockwave slows and significant material falls back onto the core (Woosley & Weaver 1995; Heger et al. 2003). Such fallback can result in the formation of a black hole instead of a neutron star. Depending on the amount of fallback, the observed explosion is expected to be lower luminosity, lower velocity and lack a radioactive tail in the light curve. In extreme cases, the shock-wave may not be revived at all and the star would simply disappear into a black hole without any electromagnetic signature (O'Connor & Ott 2011; Fryer 1999). The lower the metallicity, the lower the mass loss due to winds and larger the probability of black hole formation (Heger et al. 2003)

Stars in the 8–10 $M_\odot$ range are expected to have O-Ne-Mg cores. Neutrinos produced by electron capture on the Neon-20 and Magnesium-24 nuclei efficiently carry away the energy produced by nuclear burning. The core can collapse to form a neutron star; neutrino heating and neutrino-driven wind can power an explosion. Such an explosion is expected to have low energy, produce little Nickel-56, have an extended plateau phase and eject very little Oxygen (Kitaura et al. 2006).

Thus, there are at least five stellar outcomes that motivate a search for transients in the gap. Additional ideas for unusual transients occuring earlier in stellar evolution include the merger of main sequence stars (Soker & Tylenda 2003) and planets being swallowed by their host star (Retter & Marom 2003). I summarize theoretically predicted rates (albeit uncertain) and compare them to to rates of supernovae in Table 1.1.

1.3 A Complete Inventory

My second motivation is derived from the surge of excitement in the physics community as several large experiments probing entirely new cosmic frontiers are coming online this decade — ICECUBE[1] at the South Pole now has 86 strings and is sensitive to very high

[1] http://icecube.wisc.edu/

Table 1.1. Theoretically Predicted Rates of Transients in the Gap

Scenario	Peak Luminosity (Abs. Mag.)	Timescale (Days)	Universal Rate (Mpc^{-3} yr^{-1})	Reference
.Ia Explosion	$-15..-18$	2..7	$0.6..2\times10^{-6}$	Shen et al. 2010; Bildsten et al. 2007a
Macronovae	$-12..-16$	0.1..1	$10^{-5}..10^{-7}$	Metzger et al. 2010; Kulkarni 2005
AIC	$-13..-16$	0.1..4	$10^{-6}..10^{-8}$	Darbha et al. 2010
Fallback SN	$-4..-21$	0.5..2	5×10^{-6}	Fryer, C., priv. comm.
Type Ia SN	$-17..-20$	20..40	3.0×10^{-5}	Li et al. 2011
Core Collapse SN	$-15..-20$	30..300	7.1×10^{-5}	Li et al. 2011

energy (TeV) neutrinos; advanced LIGO[2] and advanced VIRGO[3] are gravitational wave interferometers that will come online in 2016; the Pierre Auger observatory[4] is sensitive to ultra high energy cosmic rays. Each of these endeavors have one thing in common. They are all limited in sensitivity, due to instrumental or physical effects, to the local horizon of 200 Mpc.

I eagerly look forward to searching for electromagnetic counterparts to these new phenomena. In preparation, I am motivated to systematically build a complete inventory of the explosive phenomenon in the local universe.

1.4 Thesis Outline

My thesis is organized as follows. First, I begin with a discussion of observed extremes in supernovae and novae in Chapters 2 and 3 respectively (an exemplar of extremely short timescales is presented in Appendix A). Next, I discuss details of survey design, operations and net yield in Chapter 4. Finally, I discuss three new classes of transients that bridge the gap between novae and supernovae in Chapters 5, 6 and 7. I summarize the progress to date with an eye to the future in Chapter 8.

[2]http://www.ligo.org/

[3]http://www.ego-gw.it/public/virgo/virgo.aspx

[4]http://www.auger.org/

Chapter 2

Understanding Extreme Supernovae: SN2007ax*

M. M. Kasliwal[1,2], E. O. Ofek[1], A. Gal-Yam[1], A. Rau[1], P. J. Brown[3], S. B. Cenko[4], P. B. Cameron[1], R. Quimby[1], S. R. Kulkarni[1], L. Bildsten[5], P. Milne[6]

[1] Astronomy Department, California Institute of Technology, 105-24, Pasadena, CA 91125, USA

[2] George Ellory Hale Fellow, Gordon and Betty Moore Foundation

[3] Department of Astronomy and Astrophysics, Pennsylvania State University, 525 Davey Laboratory, University Park, PA 16802, USA

[4] Space Radiation Laboratory, California Institute of Technology, MS 220-47, Pasadena, CA 91125, USA

[5] Kavli Institute for Theoretical Physics and Department of Physics, Kohn Hall, University of California, Santa Barbara, CA 93106, USA

[6] Steward Observatory, 933 N. Cherry Ave., Tucson, AZ 85721, USA

Abstract

We present multi-band photometric and optical spectroscopic observations of SN2007ax, the faintest and reddest Type Ia supernova (SN Ia) yet observed. With $M_B = -15.9$ and $(B-V)_{max} = 1.2$, this SN is over half a magnitude fainter at maximum light than any

*A version of this chapter is published with the title "SN2007ax: An Extremely Faint Type Ia Supernova" in the *The Astrophysical Journal Letters*, 2008, vol. 683, L29–L32, and is reproduced by permission of the AAS.

other SN Ia. Similar to subluminous SN2005ke, SN2007ax also appears to show excess in UV emission at late time. Traditionally, $\Delta m_{15}(B)$ has been used to parameterize the decline rate for SNe Ia. However, the B-band transition from fast to slow decline occurs sooner than 15 days for faint SNe Ia. Therefore we suggest that a more physically motivated parameter, the time of intersection of the two slopes, be used instead. Only by explaining the faintest (and the brightest) supernovae, we can thoroughly understand the physics of thermonuclear explosions. We suggest that future surveys should carefully design their cadence, depth, pointings and follow-up to find an unbiased sample of extremely faint members of this subclass of faint SNe Ia.

2.1 Introduction

Inspired by the application as a standard cosmological candle, the progress in understanding Type Ia supernovae (SNe Ia) has grown in leaps and bounds. However, the understanding of their weakest subluminous cousins has been purposefully overlooked as their atypical light curve and atypical spectra make them contaminants for cosmological studies. We suggest here some characteristics that make the physics of the explosions of faint SNe Ia intriguing in their own right.

In this paper, we present SN2007ax which, with a peak absolute magnitude of $M_B = -15.9$ and $(B-V)_{max} = 1.2$, is the faintest and reddest Type Ia supernova yet discovered. Although the class of SNe Ia is remarkably homogenous, subluminous SNe Ia show atypical spectral and light curve features (Garnavich et al. 2004, Taubenberger et al. 2008). Photometrically, not only do they fade much faster than predicted by the Phillips relation, they are also very red at maximum and (at least SN2005ke and SN2007ax) appear to show UV excess at late-time. Spectroscopically, they have broad Ti II features and moderate expansion velocities.

SN2007ax was discovered in NGC 2577 on UT 2007 Mar 21.978 by Arbour (2007) at an unfiltered magnitude of 17.2. Upper limits of >18.5 mag on Mar 17.636 and >19.0 mag on Mar 9.959 were also reported. Spectra obtained on Mar 26 by Blondin et al. (2007) and Morrell & Folatelli (2007) showed that it was a SN Ia near maximum light similar to SN1991bg.

In this paper, we present multi-epoch, multi-band imaging and spectroscopic follow up of

SN2007ax including optical, ultraviolet, and near-infrared. We summarize our observations in § 2, present our analysis and comparison with other faint SNe Ia in § 3 and discuss possible scenarios for faint thermonuclear explosions in § 4. We conclude with how future surveys can systematically design their cadence, limiting magnitude and pointings to search for more members belonging to this subclass of faint SNe Ia.

2.2 Observations and Data Reduction

The automated Palomar 60-inch telescope (Cenko et al. 2006a) started daily observations of SN2007ax on UT 2007 Mar 29 in g' and r' bands . Data were reduced using custom routines. Aperture photometry was done after image subtraction using two custom modifications of the ISIS algorithm (Alard & Lupton 1998), *hotpants*[1] and *mkdifflc* (Gal-Yam et al. 2004, Gal-Yam et al. 2008). The two reductions gave consistent results. Errors were estimated by first placing artificial sources of the same brightness and at the same distance from the galaxy center as the SN and then measuring the scatter in measured magnitudes. Finally, the zeropoint was calibrated with reference magnitudes of stars from the Sloan Digital Sky Survey (Adelman-McCarthy et al. 2007).

We triggered Target of Opportunity observations to obtain spectra with the Double Beam Spectrograph (Oke & Gunn 1982) on the Hale 200-inch telecope. Two spectra were obtained around maximum light (UT 2007 Mar 29 and Mar 30) and a third a fortnight later (Apr 13). Spectra were taken using the red grating 158/7500, blue grating 300/3990 and using a dichroic to split the light at 5500 Å . This gave us a total wavelength coverage of 3800 Å – 9000 Å and dispersion of 4.9 Å pix^{-1} and 2.1 Å pix^{-1} on the red and blue side, respectively. Data were reduced using the standard IRAF[2] package *apall*.

We triggered Swift Target of Opportunity observations for SN2007ax starting UT 2007 Mar 29.84 and obtained eight epochs of roughly five kiloseconds each distributed between the $uvw2, uvm2, uvw1, u, b$ and v bands. We also obtained a reference image over eight months after peak to subtract galaxy light. Aperture photometry was performed using a $3''$ circular

[1] http://www.astro.washington.edu/becker/hotpants.html

[2] IRAF is distributed by the National Optical Astronomy Observatories, which are operated by the Association of Universities for Research in Astronomy, Inc., under cooperative agreement with the National Science Foundation.

radius. To estimate the galaxy brightness at this location, a $3''$ aperture at the supernova position in the reference image was used. Poole et al. (2008) photometric zeropoints were applied after appropriately scaling for aperture size. For consistency with calibration, a $5''$ aperture was used in the computation of coincidence loss. The supernova is detected in $uvw1$ in four epochs, and not detected in the $uvw2$ and $uvm2$ filters. The b band light curve was independently reduced using image subtraction with consistent results. We note that due to the faintness of the supernova and brightness of galaxy background, coincidence loss is dominated by the galaxy light and not a point source, possibly introducing a systematic error in the Swift u, b, and v bands.

Further late-time $BVRI$ observations were obtained using the SLOTIS and Bok telescopes and light curves were obtained using image subtraction based on ISIS and IRAF routines. We also obtained near-infrared K' imaging using the Keck NIRC2 instrument with Natural Guide Star adaptive optics on UT 2007 Apr 4.

2.3 Analysis

We present analysis of the optical and ultra-violet light curve and optical spectrum of SN2007ax below. We also compare it to other subluminous SN Ia. We adopt a distance modulus of 32.2 (B. Tully, personal communication) to NGC 2577.

2.3.1 Optical Light Curve

We plot the multi-band light curve of SN2007ax in Figure 5.4. The key characteristic of SN2007ax is its rapid decline. Traditionally, Δm_{15} (the difference between the peak B-mag and the B-mag 15 days after the peak) has been used to parametrize the decline of the light curve. However, this parameter can be misleading when applied to the faint SNe Ia because the knee in their light curve (transition from fast initial decline to slow late-time decline) is sooner than fifteen days from the peak. Therefore, we choose to compare the light curves of subluminous Ia using three parameters first introduced by Pskovskii (1984) — initial slope (β), late-time slope (γ) and the time of intersection of the two slopes (t_b). This time of intersection parameter (defined from maximum in B-mag) was also used by Hamuy et al. (1996) as t_2^B and shown to be empirically proportional to Δm_{15} for some SNe Ia.

For the subclass of faint SNe Ia, we find that t_b is better correlated with the peak absolute B-mag than β and γ slopes of the B-band light curve. We fit an empirical relation to the intersection time as a function of peak absolute magnitude and find that $M_{\rm B} = -13.7(\pm0.5) - 0.22(\pm0.03) \times t_b$. Moreover, this transition to slower decline should represent the time at which the optical depth to thermalized radiation becomes thin. We report these three parameters for a sample of subluminous SNe Ia in Table 2.1 and and show the linear fits in Figure 2.2.

Another crucial property of subluminous SNe Ia is that the fainter they are, the redder they are at maximum. We find that SN2007ax is consistent within uncertainties of the empirical relation derived first by Garnavich et al. (2004): $M_{\rm B} = -18.7 + (B-V)_{\rm max} \times 2.68(\pm0.32)$. This relation predicts a color in the range of 1.0–1.3 mag and we observe 1.2 ± 0.1 mag. This color has been derived based on synthetic photometry of the spectra around maximum.

2.3.2 Ultraviolet Light Curve

In Figure 5.4, we compare the Swift UVOT light curve of SN2007ax to another subluminous SN Ia 2005ke (Immler et al. 2006) and a typical SN Ia 2005am (Brown et al. 2005). The key similarity between SN2005ke and SN2007ax is that both show an excess in UV starting ≈ 20 days after the peak. Immler et al. (2006) propose that SN2005ke showed a UV excess due to circumstellar interaction. Perhaps, subluminous supernovae are optically thin below 3800 Å simply due to lower production of iron-group elements. The question of whether UV excess is a more general property of faint SNe Ia merits further investigation with timely follow-up of a larger sample. With a larger sample, one could also consider whether the break in the UV light curve also depends on absolute magnitude.

2.3.3 Spectral Evolution

We compare optical spectra of SN2007ax to SN1991bg in Figure 3.10. The prominent absorption features are Ti II, O I, Si II and Ca I. The presence of intermediate mass elements like Oxygen and Titanium is indicative of the presence of unburned material or a low burning efficiency. The absorption features become broader as the supernova evolves. Comparing our spectra to SN1991bg one day, two days and sixteen days after maximum

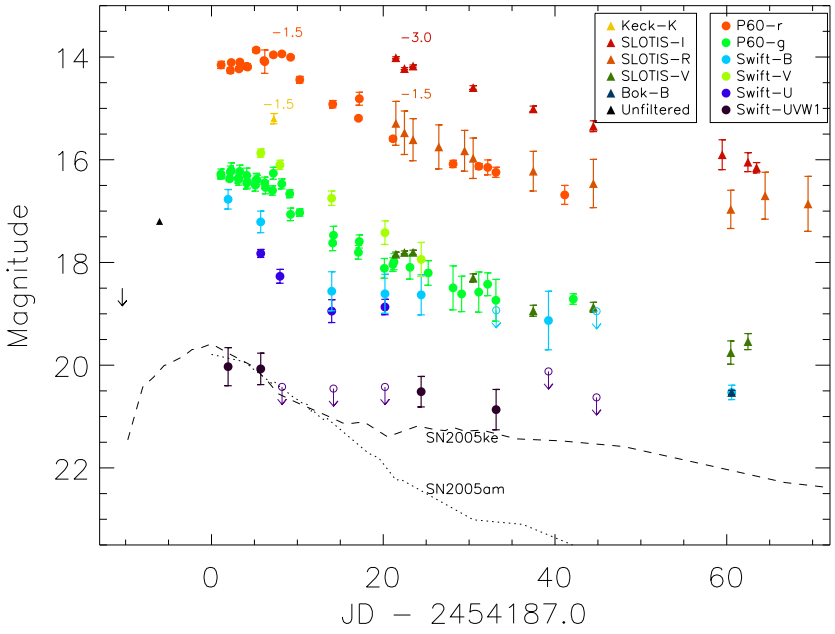

Figure 2.1 Multi-band light curve of SN2007ax based on data from P60, Swift/UVOT, SLOTIS, Bok and Keck II/NIRC2. Unfiltered magnitudes from Arbour 2007. Note that similar to subluminous SN2005ke (dashed line), SN2007ax also appears to show an excess in UV emission at $t > 20$ days while typical SNe Ia (SN2005am, dotted line) continue to decline.

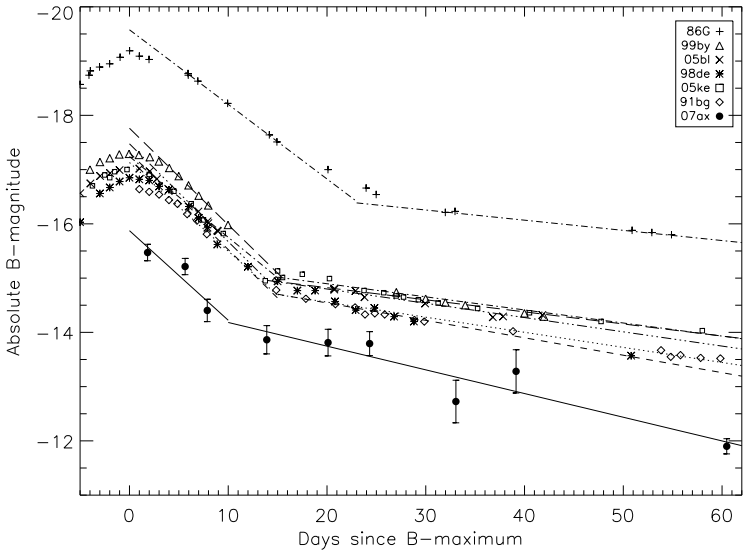

Figure 2.2 B-band light curve of SN2007ax in comparison with other subluminous SNe Ia. The best linear fits are overplotted and give the early-time and late-time slope. We note that the time of intersection, t_b of the early-time and late-time slopes is more strongly correlated with the absolute magnitude than the slopes, α and β.

in B-band, we find that the spectra are very similar. In the first epoch, we see a hint of carbon in the small bump immediately redward of the Si II feature at 6150 Å . However, the signal-to-noise ratio in the spectrum is too low for any conclusive evidence.

Using the technique described by Nugent et al. (1995), we estimate the temperature diagnostic R(Si II) — the ratio of the depths of the two Si II features at 5800 Å and 6150 Å — to be 0.33. This is smaller than what is implied by the empirical relations derived by Garnavich et al. (2004) and Taubenberger et al. (2008).

We also measure the velocity of the Si II 6150 Å line in the two epochs around maximum and we obtain 9300 km s^{-1} and 8800 km s^{-1}. This is consistent with lower velocities observed in other faint SNe Ia (Benetti et al. 2005).

2.3.4 NIR Imaging and Extinction

We measure a K′ magnitude of 16.7 ± 0.1 on UT 2007 Apr 4. We determined the contribution of galaxy light at the supernova position by fitting a Sersic profile to the galaxy using GALFIT (Peng et al. 2002). The best-fit parameters are: a Sersic index of 1.90, axis ratio

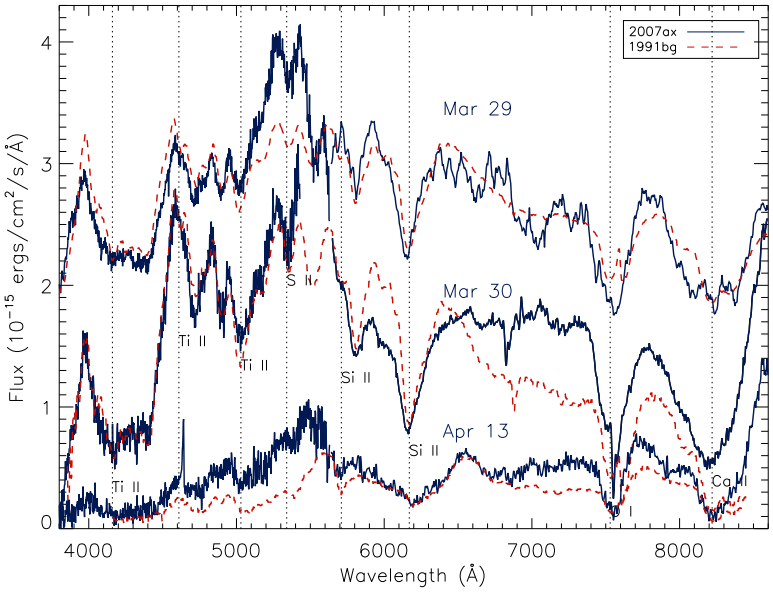

Figure 2.3 Three epochs of P200 DBSP spectra of SN2007ax (with arbitrary vertical offsets for clarity). Overplotted is another subluminous Type Ia supernova, SN1991bg, one day, two days and sixteen days after the peak (scaled by a multiplicative factor for comparison).

of 0.60, effective radius of 4.98″, position angle of 105.6° and diskiness of −0.14. We find no evidence of dust lanes in this image suggesting that the host extinction is minimal. This is also consistent with the absence of the interstellar Na D line at 5893 Å . We compute an upper limit on the equivalent width as 0.1 Å . Using the relations derived in Turatto et al. (2003), we get an upper limit of E$(B-V) < 0.01$ mag on the extinction.

Based on the Galactic position, l=201.1°, b=29.6°, the extinction along the line of sight is E$(B-V)$=0.054 mag (Schlegel et al. 1998a). Therefore, we account for $A_B = 0.23$ and A_v= 0.18 in our calculations of absolute magnitude and luminosities.

2.3.5 Bolometric Luminosity and ^{56}Ni Mass

Arnett et al. (1985) gives an estimate of the ^{56}Ni mass in the ejecta using the peak bolometric luminosity and the rise time:

$$M_{Ni} = L_{43} \times [6.31\ \exp(-t_r/8.8) + 1.43\ \exp(-t_r/111)]^{-1}$$

. For SN2007ax, the extinction-corrected peak bolometric luminosity is 2.3×10^{42} ergs s^{-1}. We estimate this by using the photometric points to calibrate our spectrum near maximum light and integrating. The rise-time is unknown and unfortunately, the literature somewhat arbitrarily assumes 17 days for faint SNe Ia and 19.5 days for typical SNe Ia. Recently, Taubenberger et al. (2008) used SN1999by early-time data to estimate a rise-time of 14 days. The only observational constraint we have for SN2007ax is that the rise-time is longer than 6 days. Thus, for the range of rise-times from 6–14 days, we find a ^{56}Ni mass of 0.05–0.09 $M_\odot$. This is consistent with other techniques to estimate ^{56}Ni of faint SNe Ia. For SN1991bg, Cappellaro et al. (1997) model the V-band light curve and obtain a mass of 0.1 $M_\odot$, and Mazzali et al. (1997) model the photospheric and nebular-epoch spectra and obtain ^{56}Ni mass of 0.07 $M_\odot$.

2.4 Discussion

To summarize, the primary observational characteristics of subluminous SNe Ia (of which SN2007ax is an extreme case) are small t_b in the optical B-band light curve, extremely red $B-V$ color at maximum, possible excess in UV emission at late-time, presence of intermediate mass elements in spectra, medium ejecta velocities, low ^{56}Ni mass in ejecta and short rise-times.

Several theoretical models have been proposed to explain faint SNe Ia — complete detonation of a sub-Chandrashekhar mass white dwarf, a delayed detonation model, a failed neutron star model and a small-scale deflagration model. The detonation of a sub-Chandrashekhar C-O white dwarf (e.g., Livne 1990, Woosley & Weaver 1994) produces more ^{56}Ni than observed and is more blue at maximum than observed (Hoeflich & Khokhlov 1996). If we consider detonation of a sub-Chandrashekhar O-Ne-Mg white dwarf (Isern et al. 1991), the total nuclear energy is smaller and the predicted ejecta velocities are lower than observed (Filippenko et al. 1992). Mazzali et al. (2007) use detailed spectral modeling to show a common explosion mechanism for all SNe Ia, likely delayed detonation. The failed neutron star model (Nomoto & Iben 1985) suggests that if the accretion rate of carbon and oxygen from a companion onto a white dwarf is high enough, it may prematurely ignite CO on the white dwarf surface. Thus, instead of a neutron star, we may see a faint SNe Ia. Small-scale deflagration models suggest that either the burning is restricted to the outer

layers or that it occurs slowly.

Another intriguing theoretical possibility recently proposed by Bildsten et al. (2007b) is faint thermonuclear supernovae from ultracompact double degenerate AM CVn systems. This supernova is tantalizingly at the brightest end of their predictions (M_V=−14 to −16, timescale = 2–6 days, $M_{ej} < 0.1$ M⊙). However, the decay time predicted by these models is much shorter and the ^{56}Ni mass less than that observed in SN2007ax. Also, the spectrum does not show any feature which suggests being powered by different radioactive material (^{48}Cr, ^{44}Ti, ^{52}Fe) produced by some of these models.

None of the above models convincingly explain all the observed characteristics of subluminous SNe Ia. SN2007ax compels the question of what is the (and whether there is) lower limit of ^{56}Ni mass in a thermonuclear explosion. Only if we can explain the extremely faint (and the extremely bright) supernovae will we thoroughly understand the limitations in physical processes involved in the thermonuclear explosion, in particular, the ^{56}Ni mass production.

Future supernova surveys which have a shorter cadence and a deeper limiting magnitude will provide invaluable clues to understanding the nature of subluminous SNe Ia. Follow-up of these supernovae with well-sampled UV light curves and well-calibrated multi-epoch UV spectra would also be important to understand the apparent excess at late-time.

We suggest how a near-future survey, for example, the Palomar Transient Factory[3], can systematically search for faint SNe Ia. The parameters of the survey design are sky coverage, cadence, depth, filter and choice of pointings. Howell (2001) shows that faint SNe Ia occur preferentially in early-type galaxies and Taubenberger et al. (2008) suggest that they occur in lower metallicity, old stellar mass populations. Since they decline by a magnitude in five days, the cadence of the search should be faster than five days so that the detection sample is complete. Since faint SNe Ia are extremely red at maximum, we should choose a red filter for the search. To maximize sky coverage, searching with a single red filter should suffice (with multi-band follow-up). Since the local universe is clumpy (e.g., ≈25% of the total light at the distance of Virgo is in the Virgo supercluster), the sky coverage must include concentrations in stellar mass, such as the Virgo, Perseus and Coma galaxy clusters. The

[3]The Palomar Transient Factory is a dedicated time-domain astronomy project to come online on Palomar 48-inch in Nov 08.

rate of normal SNe Ia is 3 per $10^{11}L_{\odot}$ per century (Scannapieco & Bildsten 2005). Li et al. (2001) estimate a rate for subluminous SNe Ia to be 16% of normal SNe Ia rate based on LOSS and BAOSS surveys. To a depth of absolute magnitude of -15.5, and with a limiting magnitude of 20.5, the survey volume would be $1.5\times\ 10^{7}$ Mpc^3. Using the 2MASS K-band luminosity function of $5.1\times10^{8}L_{\odot}\mathrm{Mpc}^{-3}$ (Karachentsev & Kutkin 2005, Kochanek et al. 2001), we expect a rate of the faintest subluminous supernovae to be ≈ 370 all sky per year. The Palomar Transient Factory plans a 5-day cadence 2700 deg^2 experiment which would give ≈ 24 faint SNe Ia per year.

We thank Nick Scoville, Milan Bogoslavejic and the Swift team for performing our Target of Opportunity observations flawlessly. We would like to thank Brent Tully for providing his catalog of nearby galaxies. LB thanks NSF grants PHY 05-51164 and AST 02-05956.

Table 2.1. Comparison of Faint Type Ia Supernovae

Supernova	Galaxy	DM	$M_{B,max}$ mag	α mag day^{-1}	β mag day^{-1}	t_b days	$(B-V)_{\max}$ mag	Reference
SN2007ax	NGC 2577	32.2	−15.9±0.2	0.16	0.04	10.3	1.2	This Paper
SN1991bg	NGC 4374	31.2	−16.6±0.3	0.16	0.03	14.8	0.8	Leibundgut et al. (1993),Filippenko et al. (1992)
SN1998de	NGC 252	34.3	−16.8±0.2	0.18	0.03	14.5	0.7	Modjaz et al. (2001)
SN2005ke	NGC 1371	31.8	−17.0±0.2	0.15	0.02	14.9	0.7	Immler et al. (2006)
SN2005bl	NGC 4070	35.1	−17.2±0.2	0.18	.03	14.0	0.6	Taubenberger et al. (2008)
SN1999by	NGC 2841	30.9	−17.3±0.2	0.18	0.02	16.0	0.5	Garnavich et al. (2004)

Table 2.2: Summary of Photometric Observations of SN2007ax

UT	MJD	Facility	Band	Exposure	Magnitude
04-Apr-2007	54194.29	Keck-NIRC2	K'	600 s	16.7 ± 0.1 mag
29-Mar-2007	54188.147	Palomar-60	r'	3×180 s	15.65 ± 0.06 mag
30-Mar-2007	54189.230	Palomar-60	r'	3×180 s	15.75 ± 0.05 mag
30-Mar-2007	54189.331	Palomar-60	r'	3×180 s	15.60 ± 0.02 mag
31-Mar-2007	54190.232	Palomar-60	r'	3×180 s	15.73 ± 0.03 mag
31-Mar-2007	54190.329	Palomar-60	r'	3×180 s	15.59 ± 0.03 mag
01-Apr-2007	54191.137	Palomar-60	r'	3×180 s	15.68 ± 0.05 mag
01-Apr-2007	54191.234	Palomar-60	r'	3×180 s	15.69 ± 0.03 mag
01-Apr-2007	54191.137	Palomar-60	r'	3×180 s	15.68 ± 0.05 mag
02-Apr-2007	54192.233	Palomar-60	r'	3×180 s	15.36 ± 0.04 mag
03-Apr-2007	54193.138	Palomar-60	r'	3×180 s	15.56 ± 0.03 mag
03-Apr-2007	54193.231	Palomar-60	r'	3×180 s	15.59 ± 0.22 mag
04-Apr-2007	54194.238	Palomar-60	r'	3×180 s	15.45 ± 0.04 mag
05-Apr-2007	54195.223	Palomar-60	r'	3×180 s	15.43 ± 0.03 mag
06-Apr-2007	54196.239	Palomar-60	r'	3×180 s	15.50 ± 0.03 mag
07-Apr-2007	54197.307	Palomar-60	r'	3×180 s	15.94 ± 0.06 mag
11-Apr-2007	54201.145	Palomar-60	r'	3×180 s	16.41 ± 0.07 mag
14-Apr-2007	54204.146	Palomar-60	r'	3×180 s	16.69 ± 0.03 mag
14-Apr-2007	54204.245	Palomar-60	r'	3×180 s	16.31 ± 0.12 mag
18-Apr-2007	54208.165	Palomar-60	r'	3×180 s	17.09 ± 0.04 mag
25-Apr-2007	54215.164	Palomar-60	r'	3×180 s	17.58 ± 0.07 mag
28-Apr-2007	54218.157	Palomar-60	r'	3×180 s	17.62 ± 0.05 mag
29-Apr-2007	54219.195	Palomar-60	r'	3×180 s	17.64 ± 0.14 mag
30-Apr-2007	54220.154	Palomar-60	r'	3×180 s	17.74 ± 0.09 mag
08-May-2007	54228.159	Palomar-60	r'	3×180 s	18.18 ± 0.18 mag

Continued on Next Page...

Table 2.2 – Continued

UT	MJD	Facility	Band	Exposure	Magnitude
29-Mar-2007	54188.127	Palomar-60	g'	$3 \times 180\,\mathrm{s}$	$16.27 \pm 0.09\,\mathrm{mag}$
29-Mar-2007	54188.142	Palomar-60	g'	$3 \times 180\,\mathrm{s}$	$16.30 \pm 0.05\,\mathrm{mag}$
30-Mar-2007	54189.128	Palomar-60	g'	$3 \times 180\,\mathrm{s}$	$16.37 \pm 0.04\,\mathrm{mag}$
30-Mar-2007	54189.222	Palomar-60	g'	$3 \times 180\,\mathrm{s}$	$16.23 \pm 0.11\,\mathrm{mag}$
30-Mar-2007	54189.323	Palomar-60	g'	$3 \times 180\,\mathrm{s}$	$16.20 \pm 0.14\,\mathrm{mag}$
31-Mar-2007	54190.129	Palomar-60	g'	$3 \times 180\,\mathrm{s}$	$16.36 \pm 0.08\,\mathrm{mag}$
31-Mar-2007	54190.225	Palomar-60	g'	$3 \times 180\,\mathrm{s}$	$16.37 \pm 0.12\,\mathrm{mag}$
31-Mar-2007	54190.321	Palomar-60	g'	$3 \times 180\,\mathrm{s}$	$16.22 \pm 0.12\,\mathrm{mag}$
01-Apr-2007	54191.130	Palomar-60	g'	$3 \times 180\,\mathrm{s}$	$16.45 \pm 0.11\,\mathrm{mag}$
01-Apr-2007	54191.227	Palomar-60	g'	$3 \times 180\,\mathrm{s}$	$16.43 \pm 0.12\,\mathrm{mag}$
01-Apr-2007	54191.130	Palomar-60	g'	$3 \times 180\,\mathrm{s}$	$16.30 \pm 0.13\,\mathrm{mag}$
02-Apr-2007	54192.130	Palomar-60	g'	$3 \times 180\,\mathrm{s}$	$16.49 \pm 0.11\,\mathrm{mag}$
02-Apr-2007	54192.226	Palomar-60	g'	$3 \times 180\,\mathrm{s}$	$16.39 \pm 0.12\,\mathrm{mag}$
02-Apr-2007	54192.322	Palomar-60	g'	$3 \times 180\,\mathrm{s}$	$16.39 \pm 0.09\,\mathrm{mag}$
03-Apr-2007	54193.224	Palomar-60	g'	$3 \times 180\,\mathrm{s}$	$16.45 \pm 0.11\,\mathrm{mag}$
03-Apr-2007	54193.320	Palomar-60	g'	$3 \times 180\,\mathrm{s}$	$16.53 \pm 0.12\,\mathrm{mag}$
04-Apr-2007	54194.132	Palomar-60	g'	$3 \times 180\,\mathrm{s}$	$16.59 \pm 0.09\,\mathrm{mag}$
04-Apr-2007	54194.230	Palomar-60	g'	$3 \times 180\,\mathrm{s}$	$16.26 \pm 0.11\,\mathrm{mag}$
05-Apr-2007	54195.216	Palomar-60	g'	$3 \times 180\,\mathrm{s}$	$16.47 \pm 0.09\,\mathrm{mag}$
06-Apr-2007	54196.138	Palomar-60	g'	$3 \times 180\,\mathrm{s}$	$16.66 \pm 0.07\,\mathrm{mag}$
06-Apr-2007	54196.231	Palomar-60	g'	$3 \times 180\,\mathrm{s}$	$17.06 \pm 0.12\,\mathrm{mag}$
07-Apr-2007	54197.300	Palomar-60	g'	$3 \times 180\,\mathrm{s}$	$17.03 \pm 0.07\,\mathrm{mag}$
11-Apr-2007	54201.138	Palomar-60	g'	$3 \times 180\,\mathrm{s}$	$17.62 \pm 0.14\,\mathrm{mag}$
11-Apr-2007	54201.235	Palomar-60	g'	$3 \times 180\,\mathrm{s}$	$17.47 \pm 0.17\,\mathrm{mag}$
14-Apr-2007	54204.139	Palomar-60	g'	$3 \times 180\,\mathrm{s}$	$17.80 \pm 0.13\,\mathrm{mag}$
14-Apr-2007	54204.237	Palomar-60	g'	$3 \times 180\,\mathrm{s}$	$17.59 \pm 0.12\,\mathrm{mag}$
17-Apr-2007	54207.159	Palomar-60	g'	$3 \times 180\,\mathrm{s}$	$18.11 \pm 0.19\,\mathrm{mag}$

Continued on Next Page...

Table 2.2 – Continued

UT	MJD	Facility	Band	Exposure	Magnitude
18-Apr-2007	54208.158	Palomar-60	g'	3×180 s	18.04 ± 0.13 mag
18-Apr-2007	54208.275	Palomar-60	g'	3×180 s	17.98 ± 0.15 mag
20-Apr-2007	54210.140	Palomar-60	g'	3×180 s	18.09 ± 0.23 mag
22-Apr-2007	54212.267	Palomar-60	g'	3×180 s	18.20 ± 0.23 mag
25-Apr-2007	54215.157	Palomar-60	g'	3×180 s	18.49 ± 0.42 mag
26-Apr-2007	54216.155	Palomar-60	g'	3×180 s	18.61 ± 0.34 mag
28-Apr-2007	54218.150	Palomar-60	g'	3×180 s	18.57 ± 0.39 mag
29-Apr-2007	54219.188	Palomar-60	g'	3×180 s	18.42 ± 0.22 mag
30-Apr-2007	54220.147	Palomar-60	g'	3×180 s	18.73 ± 0.40 mag
09-May-2007	54229.159	Palomar-60	g'	3×180 s	18.71 ± 0.10 mag
02-Apr-2007	54192.8	Swift-UVOT	v	419 s	15.87 ± 0.08 mag
04-Apr-2007	54195.0	Swift-UVOT	v	229 s	16.10 ± 0.09 mag
10-Apr-2007	54201.0	Swift-UVOT	v	227 s	16.75 ± 0.14 mag
17-Apr-2007	54207.2	Swift-UVOT	v	225 s	17.42 ± 0.23 mag
21-Apr-2007	54211.4	Swift-UVOT	v	516 s	17.94 ± 0.33 mag
29-Mar-2007	54189.0	Swift-UVOT	b	189 s	16.96 ± 0.05 mag
02-Apr-2007	54192.8	Swift-UVOT	b	419 s	17.22 ± 0.05 mag
04-Apr-2007	54195.0	Swift-UVOT	b	205 s	18.02 ± 0.11 mag
10-Apr-2007	54201.0	Swift-UVOT	b	202 s	18.57 ± 0.16 mag
17-Apr-2007	54207.2	Swift-UVOT	b	324 s	18.62 ± 0.14 mag
21-Apr-2007	54211.4	Swift-UVOT	b	679 s	18.64 ± 0.12 mag
30-Apr-2007	54220.2	Swift-UVOT	b	677 s	19.70 ± 0.29 mag
06-May-2007	54226.3	Swift-UVOT	b	134 s	19.15 ± 0.30 mag
11-May-2007	54231.9	Swift-UVOT	b	723 s	> 19.8 mag
02-Apr-2007	54192.8	Swift-UVOT	u	419 s	17.82 ± 0.08 mag
04-Apr-2007	54194.0	Swift-UVOT	u	229 s	18.26 ± 0.13 mag
10-Apr-2007	54201.0	Swift-UVOT	u	227 s	18.94 ± 0.22 mag

Continued on Next Page...

Table 2.2 – Continued

UT	MJD	Facility	Band	Exposure	Magnitude
17-Apr-2007	54207.2	Swift-UVOT	u	648 s	18.86 ± 0.14 mag
29-Mar-2007	54188.9	Swift-UVOT	$uvw1$	432 s	20.02 ± 0.47 mag
02-Apr-2007	54192.8	Swift-UVOT	$uvw1$	844 s	20.07 ± 0.40 mag
04-Apr-2007	54195.2	Swift-UVOT	$uvw1$	1669 s	> 20.42 mag
10-Apr-2007	54201.2	Swift-UVOT	$uvw1$	1369 s	> 20.45 mag
17-Apr-2007	54207.2	Swift-UVOT	$uvw1$	1620 s	> 20.42 mag
21-Apr-2007	54211.4	Swift-UVOT	$uvw1$	3400 s	20.51 ± 0.40 mag
30-Apr-2007	54220.7	Swift-UVOT	$uvw1$	3390 s	20.86 ± 0.50 mag
06-May-2007	54226.7	Swift-UVOT	$uvw1$	6681 s	> 20.12 mag
11-May-2007	54232.4	Swift-UVOT	$uvw1$	3615 s	> 20.62 mag
18-Apr-2007	54208.6	Super-LOTIS	I	13 × 60 s	17.01 ± 0.02 mag
19-Apr-2007	54209.6	Super-LOTIS	I	10 × 60 s	17.22 ± 0.02 mag
20-Apr-2007	54210.6	Super-LOTIS	I	9 × 60 s	17.18 ± 0.02 mag
27-Apr-2007	54217.6	Super-LOTIS	I	6 × 60 s	17.59 ± 0.04 mag
04-May-2007	54224.6	Super-LOTIS	I	18 × 60 s	18.00 ± 0.05 mag
11-May-2007	54231.6	Super-LOTIS	I	16 × 60 s	18.35 ± 0.10 mag
26-May-2007	54246.6	Super-LOTIS	I	18 × 60 s	18.90 ± 0.29 mag
29-May-2007	54249.6	Super-LOTIS	I	22 × 60 s	19.05 ± 0.18 mag
30-May-2007	54250.6	Super-LOTIS	I	14 × 60 s	19.15 ± 0.10 mag
18-Apr-2007	54208.6	Super-LOTIS	R	12 × 60 s	16.79 ± 0.23 mag
19-Apr-2007	54209.6	Super-LOTIS	R	12 × 60 s	16.97 ± 0.22 mag
20-Apr-2007	54210.6	Super-LOTIS	R	14 × 60 s	17.10 ± 0.20 mag
23-Apr-2007	54213.6	Super-LOTIS	R	15 × 60 s	17.24 ± 0.22 mag
26-Apr-2007	54216.6	Super-LOTIS	R	47 × 60 s	17.32 ± 0.29 mag
27-Apr-2007	54217.6	Super-LOTIS	R	12 × 60 s	17.47 ± 0.29 mag
04-May-2007	54224.6	Super-LOTIS	R	10 × 60 s	17.72 ± 0.38 mag
11-May-2007	54231.6	Super-LOTIS	R	16 × 60 s	17.96 ± 0.46 mag

Continued on Next Page...

Table 2.2 – Continued

UT	MJD	Facility	Band	Exposure	Magnitude
26-May-2007	54246.6	Super-LOTIS	R	$17 \times 60\,\mathrm{s}$	18.11 ± 0.40 mag
27-May-2007	54247.6	Super-LOTIS	R	$11 \times 60\,\mathrm{s}$	18.55 ± 0.37 mag
31-May-2007	54251.6	Super-LOTIS	R	$11 \times 60\,\mathrm{s}$	18.16 ± 0.46 mag
05-Jun-2007	54256.6	Super-LOTIS	R	$20 \times 60\,\mathrm{s}$	18.20 ± 0.54 mag
18-Apr-2007	54208.6	Super-LOTIS	V	$9 \times 60\,\mathrm{s}$	17.84 ± 0.15 mag
19-Apr-2007	54209.6	Super-LOTIS	V	$6 \times 60\,\mathrm{s}$	17.80 ± 0.15 mag
20-Apr-2007	54210.6	Super-LOTIS	V	$8 \times 60\,\mathrm{s}$	17.80 ± 0.15 mag
27-Apr-2007	54217.6	Super-LOTIS	V	$16 \times 60\,\mathrm{s}$	18.30 ± 0.15 mag
04-May-2007	54224.6	Super-LOTIS	V	$9 \times 60\,\mathrm{s}$	18.94 ± 0.15 mag
11-May-2007	54231.6	Super-LOTIS	V	$17 \times 60\,\mathrm{s}$	18.87 ± 0.15 mag
27-May-2007	54247.6	Super-LOTIS	V	$18 \times 60\,\mathrm{s}$	19.55 ± 0.23 mag
29-May-2007	54249.6	Super-LOTIS	V	$22 \times 60\,\mathrm{s}$	19.27 ± 0.16 mag
27-May-2007	54247.6	Bok-2.3m	B	$4 \times 180\,\mathrm{s}$	20.53 ± 0.04 mag

Chapter 3

Understanding Extreme Novae: P60-FasTING*

M. M. Kasliwal[1], S. B. Cenko[2], S. R. Kulkarni[1], E. O. Ofek[1], R. Quimby[1], A. Rau[3]

[1]Astronomy Department, California Institute of Technology, 105-24, Pasadena, CA 91125, USA

[2] Department of Astronomy, University of California at Berkeley, Berkeley, CA 94720, USA

[3] Max-Planck Institut fuer Extraterrestrische Physik, 85748 Garching, Germany

Abstract

We present photometric and spectroscopic follow-up of a sample of extragalactic novae discovered by the Palomar 60-inch telescope during a search for "Fast Transients In Nearest Galaxies" (P60-FasTING). Designed as a fast cadence (1-day) and deep ($g < 21$ mag) survey, P60-FasTING was particularly sensitive to short-lived and faint optical transients. The P60-FasTING nova sample includes 10 novae in M 31, 6 in M 81, 3 in M 82, 1 in NGC 2403 and 1 in NGC 891. This significantly expands the known sample of extragalactic novae beyond the Local Group, including the first discoveries in a starburst environment. Surprisingly, our photometry shows that this sample is quite inconsistent with the canonical Maximum Magnitude Rate of Decline (MMRD) relation for classical novae. Furthermore, the spectra of the P60-FasTING sample are indistinguishable from classical novae. We suggest that

*A version of this chapter is published with the title "Discovery of a new photometric sub-class of faint and fast classical novae" in the *The Astrophysical Journal*, 2011, vol. 734 and is reproduced by permission of the AAS.

we have uncovered a sub-class of faint and fast classical novae in a new phase space in luminosity-timescale of optical transients. Thus, novae span two orders of magnitude in both luminosity and time. Perhaps, the MMRD, which is characterized only by the white dwarf mass, was an over-simplification. Nova physics appears to be characterized by quite a rich four-dimensional parameter space in white dwarf mass, temperature, composition and accretion rate.

3.1 Introduction

Since the discovery of classical novae, astronomers have pursued their use as standard candles to determine distances (see Hubble 1929). Zwicky (1936) first noticed some regularity in nova light curves and termed this the "life-luminosity" relation. Arp (1956) undertook a comprehensive search for novae in M31, discovering thirty novae in 290 nights, and found a clear relation — luminous novae evolve faster than less luminous novae. The modern name for this observation is the maximum-magnitude rate-of-decline relation (MMRD relation).

The MMRD relation has attracted considerable theoretical attention (e.g., Livio 1992). The basic idea is that the relation is entirely due to the mass of the accreting white dwarf. The more massive the white dwarf, the higher the surface gravity, the higher the pressure at the base of envelope and the stronger the thermonuclear runaway (and hence, higher the peak luminosity). Also, the more massive the white dwarf, the smaller the envelope mass to attain the critical pressure for thermonuclear runaway (TNR) and hence, the faster the decline.

In more recent times, della Valle & Livio (1995) used a sample of novae in M31 and LMC to propose an arctangent relation between the peak luminosity and rate of decline. Downes & Duerbeck (2000) used a sample of Galactic novae to propose a linear relation between the same two parameters. Darnley et al. (2006) used a score of novae in M31 from POINT AGAPE survey and claimed their observations were consistent with the della Valle & Livio (1995) formulation of the MMRD.

In comparison to supernovae, classical novae are not very luminous. Hence, searches (e.g., Shafter & Irby 2001, Ciardullo et al. 1987) have traditionally focussed only on the Milky Way and its nearest neighbors (Andromeda and the Large Magellanic Cloud). Hornoch et al.

(2008) looked into archival data and found 49 nova candidates[1] in M 81 in the past 20 years — unfortunately, these candidates neither have light curves nor spectra. Ferrarese et al. (2003) undertook a search for novae using 24 orbits of the Hubble Space Telescope and found nine nova candidates in M49. Even with their sparsely sampled light curves for nine novae, they concluded that novae are not good standard candles. Another survey, CFHT-COVET[2] (aimed at finding transients in the gap between novae and supernovae) found a dozen nova candidates in many galaxies in the Virgo supercluster, including some in the far outskirts of galaxies (Kasliwal et al 2011, in prep).

Here, we report on novae discovered in high cadence monitoring observations of a representative collection of galaxies with distance less than that of the Virgo cluster. The original motivation of this search, P60-FasTING[3], was to explore rapid transients (those which last less than a couple of nights) in the nearest galaxies. A strong spectroscopic follow-up effort was a part of P60-FasTING. The survey was capable of finding novae in the major galaxies out to 4 Mpc: M 31, M 81, the star-burst M 82 and NGC 2403. We present our sample of 21 transients, which although spectroscopically indistinguishable from classical novae, photometrically occupy a new region of phase space.

The paper is organized as follows: § 3.2 describes the discovery, photometric and spectroscopic follow-up observations of this nova sample, § 3.3 describes the data analysis, § 3.4 discusses the implications and § 3.5 presents our conclusion.

[1]We use the term candidate where the light curve is very sparse and/or there is no spectrosopic confirmation.

[2]**C**anada **F**rance **H**awaii **T**elescope **CO**ma **V**irgo **E**xploration for **T**ransients

[3]**P**alomar **60**-inch **Fas**t **T**ransient **I**n **N**earest **G**alaxies

Table 3.1. Novae Discovered by P60-FasTING

Nova	Host	Discovery Date	RA(J2000)	DEC(J2000)	Offset from Host	Reference
P60-NGC2403-090314	NGC2403	2009 Mar 14.160	07:36:35.00	+65:40:20.8	101.0"W, 252.0"N	Kasliwal et al. (2009a)
P60-M82OT-090314	NGC3034	2009 Mar 14.496	09:56:12.60	+69:41:32.3	104.2"E, 48.2"N	···
P60-M81OT-090213	NGC3031	2009 Feb 13.404	09:55:35.96	+69:01:51.0	15"E, 124"S	Kasliwal et al. (2009b)
P60-M31OT-081230 (2008-12b)	NGC224	2008 Dec 30.207	00:43:05.03	+41:17:52.3	233.4"E,103.8"N	Kasliwal et al. (2009c)
P60-M81OT-081229	NGC3031	2008 Dec 29.373	09:55:38.15	+69:01:43.6	26.7"E, 131.4"S	Rau et al. (2009a)
P60-M81OT-081203	NGC3031	2008 Dec 3.303	09:55:16.92	+69:02:17.7	87.2"W, 97.4"S	Kasliwal et al. (2008a)
P60-M82OT-081119	NGC3034	2008 Nov 19.536	09:55:58.39	+69:40:56.2	29.5"E, 10.4"N	Kasliwal et al. (2008b)
P60-M81OT-081027	NGC3031	2008 Oct 27.402	09:55:36.11	+69:03:22.0	15.8"E, 33.1"S	Kasliwal et al. (2008g)
P60-M81OT-080925	NGC3031	2008 Sep 25.49	09:55:59.35	+69:05:57.1	2.35'E, 2.03'N	Kasliwal et al. (2008i)
P60-M31OT-080915 (2008-09c)	NGC224	2008 Sep 15.36	00:42:51.42	+41:01:54.0	1.34'E, 14.24'S	Kasliwal et al. (2008f)
P60-M31OT-080913 (2008-09a)	NGC224	2008 Sep 13.18	00:41:46.72	+41:07:52.1	10.8'W, 8.3'S	Kasliwal et al. (2008e)
P60-NGC891OT-080813	NGC891	2008 Aug 13.45	02:22:32.70	+42:21:56.1	8"W,59"N	Kasliwal et al. (2008c)
P60-M31OT-080723 (2008-07b)	NGC224	2008 Jul 23.33	00:43:27.28	+41:10:03.3	8.1'E,6.1'S	Kasliwal et al. (2008d)
P60-M82OT-080429	NGC3034	2008 Apr 29.24	09:55:21.00	+69:39:42.0	165" W, 64" S	Kasliwal et al. (2008h)
P60-M81OT-071213	NGC3031	2007 Dec 13.40	09:55:25.98	+69:04:34.8	40"W,40"N	Kasliwal et al. (2007)

Table 3.2. Additional M31 Novae

Nova	Discovery Date	Classification	Reference
2007-10a	54380.606	Fe II	Pietsch et al. (2007); Gal-Yam & Quimby (2007)
2007-11f	54433.716	···	Ovcharov et al. (2007)
2007-12b	54444.528	He/N	Nakamo,Hornoch Lee et al. (2007); Bode et al. (2009)
2008-08c	54708.127	···	Valcheva et al. (2008);Hornoch
2008-10b	54759.698	Fe II	Henze et al. (2008); Di Mille et al. (2008); Barsukova et al. (2008)
2008-11a	54774.438	Hybrid	Nishiyama;Hornoch Shafter et al. (2008)

3.2 Observations

3.2.1 Experiment Design

P60-FasTING was designed with the specific goal of probing new phase space, particularly, fast transients with peak luminosity in the gap between novae and supernovae. The sample of galaxies included the brightest and nearest galaxies (< 20 Mpc, majority around 10 Mpc). The survey was undertaken in a single filter (primarily Gunn-g and some Gunn-i data just around full moon). The limiting magnitude was typically Gunn-g < 21 and cadence was < 1 day. The field of view of P60 is $13.5' \times 13.5'$ and all galaxies except M31 were covered in a single pointing. For M31, five pointings were chosen to cover a larger fraction of the galaxy.

A real-time data reduction and transient search pipeline was written and implemented in April 2008. P60-FasTING ended in March 2009. The search pipeline was written in `python`. A deep reference image was constructed by combining images from several of the best seeing dark nights. Next, `wcsremap` was used to align every new image with the reference and `hotpants` was used to compute a convolution kernel prior to image subtraction (both codes supplied by A. Becker [4]). Although the image subtraction software was quite sophisticated in its convolution of the new image to match the reference prior to subtraction, we suffered from a large number of false positives. To distill the false subtraction residuals from the bonafide astrophysical sources, a variety of automatic filters were used (e.g., the shape

[4] http://www.astro.washington.edu/users/becker/c_software.html

characteristics of the PSF of the candidate, how well it resembles the PSF characteristics of other stars in the image). However, the final step in the vetting process was done by human eyes on candidate thumbnails every morning. Due to the myriad trade-offs for maximum completeness and minimum contamination, the complex issue of quantifying the completeness of the nova sample is beyond the scope of this publication.

Our survey was sensitive to classical novae only in a handful of the nearest galaxies in our sample (distance, $d < 4\,\mathrm{Mpc}$). Classical novae discovered by P60-FasTING are summarized in Table 3.1. Some novae in M31 were announced by different groups before P60-FasTING's first detection (usually due to bad weather at Palomar) — these are summarized in Table 3.2.

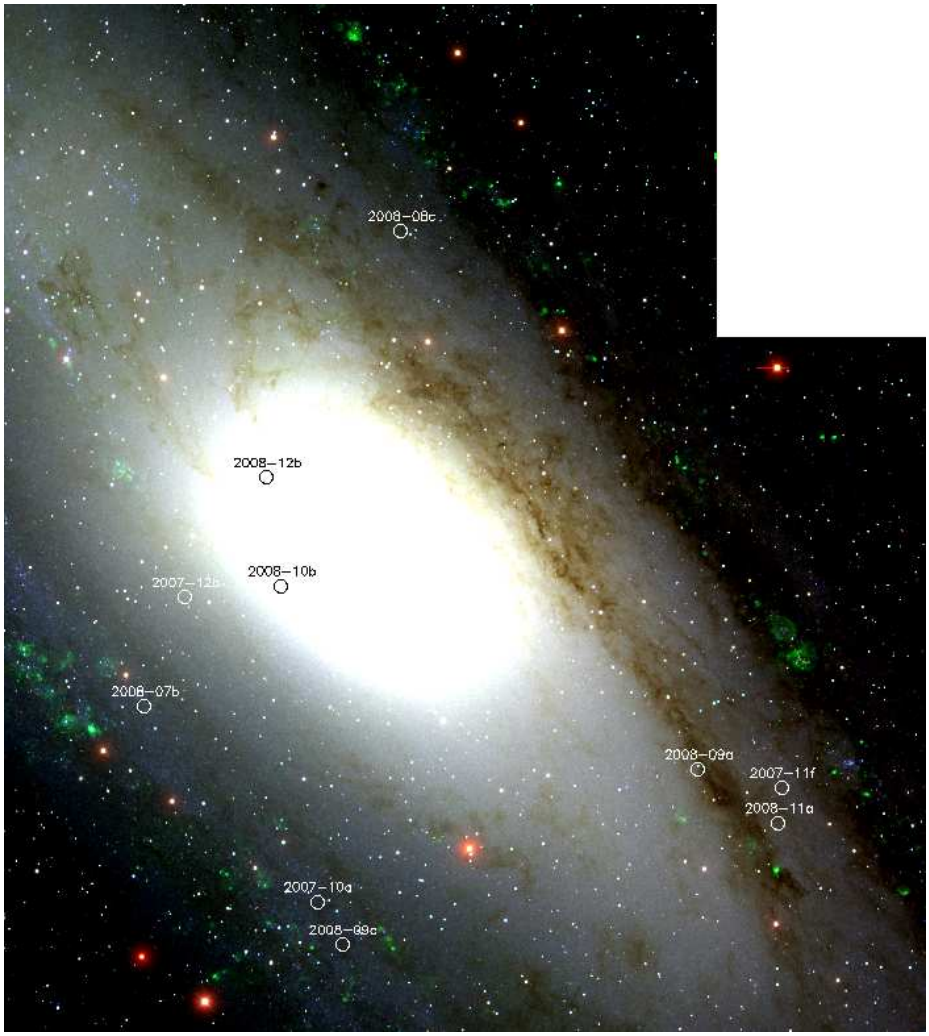

Figure 3.1 Location of ten novae in M31. Background image is a mosaic based on Massey data.

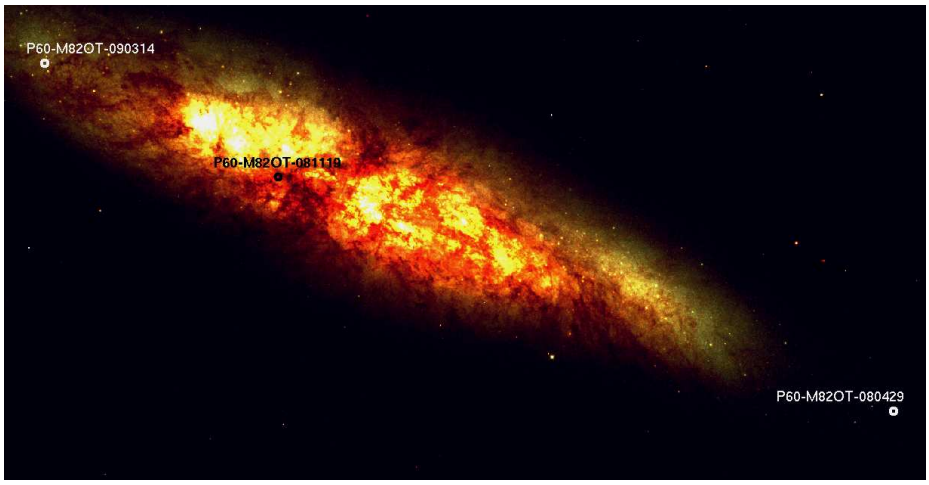

Figure 3.2 Location of three novae discovered by P60-FasTING in the starburst environment of M82. Background image is an HST/ACS mosaic.

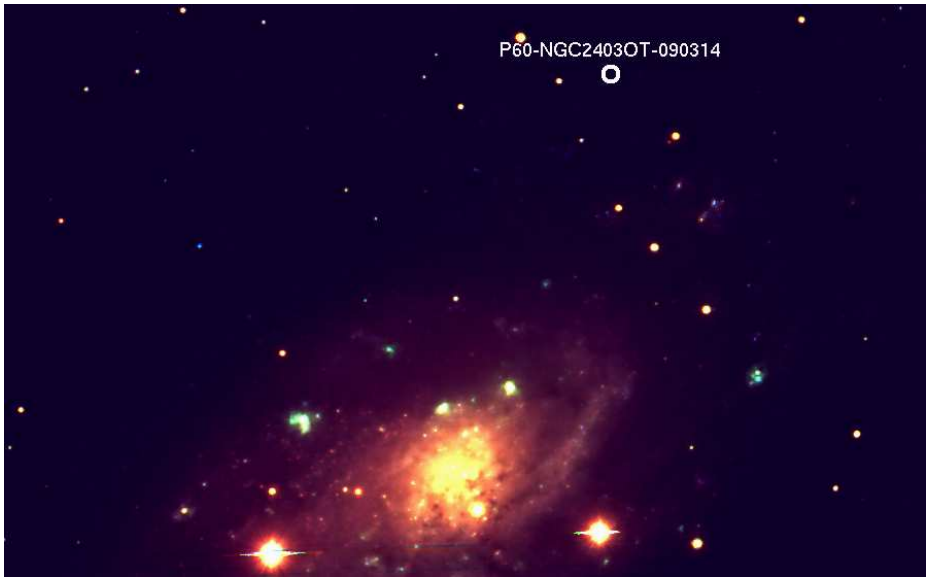

Figure 3.3 Location of one nova discovered by P60-FasTING in NGC2403. Background image is a deep co-add of P60 data.

3.2.2 Photometry

The robotic Palomar 60-inch has a standard data-reduction pipeline (Cenko et al. 2006). This pipeline performs basic detrending (flat-fielding and bias subtraction) and computes an astrometric solution. In August 2008, we added a new functionality: computation of a

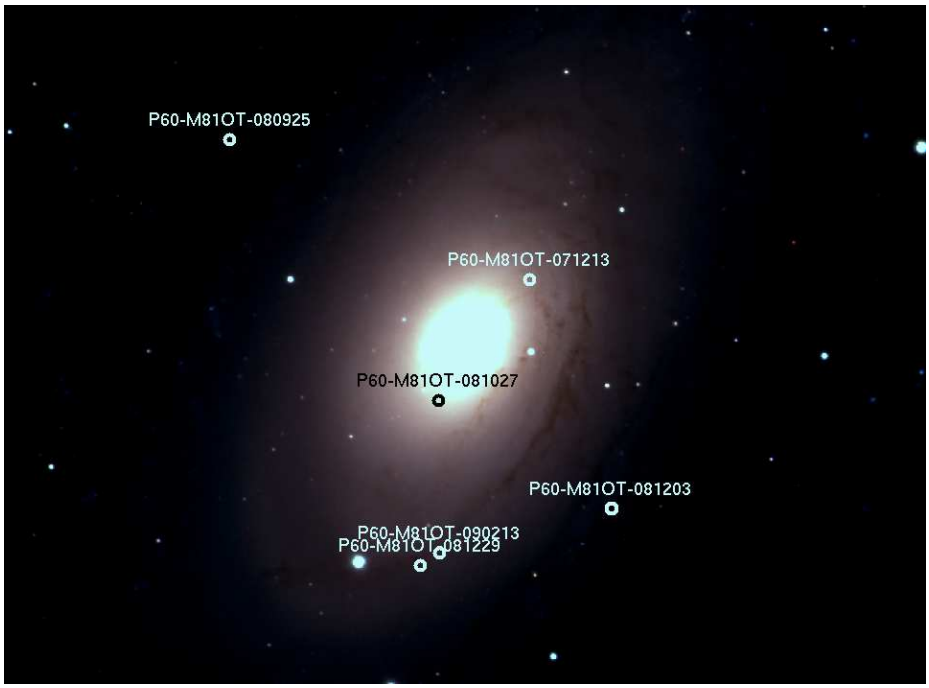

Figure 3.4 Location of six novae discovered by P60-FasTING in M81. Background image is a color mosaic using SDSS data.

photometric solution. We used the SDSS catalog where available, otherwise the NOMAD catalog. Note that where NOMAD was used (e.g., M31), the transformation from Johnson $UBVRI$ magnitudes to SDSS $ugriz$ magnitudes was done following Jordi et al. (2006).

To compute a light curve, we first measured the magnitude of the nova on the subtracted image. The subtracted image was scaled to the same flux level as the new image. Thus, we measured the magnitude of ~ 150 reference stars on the new image to compute a relative zeropoint with appropriate outlier rejection. Finally, we applied this relative zeropoint to the instrumental magnitude of the nova.

3.2.3 Spectroscopy

An integral part of P60-FasTING was follow-up spectroscopy to confirm and classify discovered candidate transients. Since we were looking for fast evolving phenomenon, we triggered our Target Of Opportunity program on the Keck I and Palomar Hale telescopes soon after

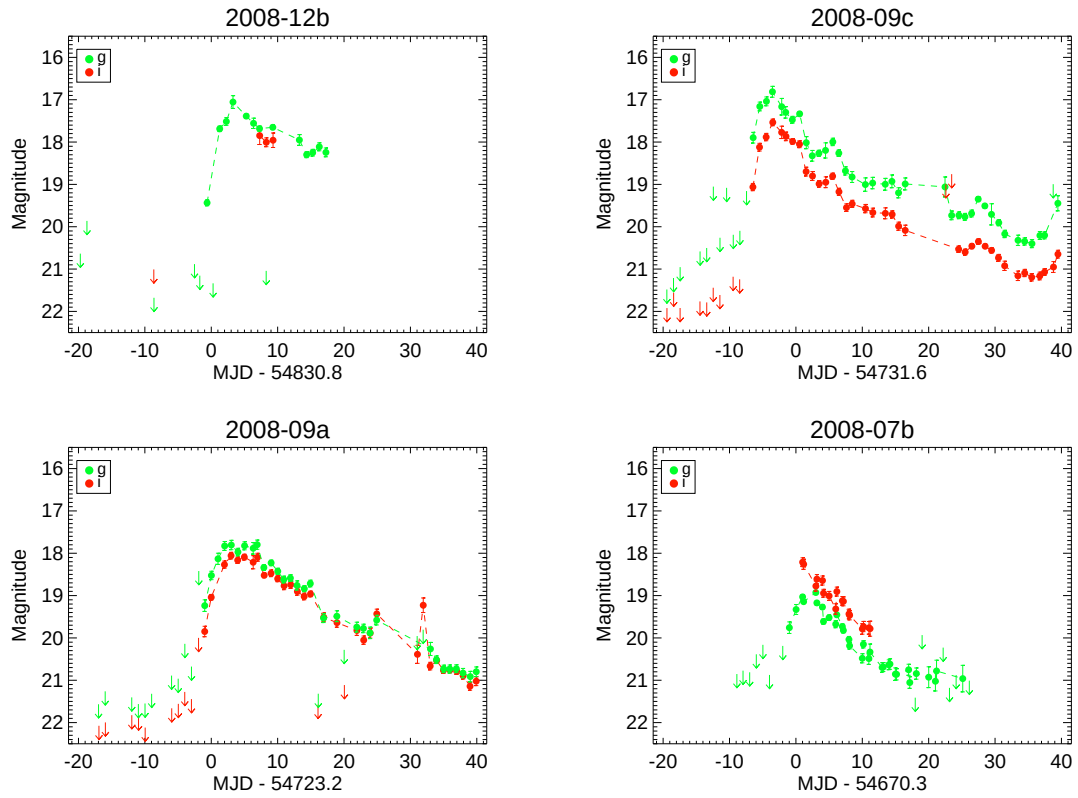

Figure 3.5 Lightcurves of novae in M31 discovered by P60-FasTING. Note the well-sampled rise.

discovery. Sometimes due to bad weather or bright moon-phase[5], neither of these was an option. We resorted to the queue-scheduled service-observed programs on Gemini or HET telescopes. A log of spectroscopic observations can be found in Table 5.1.

We emphasize that spectroscopy is crucial in distinguishing between an optical transient which happened to be co-incident with a nearby galaxy and a classical nova. For instance, we took spectra of several optical transient candidates which did not turn out to be novae: a foreground M-dwarf flare in the Milky Way spatially coincident with NGC 7640; a background supernova; a luminous blue variable in NGC 925.

Data were reduced in `iraf` using standard tasks in the NOAO package `onedspec` and the spectra are shown in Figure 3.10.

[5]Low resolution spectrographs are usually available on both these telescopes only during the dark fortnight.

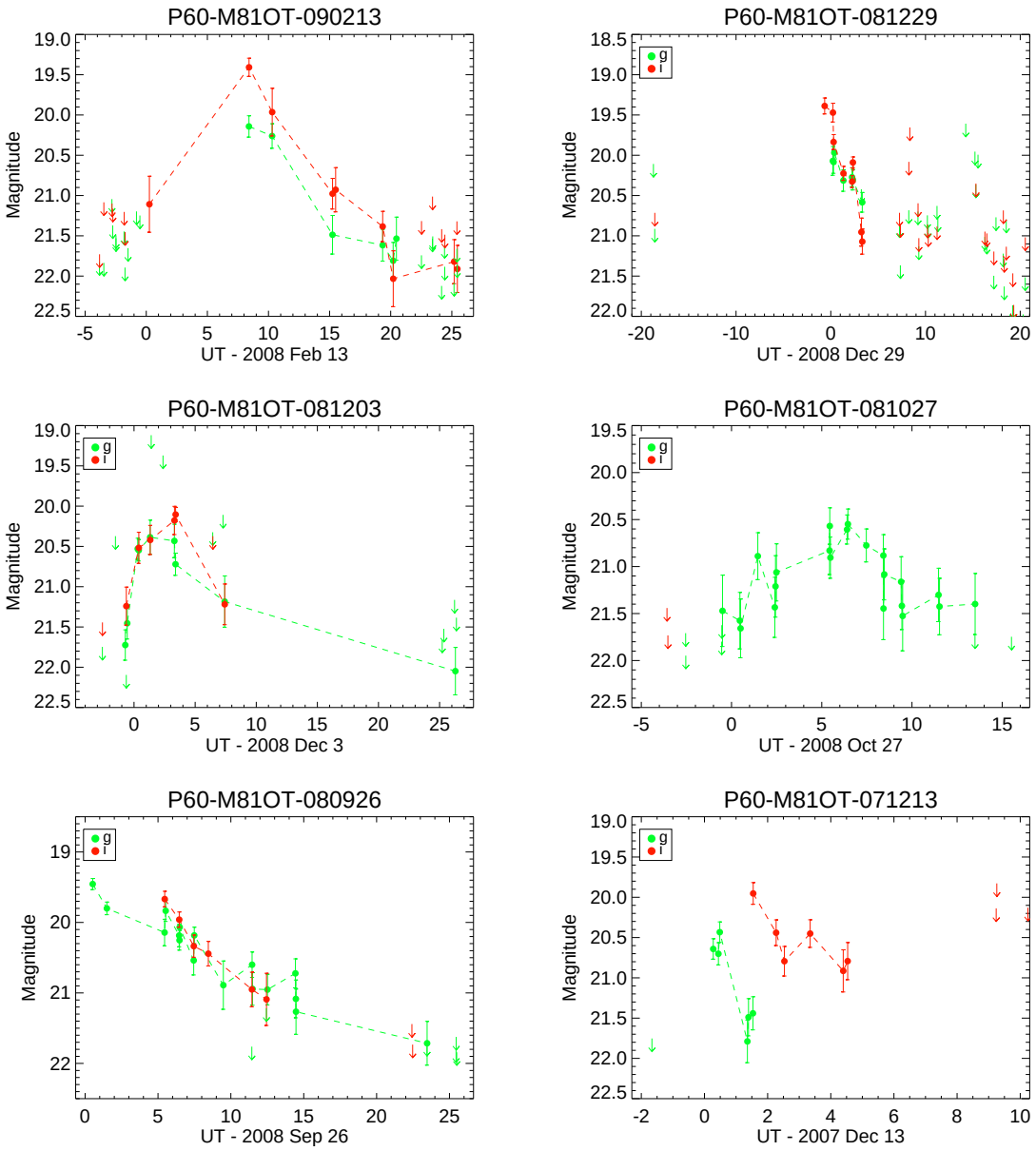

Figure 3.6 Lightcurves of novae in M81.

3.3 Analysis

The primary photometric analysis was to measure the peak absolute magnitude and rate of decline. The peak magnitude had to be corrected for extinction using spectra or colors. The primary spectroscopic analysis was to classify the spectra.

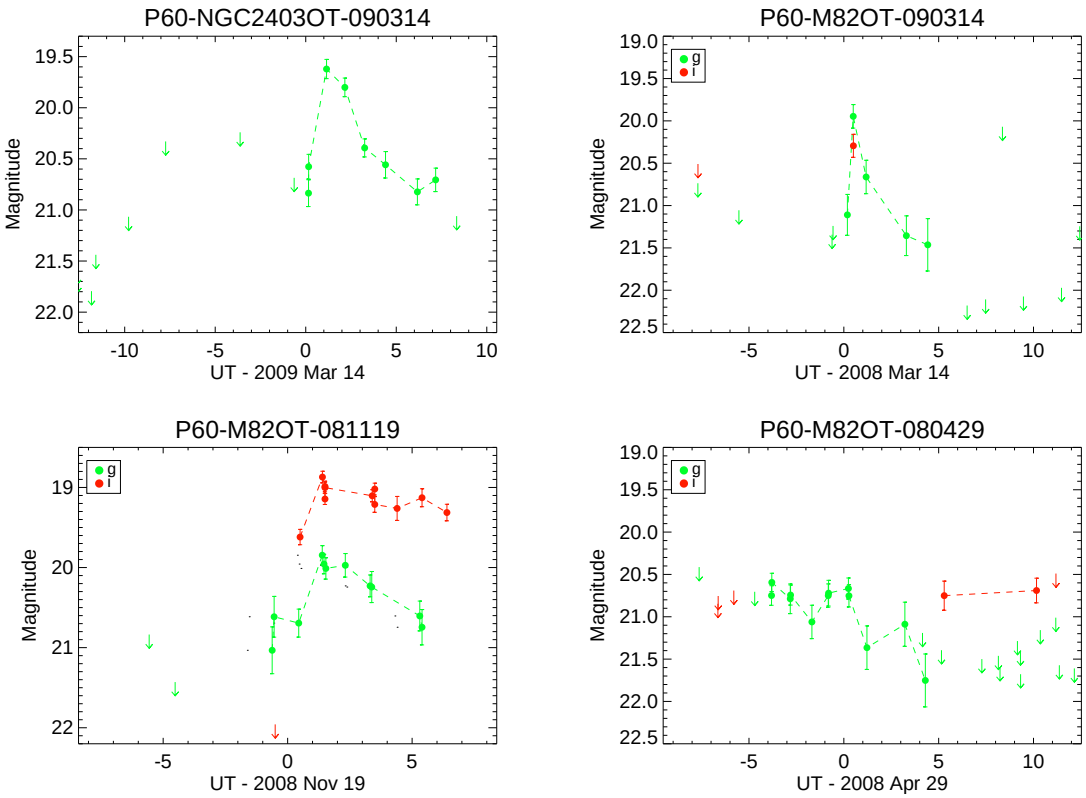

Figure 3.7 Lightcurves of novae in M82 and NGC2403. Note that P60-M82OT-081119 is much redder than typical novae.

3.3.1 Extinction

A multitude of methods have been used in the literature to measure extinction to novae. Darnley et al. (2006) compared a synthetic dust-free stellar $r-i$ map of M31 to an observed $r-i$ color map of M31 and used the difference between the maps to generate a dust map of M31. The location of the nova on this map determined how much extinction needed to be applied. This assumed that the novae were behind the galaxy and suffered extinction due to the entire column of dust. The average extinction as determined by this method is A_i=0.8. The galactic extinction along the line of sight of M31 of A_i=0.13 (Schlegel et al. 1998b). Shafter et al. (2009) compared the observed color of the new nova to that of a well-studied nova to derive the extinction. Kogure (1961) used the Balmer decrement (H_α/H_β) and attributed the excess in the ratio over the theoretical Case B value to dust.

Our preferred method of computing extinction is by using the spectroscopic Balmer

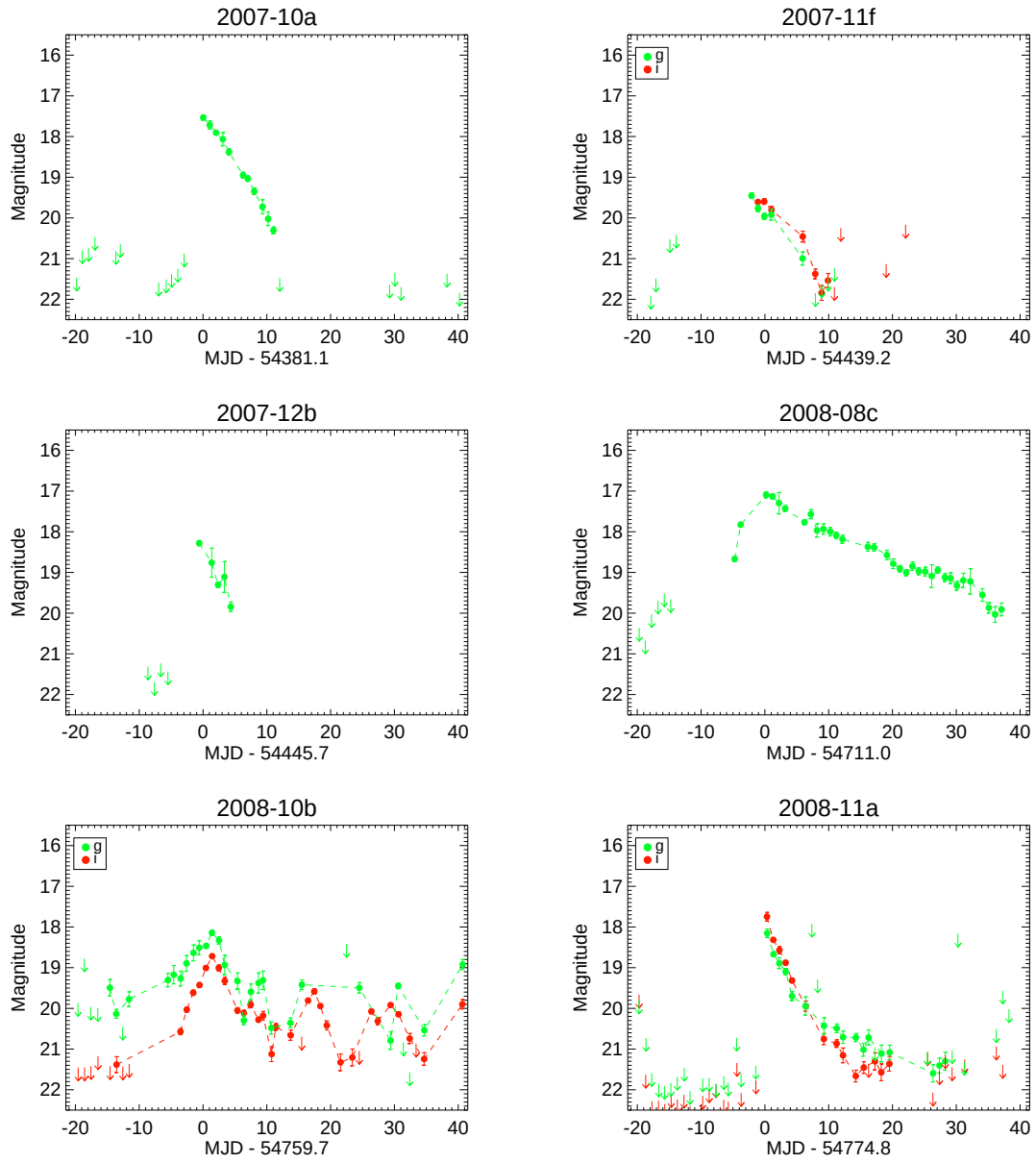

Figure 3.8 Lightcurves of additional novae in M31.

decrement where nebular spectra are available. We subtract the continuum, measure the flux ratio of the two lines, and then use:

$$A_g = 3.793 \times E(B-V) = 3.650 \times E(g-r)$$

$$= 3.650 \times \log_{10}(H_\alpha/H_\beta) - 1.75 \pm 0.14$$

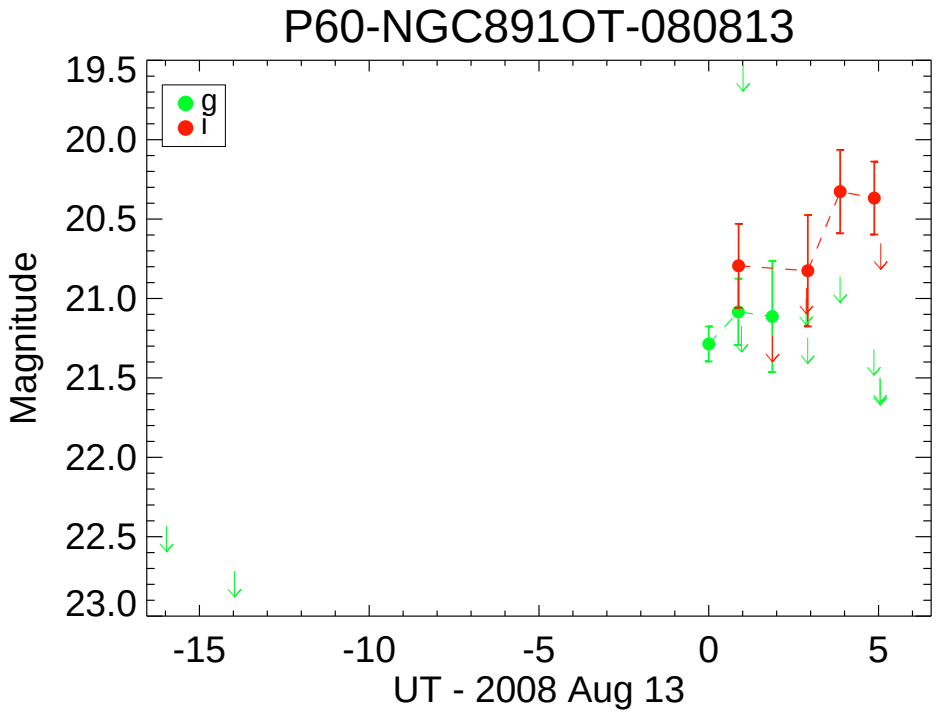

Figure 3.9 Lightcurve of possible nova in NGC 891. This was not spectroscopically confirmed and is not used in the MMRD analysis.

. The uncertainty comes from the range in expected ratios for Case B of 2.76–3.30.

Our second choice is to use the $g-i$ color of the nova at maximum, compare against the typical $g-i$ color and attribute the reddening to dust.

van den Bergh & Younger (1987) compiled photometry of several Galactic novae and derived an average color at maximum of $\langle B-V\rangle_0$=0.23 $\pm$ 0.06 mag. Following Shafter et al. (2009), we can use the colors of an A5V star (T = 8200 K) to translate $\langle B-V\rangle_0$ to $\langle g-i\rangle_0$. Using colors of an A5V star from Kraus & Hillenbrand (2007a), we get:

$$\langle g-i\rangle_0 = 1.88 - 2.15 = -0.27\,\mathrm{mag}$$

. Now,

$$A_g = 3.793 \times E(B-V) = 2.223 \times E(g-i)$$

. Hence,

$$A_g = 2.223 \times [(g-i)_{obs} - \langle g-i\rangle_0] = 2.223 \times [(g-i)_{obs} + 0.27]$$

.

For the case of M31N2007-11d (Shafter et al. 2009), where data for both the above options are available, we get consistent answers: $g - i = 0.7$ mag at maximum suggests $A_g = 0.75$ mag and a Balmer decrement of 4.6 suggests $A_g = 0.65$ mag.

If neither a color at maximum nor a spectrum at late-time is available, we use the average line-of-sight extinction to the host galaxy using the Schlegel maps. The uncertainty in extinction calculation significantly contributes to the uncertainty in the peak magnitude.

We note here that for the case of P60-M82OT-081119, the light curve was unusually red for a nova and the extinction correction may be overestimated.

3.3.2 Rate of Decline

The heterogenity in nova light curves suggests that a single parameter may not characterize the decline well. Traditionally, the time to decay from peak by one magnitude (t1), two magnitudes (t2) or three magnitudes (t3) is used. For several novae (e.g., M31N2007-10a, M31N2008-08c, M31N2008-11a), the decline is more or less linear and t1 can be approximated as half of t2. For some novae (e.g., M31N2008-10b), the light curve behavior is more complex and this simplification is not applicable. In Table 3.4, we see that t2 values (where available) are sometimes larger and sometimes smaller than twice the t1 value.

We note here that we did not have data to measure the decline of the nova in NGC 891 and hence it is excluded from further MMRD analysis.

3.3.3 Rate of Rise

Given the cadence of P60-FasTING, we were able to catch several novae on the rise. We define the rate of rise as the average slope between first detection and peak detection and summarize in Table 3.4. We find a wide range of rise-times, from $> 1.8\,\mathrm{mag\,day^{-1}}$ (e.g., M31N2008-11a) to $0.2\,\mathrm{mag\,day^{-1}}$ (e.g., M31N2008-09a). It is not clear how previous determinations of the MMRD in the literature dealt with the uncertainty in the peak magnitude due to inadequate coverage. Especially since previous surveys likely had a relatively slower cadence, missing the peak may be a substantial source of error. Slower cadence and/or shallower depth would correspond to a weaker constraint on the rise time of the nova. Due to gaps on account of weather, some of the P60 light curves have constraint weaker than

0.1 mag day^{-1} on the rate of rise. Hence, we do not use the lightcurves of P60-M81OT-080926 or P60-M82OT-080429 for subsequent analysis of the MMRD relation.

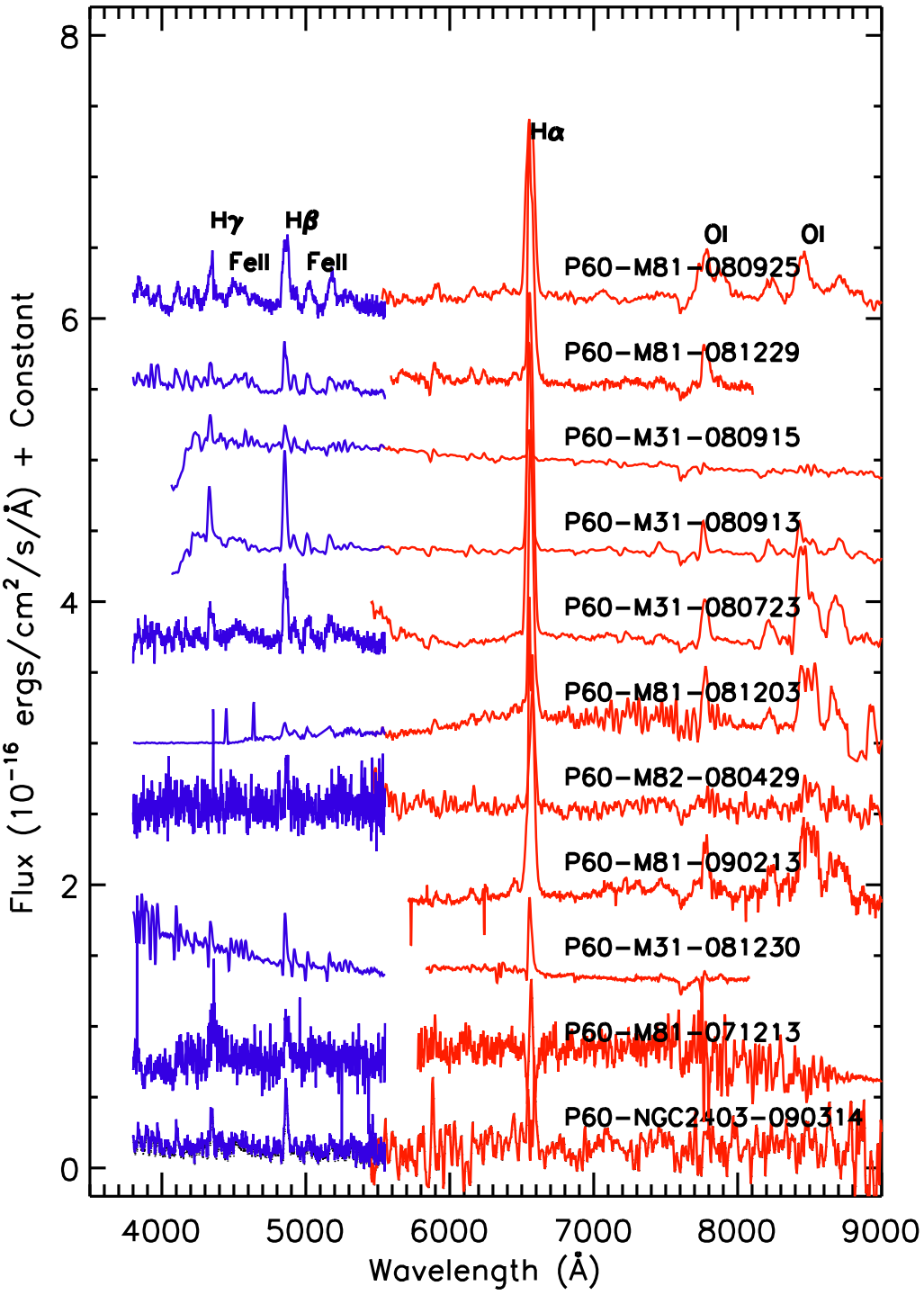

Figure 3.10 Optical spectra of P60-FasTING novae. Majority are Fe II class. Note that they have been arbitrarily offset along the y-axis for clarity.

Table 3.3. Spectroscopic Observations of P60-FasTING Novae

Nova	Spectroscopy Date	Telescope	Instrument	Classification	Observer
P60-NGC2403-090314	2009 Mar 20.145	P200	DBSP (Oke & Gunn 1982)	Fe Class?	Kasliwal,Ellis
P60-M81-090213	2009 Feb 18.510	Keck I	LRIS (Oke et al. 1995)	Fe Class	Ofek
P60-M81-081229	2008 Dec 31.40	P200	DBSP (Oke & Gunn 1982)	Fe Class	Rau,Salvato
P60-M31-081230	2008 Dec 31.104	P200	DBSP (Oke & Gunn 1982)	Fe Class	Rau,Salvato
P60-M81-081203	2008 Dec,4,5,16	P200,Gemini	DBSP,GMOS-N (Hook et al. 2004)	Fe Class	Kasliwal
P60-M81-080925	2008 Sep 29.51	P200	DBSP (Oke & Gunn 1982)	Fe Class	Quimby
P60-M31-080915	2008 Sep 20.2	HET	LRS (Hill et al. 1998)	Fe Class	Shafter
P60-M31-080913	2008 Sep 22.4	HET	LRS (Hill et al. 1998)	Fe Class	Shafter
P60-M31-080723	2008 Aug 1	P200	DBSP (Oke & Gunn 1982)	Fe Class	Ofek
P60-M82-080429	2008 May 2.28	P200	DBSP (Oke & Gunn 1982)	···	Cenko
P60-M81-071213	2007 Dec 15.565	Keck	LRIS (Oke et al. 1995)	···	Ofek

Table 3.4. Characteristics of P60-FasTING Novae

Nova	Balmer Decrement FHα/Hβ	Spectral Phase	Color at Peak $g-i$(mag)	Extinction A$_g$(mag)	Rate of Rise mag day^{-1}	Abs-Mag M$_g$(mag)	t1 days	t2 days
P60-NGC2403-090314	5.0	Nebular	···	0.8	1.3	−9.0	3.3	>6
P60-M82-090314	···	···	−0.3	0.6	>1.2	−8.5	2.4?	>3.3
P60-M81-090213	···	Nebular	0.7	2.2	0.2	−9.9	5?	>10.9
P60-M31-081230 (2008-12b)	···	···	−0.17	0.24	0.6	−7.5	12.3	
P60-M81-081229	2.4	Near-Max	0.1	0.90	>0.1	−8.7	2.9	···
P60-M81-081203	···	···	−0.03	0.53	0.7	−8.0	7.5?	>23
P60-M82-081119	···	···	0.98	2.8	0.6	−10.7	4.0	···
P60-M81-081027	···	···	···	0.3	0.2	−7.6	4.0	···
P60-M81-080926	1.4	Near-Max	-0.2	0.13	···	−8.5	8.9	14.0
P60-M31-080915 (2008-09c)	1.4	Near-Max	−0.72	0.24	0.4	−7.8	9.1	16.6
P60-M31-080913 (2008-09a)	2.5	Near-Max	−0.30	0.24	0.2	−6.8	6.3	16.0
P60-M31-080723 (2008-07b)	14.3	Nebular?	−0.20	2.5	0.2	−7.6	5.0	12.0
P60-M82-080429	6.3	Nebular?	···	1.2	···	−8.5	8.1	···
P60-M81OT-071213	3.8	Nebular?	0.5	0.4	>0.6	−7.8	1.0	···
2007-10a	···	···	···	>0.24	>1.2	−7.0	4.1?	8.6
2007-11f	···	···	−0.16	0.24	>0.1	−5.1	5.0	>8.0
2007-12b	···	···	···	>0.24	>0.6	−6.3	3.5	>5.0
2008-08c	···	···	···	>0.24	0.3	−7.5	11.0	26.3
2008-10b	···	···	−0.58	>0.24	0.2	−6.5	6.0	12.3?
2008-11a	···	···	0.41	1.5	>1.8	−7.7	2.9	7.5

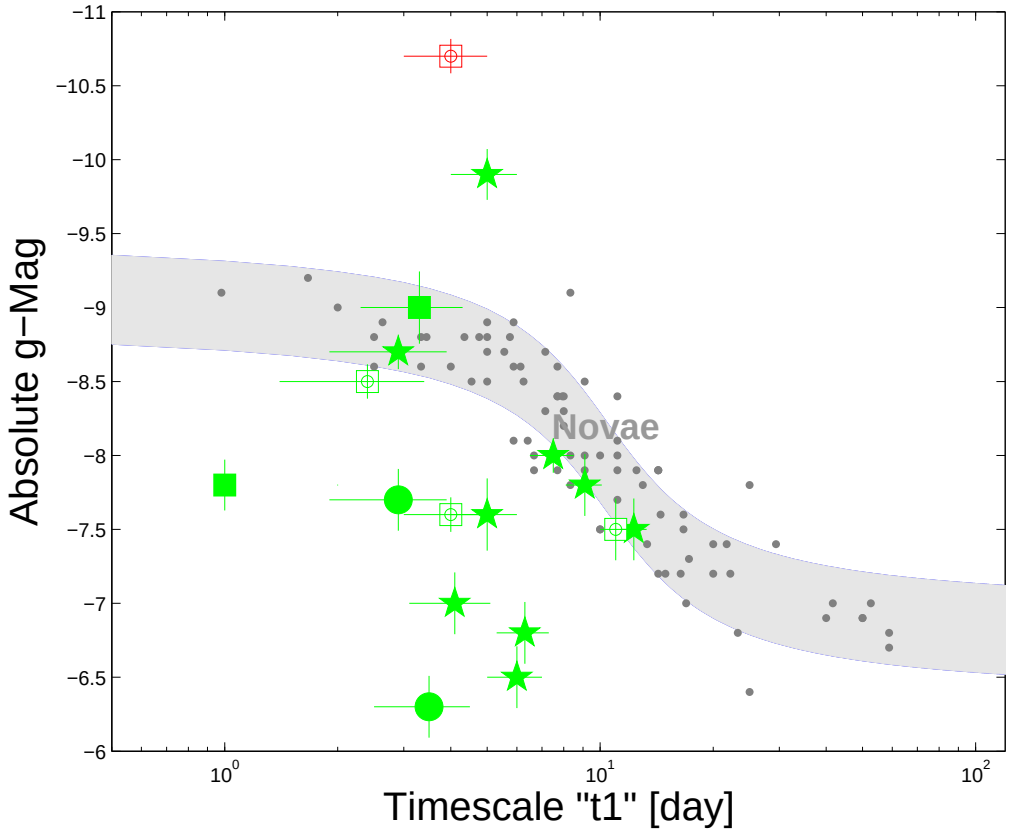

Figure 3.11 Maximum magnitude (absolute g-band) versus rate of decline (time to decay from peak by 1 mag). Gray region denotes the della Valle & Livio (1995) MMRD relation. The dark gray dots denote the nova sample used by della Valle & Livio (1995) — we derived t1 by dividing t2 by two and we converted from V-band to g-band assuming the colors of an A5V star (Shafter et al. 2009). The P60-FasTING sample is shown with symbols that denote spectral type — Fe II class (star), He/N class (circle), spectrum with no prominent features for classification (squares) and no spectrum (empty square).

3.3.4 Spectral Classification

For spectroscopy the primary analysis was to classify the novae by their spectra. The taxonomy of novae were laid out by Payne-Gaposchkin (1964) and McLaughlin (1960). The most prominent feature in all classical novae is Balmer emission. Williams (1992) propose that there is a two-component structure of the emitting gas — discrete shell and continuous

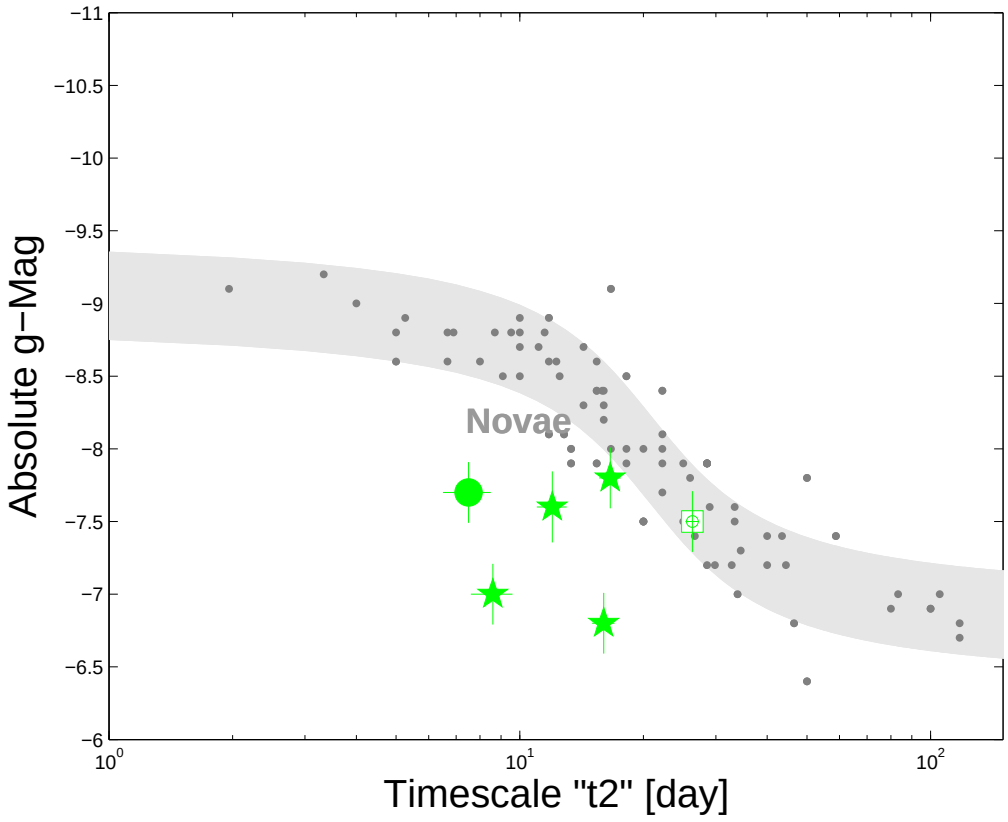

Figure 3.12 Maximum magnitude (absolute $g-$band) versus rate of decline (time to decay from peak by 2 mag). Only the six novae (P60-M31OT-080915, P60-M31OT-080913, P60-M31OT-080723, M31N2007-10a, M31N2008-08c,M31N2008-11a) with the best sampled light curves are shown. Symbols denote spectral type as in Figure 6.1.

wind. If the wind mass-loss rate is low, the effective photosphere is smaller, the radiation temperature is higher and the level of ionization of the shell is higher, resulting in a shell-dominated He/N spectrum. If the wind mass-loss rate is high, it results in a wind-dominated Fe II spectrum.

Thus, classical novae are divided into two principal families — the "Fe" class (dominated by Fe II lines, often low velocity and showing P-Cygni profiles) and the "He/N" class (dominated by He and N lines, often high velocity and flat or jagged-topped profiles). These evolve into nebular spectra with four classes based on the prominent forbidden lines — standard (e.g., [N II], [O II], [O III]), neon (e.g., [Ne V], [Ne III]), coronal (e.g., [Fe X])

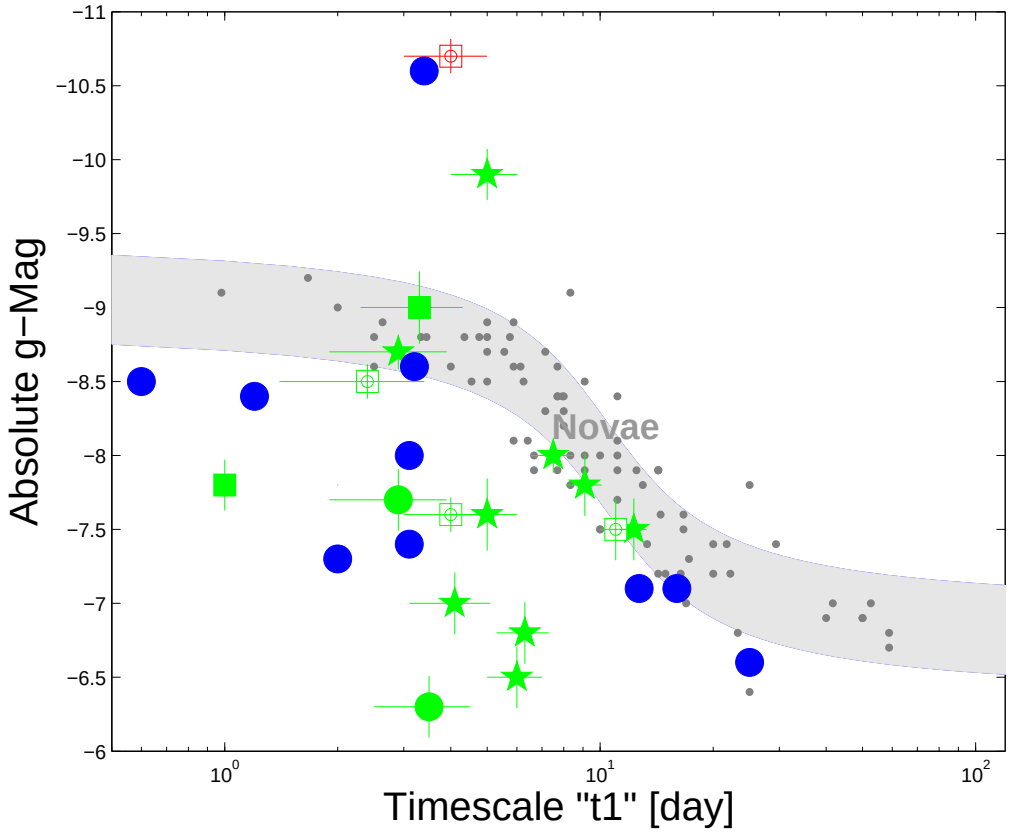

Figure 3.13 Comparison of the P60-FasTING nova sample (green symbols) with the Galactic recurrent novae (blue circles, data from Smartt (2009)). Symbols denote spectral type as in Figure 6.1.

or no forbidden lines. The Fe class novae are expected to evolve into standard or neon nebular spectra. The He/N class are expected to evolve into neon, coronal or no forbidden line spectra. Some novae are classified as "hybrid" as they start out with high velocity Fe II features and quickly evolve into showing He/N features (e.g., V745 Sco, V3890 Sgr, M31N2008-11a).

Majority of the P60-FasTING spectra show clear permitted lines from Fe II (42), Fe II (37,38) and O I. The line velocities are low and typical Gaussian FWHM are $< 2500\,\mathrm{km\ s^{-1}}$ with the exception of P60-M81-080925 where H_α velocity is $3000\,\mathrm{km\ s^{-1}}$. P60-NGC2403-090314 shows weak Fe II(42) and weak P-Cygni profiles in Balmer lines and can tentatively also be classified as Fe II class. P60-M81-071213 and P60-M82-080429 have very low SNR

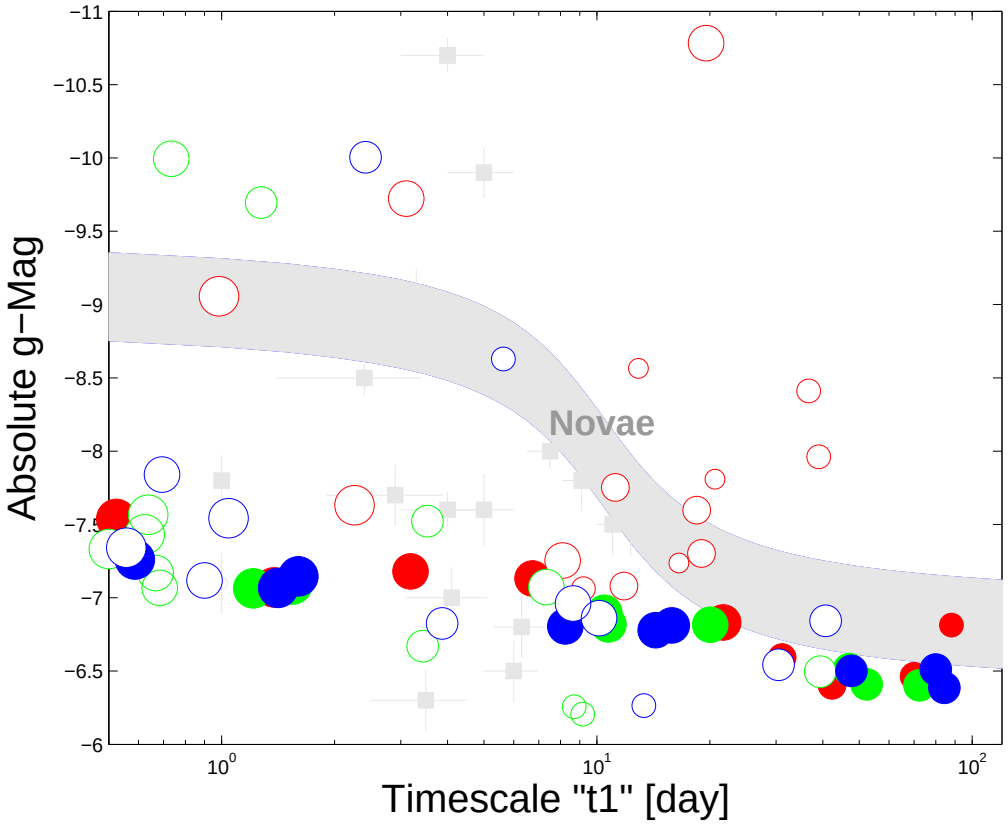

Figure 3.14 Theoretical results of Yaron et al. (2005) over a wide range of nova parameters — we use the colors of an A5V star to convert L4max to M_g and approximate t1 as $t_{ml}/3$. The size of the symbol is proportional to the mass of the white dwarf. The color of the symbol denotes temperature — 10 million K (red), 30 million K (green), 50 million K (blue). Empty circles denote lower accretion rate in the range $10^{-12.3}$–$10^{-10} M_\odot yr^{-1}$ and filled circles denote higher accretion rate in the range 10^{-9}–$10^{-6} M_\odot yr^{-1}$. Note that the density of circles is unrelated to the relative populations.

and no feature other than the Balmer lines are detected, hence, we cannot classify them. Multiple spectra of P60-M81-081203 were taken — initially, the spectra show a featureless continuum (obtained a few days prior to maximum light) and later (about a week after maximum light), evolved to show Balmer lines, Fe II (42), O I. We summarize spectral classifications in Table 5.1. For four novae in M31, other groups obtained spectra and we summarize their classification in Table 3.2.

3.4 Discussion

In comparison to traditional nova searches, P60-FasTING was designed as a faster cadence and deeper survey. Weather-permitting, galaxies in the sample were imaged every night to a mean depth of Gunn-$g < 21$ mag. Hence, P60-FasTING was sensitive to transients that are less luminous and evolve faster than classical novae.

Given that our light curves are well-sampled, and we have spectra or color measurements to correct for extinction, we can securely measure both the maximum magnitude and the rate of decline. To our surprise, as demonstrated in Figure 6.1, we find that the P60-FasTING nova sample is evidently inconsistent with the MMRD relation (della Valle & Livio 1995).

In Figure 6.1, the decay time is measured as the time to decay by one magnitude. To test whether the apparent photometric diversity is consistent with the MMRD over a longer timescale, we plot the time to decay by two magnitudes in Figure 3.12. Furthermore, we restrict this to the sub-sample of six classical novae in M31 with the best-sampled light curves (see lightcurves of P60-M31OT-080915, P60-M31OT-080913, P60-M31OT-080723, M31N2007-10a, M31N2008-08c, M31N2008-11a in Figure 3.5 and Figure 3.8). Even this sub-sample does not obey the MMRD relation. This scatter is larger than the ± 0.8 mag predicted on theoretical grounds by Shara (1981).

Despite the atypical photometric signature, the P60-FasTING nova sample shows no spectroscopic peculiarities. In Figure 6.1, the symbols indicate the spectral class — majority are Fe II class (stars), a couple are He/N class (circles), some have spectra with no prominent features for classification (filled squares) and a few have no spectra (empty squares).

We could hypothesize that some of the P60-FasTING novae are not classical but recurrent (classical novae which recur on a timescales shorter than a century) since recurrent novae are also known not to obey the MMRD relation. Recurrent novae are expected to occur in the most massive white dwarfs with high accretion rates. A small amount of mass accreted on a short timescale is sufficient to trigger thermonuclear runaway. Recently, Smartt (2009) compiled all available photometry over the past century on the ten recurrent novae in our galaxy — overplotted to compare with the P60-FasTING sample in Figure 3.13.

There are three ways to test the recurrent nova hypothesis. First, spectra of recurrent novae have high velocities and belong to either He/N or hybrid class (e.g., V3890 Sgr, V745

Sco, V394 CrA in Williams 1992 and Williams et al. 1994). We find that majority off the P60-FasTING novae do not share the spectroscopic properties of recurrent novae. P60-FasTING novae mostly belong to the Fe II class and have low velocities. Second, recurrent novae are often a few magnitudes brighter than classical novae at quiescence. Smartt (2009) suggests that recurrent novae range from $-4.1 < M_V < 3.2$ and classical novae range from $1.1 < M_V < 7.0$ at quiescence. Given the distance modulus to these galaxies, this test is within reach of 10-m class telescopes and easy with HST (e.g., see Bode et al. 2009). Third, the unambiguous test of whether an eruption is recurrent is to continue to monitor these galaxies for the next few decades until another eruption is witnessed.

In order to decipher the nature of this new sub-class of novae we turn to the fundamental physics of classical novae. The physics is governed by four parameters — mass of the white dwarf, temperature, accretion rate and composition. The MMRD relation is explained with the mass of the white dwarf being the single, dominant parameter. Perhaps, the P60-FasTING sample of faint and fast novae can be explained based on an unexplored region of this four-parameter phase space? Could some P60-FasTING novae come from hot and massive white dwarfs? If it is hot, then the thermonuclear runaway would not be as explosive and thus, the peak luminosity would be fainter. Also, the higher temperature would result in a smaller amount of envelope mass being sufficient to trigger thermonuclear runaway and thus, the timescale would be faster.

Recent theoretical efforts have explored nova diversity (e.g. Townsley & Bildsten 2004, Shen & Bildsten 2009, Epelstain et al. 2007, Jose & Hernanz 1998, Scott 2000). Yaron et al. (2005) present an extended grid of nova models to explore a wider parameter space (in mass, temperature and accretion rate) than traditionally explored for classical novae subject to physical constraints (such as conditions for thermonuclear runaway). We summarize the results of the variety of models they run in Figure 3.14. Some hot and massive white dwarfs with high accretion rates can result in a faint and fast nova population consistent with the P60-FasTING sample. Indeed, Yaron et al. (2005) predict the existence of remarkably small amplitude novae across the entire span of decay rates.

Finally, we note that more than half of the P60-FasTING nova sample is inconsistent with the MMRD. This suggests that faint and fast novae are commonplace and cannot be explained by a rare type of white dwarf.

3.5 Conclusion

We conclude that P60-FasTING has uncovered classical novae in a new region in the luminosity-timescale phase space of optical transients. Classical novae span at least two orders of magnitude in time and two orders of magnitude in luminosity. Future surveys would have a large enough sample to meaningfully constrain the relative populations of classical novae in the different areas of phase space.

P60-FasTING was designed as a pilot project, to begin to set the stage for future projects such as Palomar Transient Factory (PTF[6], Law et al. 2009, Rau et al. 2009b, Rahmer et al. 2008), PanSTARRS (PS1[7]) and Large Synoptic Survey Telescope (LSST[8]). Both PTF and PS1 are now underway. PTF is looking at several nearby galaxies with a similar depth and cadence as P60-FasTING. Among nearby galaxies, PS1 day-cadence fields only cover M31 but are a couple of magnitudes deeper. LSST will be both deeper and faster cadence and cover the visible sky. P60-FasTING is only the trailblazer for the uncovering of a wealth of information about classical novae by near-future synoptic surveys.

We thank Marina Orio for discussion, in particular the suggestion that some of the faint novae may be recurrent novae. We thank A. Shafter, M. Shara, L. Bildsten and O. Yaron for valuable feedback. We are grateful to A. Becker for making his software `hotpants` and `wcsremap` available for public use. MMK thanks the Gordon and Betty Moore Foundation for the Hale Fellowship in support of graduate study. S.B.C. is grateful for generous support from Gary and Cynthia Bengier, the Richard and Rhoda Goldman Fund, and National Science Foundation (NSF) grant AST0908886. MMK thanks the Palomar Observatory staff for their help in maximizing the efficiency and image quality of the Palomar 60-inch. Some of the data presented herein were obtained at the W.M. Keck Observatory, which is operated as a scientific partnership among the California Institute of Technology, the University of California and the National Aeronautics and Space Administration. The Observatory was made possible by the generous financial support of the W.M. Keck Foundation. The authors wish to recognize and acknowledge the very significant cultural role and reverence that the summit of Mauna Kea has always had within the indigenous Hawaiian community. We are

[6]http://www.astro.caltech.edu/ptf

[7]http://pan-starrs.ifa.hawaii.edu

[8]http://www.lsst.org

most fortunate to have the opportunity to conduct observations from this mountain.

Chapter 4

Systematic Survey Design: CFHT-COVET & PTF-TILU

4.1 Introduction

Our understanding of the landscape of optical transients in the past century has been dominated by novae and supernovae. Novae and supernovae are relatively easy to find. Novae, although fainter than supernovae by factor of 1000, are abundant (20 galaxy^{-1} year^{-1}). Supernovae, although rarer than novae (0.01 galaxy^{-1} year^{-1}), are luminous and long-lived. To find explosions at least ten times fainter and faster than supernovae, we need a deeper and higher cadence search.

Telescope time is a zero sum game — both for discovery and follow-up. The design trade-off for discovery is between cadence and survey volume. Survey volume, in turn, depends on depth and either area (blind pointings) or number of galaxies searched (targeted survey). Most surveys have optimized two out of the four parameters. For example, the Lick Observatory Supernova Search (LOSS; Filippenko et al. 2001), chose depth and galaxies and searched thousands of galaxies to 19 mag at a slow weekly cadence. LOSS found several hundred supernovae in the local universe in the past decade. The Texas Supernova Search (TSS; Quimby 2006), chose cadence and area and searched a large area daily to a shallow depth of 17 mag. TSS found a rare class of luminous supernovae. The Supernova Legacy Survey (SNLS; Astier et al. 2006) chose depth and cadence and searched a small area of 4 deg^2 to 24 mag every few days. SNLS found a large number of Type Ia supernovae at high redshifts.

Since our goal was to study explosions fainter and faster than supernovae, it was clear that our best bet would be to target galaxies in the local universe. When I started my thesis, the rates for transients in the gap, both observational constraints as well as theoretical predictions, were uncertain by order(s) of magnitude. I worked on three deep and fast cadence surveys, scaling the number of galaxies by an order of magnitude each time.

In Chapter 3, we discussed the simplest search (P60-FasTING) which targeted ≈ 60 of the nearest and brightest galaxies at a < 1 day cadence and a depth of 21 mag for one year (April 2008 to March 2009). We learned that although this search yielded two dozen novae and two supernovae, it did not include enough galaxies to find transients in the "gap". Therefore, we decided to scale our search in two phases: CFHT-COVET (≈ 500 galaxies) and PTF-TILU ($\approx 10{,}000$ galaxies).

Lesson 1: Gap transients are rarer than supernovae. Several hundred (if not several thousand) galaxies will need to be searched to uncover them.

4.2 CFHT-COVET

Using the one square degree MegaCAM camera on the 3.6 m Canada France Hawaii Telescope (CFHT), we decided to undertake "Coma and Virgo Exploration for Transients" (COVET; PI Marten van Kerkwijk). We chose seven pointings of the Virgo Cluster (Figure 4.1) and three pointings of the Coma Cluster, since they are very dense nearby galaxy concentrations. To image 10 deg^2 and cycle through each pointing twice in a single filter (r-band), we needed a total of half hour nightly, including overheads. As Megacam was only available on CFHT during dark fortnights, we proposed for a total of 30 hours. Our program was top-ranked in semester 2009A[1] and this ensured that our half-hour block indeed got systematically queue-scheduled on every night that weather allowed.

4.2.1 Real-Time Pipeline

Given the exquisite image quality and fine pixel scale (0.18 arcsec pixel^{-1}) of Megacam, we were able to architect a transient discovery pipeline with a very high detection efficiency.

[1]During semester 2008A, we obtained some data as well but the cadence was very poor due to queue scheduling priorities. Nevertheless, the data served as a dry run to test our pipelines and demonstrate the feasibility of this search.

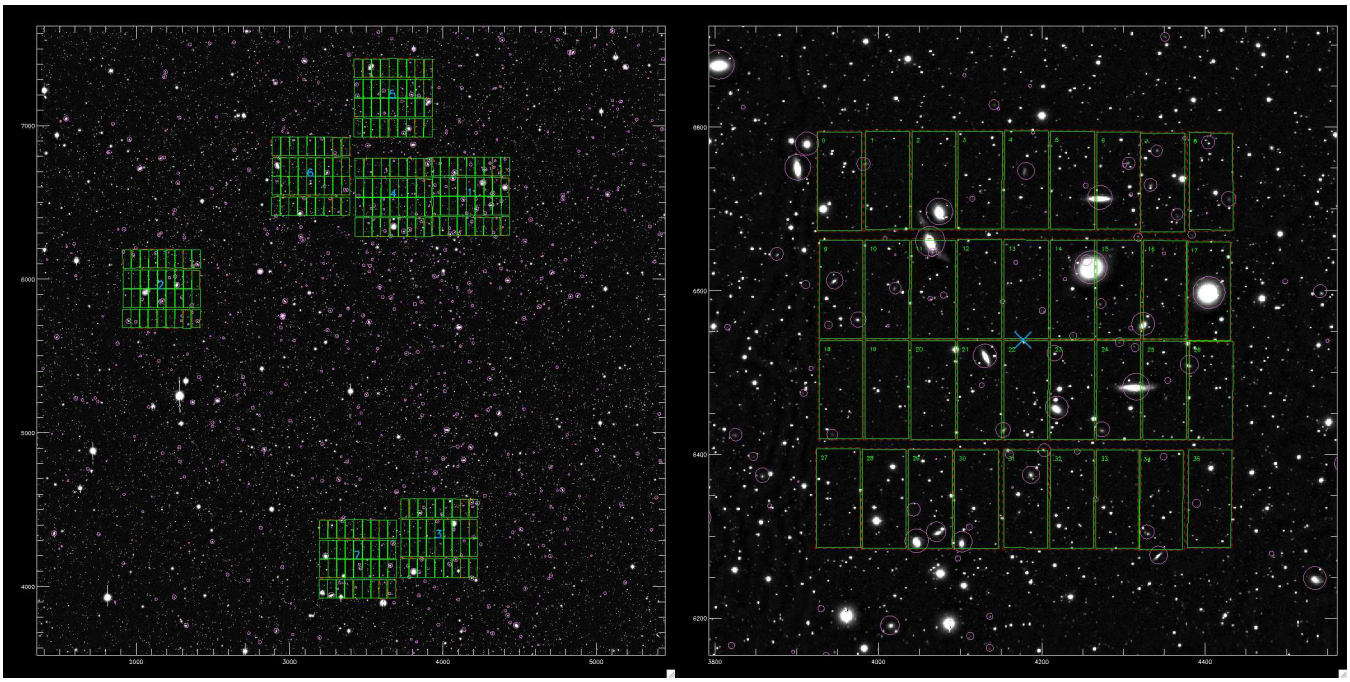

Figure 4.1 *Left:* Shown above are the seven pointings of the Virgo Cluster for our CFHT-COVET survey. Magenta circles denote galaxies in the Virgo Cluster. *Right:* Also shown is a zoomed-in view of one pointing.

We were able to probe deep down into the cores of bright galaxies and find faint transients. Furthermore, the data volume and low false positive rate allowed me to manually vet every single candidate transient by eye every morning.

Our real-time pipeline worked as follows:

1. *Ingestion and Characterisation.* Download detrended data the minute they are available on CFHT webpage, insert them into our local database, characterize them by computing seeing, zeropoint and sky, and solve for a precise World Coordinate System.

2. *Reference Image Subtraction.* Query our `postgres` database for appropriate reference image (deep combined image), precisely align the new image to it with sub-pixel accuracy, convolve the reference image point spread function (psf) and flux level to match the new image, and subtract the two. We implemented two codes developed by A. Becker[2] (`hotpants` and `wcsremap`) in our pipeline.

[2]http://www.astro.washington.edu/users/becker/

3. *Candidate Identification.* Find candidates on subtracted images, characterize their brightness and PSF, and insert them into database.

4. *Filtering.* Use multiple criteria to separate junk and moving objects from bonafide extragalactic transient candidates (e.g., filter based on whether the shape of the PSF of the candidate consistent with that of other stars in the same field)

5. *Cross-Correlation with Known Objects.* Query databases to check if there is a known asteroid, star or galaxy at that position (Minor Planet Center, Simbad, SDSS).

6. *Visualisation and Manual Vetting.* Post thumbnails of filtered candidates on a webpage for manual scanning. The webpages were generated on-the-fly (cgi scripts queried the database for candidates that fulfilled specified filtering thresholds).

7. *Follow-up.* Undertake multi-band photometry and spectroscopy of real transient candidates as necessary.

To measure the detection efficiency of our pipeline, we inserted over 100,000 fake sources with magnitudes between $18 < r < 24$ mag at random locations in images spanning a representative range in seeing conditions and galaxy surface brightness. Then, we ran these images through all the steps outlined above and checked how many sources were recovered (Figure 4.2). We found that even for an underlying host galaxy surface brightness of 18 mag arcsec^{-2}, we recovered transients with $r \approx 22$ mag with 72% efficiency and $r \approx 20$ mag with 80% efficiency. At the easier low surface brightness end, our efficiency was 90% (where 7% of the missing 10% was due to imperfect overlap between the new image and reference image).

4.2.2 Discoveries

The net result was that with a very modest investment of telescope time (30 hours), we found ≈ 140 transients. We even found a nova and supernova on the same chip in the same exposure (see Figure 4.3). The majority of transients were supernovae and active galactic nuclei in galaxies that were likely at distances much further than the targeted nearby cluster. We also found two dozen transients in the Virgo Cluster which were consistent with classical novae given their peak luminosity and light curves. The locations of several

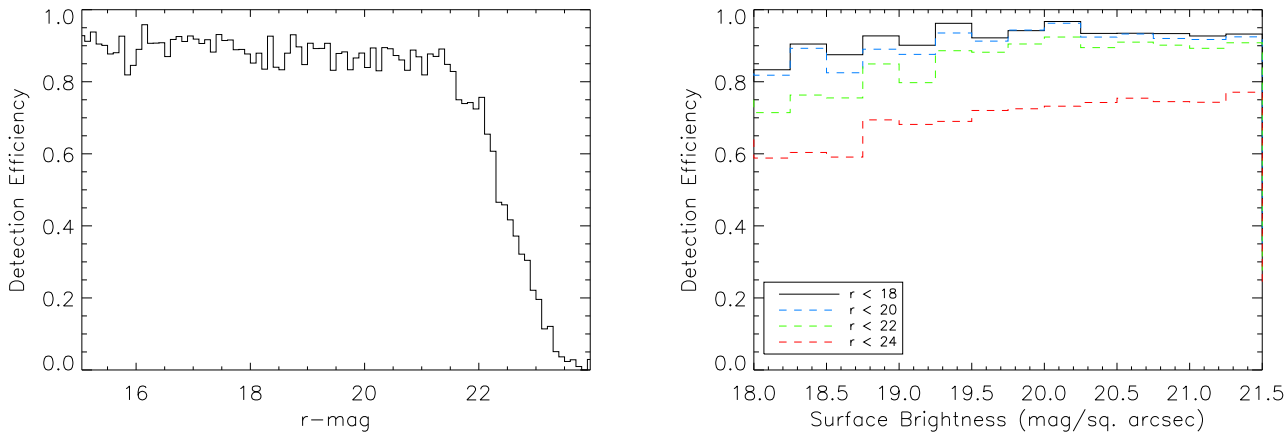

Figure 4.2 *Left:* Detection efficiency as a function of magnitude of transient. Over a range of seeing and background surface brightness conditions, we were able to recover 75% of simulated transients as faint as r≈22. *Right:* Detection efficiency as a function of underlying surface brightness of host galaxy. We could recover 72% of transients as faint as 22 mag buried under 18 mag arcsec^{-2}.

of these novae was in-between galaxies in regions of low surface brightness. For example, comparing against a map of the surface brightness of the Virgo core (Mihos et al. 2005), the locations of COVET-090420A, COVET-090423B and COVET-090423C corresponded to very low surface brightness of 23.5, 22 and 23 mag arcsec^{-2} respectively. Since 15% of the mass is expected to be in the intergalactic medium, it is not surprising that we have three inter-galactic novae.

Unfortunately, the CFHT-COVET search did not yield any new transients in the luminosity gap between novae and supernovae. However, the systematic nature of the search placed strict constraints on the rates of these events. COVET surveyed a volume at the distance of Virgo of $9.5 \times 10^{10}\,\mathrm{L}_{\odot}$-yr and at the distance of Coma of $4.4 \times 10^{11}\,\mathrm{L}_{\odot}$-yr. Therefore, it constrained the rates of transients on a timescale longer than 1 day and brighter than -9 mag to $< 7.9 \times 10^{-12}\,\mathrm{L}_{\odot}^{-1}\,\mathrm{yr}^{-1}$. COVET also constrainted the rates of transients on a timescale longer than 1 day and brighter than -13 mag to $< 1.7 \times 10^{-12}\,\mathrm{L}_{\odot}^{-1}\,\mathrm{yr}^{-1}$. For comparison, the rates of supernovae are roughly $6 \times 10^{-12}\,\mathrm{L}_{\odot}^{-1}\,\mathrm{yr}^{-1}$ (Mannucci et al. 2005).

We needed a survey that probed a significantly larger survey volume to find "gap" transients. To build survey volume in the local universe, one magnitude in depth is equivalent

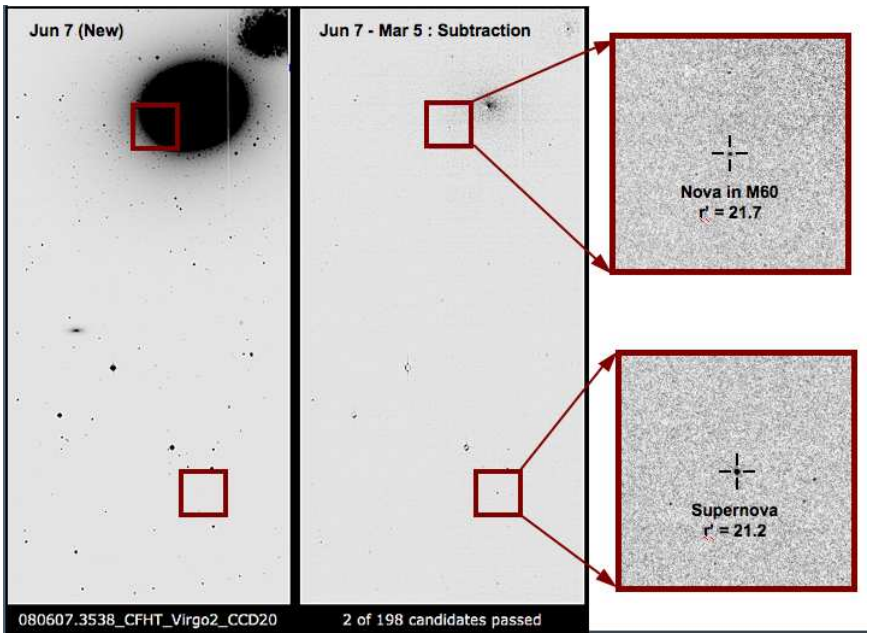

Figure 4.3 We discovered both a classical nova as well as a supernova on one of 48 chips in a single 60 s exposure with the MegaCAM camera on the CFHT.

to a factor of four in areal sky coverage. However, the follow-up challenge (especially spectroscopy) is formidable if the transients are faint. Despite Keck and Palomar Target Of Opportunity programs, we were able to spectroscopically classify only a handful of COVET transients. Therefore, we needed a wide-angle survey that surveyed thousands of galaxies in the local universe at a rapid cadence.

Lesson 2: Follow-up is key. The depth of the survey should be chosen to match the follow-up capabilities.

4.3 PTF-TILU

The Palomar Transient Factory (PTF[3]; Law et al. 2009; Rau et al. 2009b; Rahmer et al. 2008) was designed with a single dedicated goal of systematically charting the transient sky. PTF has two ongoing major experiments: a 5 day Supernova Cadence[4] and a 1 day Dynamic Cadence. My thesis project, "Transient in the Local Universe" (TILU) allowed me to design the "Dynamic Cadence" experiment.

[3]PI Shri Kulkarni; http://astro.caltech.edu/ptf

[4]In 2011, the supernova cadence is set to 3 day.

We chose a 1 day cadence[5] so as to be more sensitive to short timescale transients relative to previous supernova searches (typical cadence of a week to ten days). We chose a depth of 21 mag (60 s exposure on the Palomar 48-inch) to facilitate timely spectroscopic follow-up. This flux limit constrained our sensitivity to transients with a luminosity lower than that of supernovae to 200 Mpc. Therefore, to maximize the odds of finding rare transients, we would need to carefully optimize pointings on nearby galaxies and clusters.

4.3.1 Catalog of the Local Universe

First, I compiled a catalog collating all existing galaxy databases including NASA/IPAC Extragalactic Database (NED)[6], Hyperleda[7] and Extragalactic Distance Database (EDD)[8]. It was necessary to combine data from these sources as there were galaxies/redshifts missing in each of these compilations. The total number of galaxies within 200 Mpc was 150,000. Of the 150,000 galaxies, sizes were available for 100,000 and integrated B-band luminosities for 140,000. Wherever available, I used distances based on Tully-Fischer, Faber-Jackson, or from the Tully model (EDD estimates were used for the nearest galaxies). Otherwise, I used kinematic velocity-based distances corrected for infall of the Local Group towards Virgo. B-band magnitudes are corrected for galactic extinction, internal extinction and k-correction wherever available. Size of a galaxy is measured out to the surface brightness contour of 25 mag arcsec^{-2}. The combined catalog still captured only 50% of the starlight at 200 Mpc (Figure 4.4). We need an all-sky spectroscopic survey down to 21 mag to be 100% complete. Given how crucial this catalog is, we are undertaking a narrow-band survey during full-moon nights with PTF to complete this catalog, starting in May 2011.

Next, leveraging the clumpiness of the local universe, I used a fine grid to choose the top 200 pointings that would maximize the amount of galaxy light. I maximized the galaxy light in seven logarithmic bins in distance (uniform bins in distance modulus). I also ensured that galaxies didn't fall on chip gaps or the one non-working CCD. The resulting set of pointings gave me a factor of four more light at 200 Mpc than an equivalent number of randomly

[5]We note here that due to challenges in scheduling the robotic telescope, only a small fraction of the planned Dynamic Cadence fields were actually observed at the 1 day cadence. We now have an improved scheduler and look forward to a more successful second year of operations.

[6]http://ned.ipac.caltech.edu

[7]http://leda.univ-lyon1.fr/

[8]http://edd.ifa.hawaii.edu

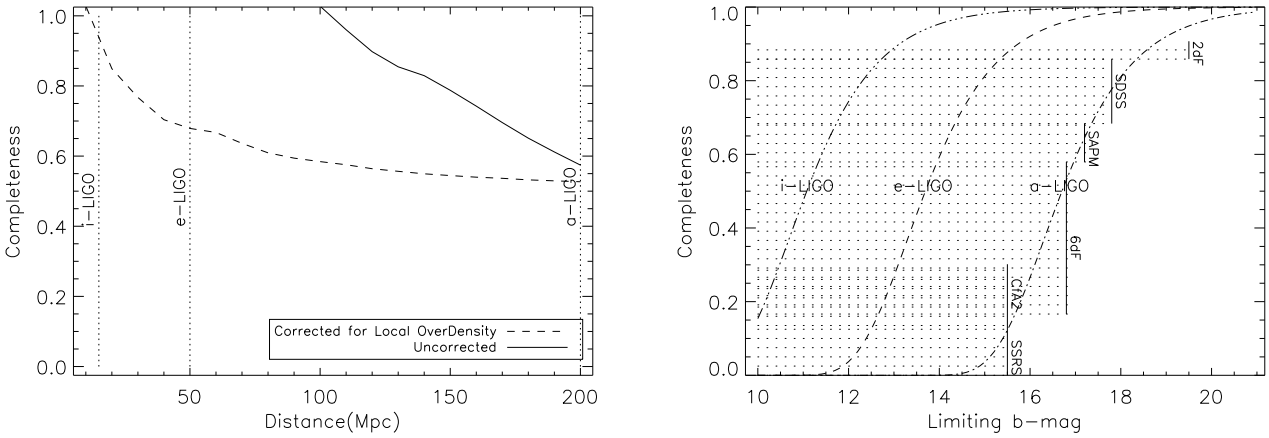

Figure 4.4 *Left:* Fraction of total theoretical light accounted for by galaxies in the catalog as a function of distance. A correction has been applied for the local overdensity by scaling the Schechter function by the observed luminosity brighter than $L_\star$. This correction is applied every 10 Mpc and is a factor of three at 10 Mpc and one at 200 Mpc. *Right:* Completeness of galaxy catalog as a function of apparent magnitude limit of survey. The largest surveys are represented by lines at the depth of the survey, the height of the line is proportional to the fraction of all-sky covered by survey. Unshaded region represents how much of the catalog is incomplete.

chosen pointings (Figure 4.5). Choosing nearby galaxies and galaxy clusters gave me the advantages of both a targeted and an untargeted survey. Since ≈ 100 pointings would be surveyed at any given time, this experiment was designed to be sensitive to transients whose rates were a few percent of the rate of supernovae (Figure 4.6).

4.3.2 Operations and Follow-Up

The design sensitivity of PTF-TILU inspired confidence. However, we also needed robust real-time operations and an arsenal of follow-up resources.

Our pipelines are completely automated and run in real-time. Discoveries from the Palomar 48-inch automatically trigger the Palomar 60-inch for multi-band follow-up during the same night without any human intervention. Automated pipelines on the 60-inch promptly return the photometry (with image subtraction relative to the Sloan Digital Sky Survey where available) to the central "Follow-Up Marshal" database. The PTF collaboration

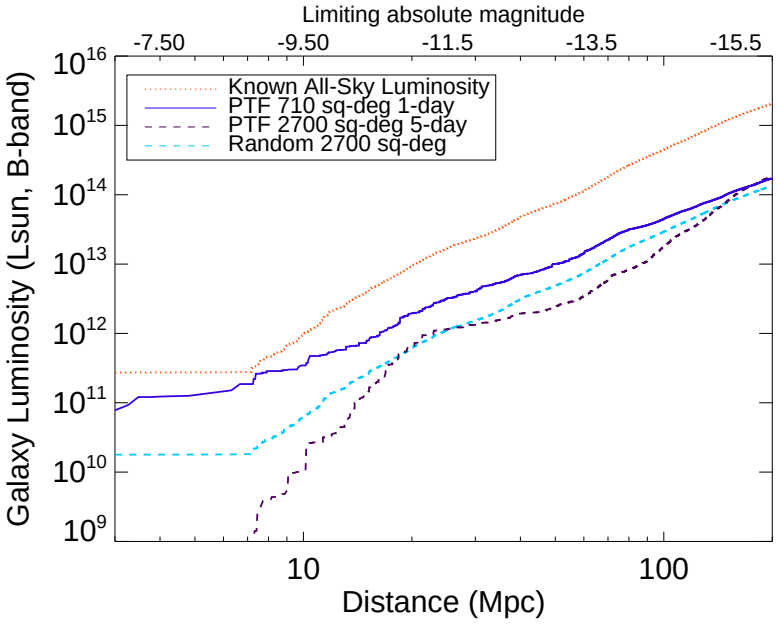

Figure 4.5 Cumulative galaxy light as a function of distance. The top axis denotes the limiting luminosity of a transient that PTF would be sensitive to at that distance. The known all-sky luminosity is shown in red, a random choice of 2700 sq deg is shown in light blue. The light in the PTF 1-day cadence experiment is shown in dark blue and the 5-day experiment is shown in purple. Note that although the 1-day experiment has a factor-of-four less area, the careful choice of galaxy light concentrations gives the same amount of light as the 5-day experiment.

---

then uses different selection criterion based on the data obtained from these two telescopes to trigger follow-up spectroscopy.

A major improvement over the CFHT-COVET pipeline described above is that PTF has an ongoing effort to completely automate the final step of manual vetting. We do this by improved machine learning algorithms as well as outsourcing the visualization step to citizen scientists via the supernova zoo portal [9]. While these efforts have been successful in netting the majority of transients, unfortunately, they are still incomplete in the especially challenging identification of faint transients buried inside bright galaxies. Therefore, I have been running a script that spatially cross-correlates the PTF discovery stream against the galaxies in this catalog (out to twice the radius of the 25 mag arcsec^{-2} contour, B_{25}). I

[9] http://supernova.galaxyzoo.org

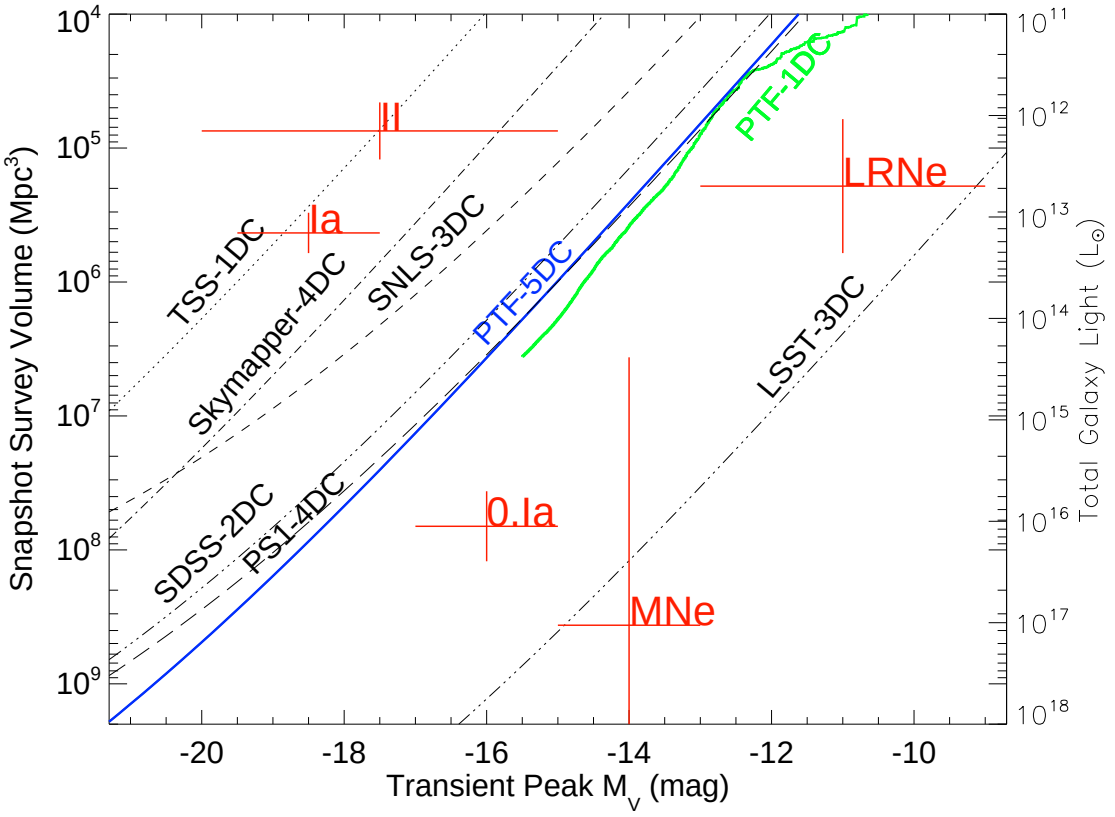

Figure 4.6 Volume probed by various surveys (in specified cadence period) as a function of transient absolute magnitude. Red plusses represent the minimum survey volume needed to detect a single transient event (the uncertainty in the y-axis is due to uncertainty in rates and the error in the x-axis represents luminosity range). Key: SDSS is the Sloan Supernova search, PS-MD is PanStarrs1 Medium Deep search, PTF-5DC is the 5-day cadence experiment and PTF-1DC is the Dynamic cadence experiment, LSST is the Large Synoptic Survey Telescope. Note that the design sensitivity of the PTF-1DC experiment is second only to LSST.

continue to manually vet this subset of PTF candidates daily for prompt follow-up.

The first and most critical step in follow-up was rapid response spectroscopy. Therefore, we applied for Target Of Opportunity (ToO) time on the Keck and Palomar telescopes. To hedge against weather and the unavailability of low resolution spectrographs when the moon is bright, we also applied for a Gemini program. The PTF collaboration has also been helpful in obtaining spectra of local universe candidates on classically scheduled nights. For multi-band follow-up, we have ToO programs on the *Swift* satellite (X-ray, UV) and *Expanded Very Large Array* (radio). As needed, we applied for time on the Hubble, Spitzer and Galex

space telescopes.

4.3.3 Discoveries

PTF obtained first light in December 2008, found its first supernova in March 2009 and was fully commissioned by July 2009. Unfortunately, the Station fire[10] shut down operations at Palomar mountain from August to November 2009. In just over a year of rolling operations, PTF has discovered and spectroscopically classified 1044 extragalactic transients (as of February 9, 2011). Of these, 270 transients were in the local universe ($z < 0.05$). We show the division of this group between core-collapse (59%) and thermonuclear (37%) supernovae in Figure 4.7. Of special note is the 4% unclassified slice. These are transients with no good match in libraries of supernova spectra. Case studies of some of these are discussed in the next few chapters.

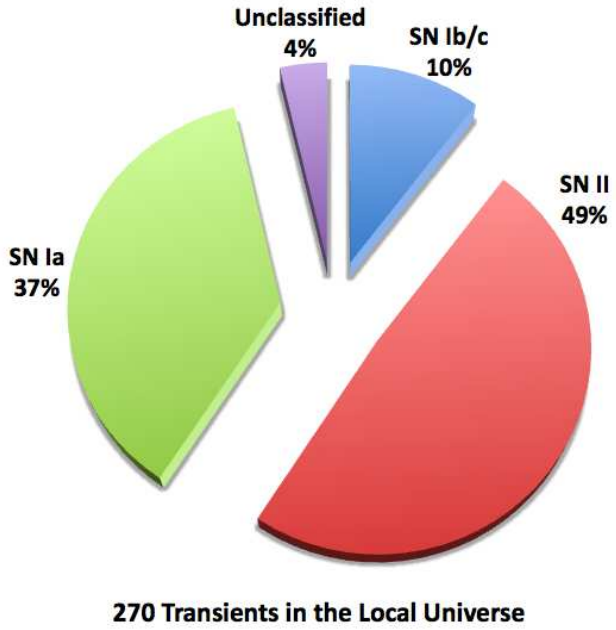

Figure 4.7 The Palomar Transient Factory has discovered 270 transients in the local universe (z<0.05). Of these, 4% have unclassified spectra, with no matches in supernova or nova libraries.

In Figure 4.8, we show the distribution of peak luminosities of PTF supernovae. SN 2007ax

[10]http://www.fs.fed.us/fire/station_fire_report.pdf

(discussed in Chapter 2) continues to be the recordholder for the faintest SN Ia. Only 16 out of 270 transients are fainter than −16 mag, i.e. 1.5%. Of these, the characteristics of 11 transients are consistent with extreme versions of hydrogen-rich core-collapse supernovae (e.g., PTF 10vdl, Gal-Yam et al. 2011); the new record-holder for the faintest Type IIP supernova is now PTF 10ehy (−13 mag). PTF 10aaxi has curious three-peaked Balmer line profiles and we are investigating this in more detail (Smith et al., in prep). PTF 10fqs and PTF 10acbp are members of a new class of explosions in the gap (discussed in Chapter 5). PTF 09dav and PTF 10iuv also appear to be yet another class of explosions in the gap (discussed in Chapter 7).

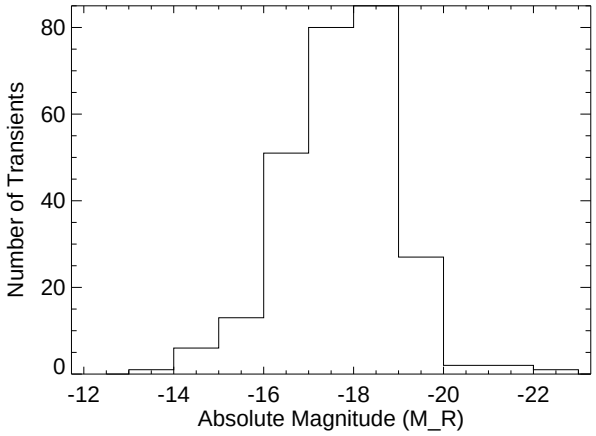

Figure 4.8 Histogram of peak R-band luminosities of PTF transients in the local universe. Note that of the 16 transients fainter than −16 mag, 11 are consistent with being faint analogs of core-collapse supernovae and 5 are peculiar transients whose physical nature is yet to be determined.

In conclusion, we have discovered multiple, distinct populations of transients in the gap. These transients are nothing like anything we have seen before and nothing like each other. It appears we have just begun to explore the tips of icebergs.

Chapter 5

A New Class in the Gap: Luminous Red Novae*

Mansi M. Kasliwal[1], Shri R. Kulkarni[1], Iair Arcavi[2], Robert M. Quimby[1], Eran O. Ofek[1], Peter Nugent[3], Janet Jacobsen[3], Avishay Gal-Yam[2], Yoav Green[2], Ofer Yaron[2], Derek B. Fox[4], Jacob L. Howell[4], S. Bradley Cenko[5], Io Kleiser[5], Joshua S. Bloom[5], Adam Miller[5], Weidong Li[5], Alexei V. Filippenko[5], Dan Starr[5], Dovi Poznanski[3,5], Nicholas M. Law[6], George Helou[7], Dale A. Frail[8], James D. Neill[1], Karl Forster[1], D. Christopher Martin[1], Shriharsh P. Tendulkar[1], Neil Gehrels[9], Jamie Kennea[4], Mark Sullivan[10], Lars Bildsten[11,12] , Richard Dekany[13] , Gustavo Rahmer[13] , David Hale[13] , Roger Smith[13] , Jeff Zolkower[13] , Viswa Velur[13] , Richard Walters[13] , John Henning[13] , Kahnh Bui[13] , Dan McKenna[13] & Cullen Blake[14]

[1] Cahill Center for Astrophysics, California Institute of Technology, Pasadena, CA, 91125, USA

[2] Benoziyo Center for Astrophysics, Faculty of Physics, The Weizmann Institute of Science, Rehovot 76100, Israel

[3] Computational Cosmology Center, Lawrence Berkeley National Laboratory, 1 Cyclotron Road, Berkeley, CA 94720, USA

[4] Astronomy and Astrophysics, Eberly College of Science, The Pennsylvania State University, University Park, PA 16802, USA

[5] Department of Astronomy, University of California, Berkeley, CA 94720-3411, USA

[6] Dunlap Institute for Astronomy and Astrophysics, University of Toronto, 50 St. George Street, Toronto M5S 3H4, Ontario, Canada

[7] Infrared Processing and Analysis Center, California Institute of Technology, Pasadena, CA 91125, USA

[8] National Radio Astronomy Observatory, Array Operations Center, Socorro, NM 87801, USA

[9] NASA-Goddard Space Flight Center, Greenbelt, MD 20771, USA

[10] Department of Physics, Oxford University, Oxford, OX1 3RH, UK

[11] Kavli Institute of Theoretical Physics, University of California Santa Barbara, Santa Barbara, CA 93106, USA

[12] Department of Physics, University of California Santa Barbara, Santa Barbara, CA 93106, USA

[13] Caltech Optical Observatories, California Institute of Technology, Pasadena, CA 91125, USA

[14] Department of Astrophysical Sciences, Princeton University, Princeton, NJ 08544, USA

Abstract

The Palomar Transient Factory (PTF) is systematically charting the optical transient and variable sky. A primary science driver of PTF is building a complete inventory of transients in the local Universe (distance less than 200 Mpc). Here, we report the discovery of PTF 10fqs, a transient in the luminosity "gap" between novae and supernovae. Located on a spiral arm of Messier 99, PTF 10fqs has a peak luminosity of $M_r = -12.3$, red color ($g - r = 1.0$) and is slowly evolving (decayed by 1 mag in 68 days). It has a spectrum dominated by intermediate-width Hα ($\approx 930\,\mathrm{km\,s^{-1}}$) and narrow calcium emission lines. The explosion signature (the light curve and spectra) is overall similar to that of M85 OT2006-1, SN 2008S, and NGC 300 OT. The origin of these events is shrouded in mystery and controversy (and in some cases, in dust). PTF 10fqs shows some evidence of a broad feature (around 8600 Å) that may suggest very large velocities ($\approx 10{,}000\,\mathrm{km\,s^{-1}}$) in this explosion. Ongoing surveys can be expected to find a few such events per year. Sensitive spectroscopy, infrared monitoring and statistics (e.g., disk versus bulge) will eventually make it possible for astronomers to unravel the nature of these mysterious explosions.

*A version of this chapter is published with the title "PTF10fqs: A Luminous Red Nova in the Spiral Galaxy Messier 99" in the *The Astrophysical Journal*, 2011, vol. 730, pp. 134 and is reproduced by permission of the AAS.

5.1 Introduction

Two reasons motivate us to search for transients in the local Universe (distance < 200 Mpc). First, the emerging areas of gravitational wave astronomy, high-energy cosmic rays, very high-energy photons, and neutrino astronomy are limited to this distance horizon either due to physical effects (optical depth) or instrumental sensitivity. Thus, to effectively search for an electromagnetic analog, understanding the full range of transient phenomena is essential. For instance, the electromagnetic counterpart to the gravitational wave signature of neutron star mergers is expected to be fainter and faster than that of supernovae (e.g., Metzger et al. 2010).

Our second motivation is one of pure exploration. The peak luminosity of novae ranges between -4 and -10 mag[1], whereas supernovae range between -15 and -22 mag. The large gap between the cataclysmic novae and the catastrophic supernovae has been noted by early observers. Theorists have proposed several intriguing scenarios producing transients in this "gap" (e.g., Bildsten et al. 2007a; Metzger et al. 2009; Shen et al. 2010; Moriya et al. 2010).

The Palomar Transient Factory[2] (PTF; see Rahmer et al. 2008; Law et al. 2009; Rau et al. 2009b) was designed to undertake a systematic exploration of the transient sky in the optical bands. One of the key projects of PTF is to build a complete inventory of transients in the local Universe. PTF has a "Dynamic" cadence experiment which undertakes frequent observations of fields, optimized for inclusion of galaxies in the local Universe. A description of the design sensitivity is given elsewhere (Kulkarni & Kasliwal 2009b). Here, we report on the discovery of PTF 10fqs, a transient in this "gap" between novae and supernovae.

5.2 Discovery

On 2010 April 16.393 (UT dates are used throughout this paper), the Palomar Transient Factory discovered an optical transient toward Messier 99 (M99; see Figure 5.1). Following the PTF discovery naming sequence, this transient was dubbed PTF 10fqs and reported via an ATEL (Kasliwal & Kulkarni 2010).

M99 (NGC 4254)[3], an Sc galaxy, is one of the brighter spiral members of the Virgo

[1] Unless explicitly noted, quoted magnitudes are in the R band.

[2] `http://www.astro.caltech.edu/ptf`

[3] `http://seds.org/messier/m/m099.html`

cluster. The recession velocity of the galaxy is about 2400 km s^{-1}. Over the past fifty years, three supernovae have been discovered in this galaxy: SN 1967H (Type II?, Fairall 1972), SN 1972Q (Type II; Barbon et al. 1973)[4], and SN 1986I (Type II; Pennypacker et al. 1989).

At discovery, the brightness of PTF 10fqs was $R = 20.0 \pm 0.2$ mag. There are no previous detections in PTF data taken on and prior to April 10. If located in M99, the absolute magnitude (for an assumed distance of 17 Mpc; Russell 2002) corresponds to $M_R = -11.1$ We concluded that the object could be (in decreasing order of probability) a foreground variable star, a young supernova, or a transient in the "gap". These possibilities can be easily distinguished by spectroscopic observations.

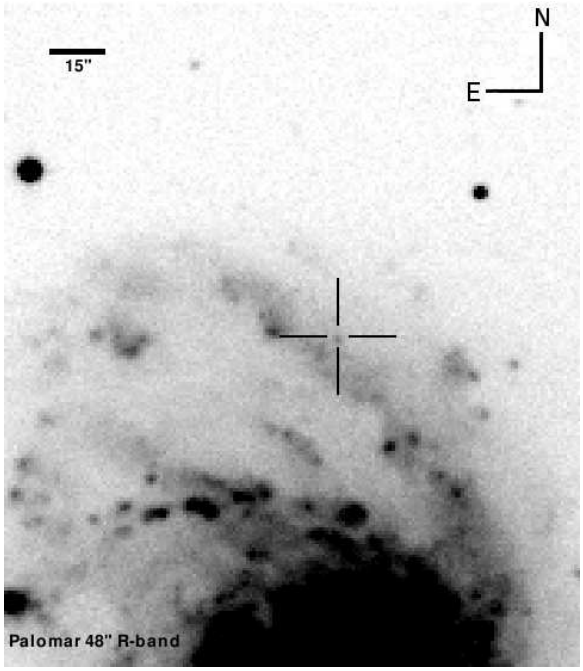

Figure 5.1 The discovery image of PTF 10fqs (obtained with the Palomar Oschin 48-inch telescope on 2010 Apr 16.393). The transient is marked by a cross and located at α(J2000) = $12^h18^m50.16^s$ and δ(J2000) = $+14°26'39.2''$. With respect to the host-galaxy nucleus, the transient is offset by $8.1''$ E and $99.9''$ N.

[4]Curiously, the reported position of SN 1972Q was only $3.6''$ from PTF 10fqs. We did a careful registration of the discovery image of SN 1972Q (Barbon et al. 1973) and PTF 10fqs and find that the offset is actually $11.0''$ E,$0.8''$ S.

5.3 Follow-Up Observations

5.3.1 Spectra

We triggered our Target-of-Opportunity (TOO) program on the 8-m Gemini-South telescope. On 2010 April 18.227, the Gemini Observatory staff observed PTF 10fqs with the Gemini Multi-Object Spectrograph (GMOS; Hook et al. 2004). The parameters for the observations were: R400 grating, order-blocking filter GG455_G039, and a 1.0″ slit. Two 10-min integrations centered on 6700 and 6800 Å were obtained. The two observations allowed for coverage of the gap between the chips. The package `gemini gmos` working in the `iraf` framework was used to reduce the data. The spectrum is shown in Figure 5.2.

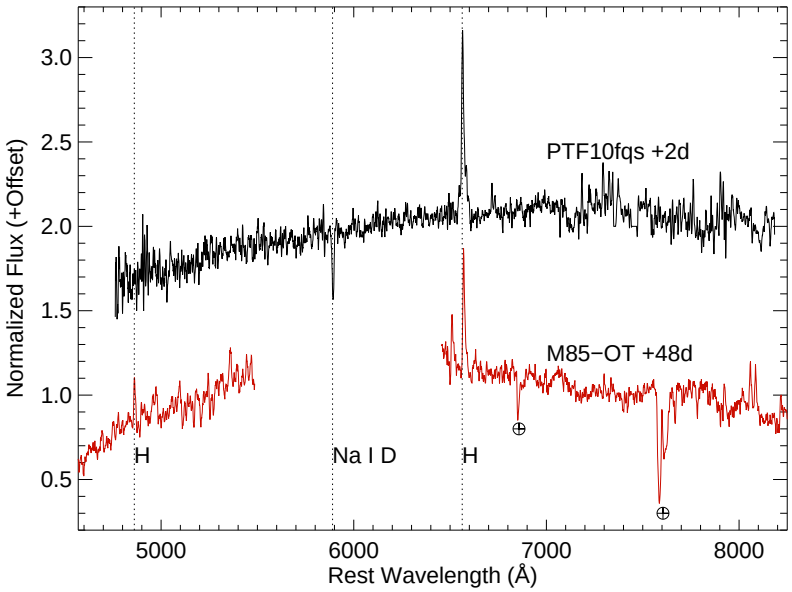

Figure 5.2 Gemini GMOS spectrum of PTF 10fqs (black) taken two days after discovery. The wavelength coverage is continuous over the range 4600 to 8800 Å. The most prominent emission feature is Hα. Plotted below for comparison, the spectrum of M85OT-2006-1 (red; Kulkarni et al. 2007)

The most prominent emission feature is an intermediate width (13 Å, 600 km s^{-1})[5] Hα line consistent with the recession velocity of the galaxy (2400 km s^{-1}; see below). Hβ was not detected. From this spectrum alone, we concluded that PTF 10fqs is in M99 and the

[5]The velocity quoted here is corrected for instrumental resolution and is measured as the Gaussian Full Width Half Maximum (GFWHM) of the emission line.

Table 5.1. Log of Spectroscopic Observations

Date (UT 2010)	MJD	Exposure	Facility	Grating/Grism
Apr 18.23	55304.23	2× 600 s	Gemini-S/GMOS	400
Apr 21.31	55307.31	2× 800 s	HET/LRS	360
Apr 25.29	55311.29	2× 600 s	HET/LRS	360
Apr 30.12	55316.12	2× 600 s	HET/LRS	360
May 3.28	55319.28	2× 600 s	HET/LRS	360
May 15.26	55331.26	3×600 s	Keck I/LRIS	831
May 15.26	55331.26	1×2000 s	Keck I/LRIS	300
May 15.31	55331.31	3×650 s	Keck I/LRIS	600

intermediate line width made it unlikely to be a supernova. PTF 10fqs appeared to be a transient in the "gap," and we initiated extensive multi-band follow-up observations.

We continued to monitor the spectral evolution with the Marcario Low-Resolution Spectrograph (LRS; Hill et al. 1998) on the Hobby Eberly Telescope[6]. We used the G1 grating, with a 2″ slit and a GG385 order-blocking filter, providing resolution $R = \lambda/\Delta\lambda \approx 360$ over 4200–9200 Å. Data were reduced using the `onedspec` package in the `iraf` environment, with cosmic-ray rejection via the `la_cosmic` package (van Dokkum 2001), and with spectrophotometric corrections applied using standard-star observations (specifically, BD332642).

On May 15, we also obtained relatively higher resolution spectroscopic observations and relatively better blue coverage with the Low Resolution Imaging Spectrograph (Oke et al. 1995) on the Keck I telescope. First, we used the 831/8200 grating centered on 7905 Å to get higher resolution spectra of the Calcium lines. On the blue side, we used the 300/5000 grism to cover Ca H+K lines. For higher resolution covering the Balmer lines, we used the 600/7500 grating (centered on 7201 Å) in conjunction with the 600/4000 grism.

The log of spectroscopic observations in given in Table 5.1. The spectral evolution is shown in Figure 5.3.

[6]Director's Discretionary Time, PI D. Fox

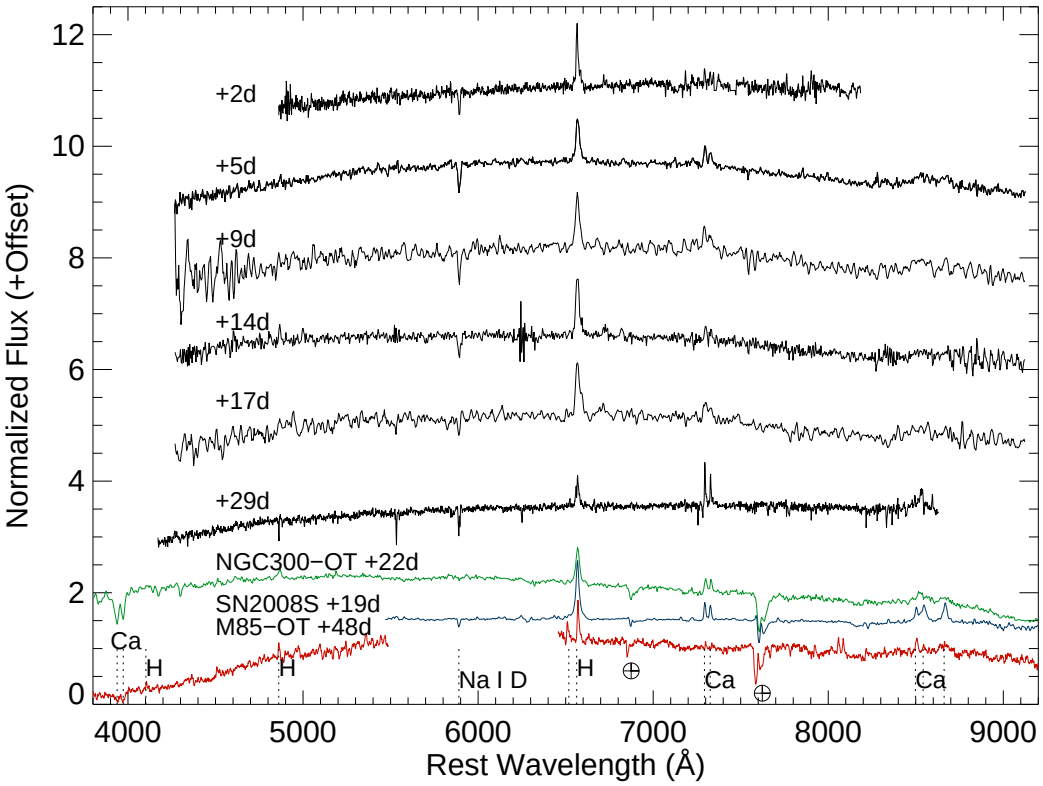

Figure 5.3 Spectra of PTF 10fqs at various epochs (phase in days is defined relative to discovery epoch). Also shown are spectra of NGC 300-OT (Bond et al. 2009), M85OT2006-1 (Kulkarni et al. 2007) and SN2008S (Botticella et al. 2009). The wavelength has been corrected for the recession velocity of each galaxy ($z = 0.0024$ for M85, $z = 0.008$ for M99, $z = 0.00048$ for NGC 300 and $z = 0.00016$ for NGC 6946).

5.3.2 Optical and Near-Infrared Imaging

Observations with the robotic Palomar 60-inch telescope (Cenko et al. 2006b) on April 20.4 confirmed that PTF 10fqs was rising ($r = 19.4 \pm 0.1$ mag) and red ($g - r = 1.0$ mag). We show the photometric evolution in *gri*-bands in Figure 5.4 and Table 5.6. On April 27.2, the light curve peaked at $r = 18.9 \pm 0.1$ mag corresponding to $M_r = -12.3$ (correcting for foreground Galactic extinction of E(B-V)=0.039; Schlegel et al. 1998b). Aperture photometry was done after image subtraction using a custom modification of the CPM algorithm, *mkdifflc* (Gal-Yam et al. 2004). Template images for subtraction and reference magnitudes for zeropoint computation were taken from the Sloan Digital Sky Survey (Abazajian et al. 2009).

Near-infrared images were obtained with the Peters Automated Infrared Imaging Telescope (PAIRITEL; Bloom et al. 2006a), and reduced by an automated reduction pipeline. We lack sufficiently deep template images, which are free of light from PTF 10fqs, to perform reliable image subtraction. Thus, we measure the flux from the source in a small circular aperture, removing the sky with a nearby background region, and adopt a systematic error of 0.2 mag in the J and H bands and 0.3 mag in K_s band. The values reported in Table 5.6 have been calibrated against the 2MASS system (Cohen et al. 2003).

5.3.3 Radio Observations

We observed PTF 10fqs with the EVLA on April 20.19–20.26 at central frequencies of 4.96 GHz and 8.46 GHz. We added together two adjacent 128 MHz subbands with full polarization to maximize continuum sensitivity. Amplitude and bandpass calibration was achieved using a single observation of J1331+3030, and phase calibration was carried out every 10 min by switching between the target field and the point source J1239+0730. The visibility data were calibrated and imaged in the *AIPS* package following standard practice.

A radio point source was not detected at the position of the transient. After removing extended emission from the host galaxy, the 3σ limits for a point source are 93 μJy and 63 μJy at 4.96 GHz and 8.46 GHz, respectively. At the distance of M99, this corresponds to $L_\nu < 2.1 \times 10^{25}$ erg s^{-1} Hz^{-1}. Comparing with the compilation in Chevalier et al. (2006), this upper limit is at the level of the faintest Type II-P (SN 2004dj; Beswick et al. 2005) and Type Ic (SN 2002ap; Berger et al. 2002) supernovae. As noted by Berger et al. (2009),

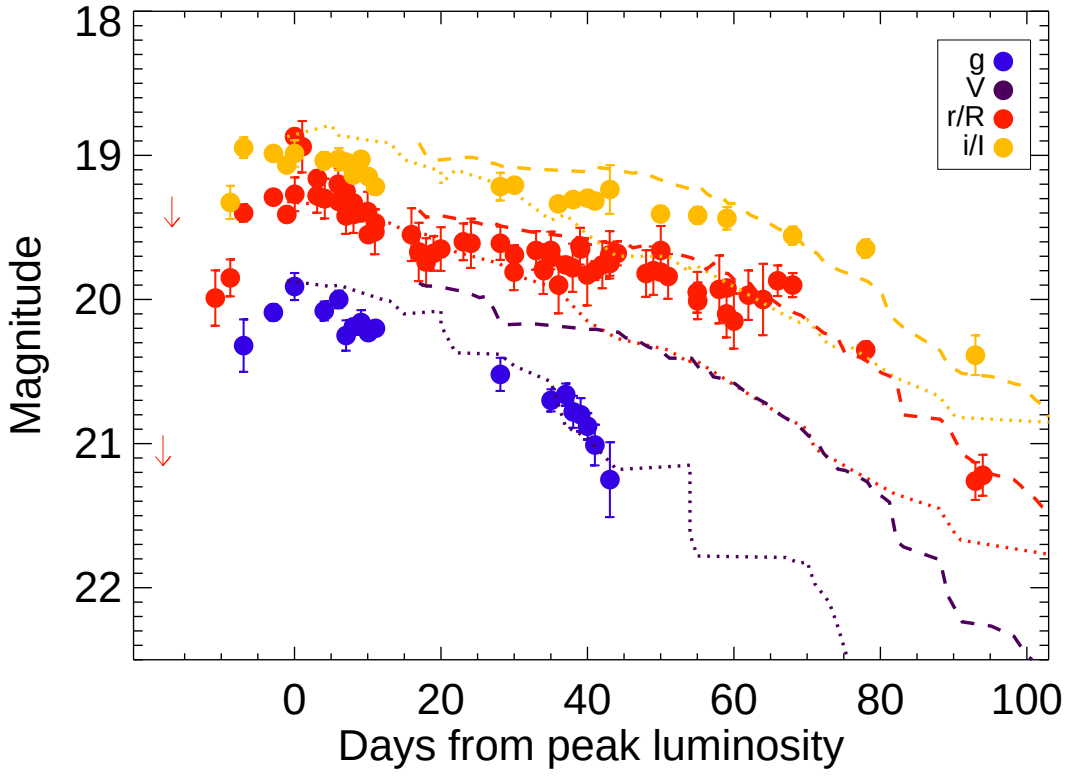

Figure 5.4 Multi-band light curve of PTF 10fqs obtained with the Palomar 48-inch (squares) and Palomar 60-inch (circles) telescopes. Upper limits are denoted by downward arrows. Note that the evolution is relatively faster in the g-band compared to r-band. Also shown for comparison are the VRI-band lightcurves of SN2008S (dotted; Botticella et al. 2009) and NGC300-OT (dashed; Bond et al. 2009). The light curves are shifted vertically by a constant (+3 mag for SN2008S and +5.2 mag for NGC300-OT) such that their R-band light curves are at the same level as the r-band light curve of PTF 10fqs.

Table 5.2. Broadband Measurements of PTF 10fqs

Date (UT 2010)	MJD	Filter	Magnitude/Flux	ν (Hz)	νF_ν (erg cm^{-2} s^{-1})	Facility
Apr 20.23	55306.23	4.96 GHz	<93 μJy	4.960×10^9	4.613×10^{-18}	EVLA
Apr 20.23	55306.23	8.46 GHz	<63 μJy	8.460×10^9	5.330×10^{-18}	EVLA
Apr 20.466	55306.466	0.3–10 keV	$<4.6\times10^{-4}$ cps	4.200×10^{17}	2.864×10^{-15}	*Swift*/XRT
Apr 24.646	55310.646	NUV (AB)	>22.7 mag	1.295×10^{15}	3.885×10^{-14}	*GALEX*

the nearby NGC300-OT was also not detected in the radio to deeper luminosity limits.

5.3.4 Ultraviolet Observations

We observed PTF 10fqs with *GALEX* (Martin et al. 2005) on two consecutive orbits starting at 2010 April 24.387 (total exposure of 2846 s). All images were reduced and coadded using the standard *GALEX* pipeline and calibration (Morrissey et al. 2007).

To create a reference image, we coadded 22 images of M99 prior to 2005 April 2 (total exposure of 18571 s). Next, we subtracted the reference image from observations of PTF 10fqs (see Figure 5.6). No source is detected. We find a 3σ upper limit of NUV 22.7 AB mag in an aperture consistent with a *GALEX* point source ($7.5'' \times 7.5''$).

To constrain the pre-explosion counterpart, we measured the limiting magnitude at the position of PTF 10fqs in the coadded reference image. The faintest detected object consistent with being a point source within the galaxy had NUV = 20.1 AB mag. The 3σ limit based on measuring the sky root-mean square (rms) is NUV > 21.8 AB mag.

5.3.5 X-Ray Observations

We observed PTF10fqs with *Swift*/XRT on April 20.466 for 2507.3 s and April 22.024 for 2623.5 s. No source is detected to a 3σ limiting count rate (assuming an $18''$ radius) of 4.6×10^{-4} counts s^{-1}. Assuming a power-law model with a photon index of two, this corresponds to a flux limit of 1.6×10^{-14} erg cm^{-2} s^{-1}.

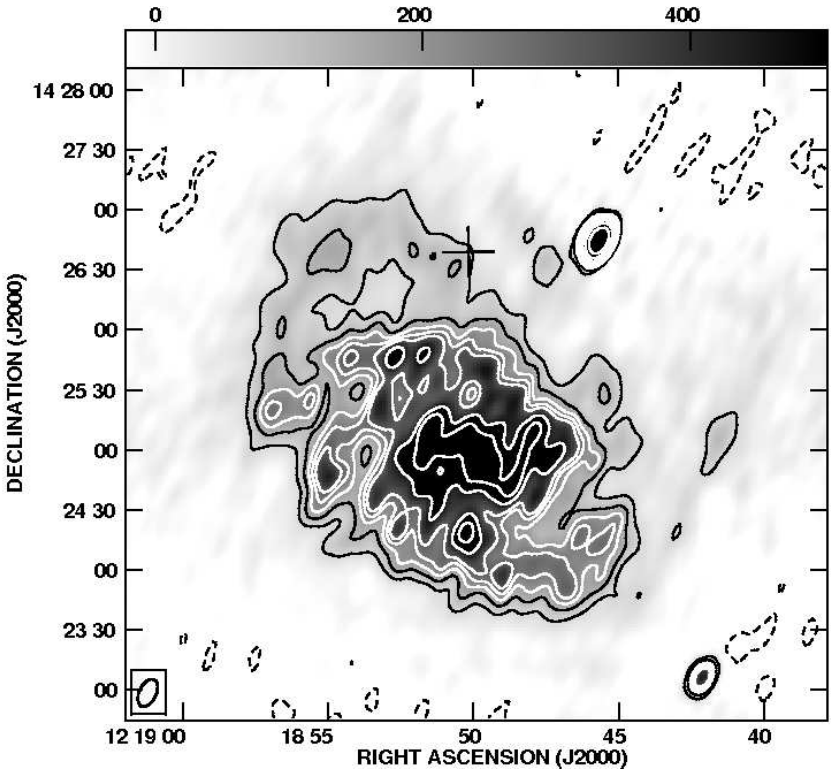

Figure 5.5 Observation of PTF 10fqs (denoted by a plus sign) with the EVLA at 4.96 GHz, just four days after discovery. The gray-scale range is -40 to 1000 μJy per beam and the size of the synthesized beam is shown at the bottom-left corner.

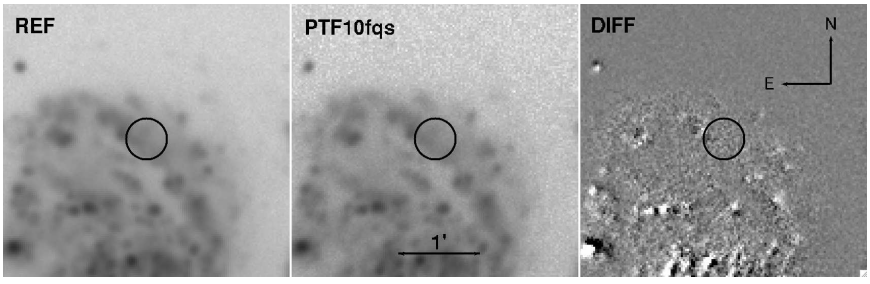

Figure 5.6 Observation of PTF 10fqs with *GALEX*. Reference data are taken from 22 images between 28 March 2005 and 2 April 2005 (left panel). Observations of PTF 10fqs were taken on 24 April 2010 (center panel). No source is detected in the difference image (right panel).

5.4 Archival Data

5.4.1 Hubble Space Telescope (HST)

A query to the Hubble Legacy archive returned *HST* images of M99 in the F606W (2001), F336W (2009), and F814W (2009) filters. We multidrizzled this data (PI Regan, Proposal ID 11966) and registered our Gemini/GMOS acquisition image with the *HST/WFPC2* images. Unfortunately, PTF 10fqs is just off the edge of the chip for the F606W filter image.

The total 1σ registration error, added in quadrature, was 0.59 pixels. The sources of error are as follows: centroiding error (0.17 in x, 0.30 in y), registration error between the Gemini image and HST/F814W image (0.19 in x, 0.44 in y) and registration error between HST/F814W image and HST/F336W image (0.04 in x, 0.02 in y). Hence, in Figure 5.7 we plot a 5σ radius of 3 pixels or $0.27''$.

No source is detected at the location of PTF 10fqs. To estimate the limiting magnitude, we ran sextractor and performed photometry following Holtzman et al. (1995). We find 3σ limiting Vega magnitudes of $I > 26.9$ and $U > 26$ in the 1800 s and 6600 s exposures, respectively.

5.4.2 Spitzer Space Telescope

M99 was part of the sample of the SIRTF Nearby Galaxies Survey (SINGS) galaxies (Kennicutt et al. 2003). This program undertook IRAC and MIPS imaging in 2004–2005. No point source is detected at the location of PTF 10fqs (see Figure 5.8). We downloaded IRAC images from the final data release of SINGS and MIPS images from the standard *Spitzer* pipeline. Computed upper limits (see Table 5.3) assume a 2-pixel aperture radius and sky-rms based on a 20×20 pixel box at the location.

5.4.3 Katzman Automatic Imaging Telescope

The 0.76 m Katzman Automatic Imaging Telescope (KAIT[7]; Li et al. 2000; Filippenko et al. 2001) had extensively imaged M99 in the past decade — 113 images in the period 1999–2010. We stacked the images in each season and find no point source at the location of

[7] http://astro.berkeley.edu/∼bait/kait.html

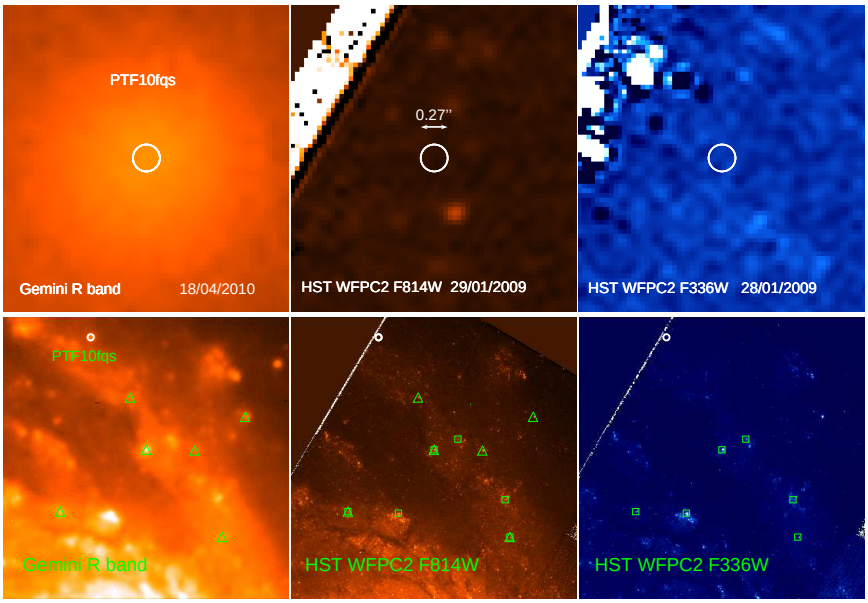

Figure 5.7 HST/F814W and HST/F336W observations from 2009. *Top panel:* Zoomed-in view ($2.8'' \times 2.6''$) to show the absence of a pre-explosion counterpart. This rules out red supergiants fainter than $M_V = -3$ mag and blue supergiants fainter than $M_V = -4.3$ mag. *Bottom panel:* Zoomed-out view ($81.2'' \times 82.1''$) to show registration stars. Stars used to register the Gemini/R-band image with the HST/F814W image are denoted by triangles. Stars used to register the HST/F814W image with the HST/F336W are denoted by squares.

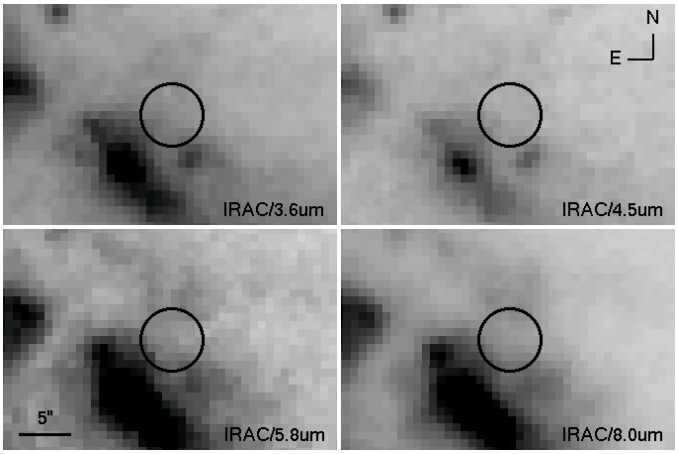

Figure 5.8 Pre-explosion observations with *Spitzer*/IRAC. No source is found to be consistent with PTF 10fqs.

Table 5.3. Progenitor constraints for PTF 10fqs

Date	Filter	Magnitude/Flux	Facility
2005	NUV (AB)	>21.8 mag	*GALEX*
2009	F336W (Vega U)	>26 mag	*HST*/WFPC2
2009	F814W (Vega I)	>26.9 mag	*HST*/WFPC2
2004	3.6 μm	<5.3 μJy	*Spitzer*/IRAC
2004	4.5 μm	<3.5 μJy	*Spitzer*/IRAC
2004	5.8 μm	<51 μJy	*Spitzer*/IRAC
2004	8.0 μm	<344 μJy	*Spitzer*/IRAC
2004	23.68 μm	<240 μJy	*Spitzer*/MIPS

PTF 10fqs. Limiting magnitudes for each season are summarized in Table 5.4.

5.4.4 DeepSky Imaging

DeepSky[8] (Nugent 2009) also has imaging at the position of this field over the interval 2006–2008. No point source is detected in a yearly sum of these images (see Table 5.4).

5.5 Analysis

5.5.1 SED

We fit a blackbody spectrum to the optical and near-infrared fluxes of PTF10 fqs without taking into account any local extinction. The best fit gives a lower limit on the temperature of ~ 3900 K.

5.5.2 Spectral Modelling

We combined the four spectra obtained with HET (between +5 days and +17 days). The most prominent (narrow) features in the spectra of PTF 10fqs are Hα, [Ca II], the Ca II near-IR triplet, Na I D, and Hβ. The measured line fluxes and equivalent widths are summarized in Table 5.5. The Hα FWHM is ≈ 930 km s^{-1} (taking into account the instrumental

[8]http://supernova.lbl.gov/∼nugent/deepsky.html.

Table 5.4. Historical Optical Observations

Date Range (UT)	Exposure (seconds)	Limiting Mag (R band)	Facility
1998-12-27 – 1999-06-01	680.0	> 20.4	KAIT
1999-11-26 – 2000-06-07	567.0	> 20.4	KAIT
2001-04-11 – 2001-06-07	192.0	> 20.1	KAIT
2002-01-14 – 2002-06-08	486.0	> 20.4	KAIT
2003-01-15 – 2003-06-04	318.0	> 20.4	KAIT
2004-01-29 – 2004-06-16	392.0	> 20.3	KAIT
2004-12-25 – 2005-06-01	110.0	> 20.3	KAIT
2006-01-12 – 2006-05-18	665.7	> 22.2	DeepSky
2006-03-24 – 2006-05-18	78.0	> 20.4	KAIT
2007-01-04 – 2007-05-06	1749.9	> 22.4	DeepSky
2007-01-13 – 2007-06-04	178.0	> 20.4	KAIT
2007-12-22 – 2008-06-16	332.0	> 20.4	KAIT
2008-05-18 – 2008-05-18	241.2	> 20.7	DeepSky
2009-03-28 – 2009-04-27	64.0	> 20.3	KAIT
2010-02-11 – 2010-03-22	32.0	> 20.0	KAIT

Note. — All images in a season were stacked.

Table 5.5. Spectral Features of PTF 10fqs

Line	Obs λ (Å)	Flux (erg cm^{-2} s^{-1})	Eq. Width Å
Hα	6621.2	1.0×10^{-15}	-19.9
Hβ	4907.3	1.3×10^{-16}	-3.7
Na I D	5939.0	-3.1×10^{-16}	6.4
[Ca II]	7355.8	2.9×10^{-16}	-6.1
[Ca II]	7387.2	1.8×10^{-16}	-3.7

Note. — Above line fluxes are measured on combined HET spectra (phase between +5 days and +17 days).

resolution).

The Ca II near-IR triplet is of particular interest. The HET spectra appear to show a flux excess longward of 8300 Å beyond that expected from a simple, low-order polynomial fit to the continuum. Together with a possible broad flux deficit near 8300 Å, the overall effect suggests a P-Cygni profile. If we fit three Gaussians, the Ca II near-IR triplet features are broader than the [Ca II] doublet, and quite likely even broader than the narrow component of the Hα profile. There is a surplus of flux at 8600 Å, which falls right between the 8498.02, 8542.09 Å pair and the more isolated 8662.14 Å line, such as one would expect from an underlying broad feature.

We test this hypothesis further with SYNOW (Jeffery & Branch 1990) modelling. We do not get a good fit to the overall shape of the spectrum with an extinguished blackbody of any temperature (assuming standard dust). To fit the red end of the spectrum, we need high temperature and extinction (consistent with the strong Na I D absorption). We find that in addition to narrow emission from Ca II IR, there is also a likely underlying broad component (see Figure 6.3). The width (FWHM) of this feature is $\approx$10,000 km s^{-1}.

A caveat to this interpretation is that a similar broad feature is not seen in the Hα profile. However, as noted below (§ 5.6.2), reinspection of the spectra of related transients shows

possible evidence of a similar broad feature. Thus, we cautiously accept the interpretation that in addition to the low-velocity outflow seen in Hα, there is a higher velocity outflow in this explosion.

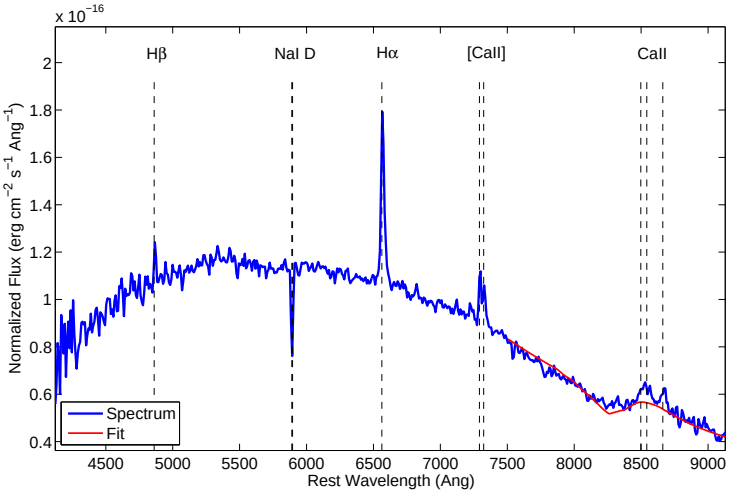

Figure 5.9 SYNOW fit to summed HET spectra of PTF 10fqs. Note the broad, possibly P Cygni, feature under the Ca II near-IR triplet.

5.6 What is PTF 10fqs?

In a nutshell, PTF 10fqs is a red transient with a peak luminosity of $M_r = -12.3$ and a spectrum dominated by Hα, [Ca II], and Ca II emission. The width of the Hα line is ≈ 930 km s^{-1}, and there is some evidence for a $\approx 10{,}000$ km s^{-1} broad Ca II IR feature.

The peak absolute magnitude and the Hα line width of PTF 10fqs are similar to those seen in M85OT2006-1 (hereafter, M85-OT; Kulkarni et al. 2007), SN 2008S (Prieto et al. 2008b; Smith et al. 2009), and NGC 300-OT (Bond et al. 2009; Berger et al. 2009). However, there are some differences amongst these four sources. Thus, to aid a better classification, we review the similarities and differences between these four sources.

5.6.1 The Light Curve

The light curves of all four transients (PTF 10fqs, SN 2008S, NGC 300-OT, and M85-OT) were red and evolved slowly for the first couple of months. PTF 10fqs had a well-sampled rise

(Figure 5.4) — it rose by 1.1 mag in r-band in 10.8 days. After maximum, PTF 10fqs declined slowly in r-band by 1 mag in 68 days. Subsequently, it evolved more rapidly, declining by the next 1.3 mag in 16 days. PTF 10fqs had $g-r$=1.0 at peak and declined relatively faster in g-band (1 mag in 40 days) than r-band. In comparison, SN 2008S declined by 1 mag in 51 days in R-band and 44 days in V-band. The epoch of maximum light is uncertain for NGC 300-OT due to lack of observations and is constrained to be anywhere between April 24 and May 15, 2008 (Bond et al. 2009). If we assume it to be April 27, the evolution in R-band and I-band are similar to that for PTF 10fqs (Figure 5.4).

5.6.2 The Spectrum

The spectral evolution of SN 2008S (Botticella et al. 2009) and NGC 300-OT (Berger et al. 2009) were very well studied as they were in very nearby galaxies. We took this opportunity to reanalyze the spectrum of M85-OT reported by (Kulkarni et al. 2007)[9].

Armed thus, we compare and contrast the spectral features of these four transients (see Figure 5.10).

- The Hα profile of SN 2008S showed a narrow component (unshocked circumstellar material [CSM]; $\approx$250 km s^{-1}), an intermediate component (shocked material between the ejecta and the CSM; $\approx$1000 km s^{-1}), and a broad component (underlying ejecta emission; $\approx$3000 km s^{-1}). NGC 300-OT exhibited narrow (560 km s^{-1}) and intermediate-width components (1100 km s^{-1}). M85-OT only had a narrow component (350 km s^{-1}). PTF 10fqs shows an intermediate-width component (930 km s^{-1}) in the Hα emission line.

- SN 2008S had an Hα/Hβ ratio that evolved from 4 to 10. NGC 300-OT had a ratio of 6, while M85-OT showed a ratio of 3.5. PTF 10fqs has a ratio of 6.5. All events show flux ratios higher than 3.1 (the expectation from Case B recombination). This may be evidence for collisional excitation (Drake & Ulrich 1980).

[9]In addition to the features mentioned by Kulkarni et al. 2007, we can securely identify Ca II H&K and see evidence of [Ca II] and the Ca II near-IR triplet. Furthermore, we can identify the lines previously marked "unidentified": 4115 Å is Hγ, 6428 Å is likely Fe II (multiplet 74), 6527 Å is likely Fe II (multiplets 40 and 92).

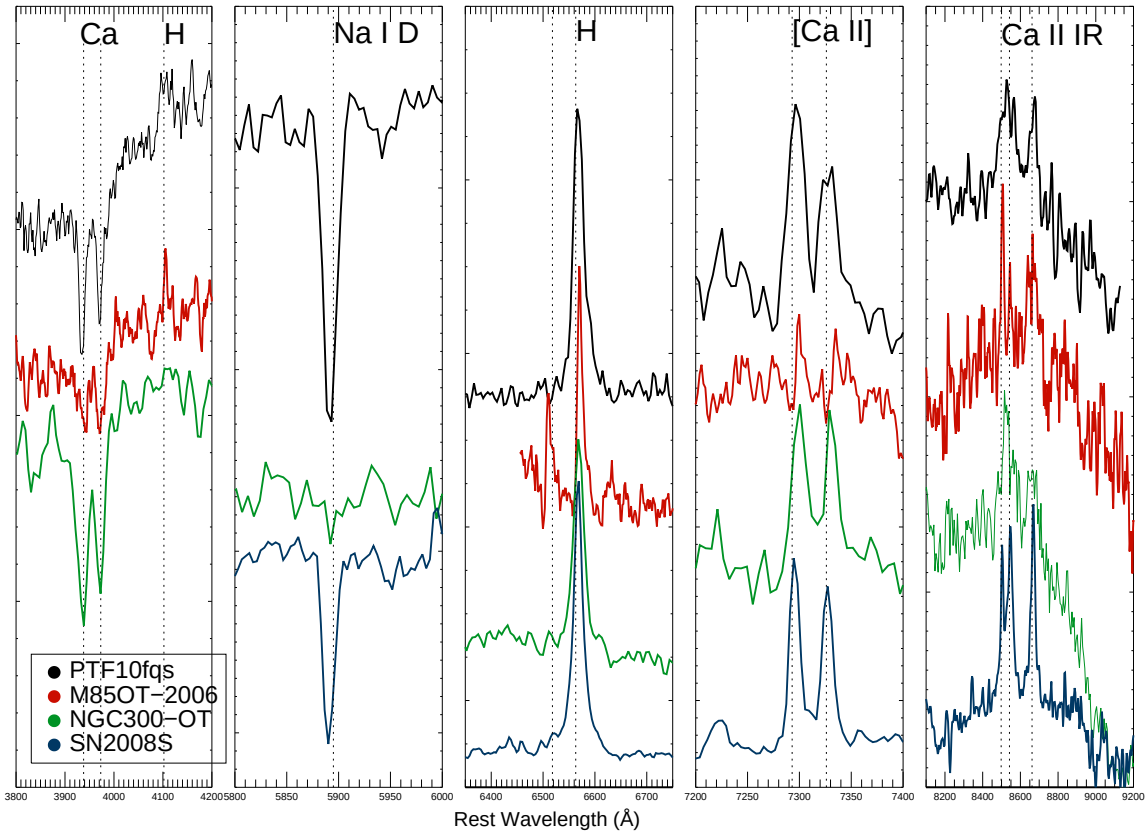

Figure 5.10 Comparison of specific lines in spectra of PTF 10fqs (black), M85-OT (red; Kulkarni et al. 2007), SN2008s (blue; Botticella et al. 2009) and NGC 300-OT (green; Bond et al. 2009). *From left to right:* Panel 1 shows Ca II H&K in all three transients. Panel 2 shows the extreme Na I D absorption in PTF 10fqs. Panel 3 shows the similar Hα widths in all three transients. Note the presence of Fe II in M85-OT. Panel 4 shows narrow [Ca II] in all three transients. Panel 5 shows Ca II near-IR triplet. Note that in addition to the narrow lines, there is possibly an underlying broad feature.

- PTF 10fqs, NGC 300-OT and SN 2008S exhibit three calcium features: Ca II H&K in absorption, [Ca II] and Ca II near-IR triplet in emission. A reanalysis of M85-OT shows Ca II H&K, as well as lower signal-to-noise ratio detections of both [Ca II] and Ca II IR. Smith et al. 2009 show a similarity between the spectra of SN2008S and a Galactic hypergiant (IRC+10420) and suggest that strong [Ca II] is due to destruction of dust grains.

- As noted earlier (see also Figure 6.3), there is evidence for a broad feature around 8600 Å in the spectrum of PTF 10fqs. Motivated by this finding, we reinspected the spectra of previous transients and found that a similar broad feature may also be present in the spectra of M85-OT and NGC 300-OT.

- Narrow Fe II lines are visible in NGC 300-OT and SN 2008S. Reanalysis of M85-OT spectra possibly shows Fe II(74) and Fe II (40, 92).

- For SN 2008S, Na I D evolves from strong absorption at early times to emission at very late times. This suggests a very dense CSM. O I λ7774 is also in emission at late times. For NGC 300-OT, Na I D has a much lower equivalent width at early times, but it also evolves from absorption to emission. Neither Na I D nor O I are seen in M85-OT, but there is possibly K I in emission. PTF 10fqs has an equivalent width of Na I D of 6.4, higher than SN 2008S (2.3–4.4) and NGC 300-OT (1.0–2.1). The equivalent width of Na I D is too high to apply a standard correlation to estimate extinction.

5.6.3 The Pre-Explosion Counterpart

We plot the upper limits on the pre-explosion counterpart for PTF10fqs in Figure 5.11. The most constraining limits are in the optical. Following the Geneva stellar evolution tracks (Lejeune & Schaerer 2001) for unenshrouded stars, the luminosity limit of $M_I > -4.3$ corresponds to a progenitor mass $<4\,M_\odot$. If there was extinction of, say 1.5 mag, this would change the limit to $<7\,M_\odot$. None of SN 2008S, NGC 300-OT, M85-OT, and PTF 10fqs have an optical counterpart in deep, pre-explosion optical images. The limits in all cases are deep enough to at least rule out red supergiants and blue supergiants.

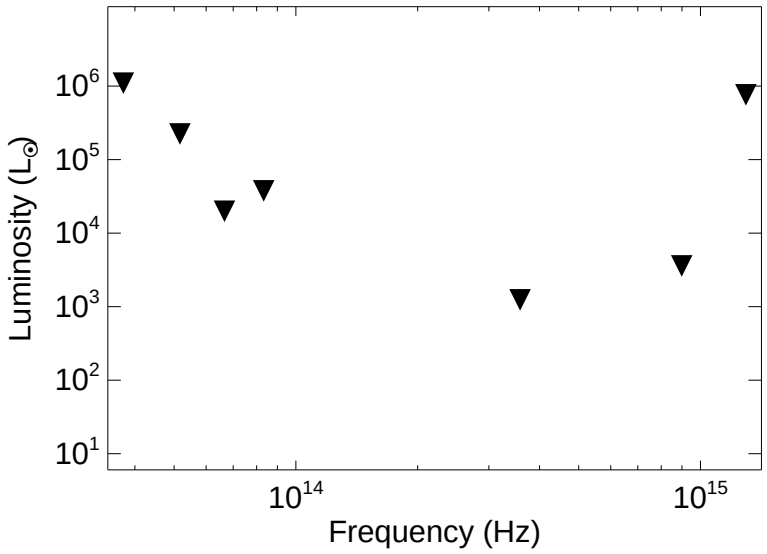

Figure 5.11 Spectral energy distribution (mid-IR to UV) constraints on the pre-explosion counterpart of PTF 10fqs. Upper limits are denoted by downward arrows.

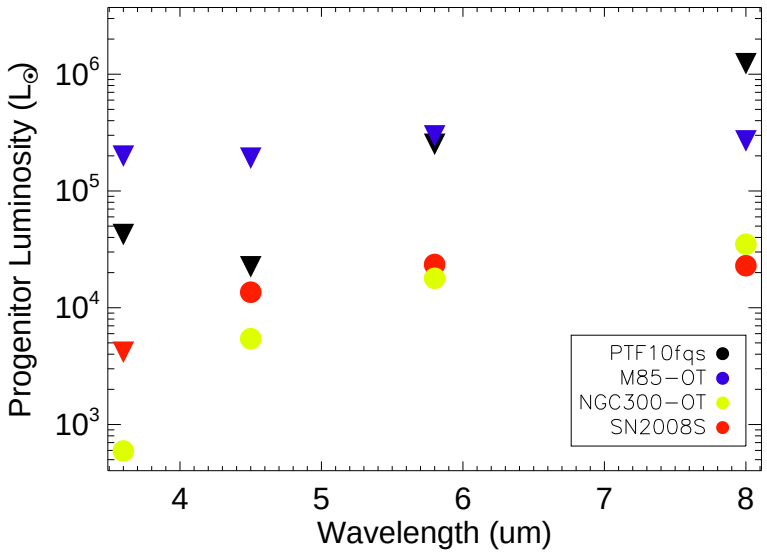

Figure 5.12 Pre-explosion detections (circles) or upper limits (downward triangles) from *Spitzer* for PTF 10fqs, SN 2008S, NGC 300-OT, and M85-OT. The non-detection of a progenitor for PTF 10fqs and M85-OT does not rule out a progenitor of luminosity comparable to that detected for NGC 300-OT and SN 2008S.

For both SN 2008S and NGC 300-OT, an extremely red and luminous mid-infrared pre-explosion counterpart is seen (Prieto et al. 2008b; Thompson et al. 2009). Recently, Khan et al. (2010) showed that such progenitors are as rare as 1 per galaxy (and possibly associated with a very short-lived phase of many massive stars). Thus, both of these transients can be reasonably associated with massive stars. Unfortunately, the large distance to M85 and M99 means that the pre-explosion *Spitzer* limits on M85-OT and PTF 10fqs are not deep enough by a factor of few to constrain their progenitors to similar depths (see Figure 5.12).

5.6.4 The Large-Scale Environment

M85-OT is located in the lenticular galaxy M85 (also in the Virgo cluster). Fortunately, this galaxy was observed with *HST* for the ACS Virgo Cluster Survey as well as for a GO program. The transient is not associated with any star-forming region and the absolute magnitude of the progenitor is fainter than $M_g \approx -4$ ($< 7\,\mathrm{M}_\odot$ not correcting for extinction; Ofek et al. 2008). Thus, a massive-star origin is quite unlikely.

In contrast, SN 2008S, NGC 300-OT, and PTF 10fqs occurred in star-forming galaxies. It may be worth noting here that three supernovae (all of the core-collapse variety) have previously been discovered in the host galaxy of PTF 10fqs. It is perhaps of some significance that eight supernovae (six core-collapse, two unclassified) were discovered in NGC 6946 in addition to SN 2008S. Only one supernova (of Type Ia) has been discovered in NGC 300. Small-number statistics and discovery bias (incompleteness from variety of different searches) notwithstanding, we make the suggestion that galaxies with a high supernova rate preferentially produce luminous red novae. If this suggestion is correct, then it would be worth the effort to systematically maintain close vigilance on the nearest galaxies having large supernova rates.

Kulkarni et al. 2007 suggested that V838 Mon, V4332 Sgr and M31 RV may also be luminous, red novae. We note here that the two Galactic sources are located in star-forming regions. Specifically, V838 Mon is in a young (25 Myr) star cluster and may even have a B3 companion (Afşar & Bond 2007). V4332 Sgr (Martini et al. 1999) is located towards the inner Galaxy (in Sagittarius). On the other hand, M31 RV is located in the bulge of M31. *HST* observations (undertaken with WFPC2 in parallel mode) taken about

a decade ago show that the immediate environs of M31-RV are typical bulge-population stars (Bond & Siegel 2006). No unusual remnant star is seen at the astrometric position of M31 RV, nor any evidence of a light echo (consistent with the absence of dense circumstellar or interstellar gas that is essential to form echoes). Separately, there is no evidence for any luminous outbursts in this area in the period 1942–1993 (Boschi & Munari 2004). Thus, M31 RV appears to have been a cataclysmic event in the bulge of M31.

5.7 Conclusion

PTF 10fqs is the fourth member of a class of extragalactic transients[10] which possess a peak luminosity between that of novae and supernovae, and have spectral and photometric evolution that bear no resemblance to either supernovae or novae. The other members of this class are M85-OT, NGC 300-OT and SN 2008S.

NGC 300-OT and SN 2008S are remarkable for their very bright mid-infrared progenitors. Though sensitive pre-explosion observations of M85-OT and PTF 10fqs do exist, the large distance to the Virgo Cluster (17 Mpc) relative to that of NGC 300 (1.9 Mpc) and NGC6946 (5.7 Mpc) results in weak constraints on the luminosity of any pre-explosion star. PTF 10fqs, NGC 300-OT, and SN 2008S occurred in star-forming regions whereas M85-OT was in the bulge. *Prima facie*, this group of explosive events can be divided into a disk and a bulge group.

The discovery of PTF 10fqs in itself cannot address whether the two groups of luminous, red novae are one and the same. The proposed models to explain this group are diverse: electron capture within an extreme asymptotic giant branch (AGB) star, common-envelope phase (stellar merger), inspiral of a giant planet into the envelope of an aging parent star, a most peculiar nova, and a most peculiar supernova.

The possible evidence of the broad feature centered around the Ca II near-IR triplet with an inferred velocity spread of 10,000 km s^{-1} may be an important clue. It would mean that these events possess both a low- and a high-velocity outflow. By comparison with other astronomical sources, one can envisage a high-velocity polar outflow and a slower equatorial outflow (but with a larger mass). To this end, continued sensitive spectroscopy of PTF 10fqs (and of course other such future events) would be very valuable.

[10]Henceforth we use the term "luminous red novae" as a functional short name for such events.

The "Transients in the Local Universe" key project of the Palomar Transient Factory is designed to systematically unveil events in the gap between novae and supernovae. It surveys $\approx$20,000 nearby galaxies ($d < 200$ Mpc) yearly at 1-day cadence and a depth of $R < 21$ mag. (If the maximum luminosity of this class is -14 mag, then we would be sensitive to events out to 100 Mpc.) Furthermore, *Spitzer* has a growing archive of deep images of nearby galaxies (e.g., SINGS, Kennicutt et al. 2003; LVL, Dale et al. 2009; and S4G, Sheth et al. 2010), and *WISE* (Wright et al. 2010) has an ongoing all-sky survey in the mid-IR. This will allow us to probe deeper in search of the pre-explosion counterpart and possibly present a new channel for discovery of luminous red novae. The discovery of PTF 10fqs is only the harbinger of the uncovering of a large sample of such transients to unveil the nature of this new class of explosions.

Acknowledgments.

M.M.K. thanks the Gordon and Betty Moore Foundation for a Hale Fellowship in support of graduate study. The Weizmann Institute PTF participation is supported in part by the Israel Science Foundation via grants to AGY. The Weizmann-Caltech collaborative PTF effort is supported by the US-Israel Binational Science Foundation. AGY and MS are jointly supported by the "making connections" Weizmann-UK program. AGY further acknowledges support by a Marie Curie IRG fellowship and the Peter and Patricia Gruber Award, as well as funding by the Benoziyo Center for Astrophysics and the Yeda-Sela center at the Weizmann Institute. A.V.F.'s group and KAIT are supported by National Science Foundation (NSF) grant AST-0908886, the Sylvia & Jim Katzman Foundation, the Richard & Rhoda Goldman Fund, Gary and Cynthia Bengier, and the TABASGO Foundation; additional funding was provided by NASA through *Spitzer* grant 1322321, as well as *HST* grant AR-11248 from the Space Telescope Science Institute, which is operated by Associated Universities for Research in Astronomy, Inc., under NASA contract NAS 5-26555. J.S.B. and his group are partially funded by a DOE SciDAC grant. E.O.O. and D.P. are supported by the Einstein fellowship. L.B. is supported by the National Science Foundation under grants PHY 05-51164 and AST 07-07633.

We are grateful to the staff of the Gemini Observatory for their promptness and high efficiency in attending to our TOO request. Likewise, we thank the staff of the Very Large Array and the Hobby Eberly Telescope. We acknowledge the following internet repositories:

SEDS (Messier Objects) and GOLDMine (Virgo Cluster). Finally, as always, we are grateful to the librarians who maintain the ADS, the NED, and SIMBAD data systems.

The Hobby-Eberly Telescope (HET) is a joint project of the University of Texas at Austin, the Pennsylvania State University, Stanford University, Ludwig-Maximillians-Universität München, and Georg-August-Universität Göttingen. The HET is named in honor of its principal benefactors, William P. Hobby and Robert E. Eberly. The Marcario Low-Resolution Spectrograph is named for Mike Marcario of High Lonesome Optics, who fabricated several optics for the instrument but died before its completion; it is a joint project of the Hobby-Eberly Telescope partnership and the Instituto de Astronomía de la Universidad Nacional Autónoma de México. *GALEX* (Galaxy Evolution Explorer) is a NASA Small Explorer, launched in 2003 April. We gratefully acknowledge NASA's support for construction, operation, and science analysis for the *GALEX* mission, developed in cooperation with the Centre National d'Etudes Spatiales of France and the Korean Ministry of Science and Technology. PAIRITEL is operated by the Smithsonian Astrophysical Observatory (SAO) and was made possible by a grant from the Harvard University Milton Fund, the camera loan from the University of Virginia, and the continued support of the SAO and UC Berkeley. The Expanded Very Large Array is operated by the National Radio Astronomy Observatory, a facility of the NSF operated under cooperative agreement by Associated Universities, Inc.

Table 5.6: Optical and Near-Infrared Light Curve

MJD	**Filter**	**Magnitude**	**Facility**
55295.2	*Mould-R*	>20.94	Palomar 48-in
55296.5	*Mould-R*	>19.28	Palomar 48-in
55302.4	*Mould-R*	19.99 ± 0.19	Palomar 48-in
55313.2	*Mould-R*	19.27 ± 0.11	Palomar 48-in
55316.3	*Mould-R*	19.28 ± 0.11	Palomar 48-in
55317.3	*Mould-R*	19.30 ± 0.13	Palomar 48-in
55319.2	*Mould-R*	19.20 ± 0.10	Palomar 48-in
55320.2	*Mould-R*	19.42 ± 0.12	Palomar 48-in
55321.3	*Mould-R*	19.41 ± 0.12	Palomar 48-in
55323.2	*Mould-R*	19.39 ± 0.13	Palomar 48-in
55324.2	*Mould-R*	19.53 ± 0.15	Palomar 48-in
55329.2	*Mould-R*	19.55 ± 0.18	Palomar 48-in
55330.2	*Mould-R*	19.67 ± 0.20	Palomar 48-in
55331.2	*Mould-R*	19.74 ± 0.16	Palomar 48-in
55332.2	*Mould-R*	19.68 ± 0.11	Palomar 48-in
55333.2	*Mould-R*	19.65 ± 0.15	Palomar 48-in
55336.3	*Mould-R*	19.60 ± 0.12	Palomar 48-in
55337.3	*Mould-R*	19.61 ± 0.17	Palomar 48-in
55343.2	*Mould-R*	19.81 ± 0.12	Palomar 48-in
55346.2	*Mould-R*	19.66 ± 0.13	Palomar 48-in
55347.2	*Mould-R*	19.79 ± 0.17	Palomar 48-in
55348.2	*Mould-R*	19.66 ± 0.13	Palomar 48-in
55349.3	*Mould-R*	19.90 ± 0.19	Palomar 48-in
55351.2	*Mould-R*	19.78 ± 0.16	Palomar 48-in
55352.2	*Mould-R*	19.63 ± 0.12	Palomar 48-in
55353.2	*Mould-R*	19.83 ± 0.21	Palomar 48-in

Continued on Next Page...

Table 5.6 – Continued

MJD	Filter	Magnitude	Facility
55355.2	*Mould-R*	19.76 ± 0.16	Palomar 48-in
55356.2	*Mould-R*	19.69 ± 0.16	Palomar 48-in
55361.2	*Mould-R*	19.82 ± 0.16	Palomar 48-in
55362.2	*Mould-R*	19.80 ± 0.16	Palomar 48-in
55363.2	*Mould-R*	19.66 ± 0.16	Palomar 48-in
55364.2	*Mould-R*	19.84 ± 0.15	Palomar 48-in
55368.2	*Mould-R*	19.95 ± 0.14	Palomar 48-in
55371.2	*Mould-R*	19.93 ± 0.23	Palomar 48-in
55372.2	*Mould-R*	20.10 ± 0.16	Palomar 48-in
55373.2	*Mould-R*	20.15 ± 0.19	Palomar 48-in
55375.2	*Mould-R*	19.97 ± 0.17	Palomar 48-in
55377.2	*Mould-R*	20.00 ± 0.24	Palomar 48-in
55379.2	*Mould-R*	19.87 ± 0.10	Palomar 48-in
55304.4	r	19.85 ± 0.12	Palomar 60-in
55306.3	r	19.40 ± 0.05	Palomar 60-in
55310.3	r	19.29 ± 0.03	Palomar 60-in
55312.1	r	19.41 ± 0.03	Palomar 60-in
55313.2	r	18.87 ± 0.05	Palomar 60-in
55314.2	r	18.94 ± 0.17	Palomar 60-in
55316.3	r	19.16 ± 0.05	Palomar 60-in
55317.3	r	19.30 ± 0.05	Palomar 60-in
55319.2	r	19.32 ± 0.04	Palomar 60-in
55320.2	r	19.25 ± 0.01	Palomar 60-in
55321.2	r	19.33 ± 0.02	Palomar 60-in
55322.3	r	19.40 ± 0.02	Palomar 60-in
55323.3	r	19.55 ± 0.04	Palomar 60-in
55324.3	r	19.47 ± 0.02	Palomar 60-in

Continued on Next Page...

Table 5.6 – Continued

MJD	Filter	Magnitude	Facility
55341.3	r	19.61 ± 0.11	Palomar 60-in
55343.2	r	19.69 ± 0.06	Palomar 60-in
55347.3	r	19.80 ± 0.04	Palomar 60-in
55348.2	r	19.71 ± 0.01	Palomar 60-in
55350.2	r	19.76 ± 0.03	Palomar 60-in
55352.3	r	19.65 ± 0.03	Palomar 60-in
55354.2	r	19.80 ± 0.06	Palomar 60-in
55356.3	r	19.75 ± 0.08	Palomar 60-in
55357.3	r	19.68 ± 0.08	Palomar 60-in
55363.2	r	19.81 ± 0.03	Palomar 60-in
55368.3	r	20.01 ± 0.12	Palomar 60-in
55372.2	r	19.92 ± 0.03	Palomar 60-in
55381.2	r	19.90 ± 0.08	Palomar 60-in
55391.2	r	20.35 ± 0.05	Palomar 60-in
55406.2	r	21.26 ± 0.13	Palomar 60-in
55407.2	r	21.22 ± 0.14	Palomar 60-in
55306.3	g	20.32 ± 0.18	Palomar 60-in
55310.3	g	20.09 ± 0.05	Palomar 60-in
55313.2	g	19.91 ± 0.09	Palomar 60-in
55317.3	g	20.08 ± 0.06	Palomar 60-in
55319.2	g	20.00 ± 0.06	Palomar 60-in
55320.2	g	20.25 ± 0.10	Palomar 60-in
55321.2	g	20.19 ± 0.03	Palomar 60-in
55322.3	g	20.16 ± 0.08	Palomar 60-in
55323.3	g	20.23 ± 0.04	Palomar 60-in
55324.3	g	20.20 ± 0.02	Palomar 60-in
55341.3	g	20.52 ± 0.11	Palomar 60-in

Continued on Next Page...

Table 5.6 – Continued

MJD	Filter	Magnitude	Facility
55348.2	g	20.70 ± 0.07	Palomar 60-in
55350.2	g	20.66 ± 0.07	Palomar 60-in
55351.3	g	20.78 ± 0.11	Palomar 60-in
55352.3	g	20.80 ± 0.11	Palomar 60-in
55353.2	g	20.88 ± 0.09	Palomar 60-in
55354.2	g	21.01 ± 0.14	Palomar 60-in
55356.3	g	21.25 ± 0.25	Palomar 60-in
55304.4	i	19.32 ± 0.11	Palomar 60-in
55306.3	i	18.94 ± 0.07	Palomar 60-in
55310.3	i	18.98 ± 0.03	Palomar 60-in
55312.2	i	19.06 ± 0.04	Palomar 60-in
55313.2	i	18.98 ± 0.09	Palomar 60-in
55317.3	i	19.03 ± 0.06	Palomar 60-in
55319.2	i	19.02 ± 0.07	Palomar 60-in
55320.2	i	19.04 ± 0.03	Palomar 60-in
55321.2	i	19.13 ± 0.03	Palomar 60-in
55322.3	i	19.02 ± 0.04	Palomar 60-in
55323.3	i	19.14 ± 0.03	Palomar 60-in
55324.2	i	19.21 ± 0.04	Palomar 60-in
55341.3	i	19.21 ± 0.09	Palomar 60-in
55343.2	i	19.20 ± 0.02	Palomar 60-in
55349.2	i	19.33 ± 0.02	Palomar 60-in
55351.3	i	19.30 ± 0.03	Palomar 60-in
55353.2	i	19.29 ± 0.05	Palomar 60-in
55354.2	i	19.31 ± 0.03	Palomar 60-in
55356.3	i	19.23 ± 0.16	Palomar 60-in
55363.2	i	19.40 ± 0.05	Palomar 60-in

Continued on Next Page...

Table 5.6 – Continued

MJD	Filter	Magnitude	Facility
55368.3	i	19.41 ± 0.05	Palomar 60-in
55372.2	i	19.43 ± 0.07	Palomar 60-in
55381.2	i	19.55 ± 0.06	Palomar 60-in
55391.2	i	19.64 ± 0.06	Palomar 60-in
55406.2	i	20.38 ± 0.13	Palomar 60-in
55307.2	J	18.14 ± 0.29	PAIRITEL
55315.2	J	18.37 ± 0.39	PAIRITEL
55317.2	J	17.89 ± 0.30	PAIRITEL
55319.2	J	17.86 ± 0.26	PAIRITEL
55321.2	J	17.94 ± 0.24	PAIRITEL
55322.2	J	18.38 ± 0.25	PAIRITEL
55324.2	J	17.88 ± 0.21	PAIRITEL
55325.2	J	17.55 ± 0.32	PAIRITEL
55327.2	J	17.86 ± 0.25	PAIRITEL
55331.2	J	17.25 ± 0.18	PAIRITEL
55333.2	J	17.82 ± 0.24	PAIRITEL
55369.2	J	17.78 ± 0.31	PAIRITEL
55307.2	H	17.35 ± 0.21	PAIRITEL
55315.2	H	17.37 ± 0.27	PAIRITEL
55317.2	H	17.14 ± 0.22	PAIRITEL
55319.2	H	16.81 ± 0.27	PAIRITEL
55321.2	H	17.75 ± 0.18	PAIRITEL
55322.2	H	17.25 ± 0.16	PAIRITEL
55324.2	H	17.22 ± 0.20	PAIRITEL
55325.2	H	17.19 ± 0.30	PAIRITEL
55327.2	H	17.02 ± 0.20	PAIRITEL
55331.2	H	16.97 ± 0.32	PAIRITEL

Continued on Next Page...

Table 5.6 – Continued

MJD	**Filter**	**Magnitude**	**Facility**
55333.2	*H*	17.07 ± 0.29	PAIRITEL
55369.2	*H*	17.22 ± 0.22	PAIRITEL
55307.2	*K*	16.17 ± 0.18	PAIRITEL
55315.2	*K*	16.56 ± 0.31	PAIRITEL
55317.2	*K*	16.84 ± 0.19	PAIRITEL
55319.2	*K*	16.90 ± 0.25	PAIRITEL
55321.2	*K*	16.84 ± 0.40	PAIRITEL
55322.2	*K*	16.69 ± 0.21	PAIRITEL
55324.2	*K*	16.29 ± 0.15	PAIRITEL
55325.2	*K*	16.73 ± 0.18	PAIRITEL
55327.2	*K*	16.65 ± 0.22	PAIRITEL
55331.2	*K*	>15.80	PAIRITEL
55333.2	*K*	>16.60	PAIRITEL
55369.2	*K*	>16.36	PAIRITEL

Chapter 6

Another Class in the Gap: The Ephemeral PTF10bhp⋆

Mansi M. Kasliwal[1], S. R. Kulkarni[1], Avishay Gal-Yam[2], Ofer Yaron[2], Robert M. Quimby[1], Eran O. Ofek[1], Peter Nugent[3], Dovi Poznanski[3,12], Janet Jacobsen[3], Assaf Sternberg[2], Iair Arcavi[2], D. Andrew Howell[4,16], Mark Sullivan[5], Douglas J Rich[6], Paul F Burke[7], Joseph Brimacombe MB ChB FRCA MD[8,9], Dan Milisavljevic[10], Robert Fesen[10], Lars Bildsten[11,16], Ken Shen[12], S. Bradley Cenko[12], Joshua S. Bloom[12], Eric Hsiao[3], Nicholas M. Law[13], Neil Gehrels[14], Stefan Immler[14], Richard Dekany[15], Gustavo Rahmer[15], David Hale[15], Roger Smith[15], Jeff Zolkower[15], Viswa Velur[15], Richard Walters[15], John Henning[15], Kahnh Bui[15] & Dan McKenna[15]

[1] Cahill Center for Astrophysics, California Institute of Technology, Pasadena, CA, 91125, USA

[2] Benoziyo Center for Astrophysics, Faculty of Physics, The Weizmann Institute of Science, Rehovot 76100, Israel

[3] Computational Cosmology Center, Lawrence Berkeley National Laboratory, 1 Cyclotron Road, Berkeley, CA 94720, USA

[4] Las Cumbres Observatory Global Telescope Network, Inc, Santa Barbara, CA, 93117, USA

[5] Department of Physics, Oxford University, Oxford, OX1 3RH, UK

[6] Rich Observatory, 62 Wessnette Dr., Hampden, Maine USA

[7] Burke Observatory, 19 Berry Rd., Pittsfield, Maine USA

[8] New Mexico Skies Observatory, Mayhill New Mexico, USA

[9] James Cook University, Cairns, Australia

[10] 6127 Wilder Lab, Department of Physics and Astronomy, Dartmouth College, Hanover, NH, 03755, USA

[11] Kavli Institute of Theoretical Physics, University of California Santa Barbara, Santa Barbara, CA 93106, USA

[12] Department of Astronomy, 601 Campbell Hall, University of California, Berkeley, CA 94720-3411, USA

[13] Dunlap Institute for Astronomy and Astrophysics, University of Toronto, 50 St. George Street, Toronto M5S 3H4, Ontario, Canada

[14] NASA-Goddard Space Flight Center, Greenbelt, MD 20771, USA

[15] Caltech Optical Observatories, California Institute of Technology, Pasadena, CA 91125, USA

[16] Department of Physics, University of California Santa Barbara, Santa Barbara, CA 93106, USA

Abstract

We present the discovery, photometric and spectroscopic follow-up observations of SN 2010X (PTF 10bhp). This supernova decays exponentially with $\tau_d = 5$ days, and rivals the current recordholder in speed, SN 2002bj. SN 2010X peaks at $M_r = -17$ mag and has mean velocities of 10,000 km s^{-1}. Our light curve modeling suggests a radioactivity powered event and an ejecta mass of 0.16 $M_\odot$. If powered by Nickel, we show that the Nickel mass must be very small (≈ 0.02 $M_\odot$) and that the supernova quickly becomes optically thin to γ-rays. Our spectral modeling suggests that SN 2010X and SN 2002bj have similar chemical compositions and that one of Aluminum or Helium is present. If Aluminum is present, we speculate that this may be an accretion induced collapse of an O-Ne-Mg white dwarf. If Helium is present, all observables of SN 2010X are consistent with being a thermonuclear Helium shell detonation on a white dwarf, a ".Ia" explosion. With the 1-day dynamic-cadence experiment on the Palomar Transient Factory, we expect to annually discover a few such events.

*A version of this chapter is published with the title "Rapidly decaying supernova 2010X: a candidate ".Ia" explosion" in *The Astrophysical Journal Letters*, 2010, vol. 683, L29–L32, and is reproduced by permission of the AAS.

6.1 Introduction

Our present knowledge of cosmic explosions is arguably biased by the searches themselves. In particular, the cadence and depth of many supernovae searches are designed to efficiently discover supernovae of type Ia (SNe Ia). A repeat visit to the sky on timescales of five days maximizes sky coverage and is still sufficient to catch SNe Ia on the rise. The brilliance of these events, peak absolute visual magnitude of -19, sets the sensitivity of the searches. Conversely, fainter events and those with a shorter characteristic lifetime are likely to be missed in such searches.

To illustrate the unexplored nature of this phase space, we plot the luminosity of optical transients versus their characteristic timescale (Figure 6.1). SNe Ia are confined to a narrow band (Phillips 1993) with decay timescales ranging from twelve days to three weeks. Classical novae span a large range of timescales albeit at considerably lower luminosities.

Figure 6.1 brings two white-spaces to attention: the wide "gap" in luminosity between novae and supernovae, and the apparent paucity of luminous events on short timescales.

Next, we discuss currently known exemplars of "faint" (i.e., lower luminosity than SNe Ia) and "fast" (i.e., faster than SN 2007ax) transients. SN 2005E occurred in the halo of its host galaxy and has been proposed as a Helium detonation on a binary white dwarf (Perets et al. 2010b). SN 2005cz has been proposed to have a massive star origin (Kawabata et al. 2010). SN 2008ha is also being widely debated both as a deflagration of a white dwarf (Foley et al. 2009b,a) and core-collapse of a massive star (Valenti et al. 2009).

Until recently, the fastest event known was SN 2002bj (Poznanski et al. 2010). It decayed by one magnitude in five days and was quite spectroscopically peculiar. The origin of this event is not yet clear.

The Palomar Transient Factory[1] (PTF) was motivated in great measure to systematically explore the phase space for fast and faint explosive transients (Law et al. 2009; Rau et al. 2009b). Here, we present the discovery of a fast event, SN 2010X (PTF 10bhp).

[1] http://www.astro.caltech.edu/ptf

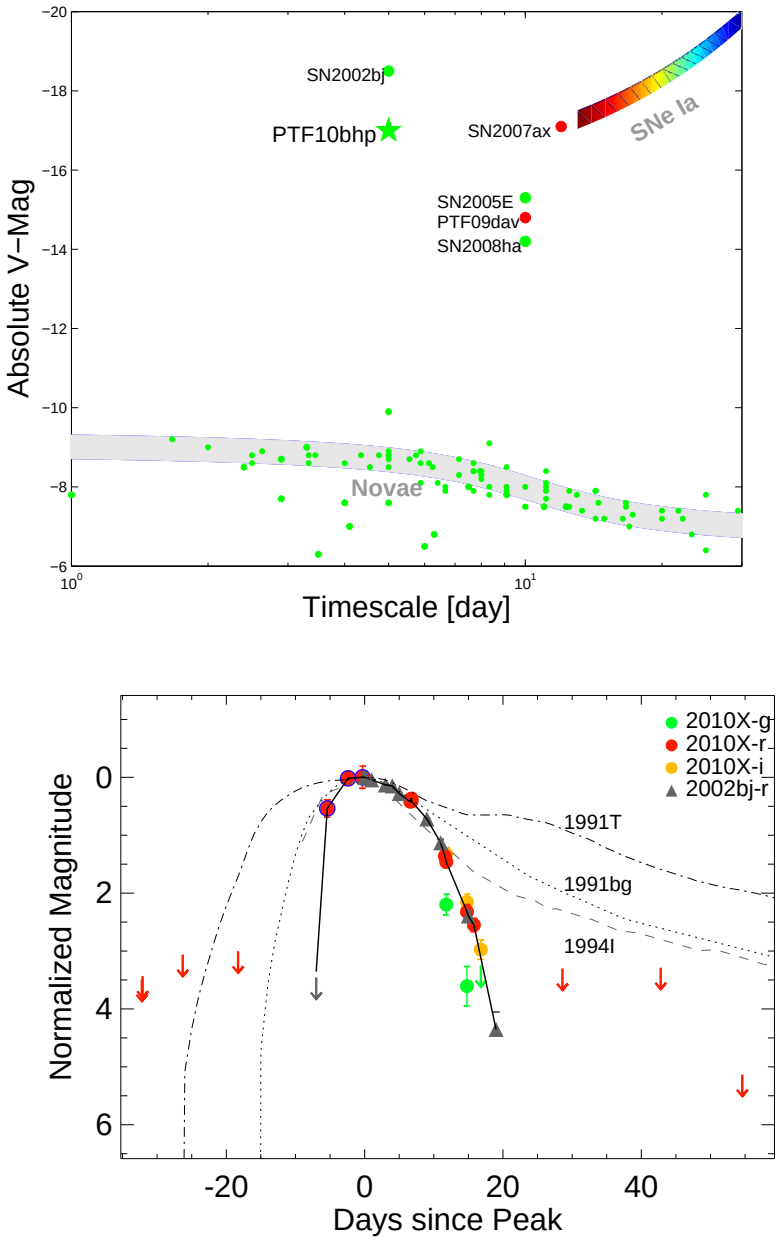

Figure 6.1 **Top:** The phase space of cosmic explosive transients. The color for each event represents the color at peak brightness. The band to the top right denotes supernovae of type Ia. The fastest such event is SN 2007ax (Kasliwal et al. 2008j). Classical novae occupy a band between −6 and −10 magnitude. Note that the only two transients with a timescale shorter than ten days are SN 2010X (PTF 10bhp) and SN 2002bj. **Bottom:** The multi-band optical light curve of SN 2010X (colored circles; green is g-band, red is r-band, orange is i-band). Three white light measurements have been calibrated to r-band and denoted by red circles with blue outline. Downward arrows represent upper limits. All light curves are normalized and shifted so that peak magnitude is zero and the time at peak is set to zero. For SN 2010X the epoch of maximum light is at MJD of 55239.5. The fast evolution of SN 2010X is compared to the current recordholder for fast supernovae, SN2002bj (gray triangles; r-band; Poznanski et al. 2010). Also shown is a prototypical "fast" Type Ic supernova, SN1994I (dashed line; Richmond et al. 1996) and templates [2] of the fast Type Ia SN1991bg and slow Type Ia SN1991T (Nugent et al. 2002). Note the rapid rise and the spectacular decay of SN 2010X and SN 2002bj relative to the other Type I exemplars.

6.2 Discovery

On UT 2010 February 7.07, D. Rich of Hampden, Maine, discovered a transient in the galaxy NGC 1573A at RA(J2000)=$04^{\rm h}48^{\rm m}27.7^{\rm s}$ and Dec(J2000)=$+73^\circ28'13''$. The discovery was confirmed by P. Burke of Pittsfield, Maine, upon which a notification was issued (CBET 2166; Rich & Burke 2010) and the transient dubbed SN2010X. On UT 2010 February 19.13, the Palomar Transient Factory independently detected this same transient and the pipeline assigned the name, PTF 10bhp. PTF had previously undertaken observations of this field (as a part of the dynamic cadence experiment) on January 11, 17 and 25 but with no detection.

6.3 Optical Light Curve

Energized by the apparent rapid fading, we initiated follow-up observations. The photometric observations from the 2-m Faulkes North Telescope (FTN) of the Las Cumbres Observatory Global Telescope (LCOGT), PTF, the Palomar Hale 200-inch telescope (P200), as well as white light observations provided by our amateur astronomer colleagues are summarized in Figure 6.1.

SN 2010X is located close to the nucleus of its host galaxy ($4.4''$ E, $6.0''$ N) and as such galaxy light subtraction is critical to produce reliable photometry. The images were subtracted from a template image using the software `hotpants` and `wcsremap` to measure a convolution kernel and align the images respectively (both codes supplied by A. Becker[3]). Aperture photometry was performed on each of these in a self-consistent manner using the same set of 22 calibration stars. Conversions from USNO-B1 magnitudes to SDSS gri magnitudes were done adopting Jordi et al. (2006). The resulting light curve is plotted in Figure 6.1.

Overplotting SN 2002bj, we find that light curves of the two supernovae are remarkably similar. Linearly fitting all the r-band detections post maximum light, we measure that SN 2010X decayed by 0.23 ± 0.01 mag day^{-1}. The corresponding exponential timescale (in the r-band) is $\tau_d = 4.7 \pm 0.2$ days.

The foreground Galactic extinction along the line of sight is E($B-V$)=0.146 or A$_r$=0.4

[3]http://www.astro.washington.edu/users/becker/c_software.html

(Schlegel et al. 1998b). The redshift of NGC 1573A is 0.015. Assuming standard cosmology (and h_0=0.72), we adopt a distance of 62.5 Mpc and a distance modulus of 34.0. Thus, the peak absolute magnitude of SN 2010X is $M_r \approx -17.0$ mag, 1.5 mag less luminous than SN2002bj.

6.4 Spectroscopic Follow-Up

On February 8 and 9, the first spectra (Figure 6.2) to classify the nature of this transient were taken with CCDS on the 2.4 m Hiltner telescope of the MDM observatory (CBET 2167, Milisavljevic & Fesen 2010). Comparison with a library of supernova spectra using SNID (Blondin & Tonry 2007) showed resemblance to the Type Ic supernovae SN 1994I and SN 2004aw a few days before maximum light. Further observations (Figure 6.2) were undertaken on Gemini-North/GMOS (Feb 23), Keck I/LRIS (Mar 7) and the Hale 200-inch/DBSP (Mar 18) telescopes. No perfect matches to Ic (or Ia, Ib) templates were found for these spectra. The velocity evolved from 12000 km s^{-1} before maximum to 9000 km s^{-1} at late-time.

We used SYNOW (Jeffery & Branch 1990) to infer elements in the spectra of SN 2010X (Figure 6.3). The most prominent identifications are oxygen (O I lines), Calcium (both Ca II IR triplet and Ca II H+K on the blue side), Carbon (C II lines), Titanium (Ti II) and Chromium (Cr II). Ti II and Cr II explain the broad blue features and adding Fe II improves the fit slightly. There is also some evidence for Mg I albeit based on single line.

The presence of Helium (He I), Sodium (Na D) and Aluminum (Al II) is less clear and we illustrate this dilemma in the inset of Figure 6.3. He I has three relevant lines: 5876 Å , 6678 Å and 7065 Å . The absorption feature around 5700 Å can be explained by both He I as well as Na D. The absorption feature around 6850 Å can be explained by Al II or He I. Since the central He I line is not prominent, SYNOW suggests that the combination of Na D and Al II is a better fit. However, Branch (2003) discusses that this central He I line is a singlet transition and this may both be suppressed and blueshifted in non-LTE relative to the other two He I triplet transitions. Therefore, we cannot conclusively say whether or not Helium is present in SN 2010X.

Comparing the spectra, SN 2002bj has substantially lower velocities (4000 km s^{-1} at +7d vs. 10,000 km s^{-1} at +10d) and a bluer continuum ($g-r$=0.2 at +12d vs. $g-r$=1.2

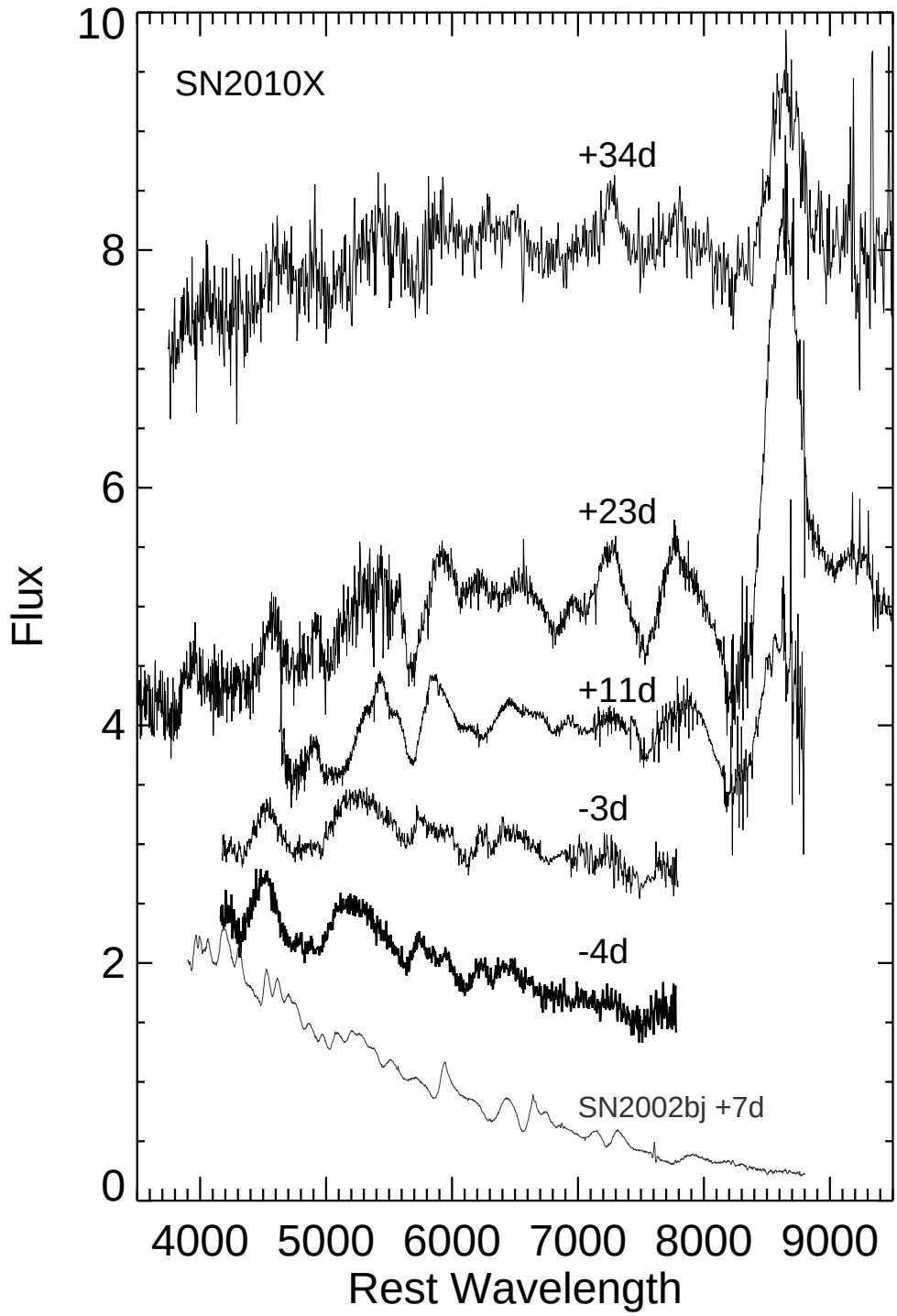

Figure 6.2 Spectroscopic follow-up of SN 2010X by MDM, Gemini, Keck and Palomar Observatories. The phase of the spectra relative to maximum light is labeled. Note the velocity evolution. Also shown is a spectrum of SN 2002bj (Poznanski et al. 2010).

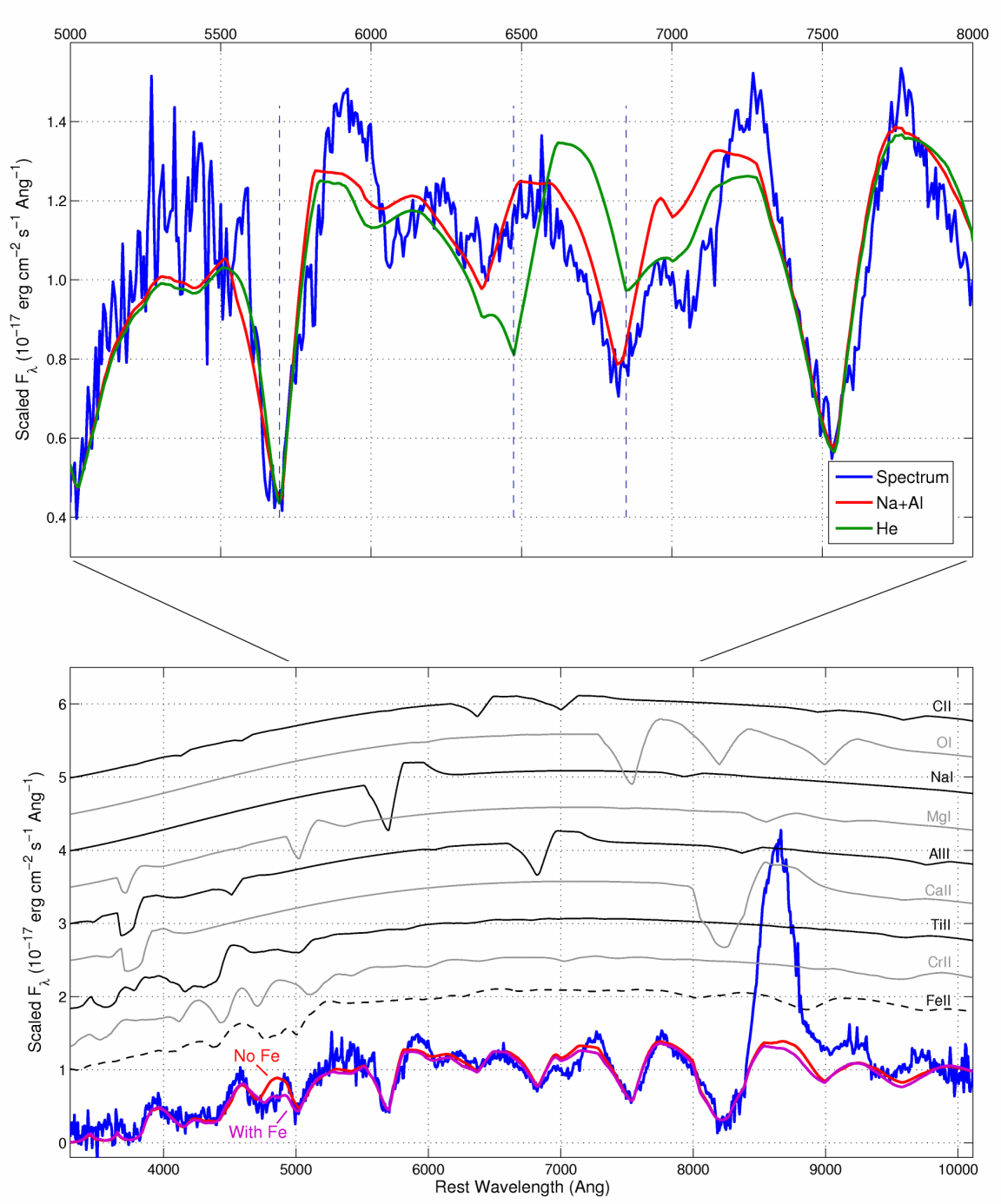

Figure 6.3 SYNOW fit to the Keck spectrum (+23 days) of SN 2010X. Lines contributed by each ion are shown. Fits with (purple) and without (red) Iron are overplotted on the data (blue). **Top Panel:** The dilemma of whether SN 2010X has Helium or a combination of Sodium and Aluminum. The vertical dashed lines show Helium at 9500 km s^{-1}. In non-LTE, the singlet transition of λ6678 may be suppressed relative to the λ7065 and λ5876 triplet transition Helium lines.

at +23d) than SN 2010X. Consistent with the SYNOW fit shown in Poznanski et al. 2010, the elements in common between the two supernovae are O I, C II and Mg II. The primary difference is the presence of Ca II in SN 2010X and presence of S II in SN 2002bj. We re-fit the spectrum of SN 2002bj with the same elements as in SN 2010X. We find that the presence of Al II vs. He I is just as ambiguous for SN 2002bj as SN 2010X. Similar to SN 2010X, including Fe II improves the fit but the presence of Fe-group elements in SN 2002bj is not conclusive.

6.5 Modeling the Light Curve

The excellent match between the normalized light curves of SN 2010X and SN 2002bj (see Figure 6.1) suggests that these two SNe belong to the same class of explosions. Combining the two data sets allows a robust determination of the rise time[4] ($\tau_r \approx 6\,\mathrm{d}$) and the subsequent exponential decay ($\tau_d \approx 5\,\mathrm{d}$).

The peak bolometric luminosity of SN 2010X is $L_{\rm peak} = 10^{42}\,\mathrm{erg\,s^{-1}}$. While the expansion speed varies from 12,000 $\mathrm{km\,s^{-1}}$ at early times to 9,000 $\mathrm{km\,s^{-1}}$ at late times, we accept $v_s \approx 10,000\,\mathrm{km\,s^{-1}}$ as a representative value.

The rise time in an explosion is the geometric mean of the initial photon diffusion timescale and the initial hydrodynamic time scale[5]. Thus, ${\tau_r}^2 \propto \kappa M_{\rm ej}/v_s$ where κ is the opacity. Assuming that the mean opacity of SN 2010X is the same as that for SNe Ia events, (for which, following Hayden et al. 2010, we adopt the following: $M_{\rm ej} \approx 1.4\,M_\odot$, $v_s = 10^9\,\mathrm{cm\,s^{-1}}$ and $\tau_r \approx 17.5\,\mathrm{d}$), we obtain $M_{\rm ej} \approx 0.16\,M_\odot$. This gives an explosion energy, $E_0 = 1/2 M_{\rm ej} v_s^2 \approx 1.7 \times 10^{50}\,\mathrm{erg}$.

Next, we investigate a physical model that satisfactorily accounts for the rise time, the decay time, the peak luminosity and the expansion velocity.

6.5.1 Pure Explosion

The simplest model is an explosion in which all the explosive energy (E_0) is deposited instantaneously into the ejecta. The peak luminosity is then $E_0/t_d(0)$ where $t_d(0) \propto \kappa M_{\rm ej}/R_0$ is the initial photon diffusion time; here, R_0 is the radius of the progenitor. Following peak

[4] time from explosion to peak brightness

[5] The derivation can be found in the textbooks, Arnett 1996 and Padmanabhan 2001.

luminosity, the decay is rapid: $\log(L) \propto -(t/\tau_r)^2$. The virtue of this model is that one can obtain an arbitrarily rapid rate of decay since, over any limited stretch of time, the light curve can be approximated by a linear decay with the desired value for the slope.

For SN 2010X, we find $R_0 \sim 4 \times 10^{12}$ cm. The large inferred radius would make sense if the progenitor had an envelope (as in type II supernovae). The absence of hydrogen at any phase of the supernova (see § 6.4) argues strongly against this model. Hence, we reject this hypothesis.

6.5.2 Radioactivity Powered Explosion

The next level of models is that developed for SNe Ia explosions, where the peak luminosity and subsequent decay is governed by radioactive material present in the ejecta. In this model, expansion decreases the store of internal energy whereas radioactivity increases it. If the photon diffusion time-scale is long, most of the radioactive energy goes into expansion. Once the diffusion time-scale becomes smaller than the expansion time-scale, the light curve tracks the radioactive luminosity (Arnett 1982), provided that there is sufficient optical depth for the γ-rays emitted during radioactive decay to undergo multiple scatterings and lose their energy to electrons.

The primary source of luminosity in a SN Ia model is the heat provided by γ-rays emitted as ^{56}Ni decays to ^{56}Co and then to ^{56}Fe. In SNe Ia, the column density of the ejecta is thick enough to trap the γ-rays and successive Compton scatterings extract energy from the γ-rays (at least for the first month). However, given the small ejecta mass for SN 2010X, attention has to be paid to the possibility that γ-rays from decaying nuclei may escape without depositing their energy into the ejecta.

The electron (Thompson) optical depth is:

$$\begin{aligned} \tau_e &= n_e R \sigma_T = \frac{3}{4\pi} \frac{M_{\rm ej}}{m_p} \frac{Z}{A} \frac{\sigma_T}{R^2} \\ &\sim 9 \left(\frac{M_{\rm ej}}{0.16 M_\odot} \right) \left(\frac{t}{15\,{\rm day}} \right)^{-2} \end{aligned} \tag{6.1}$$

where Z is the atomic number, A is the mass number, m_p is mass of proton, σ_T is the Thompson cross-section and $R \sim 6(\mathrm{t/day})\,\mathrm{AU}$ is the radius at time t.

Thus, there appears to be sufficient optical depth at the epoch of peak luminosity to trap

most of the γ-rays. Thus, for SN 2010X, the peak luminosity of $10^{42}\,\mathrm{erg\,s^{-1}}$ corresponds to ^{56}Ni mass of about $0.02\,M_{\odot}$ — a very small amount by the standards of most supernovae. For SN 2002bj, the peak luminosity was $10^{43}\,\mathrm{erg\,s^{-1}}$ (Poznanski et al. 2010) and the inferred ^{56}Ni mass was correspondingly larger, $0.2\,M_{\odot}$.

Next, we use a fitting formula (as given in Kulkarni 2005; Equation 47) to estimate the fraction of γ-rays which are effectively absorbed inside the ejecta, $\eta(\tau_e)$. The kinetic energy of positrons (3.5% of $L_{\rm Co}$; Sollerman et al. 2002) dominates by day 51. Hence, the radiated luminosity, $L_{\rm rad} = (0.965\eta + 0.035)L_{\rm Co} + \eta L_{\rm Ni}$ where $L_{\rm Ni}$ is the radioactive power released by the decay of ^{56}Ni, and $L_{\rm Co}$ by the daughter ^{56}Co. In Figure 7.7, we display the luminosity due to radioactivity and that actually trapped in the ejecta — the latter shows a satisfactory agreement with the observations.

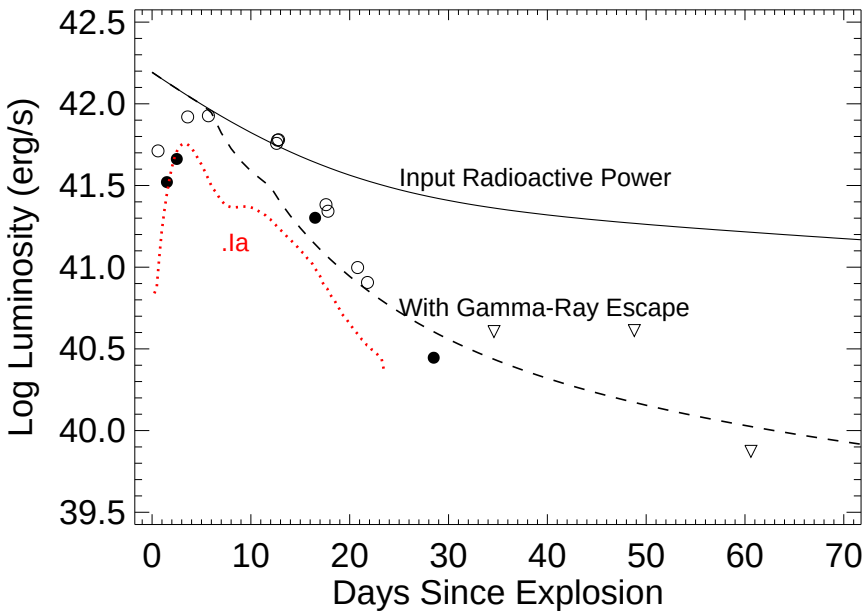

Figure 6.4 Shown above is the radioactive luminosity (solid line) and absorbed luminosity (dashed line) for the following model parameters: $M_{\rm ej} = 0.16\,M_{\odot}$, $M_{\rm Ni} = 0.02\,M_{\odot}$ and $v = 10^{9}\,\mathrm{cm\,s^{-1}}$. Also shown is a quasi-bolometric light curve of SN 2010X estimated by (a) computing $\nu \mathrm{F}_{\nu}$ in r-band (empty circles are detections, inverted triangles are upper limits), and (b) integrating the optical spectrum (filled circles). Also shown is a comparison to a ".Ia" light curve (red dotted line; Shen et al. 2010) assuming: $\mathrm{M_{wd}}$=1.2 $\mathrm{M_{\odot}}$, $\mathrm{M_{env}}$=0.05 $\mathrm{M_{\odot}}$, $\mathrm{M_{ej}}$=0.036 $\mathrm{M_{\odot}}$, $\mathrm{M_{Fe}}$= 0.005 $\mathrm{M_{\odot}}$, $\mathrm{M_{Ni}}$=0.02 $\mathrm{M_{\odot}}$, $\mathrm{M_{Cr}}$= 0.0002 $\mathrm{M_{\odot}}$.

6.5.2.1 Possible X-Ray Signature

An optically thin ejecta opens up the possibility of detecting the γ-rays (or degraded hard X-rays) emitted during β-decay. The *Swift* Observatory observed SN 2010X for 9758.7 s on MJD 55248.775 (9 days past peak). We constrain the X-ray flux[6] to be less than 0.00050 counts s^{-1} or $7.7{\times}10^{39}$ erg s^{-1}. By this epoch, our model shows that $L_\gamma \sim 10^{41}\,\mathrm{erg\,s^{-1}}$. Since photon number is conserved in scattering, the luminosity in the *Swift* band is expected to be a factor of 200 smaller and hence, the upper limit is not constraining.

6.6 Environment

The host of SN 2010X, NGC 1573A, is a small (1.6′ diameter), spiral galaxy variously classified as Sb (UGC) and SABbc (RC3). The host of SN 2002bj, NGC 1821, is a small (1.1′ diameter), barred irregular galaxy classified as IB(s)m. Both transients occurred close to the galaxy nucleus — 2.3 kpc for SN 2010X and 1.8 kpc for SN 2002bj. In Figure 6.5, we show the location of the supernovae in deep images of the galaxy.

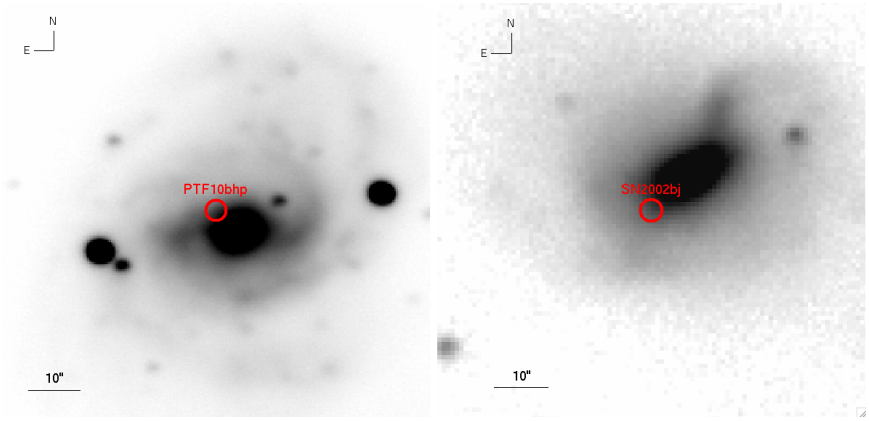

Figure 6.5 *Left:* R-band image of NGC 1573A, the host of SN 2010X, taken with the Large Format Camera on the Palomar 200-inch telescope. *Right:* Sum of all available Deepsky [7] (Nugent 2009) images of NGC1821, the host of SN2002bj.

[6] We note that the six photons in the XRT HPD PSF of 0.3′are likely from the galaxy nucleus.

6.7 Conclusion

To summarize, SN 2010X is the second member of a class of supernovae that declines exponentially on timescales shorter than 5 days. Relative to SN 2002bj, SN 2010X is less luminous by 1.5 mag ($M_R \approx -17$) and has higher velocities (10,000 km s^{-1}) by more than a factor of two. Both events have a small inferred ejecta mass. Both events are spectroscopically different from any other type I supernovae. The spectra for both supernovae can be modeled with mostly similar elements (C, O, Mg, Si, Ti and Fe). The evidence (or lack thereof) for Helium is not conclusive in both cases.

If SN 2010X is powered by radioactive ^{56}Ni, the combination of a rapid rise time and low peak luminosity constrains the Nickel mass to be small, $0.02\,M_\odot$. ^{56}Ni constitutes $\approx$13% of ejecta. However, under the same assumptions, ^{56}Ni would constitute bulk of the ejecta mass for SN 2002bj. Thus, while in both cases the ejecta mass remains the same, the nucleo-synthesis may be strongly variable. We also show that given the small ejecta mass, γ-rays from decaying ^{56}Ni can start escaping from the ejecta shortly after peak brightness. This early escape reasonably accounts for the rapid decay of the light curve of SN 2010X.

Perets et al. (2010a) have argued that S Andromeda (the first recorded SN in Andromeda) and SN 1939B (the first recorded SN in Virgo) are also like SN 2002bj. The claim primarily rests on rapid rise and rapid decay at early-time. It is of some interest to note that the late-time (2 months to nearly 1 year) decay rates, 0.03 mag/day for S Andromeda and 0.02 mag/day for SN 1939B (Perets et al. 2010a), are consistent with ^{56}Co decay (with some escape of γ-rays). A consistent explanation would require a two-zone model: comparable amount of ^{56}Ni in a slowly expanding core (to account for the late time light curve) and a rapidly expanding shell (to account for the rapid decay seen after peak brightness).

An alternative model is that the early-time emission is powered by another suitably rapidly decaying radio-active element(s). If powered solely by ^{48}Cr, 0.02 $M_\odot$ is adequate. Recently, Shen et al. 2010 computed models and observables for ".Ia" explosions (Bildsten et al. 2007a) powered by ^{48}Cr, ^{52}Fe and ^{56}Ni: rise time between 2–10 days, ejecta velocity between 9000–13000 km s^{-1}, peak luminosity between $0.5–5\times10^{42}$ erg s^{-1} and presence of Ca II and Ti II in the spectra. The properties of SN 2010X are consistent with all these predictions. Specifically, the light curve model presented for a core mass of 1.2 $M_\odot$ and envelope mass of 0.05 $M_\odot$ is a reasonable match (Figure 7.7). Furthermore, Shen et al.

2010 also discuss that the presence of Helium in the spectra may be a non-LTE effect.

If Aluminum is indeed present in the spectra, the avenue for a speculative scenario opens up. Neither ^{26}Al nor ^{27}Al is a product of Helium burning. Aluminum can be made via explosive burning of Neon and/or Carbon (Arnett & Bazan 1997; Woosley & Weaver 1980). Perhaps, SN 2010X is the outcome of accretion induced collapse of an O-Ne-Mg white dwarf (Metzger et al. 2009).

Finally, we note that the rich, star-forming environment of SN 2010X and SN 2002bj does not preclude a massive star origin. Fallback events, where a massive star collapses into a black hole, are also expected to be fast declining (Fryer et al. 2009; Moriya et al. 2010). However, the velocities expected from these models are significantly lower than observed and the spectra are more substantially dominated by intermediate mass elements.

Regardless of all these rich possibilities, it is clear that further progress in understanding the nature of these ephemeral transients would require a larger sample. Fortunately, PTF, especially as it moves to "dynamic" 1-day cadence (Law et al. 2009) targetting nearby galaxies and clusters, is well equipped to annually find a few such events. Late-time photometry is important to look for tell-tale signatures of ^{56}Co decay. Sensitive optical (or better still, ultra-violet) spectroscopy may directly reveal the radioactive element(s) powering these events. It is also not inconceivable (given the history of S Andromeda and SN 1939B) that we will be lucky enough to observe a local analog of such an event with the hard X-ray mission, NuSTAR (Harrison et al. 2010).

Acknowledgments

MMK thanks the Gordon and Betty Moore Foundation for a Hale Fellowship in support of graduate study. MMK thanks the Pumarth Headquarters in Indore, India for their warm hospitality while writing this manuscript.

We thank the referee for accepting this paper on a timescale faster than that characterizing the rapid photometric evolution of this supernova!

We would like to acknowledge the following discussions: MMK & Paolo Mazzali, AGY & David Branch, SRK & Xiaofeng Wang, DAH & Ryan Foley, MMK & Rollin Thomas. We are grateful to the staff of the Gemini Observatory and Swift Observatory for efficiently executing TOO triggers. We thank the librarians who maintain the ADS, the NED, and SIMBAD data systems.

The Weizmann Institute PTF participation is supported by grants to AGY from the Israel Science Foundation and the US-Israel Binational Science Foundation. EOO and DP are supported by an Einstein Fellowship. SBC is grateful for support from Gary and Cynthia Bengier and the Richard and Rhoda Goldman Fund. Computational resources and data storage were contributed by NERSC, supported by U.S. DoE contract DE-AC02-05CH11231. PEN acknowledges support from the US DoE contract DE-FG02-06ER06-04.

Table 6.1. Optical Light Curve of PTF 10bhp

MJD	Filter	Mag	Facility
55207.3	r	<20.91	Palomar 48-in
55207.4	r	<20.85	Palomar 48-in
55213.2	r	<20.48	Palomar 48-in
55221.2	r	<20.42	Palomar 48-in
55234.1	r	17.95 ± 0.15	Rich
55237.1	r	17.43 ± 0.12	Rich
55239.2	r	17.41 ± 0.19	Brimacombe
55246.1	r	17.84 ± 0.09	Palomar 48-in
55246.2	r	17.79 ± 0.10	Palomar 48-in
55246.3	r	17.78 ± 0.09	Palomar 48-in
55246.3	r	17.83 ± 0.09	Palomar 48-in
55251.1	r	18.77 ± 0.12	Palomar 48-in
55251.3	g	19.61 ± 0.18	LCOGT/FTN
55251.3	r	18.87 ± 0.10	LCOGT/FTN
55251.3	i	18.74 ± 0.12	LCOGT/FTN
55254.3	g	21.02 ± 0.34	LCOGT/FTN
55254.3	r	19.74 ± 0.13	LCOGT/FTN
55254.3	i	19.57 ± 0.14	LCOGT/FTN
55255.3	r	19.96 ± 0.11	LCOGT/FTN
55256.3	g	<20.66	LCOGT/FTN
55256.3	i	20.39 ± 0.17	LCOGT/FTN
55268.1	r	<20.72	Palomar 48-in
55282.3	r	<20.70	LCOGT/FTN
55294.1	r	<22.55	Palomar 200-in

Chapter 7

Yet Another Class in the Gap: Calcium-rich Halo Transients*

Mansi M. Kasliwal[1], S. R. Kulkarni[1], Avishay Gal-Yam[2], Lars Bildsten[3,4], Robert M. Quimby[1], Eran O. Ofek[1], Assaf Horesh[1], Peter Nugent[5], Mark Sullivan[6], D. Andrew Howell[4,7], Ofer Yaron[2], Iair Arcavi[2], Sagi Ben-Ami[2], Assaf Sternberg[2], Dong Xu[2], S. Bradley Cenko[8], Dovi Poznanski[5,8], Joshua S. Bloom[8], Alex Filippenko[8], Jeff Silverman[8], Nicholas M. Law[9], Neil Gehrels[10], Richard Dekany[11], Gustavo Rahmer[11], David Hale[11], Janet Jacobsen[5], Roger Smith[11], Jeff Zolkower[11], Viswa Velur[11], Richard Walters[11], John Henning[11], Khanh Bui[11] & Dan McKenna[11]

[1] Cahill Center for Astrophysics, California Institute of Technology, Pasadena, CA, 91125, USA

[2] Benoziyo Center for Astrophysics, Faculty of Physics, The Weizmann Institute of Science, Rehovot 76100, Israel

[3] Department of Physics, University of California Santa Barbara, Santa Barbara, CA 93106, USA

[4] Kavli Institute of Theoretical Physics, University of California Santa Barbara, Santa Barbara, CA 93106, USA

[5] Computational Cosmology Center, Lawrence Berkeley National Laboratory, 1 Cyclotron Road, Berkeley, CA 94720, USA

[6] Department of Physics, Oxford University, Oxford, OX1 3RH, UK

[7] Las Cumbres Observatory Global Telescope Network, Inc, Santa Barbara, CA, 93117, USA

[8] Department of Astronomy, 601 Campbell Hall, University of California, Berkeley, CA 94720-3411, USA

[9] Dunlap Institute for Astronomy and Astrophysics, University of Toronto, 50 St. George Street, Toronto M5S 3H4, Ontario, Canada

[10] NASA-Goddard Space Flight Center, Greenbelt, MD 20771, USA

[11] Caltech Optical Observatories, California Institute of Technology, Pasadena, CA 91125, USA

Abstract

We present two mysterious transients (PTF 09dav, PTF 10iuv) with five distinguishing characteristics: peak luminosity in the gap between novae and supernovae ($M_R \approx -15$), rapid photometric evolution ($t_{rise} \approx 12$ days), large photospheric velocities ($\approx 10{,}000$ km s^{-1}), early spectroscopic evolution into nebular phase (≈ 3 months) and nebular spectra dominated by Calcium. Additionally, both transients are located 40 kpc away from their putative hosts and have no underlying host brighter than -11. We present extensive follow-up which rules out standard thermonuclear and core-collapse explosions. If the progenitor is a massive star, a non-standard channel specific to a low-metallicity environment needs to be invoked (e.g., ejecta fallback leading to black hole formation). If the progenitor is a white dwarf, we need a scenario that can explain both hydrogen in the nebular phase (e.g., shockfront interaction with a previously ejected nova shell) and preference for remote locations (e.g., age).

7.1 Introduction

In the past decade, supernova surveys targeting nearby, luminous galaxies have been immensely successful as the total starlight searched is significantly larger than blind pointings of equal area. Recently, untargeted wide-angle transient surveys have also been successful with the added advantage of finding supernovae independent of a host galaxy bias. The Palomar Transient Factory (PTF; Law et al. 2009; Rau et al. 2009b) has an ongoing Dynamic Cadence experiment that combines the advantages of both a targeted and an

*A version of this chapter will shortly be published in *The Astrophysical Journal*, and is reproduced by permission of the AAS.

untargeted survey. This experiment searches wide-angle pointings on local ($d < 200$ Mpc) galaxy light concentrations at a 1-day cadence to a depth of 21 mag. The depth, cadence and locality allows us to find transients fainter, faster and rarer than supernovae. Furthermore, this facilitates the discovery of intra-cluster transients as well as transients in the farflung outskirts of their host galaxies.

The location of a transient explosion has long been exploited as a clue to determining its nature. It has been suggested that the classical nova population is bimodal, depending on whether it is in the disk or bulge of the galaxy (Shafter et al. 2011). Several studies of supernova host galaxy properties, as well as the site of the supernova within the host galaxy, have been undertaken (van den Bergh 1997; Prieto et al. 2008a; Hakobyan et al. 2009; Boissier & Prantzos 2009; Anderson & James 2009). Core-collapse supernovae (SN CC) and more luminous Type Ia supernovae (SN Ia) are preferentially found in late-type galaxies. Type Ic supernovae are not found in dwarfs (Arcavi et al. 2010) and Type Ibc supernovae are more centrally concentrated (Anderson & James 2009). Although 15% of the stellar mass is expected to be in the inter-galactic medium, only a handful of intra-cluster supernovae have been discovered (Gal-Yam et al. 2003; Sand et al. 2011).

The sample of discoveries from the Palomar Transient Factory is homogenous and and has been systematically followed up. We present the offset distribution of all PTF supernovae with a redshift < 0.1 in § 1. The focus of this paper are two unclassified transients which are also outliers on the offset distribution: PTF 09dav and PTF 10iuv. These two transients have four distinguishing characteristics. Both are offset from their hosts by 40 kpc and have no underlying host to a limiting absolute magnitude of -11. Both transients have peak luminosities in the gap between novae and supernovae. Both rise and decline much faster than supernovae. Both entered the nebular stage soon after explosion and showed peculiar Calcium-dominated ejecta. These properties are reminiscent of only one other explosion discussed in the literature, SN 2005E (Perets et al. 2010b).

We present observations of PTF09dav and PTF10iuv in § 3 and § 4 respectively, analysis in § 5, discussion in § 6 and conclusion in § 7.

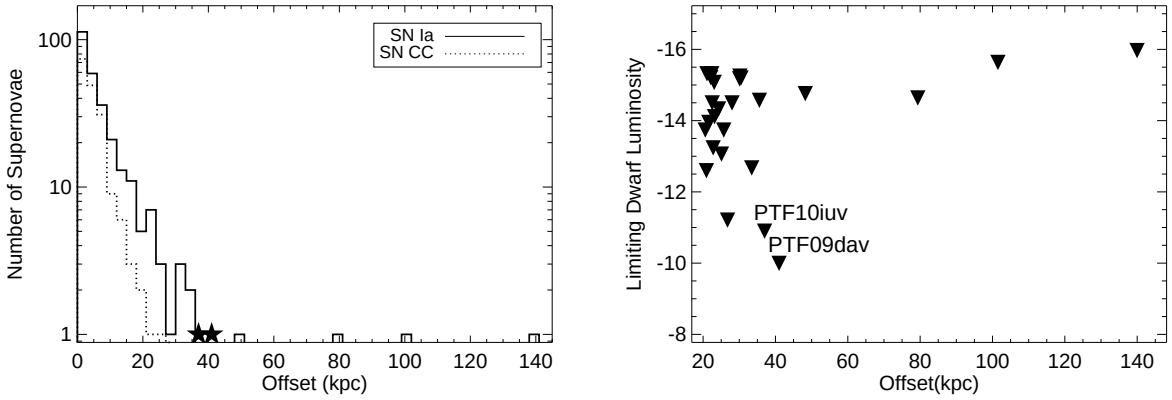

Figure 7.1 *Left:* Histogram of offsets from host galaxy for 520 spectroscopically classified transients discovered by the Palomar Transient Factory with z<0.1. Stars denote the location of PTF 10iuv and PTF 09dav. *Right:* Upper limits for an underlying dwarf host (M_R) for transients with offset greater than 20 kpc.

7.2 Offset Distribution of PTF Supernovae

In just over a year, the Palomar Transient Factory discovered and spectroscopically confirmed 1040 extragalactic transients. We limit the study of the offset distribution of PTF supernovae to a sub-sample of of 520 transients with $z < 0.1$, in order to constrain the luminosity of underlying host galaxies to -16. We compute precise offsets from the host galaxies for each transient and the resulting histogram is shown in Figure 7.1. We split the population into core-collapse supernovae and thermonuclear supernovae. We find that the core-collapse and thermonuclear population show similar distributions out to ~ 9 kpc suggesting that the average distribution is proportional to star light. Beyond 9 kpc, the thermonuclear population shows a heavy extended tail suggesting a second parameter governing their rate or perhaps even two progenitor populations.

Next, we take a closer look at the population with offsets larger than 20 kpc. We co-add available pre-explosion data to derive limiting magnitudes on a dwarf satellite host at the location of the supernova (see Figure 7.1). Of the 520 transients, 9 SN Ia, 0 SN CC and 2 unclassified transients have offsets larger than 30 kpc. PTF 09cex, PTF 10fjg, PTF 10xua, PTF 10xgb and PTF 10xgc (30–36 kpc) have spectroscopically confirmed host redshifts. PTF 10qht (79 kpc) and PTF 10qyx (48 kpc) are likely intra-cluster supernovae. The fur-

thest offset SN Ia, PTF10ops (140 kpc) is the subject of another paper (Maguire et al. in prep).

Note two more outliers on this distribution which are unclassified: PTF 09dav is offset from a spiral host by 40 kpc; PTF 10iuv is in a galaxy cluster with early-type and late-type galaxies and the closest galaxy is 37 kpc away. The limiting dwarf host luminosities are −10 and −11 for PTF 09dav and PTF 10iuv respectively.

7.3 Observations: PTF09dav

We presented the discovery, light curve and photospheric spectra of PTF09dav in a companion paper by Sullivan et al. 2011 (hereafter, Paper I). Here we present late-time imaging and nebular spectroscopy of PTF09dav.

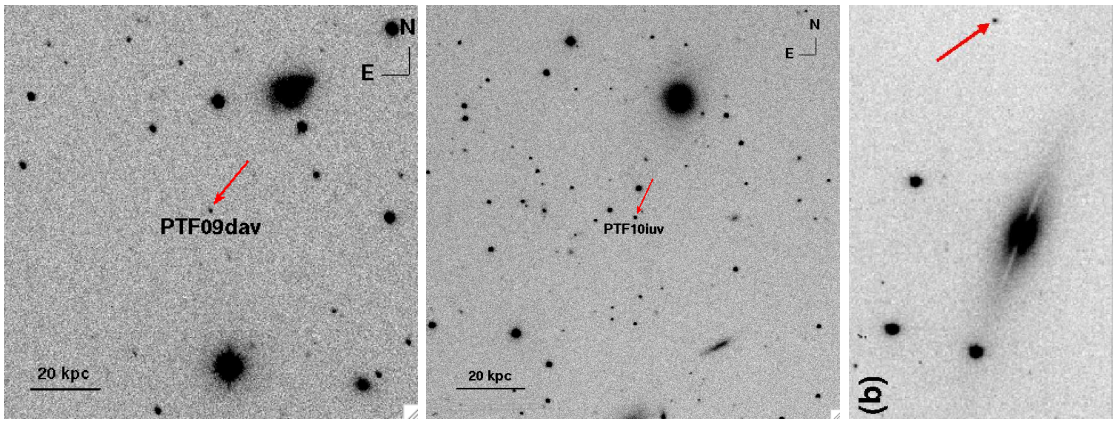

Figure 7.2 *Left:* PTF 09dav is offset from its late-type host by 40 kpc. *Center:* PTF 10iuv is offset from a galaxy group with early-type and late-type galaxies, the nearest host is 37 kpc away. *Right:* SN 2005E (Perets et al. 2010) is offset from its edge-on host by 23 kpc.

7.3.1 Late-time Imaging

We obtained deep imaging in the g-band and R-band filters at the position of PTF09dav with the Low Resolution Imaging Spectrograph (LRIS; Oke et al. 1995) on the Keck I telescope on UT 2010 May 15.603 and Jul 9.584. We registered these images with a Palomar 60-inch image of PTF09dav. No source is detected to a 3σ limiting magnitude of 26 mag (Table 7.1, Figure 7.3). This constrains any satellite, dwarf host to be fainter than $M_g =$

-10.1.

We obtained deep imaging in the K'-band with Laser Guide Star Adaptive Optics (LGS-AO; Wizinowich et al. 2006; van Dam et al. 2006) on the Keck II telescope and the Near Infrared Camera 2 (NIRC2). On 2010 Jun 17.568, we obtained 10 images of 10 s co-added integrations. Zeropoint was derived relative to the 2MASS catalog (Skrutskie et al. 2006). No source was detected to a 3σ limiting magnitude of 21.1 mag.

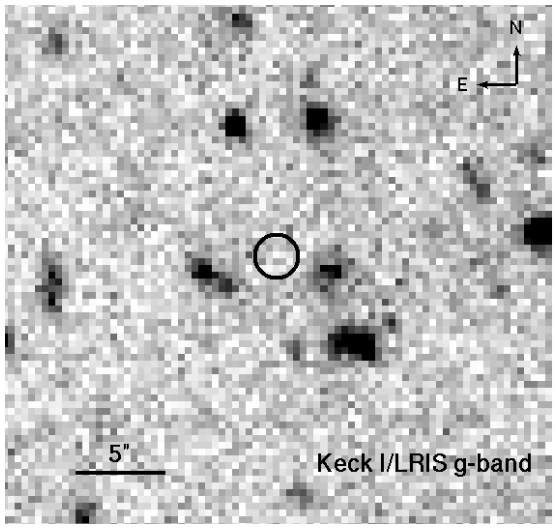

Figure 7.3 Deep late-time g-band imaging with Keck I/LRIS showing no host galaxy under the position of PTF09dav. The registration accuracy is $0.241''$. We denote the position of PTF09dav with a 5σ position error circle.

7.3.2 Nebular Spectroscopy

On 2009 November 11, only three months after maximum light, a spectrum with LRIS on Keck I revealed that PTF09dav had become nebular. The timescale to become nebular was surprising, as it was faster than typical supernovae by a factor of few. Furthermore, only two emission features are seen — Hα and [Ca II]. The width, redshift and flux of the lines is summarized in Table 7.2. The absence of Ca II IR triplet is indicative of a low circumstellar density. The presence of Hα is usually interpreted as the interaction of a massive star wind with the circumstellar environment. However, no Hα was seen in the photospheric spectra presented in Paper I. These characteristics of the nebular spectrum are unprecedented and no match can be found in supernova libraries.

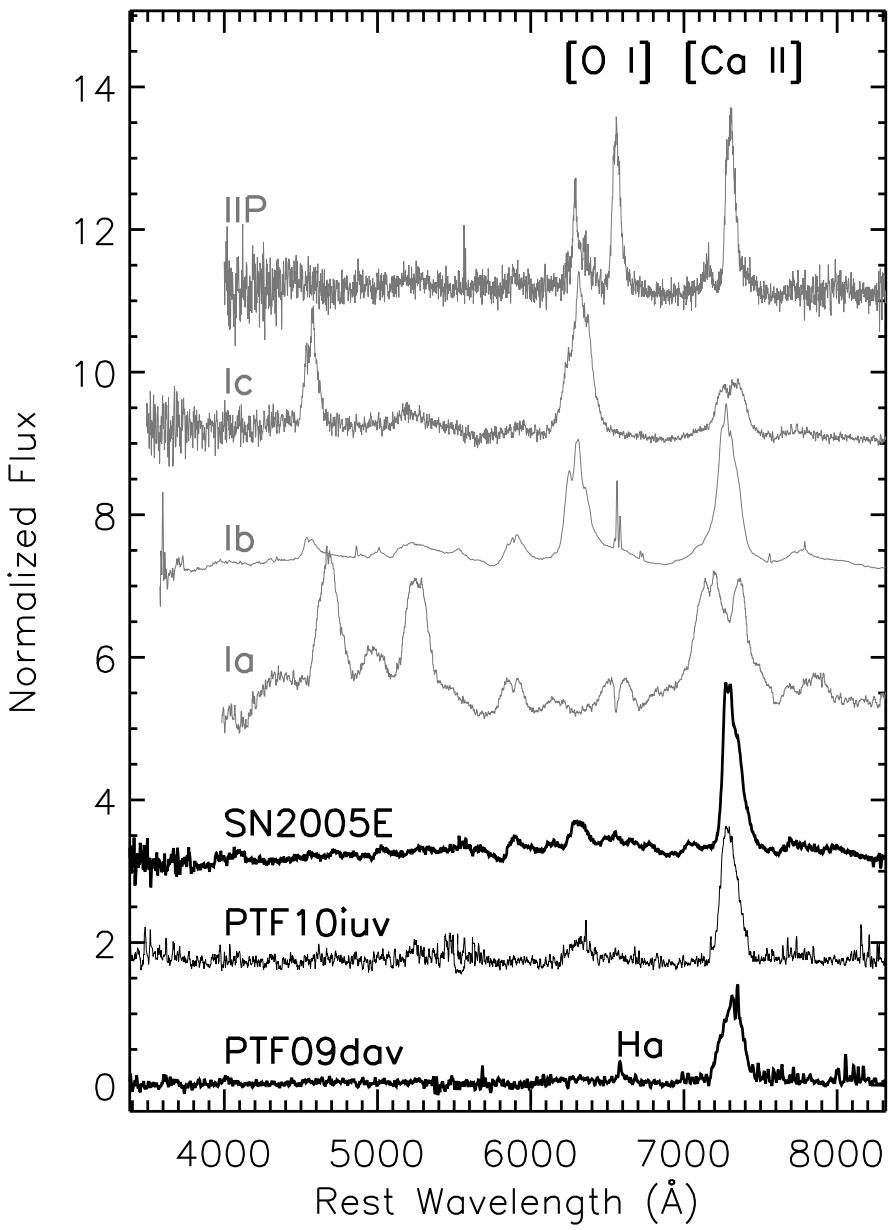

Figure 7.4 Nebular Spectra of PTF09dav, PTF10iuv and SN2005E. All three are very Calcium-rich. Also shown for comparison, nebular spectra of a Type Ia (SN1986G +257 d; Asiago Catalog), Type Ib (SN2007C +165 d; (Taubenberger et al. 2009)), Type Ic (SN2002ap +249 d; (Gal-Yam et al. 2002)) and Type IIP (SN2004et +454 d; (Sahu et al. 2006)) supernova. The nebular spectra of Type Ia supernovae are dominated by [Fe II], [Fe III] and [Co III] lines. The nebular spectra of core-collapse supernovae has a much lower ratio of Calcium to Oxygen.

7.4 Observations: PTF10iuv

7.4.1 Discovery and Light Curve

On UT 2010 May 31.241, the Palomar Transient Factory discovered a new transient, PTF 10iuv. The location of this transient was α(J2000) = $17^h16^m54.27^s$ and δ(J2000) = $+31°33'51.7''$ and brightness was $R = 21.2$ mag. We monitored the light curve of this transient with the Palomar 60-inch (P60) telescope in $Bgriz$ filters for three months. Late-time photometric observations were taken with the Large Format Camera (LFC) on the Palomar 200-inch telescope and LRIS on the Keck I telescope.

Data was reduced following standard procedures and aperture photometry was performed. Photometric calibration was done relative to photometry of field stars from the Sloan Digital Sky Survey (Abazajian et al. 2009). A common set of calibration stars were chosen for P48, P60, LFC and LRIS data for consistency. Conversion from $ugriz$ to B-band was done following Jordi et al. 2006.

The light curve is summarized in Figure 7.5. PTF10iuv peaked on Jun 10 with R=19.0 mag. It rapidly rose by 3 mag in 12 days, followed by a rapid decline at the rate of 1 mag in 12 days for one month. Subsequently, PTF 10iuv evolved slowly at the rate of 0.02 mag day^{-1} for three months, followed by 0.005 mag day^{-1}. The color was neither extremely red nor blue. It evolved from $g - i \approx 0.4$ near maximum to $g - i \approx 0.7$ one month later.

7.4.2 Spectroscopy

On Jun 7, we obtained a classification spectrum using ISIS on the WHT telescope. Subsequently, we continued to monitor the evolution with the Keck I (LRIS) and Keck II (DEIMOS) telescopes until the spectra became completely nebular (Figure 7.6).

The spectra evolved to show prominent Helium features, resembling Type Ib spectra. The Calcium lines become stronger with time, especially [Ca II] relative to O I. As with PTF09dav, the spectrum of PTF10iuv also became nebular in only 3 months. Both showed prominent Calcium emission (Table 7.2, Figure 7.4). Unlike PTF09dav, PTF10iuv showed O I emission.

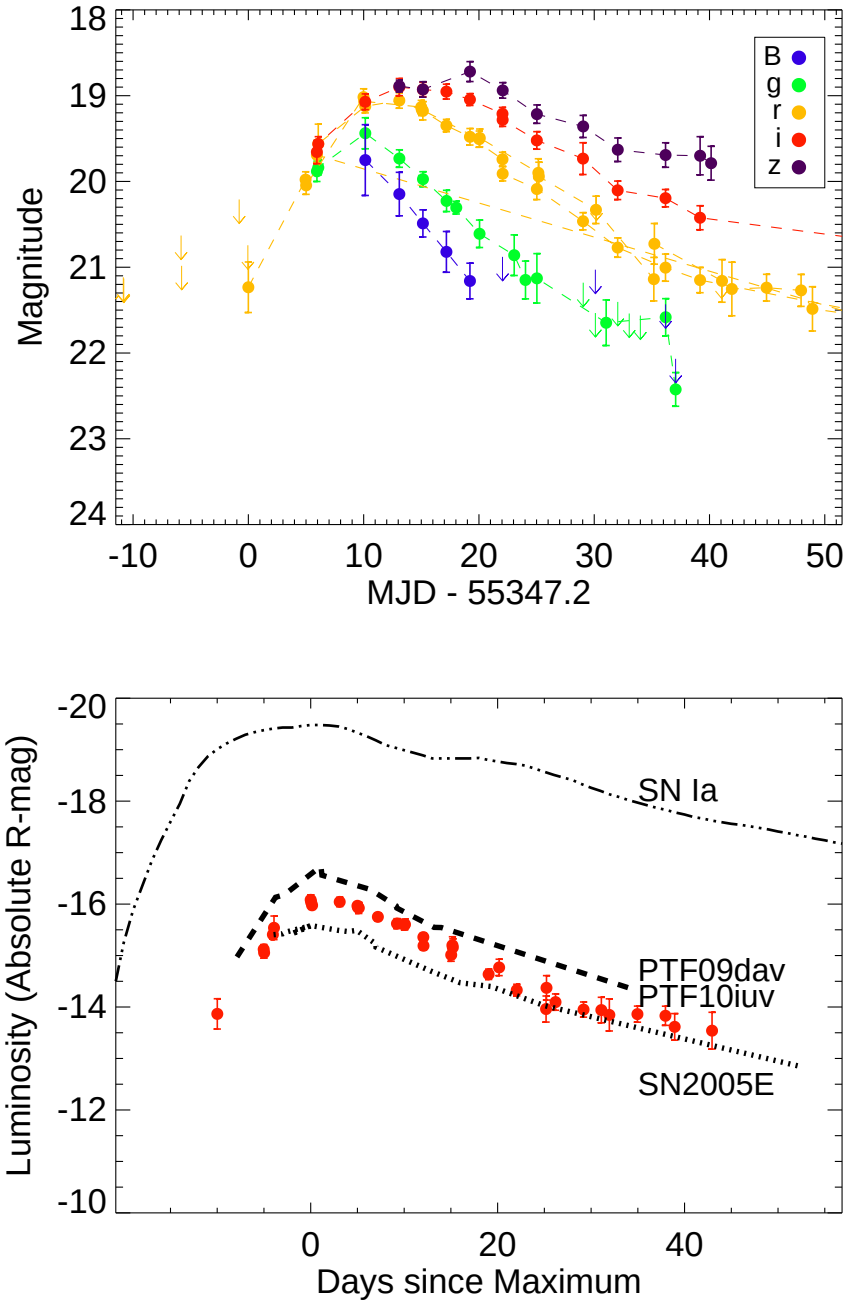

Figure 7.5 Light curve of PTF10iuv. *Top:* Note the rapid rise of 3 mag in 12 days, followed by the rapid decline at the rate of 1 mag in 12 days. *Bottom: R*-band light curves of PTF 10iuv (circles), PTF 09dav (dashed line) and SN 2005E (dotted line). All three events are subluminous, red and evolve very rapidly compared to supernovae. For comparison, we show a normal Type Ia supernova (dot-dash line).

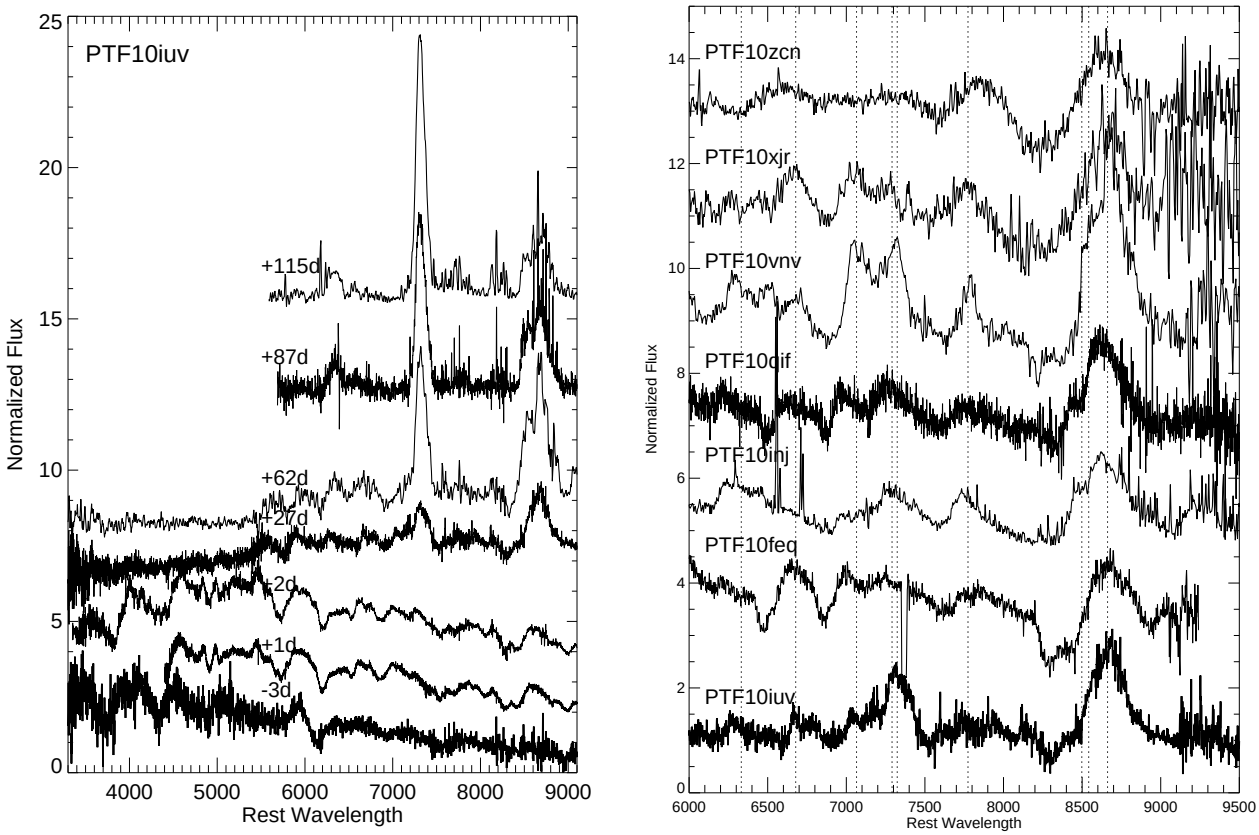

Figure 7.6 *Left:* Spectral evolution of PTF 10iuv. *Right:* Comparison of PTF10iuv to other Type Ib supernovae about a month after maximum light. Note the strength of the [Ca II] line relative to O I.

Table 7.1. Late-time Photometry of PTF09dav

Date UT 2010	Phase days	Facility	Exposure sec	Filter	Magnitude mag
May 15.612	279.7	Keck I/LRIS	1230	g	>26.0
May 15.614	279.7	Keck I/LRIS	1030	R	>24.8
Jun 17.568	313.7	Keck II/NIRC2	100	K'	>21.1
July 9.584	334.7	Keck I/LRIS	1450	g	>25.4
July 9.584	334.7	Keck I/LRIS	1200	R	>26.2

7.4.3 Radio Observations

We observed PTF 10iuv with the Expanded Very Large Array on 2010 Aug 25.060. We observed in X-band (8.46 GHz) and added together two adjacent 128 MHz subbands with full polarization to maximize continuum sensitivity. Amplitude and bandpass calibration was achieved using the archival value of flux for J1721+3542, and phase calibration was carried out every 10 min by switching between the target field and the point source J1721+3542. The visibility data were calibrated and imaged in the *AIPS* package following standard practice.

The transient was not detected with a 3σ upper limit of 189μ Jy. This corresponds to $L_\nu < 2.0 \times 10^{27}$ erg s^{-1} Hz^{-1}.

7.5 Analysis

7.5.1 Modeling the Light Curve: Radioactivity?

The light curve of PTF 10iuv is very well-sampled. The rising portion of the light curve can constrain the ejecta mass and the late-time decay can constrain the radioactive mass. Therefore, we can test the hypothesis of whether this explosion is radioactively powered by Nickel-56 as in Type Ia supernovae.

$M_{ej} \propto v\ t_r^2$ (Arnett 1982). Therefore, assuming the same opacity, we can derive an ejecta mass by scaling relative to a normal Type Ia supernova with parameters $1.4\,M_\odot$,

Table 7.2. Lines in Nebular Spectra

Transient	Ion	Line Center Å	Shift[a] km s^{-1}	Flux erg cm^{-2} s^{-1}	Width Å	Velocity Width km s^{-1}
PTF09dav	Hα	6820.4	840	7.6×10^{-17}	23.5	1000
PTF09dav	[Ca II]	7579.1	250	2.0×10^{-15}	166.1	6600
PTF10iuv	O I	6467.7	−460	1.7×10^{-16}	170.8	8090
PTF10iuv	[Ca II]	7465.4	−410	8.0×10^{-16}	134.2	5510
PTF10iuv	Ca II	8827.3	2150	9.4×10^{-16}	312.8	10950
SN2005E	O I	6360.6	−1120	2.0×10^{-15}	107.8	5110
SN2005E	[Ca II]	7367.0	−17	1.5×10^{-14}	127.6	5240
SN2005E	Ca II	8710.4	2530	2.7×10^{-14}	299.0	10470

Note. — [a] Note that this shift is computed relative to the velocity of the putative host galaxy.

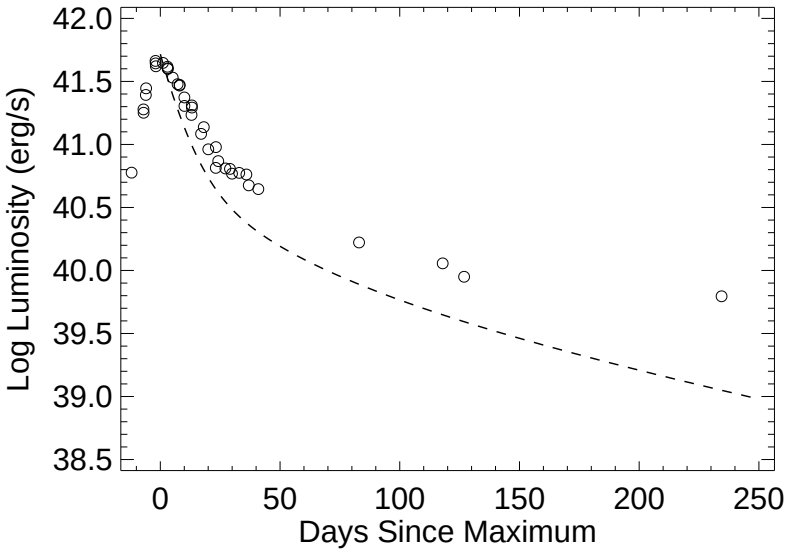

Figure 7.7 Modelling the light curve of PTF 10iuv (empty circles) with radioactive Nickel-56 decay (dashed line). We assumed an ejecta mass of 0.46 $M_\odot$ and Nickel mass of 0.016 $M_\odot$.

11000 km s^{-1} and 17.4 days. PTF 10iuv has a rise-time of 12 days, average photospheric velocity of 7600 km s^{-1} and hence, an ejecta mass of 0.46 $M_{\odot}$. PTF 09dav has the same rise time but a lower velocity of 6000 km s^{-1}, giving an ejecta mass of 0.36 $M_{\odot}$. There is no data to constrain the rise-time of SN2005E. Assuming it was also 12 days and using its photospheric velocity of 11,000 km s^{-1}, we get an ejecta mass of 0.67 $M_{\odot}$.

For PTF 10iuv, given the peak luminosity of 4.6×10^{41} erg s^{-1} and 12 day rise, we can derive a Nickel-56 mass of 0.016 $M_{\odot}$. However, we find that the late-time photometry is inconsistent with what is expected from radioactive decay of Nickel-56 (Figure 7.7). Thus, there should either be a radioactive species other than Nickel-56 or another source powering the light curve. Modeling of different combinations of other additional radioactive species (Chromium-48, Titanium-44 and Iron-52) in the context of Helium shell detonations on small (Waldman et al. 2010) and large CO white-dwarf cores (Shen et al. 2010) has been undertaken. These efforts were limited by the missing light curve data in the rising and very late phase of SN 2005E. The well-sampled light curve of PTF 10iuv should be able to better constrain these models.

7.5.2 Comparison to Type Ia and Type Ib Supernovae

In Paper I, we discuss that although the photospheric spectra of PTF 09dav share some similarities to Type Ia supernovae, there are several differences: (i) PTF 09dav does not obey the Phillips relation (not even the modified relation for subluminous Type Ia that is obeyed by the faintest SN Ia 2007ax; Kasliwal et al. 2008j), (ii) The photospheric spectra have Scandium and Strontium (elements usually seen only in core-collapse supernovae), (iii) Here, we show that the nebular spectrum of PTF 09dav does not show any Fe-peak elements, which is inconsistent with nebular spectra of all Type Ia supernovae (Figure 7.4).

The photospheric spectra of PTF 10iuv around maximum light resemble Type Ib supernovae. However, a month after maximum, Calcium emission starts to become prominent. We have spectra at this phase of six other Type Ib supernovae from PTF (Figure 7.6). While the Calcium IR triplet becomes prominent for all the Type Ib supernovae as they evolve, the [Ca II] doublet is especially prominent for PTF 10iuv. PTF 10vnv and PTF 10inj also show [Ca II], but the relative flux ratio of [Ca II] to O I is much lower than that seen in PTF 10iuv. In the nebular phase, the flux ratio of [Ca II] to [O I] is also much lower for

Type Ib supernovae relative to PTF 10iuv (Figure 7.4). Furthermore, the light curve is less luminous by at least two magnitudes and evolves faster by at least a factor of two.

7.5.3 Constraint on Electron Density

Using the flux ratio between [Ca II] and Ca II IR triplet, we can constrain the density given a temperature. For PTF10iuv, the nebular spectrum at +87 d gives a ratio of 0.86 and the spectrum at +115 d gives a ratio of 1.8. For PTF09dav, the nebular spectrum at +94 d gives a ratio of >2.2 (assumed width of 300 Å, 3σ limit is 3×10^{-18} erg cm^{-2} s^{-1} Å^{-1}). For SN 2005E, the ratio at +65 d is 0.55 (Perets et al. 2010b). Following Figure 2 of Ferland & Persson 1989, assuming a temperature around 4500 K, the electron density is of the order of 10^9cm^{-3} and decreases by a factor of few in a couple of months.

7.5.4 Modeling the Nebular Spectra

Next, we estimate the mass of the dominant species in the ejecta using the nebular spectrum.

We estimate the oxygen mass based on the luminosity of the [O I] line in the nebular phase. We can assume the high density limit holds ($>10^6$ cm^{-3}) and estimate the oxygen mass as:

$$M_O = 10^8 f_{[OI]} D_{Mpc}^2 e^{(2.28/T_4)} M_\odot$$

(Uomoto 1986). Assuming a temperature of 4500 K, we get 0.025 $M_\odot$ of Oxygen for PTF 10iuv and 0.037 $M_\odot$ for SN 2005E. Note that the oxygen mass is consistent with the mass derived in Perets et al. 2010b. A cautionary note here is that this calculation is extremely sensitive to temperature. A difference of 500 K in temperature changes this estimate by a factor of two.

The luminosity in [Ca II] nebular emission for SN 2005E, two months after maximum was 2×10^{39} erg s^{-1} and the derived ejecta mass was 0.135 $M_\odot$ (Perets et al. 2010b). The [Ca II] nebular luminosity is a factor of 2.5 smaller for PTF 10iuv and factor of 2.6 larger for PTF 09dav relative to SN 2005E. Under similar conditions, this may be representative of the range in Calcium mass for these events.

Assuming an average ejecta velocity of 6000 km s^{-1} for three months and an average electron density of 10^9 cm^{-3}, we can derive the total number of electrons. Depending on

which species is dominant (e.g., Calcium, Hydrogen, Oxygen), we can roughly estimate the mass as $2\,M_{\odot}\frac{A}{40}\frac{0.5}{Z/A}$.

7.6 Discussion

The answer to the fundamental question of whether the progenitor of this class of transients is a white dwarf or a massive star is not clear. We discuss each of the two possibilities below.

7.6.1 A Massive Star?

Four lines of evidence suggest a massive star origin. First, the presence of Hα in emission in PTF 09dav suggest a massive star wind interacting with circumstellar medium. Second, the presence of Scandium and Strontium in the photospheric spectra of PTF 09dav suggests conditions (e.g., lower temperature) usually seen in core-collapse. Third, the absence of Fe-group elements seen in all thermonuclear explosions and similarity to nebular spectra of core-collapse (albeit with significantly enhanced Calcium) suggests this is a core-collapse. Fourth, the inconsistency of the light curve of PTF 10iuv with a radioactive Nickel-56 powered explosion and disobedience of the Phillips relation suggest this is not a regular Type Ia supernova.

The biggest challenge to this hypothesis are the deep broad-band, Hα and ultra-violet imaging limits against in situ star formation. Next, we discuss the odds of finding a massive star in such remote locations. Assuming that this is possible, we discuss possible explosion channels.

7.6.1.1 Star formation in the outskirts?

Perets et al. 2010b convincingly argue against the progenitors being hypervelocity stars formed in the disk. A more feasible option that allows massive stars to traverse large distances is tidal stripping during galaxy interactions. This is especially intriguing given the galaxy group surrounding the location of PTF 10iuv.

Star formation in intra-cluster environments has also been well studied. It has been shown that roughly 15% of the cluster's mass is in the intra-cluster medium. Both an old component and a young component are expected (Mullan et al. 2011; Williams et al.

2007). Sivanandam et al. 2009 show that 50% of metals come from intra-cluster supernovae. Mullan et al. 2011 presented a study of tidal tails of interacting galaxies and found young star clusters formed in situ in half the sample. Moreover, recent systematic surveys (Werk et al. 2010b, 2008) suggest that star formation in the far outskirts of non-interacting galaxies is also possible. About 10% of the galaxies in this study had outlying HII regions with offsets between 20 kpc and 40 kpc.

7.6.1.2 Fallback Supernova?

Assuming there was some in situ star formation, since the IMF is quite universal and varies little over a wide range of metallicity (e.g., Myers et al. 2011), one would expect regular core-collapse supernovae in the outskirts as well. However, the absence of regular core-collapse supernovae with offsets larger than 30 kpc in the PTF sample appears to be at odds with the progenitors being massive stars (Figure 7.1).

A possible resolution is if the fate of massive stars in very low metallicity environments is very different. Specifically, the lower metallicity in the outskirts lowers the mass-loss rate, and it is expected that a larger fraction of massive stars would collapse directly to a black hole (e.g., Heger et al. 2003, O'Connor & Ott 2011). Such a collapse results in a subluminous explosion or no explosion at all. This could explain both the small numbers of core-collapse supernovae in the outskirts and the dearth of regular Type Ib/c supernovae in low metallicity environments. This is also consistent with studies that show that regular Type Ib/c supernovae are more centrally concentrated relative to Type II supernovae (Anderson & James 2009). Some of the missing Type Ib/c explosions in low metallicity environments (outer parts of galaxies, dwarf galaxies) could be subluminous and short-lived fallback events. Fallback of some ejecta onto the proto-neutron star to form the blackhole could explain the low ejecta mass, fast evolution and absence of heavy elements observed in this class. It would not be surprising then that the first fallback events observed are located in the outskirts of their hosts.

An important caveat here is that PTF 10iuv and SN 2005E were hydrogen-free. The mass-loss would have to be tuned to be high enough to expel the hydrogen, low enough such that there is fallback on the core, yet not too low such that there is no explosion at all. Kawabata et al. 2010 proposed an alternate scenario where the hydrogen was removed

by close binary interaction.

7.6.2 A White Dwarf?

All other lines of evidence suggest a white dwarf origin. The absence of a dwarf satellite galaxy host to deep limits for all three events, combined with deep Hα and ultra-violet limits for SN 2005E, suggests that a recent episode of in situ star formation is unlikely.

If we invoke white dwarf scenarios, there are three options that explain the intermediate luminosity. First, accretion induced collapse (AIC) of a rapidly rotating white dwarf into a neutron star (Metzger et al. 2009). However, AIC predicts a spectrum dominated by intermediate mass elements, much higher velocities (0.1 c) and much more rapid rise (1 day) and decline (4–5 days) than what is observed. Second, a ".Ia" explosion following the final Helium flash in an ultra-compact white-dwarf white-dwarf binary (Bildsten et al. 2007a; Shen et al. 2010). The observed rise-time is too slow for a ".Ia" explosion. Third, a sub-Chandrashekhar mass white dwarf deflagration (Woosley & Weaver 1994) is also expected to give lower luminosity Type Ia supernovae. However, the late-time light curve and absence of Fe-peak elements in the nebular spectra are inconsistent with this model. The presence of Helium in SN 2005E and PTF 10iuv can be explained for some white dwarf models. However, the presence of hydrogen poses a major challenge to all three models.

One possible scenario to explain late-time hydrogen in a white-dwarf explosion is as follows: Consider a binary where mass-transfer is from a hydrogen rich companion star onto a white dwarf. This accretion initially proceeded at a low rate, resulting in a series of nova eruptions prior to the sub-Chandrashekhar explosion or Helium-shell detonation. The photons from the final explosion would eventually reach one of the previously ejected nova shells and the interaction would give Hα emission.

Quantitatively, the distance to this nova shell would be the speed of light multiplied by 95 days, i.e., 2.5×10^{17} cm. Given the velocity of 1000 km s^{-1} to traverse this distance, the nova eruption would then have occured 78 years ago. A rough estimate for the mass of hydrogen needed to sutain the observed luminosity is $0.0004\,\mathrm{M}_{\odot}\frac{t}{1\,hour}\frac{1}{n}$, where n is the number of times the same hydrogen atom gets excited in the time t.

7.7 Conclusion

Three transients, PTF 09dav, PTF 10iuv and SN 2005E, share the following common properties — low peak luminosity, fast photometric evolution, large photospheric velocities, quick evolution to nebular phase, Calcium-dominated ejecta and location in the outskirts of their putative host galaxies. This set of properties in conjunction with peculiarities specific to each of them (e.g., presence of hydrogen, scandium and strontium in PTF 09dav, intracluster environment of PTF 10iuv, strong constraints againt star formation in SN 2005E) warrants a creative modification of standard thermonuclear or standard core-collapse scenarios.

We can estimate a lower limit on the rate of this class of events by comparing to the rate of Type Ia supernovae discovered by PTF in the same volume in the same time. Within 200 Mpc, we found 100 Type Ia supernovae and 2 such events. Therefore, the rate is $>6\times10^{-7}\mathrm{Mpc}^{-3}\mathrm{yr}^{-1}$. We emphasize this is a lower limit as a few days of bad weather would be much more detrimental for finding these short-lived and lower luminosity transients compared to SN Ia. This rate of 2% relative to Type Ia supernovae is consistent with the relative rate of 7±5% estimated by (Perets et al. 2010b)[1].

To understand the origin, it is essential to first address whether the location is a red herring or the most important clue. Progress theoretically requires more quantitative modelling of the metallicity dependence of core-collapse to black holes scenario. Progress observationally requires a larger sample of discoveries as intensely followed up as PTF 10iuv. Fortunately, ongoing synoptic surveys such as the Palomar Transient Factory, are well-poised to uncover and follow-up new members of this class.

[1]Unfortunately, the other possible candidates from the KAIT survey which may belong to this class given some spectroscopic similarity have too poorly sampled light curves to constrain the photometric properties

Chapter 8

Summary

8.1 Framework of Explosions: 2011

I end how I began. The framework of cosmic explosions today (Figure 8.1) has been systematically colored with multiple, new populations of transients in the white spaces. I discuss the progress on understanding each of the new classes below:

1. *Observations of a ".Ia" Explosion:* PTF 10bhp (Chapter 6) can be reasonably argued to be a protypical ".Ia" explosion: short rise-time of 6 days, exponential decline of 5 days, peak luminosity of -17 mag, velocities of 9000 km s^{-1} and ejecta composition of Ca II, Ti II and He I. All lines of evidence appear to be consistent with a Helium detonation in an ultra-compact white dwarf (AMCVn) system. The only other supernova with as fast a photospheric evolution is SN 2002bj (identified as so eight years after explosion by an archive search; Poznanski et al. 2010). However, the lower velocities (4000 km s^{-1}) and the higher peak luminosity (-18.5 mag) make the case for SN 2002bj as a ".Ia" explosion less clear. An unfortunate circumstance with PTF 10bhp was that it was too close to the sun at the time of discovery. With future events, efforts to better quantify the late-time photometric evolution and the late-time nebular spectrum to directly measure ejecta masses will be undertaken. There has been steady progress on constraining the Galactic AMCVn population (Roelofs et al. 2007; Nelemans et al. 2001) and recently, candidates that will merge within the Hubble time have also been identified (Kilic et al. 2011a). Further progress here requires a larger sample to constrain the rates and hence, constrain the fraction of AMCVn

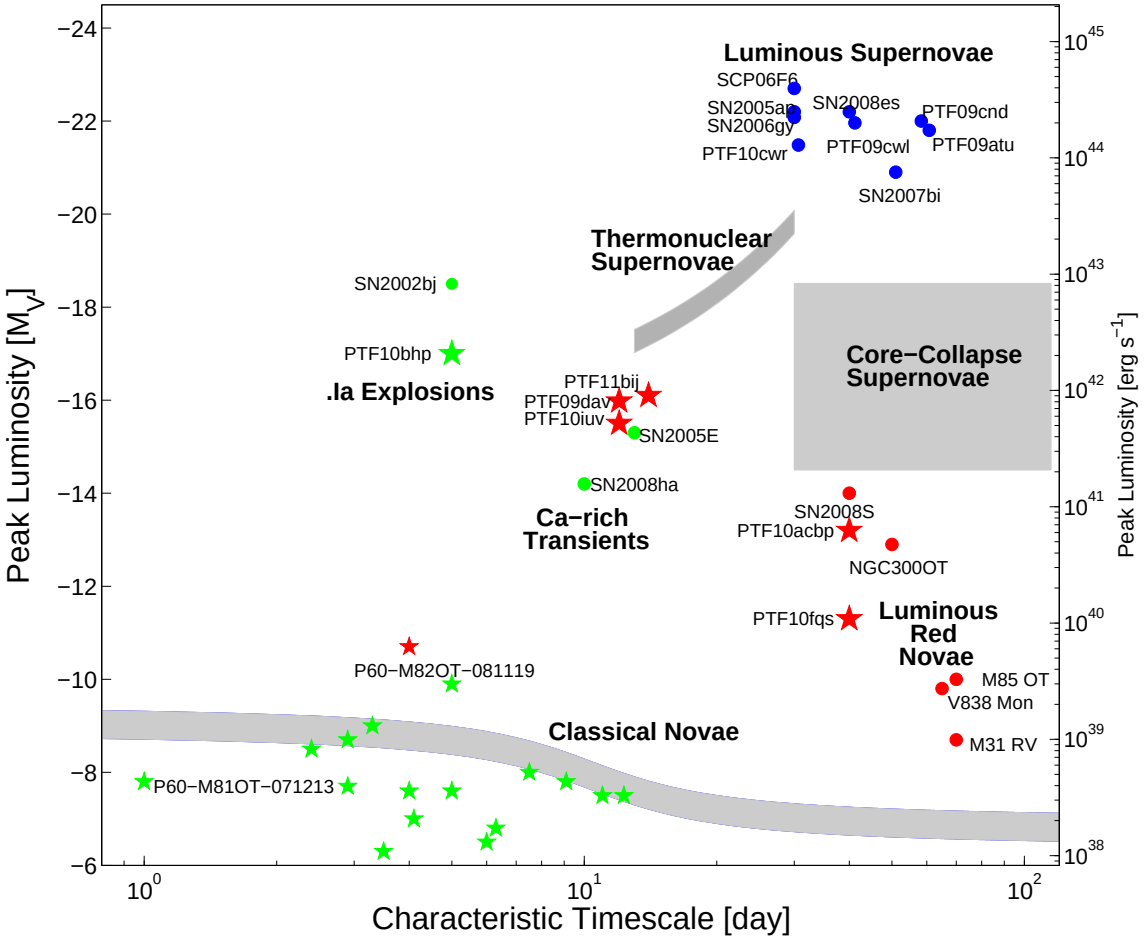

Figure 8.1 Framework of Cosmic Explosions in the Year 2011. Note that until 2005 (Figure 1.1), we only knew about three classes (denoted by gray bands). Systematic surveys, serendpitous discoveries and archival searches have yielded multiple, new classes of transients. Discoveries presented in thesis Chapters 3, 5, 6 and 7 are denoted by $\star$.

(Brown et al. 2011) that undergo such an explosion.

2. *Luminous Red Novae:* The defining characteristics of the emerging class of luminous red novae (LRN) are: large amplitude (>7 mag), peak luminosity intermediate between novae and supernovae (-6 to -14 mag), very red colors and long-lived infrared emission. When the first LRN was discovered (Kulkarni et al. 2007), the similarities to three Galactic explosions (including V838 Mon) suggested a common origin. Since then, 5 more extragalactic and 1 more Galactic LRN have been discovered. Recent developments suggest there may be two progenitor channels.

First, a less luminous but likely more prolific channel is the merger of main sequence stars. In particular, the well-sampled ten year baseline of V1309 Sco showed clear evidence of a decaying orbital period prior to eruption (Tylenda et al. 2011). As the orbital period decayed, the second maximum in the light curve became weaker as the secondary was engulfed by the primary. This suggests that it was a mergeburst of a K-type main sequence star and a lower mass companion. The distance estimate is uncertain and the peak luminosity is ≈ -6 mag. It is plausible that other Galactic events also have similar origin, with higher luminosity corresponding to higher masses of the stars in the binary. However, this channel cannot be arbitrary scaled up in luminosity beyond -10 mag.

Second, a more luminous but rarer channel is electron-capture supernovae in extreme Asymptotic Giant Branch (eAGB) stars. PTF has discovered two extragalactic LRN: PTF 10fqs (discussed in Chapter 5) and PTF 10acbp (Kasliwal et al. 2010). We estimate a lower limit on the rate of $> 7\times10^{-5}$ Mpc^{-3} (based on finding 2 LRN in the same volume as 13 core-collapse supernovae). The fundamental differences between the extra-galactic and Galactic populations are: higher peak luminosity range (-10 to -14 mag), higher velocities (10,000 km s^{-1}) and an infrared progenitor vs. optical progenitor. Based on the two nearest events, NGC300-OT and SN 2008S, the progenitor in the mid-infrared has been identified to be at the extremely luminous and red end of the AGB branch (Prieto et al. 2008b; Thompson et al. 2009). Thermal pulses could result in significant dust formation and are consistent with the deep limits on an optical progenitor. The luminosities, velocities and longevity in the redder bands are all consistent with electron capture in an O-Ne-Mg core of an eAGB star.

Further progress to understand LRN will likely come from the mid-infrared. The discovery of PTF 10acbp prompted us to search the WISE[1] data stream for Luminous Red Novae. The subsequent detection (despite the large distance of 60 Mpc) motivated us to search for the older LRN (Cutri et al. 2011; Hoffman et al. 2011). Five were detected, including two that exploded two years ago, and this opened a new channel to discover LRN. Given that WISE made two all-sky scans separated by six months, we will be searching this data for all LRN to obtain the best estimate yet of their

[1] http://www.nasa.gov/wise

rates. There is also a proposal to NASA (PI J. Bloom) to revive the WISE mission for 1 year. This mission, called WITS (WIse Transient Survey), would be dedicated to time-domain astronomy.

3. *Calcium-rich Halo Transients:* PTF 09dav, PTF 10iuv, PTF 11bij (see Chapter 7) and SN 2005E (Perets et al. 2010b) appear to constitute a family of transients in the farflung outskirts of their hosts with the following characteristics: peak luminosity lower than supernovae (-14 to -16 mag), rise time of 12 days, large photospheric velocities ($\approx$10,000 km s^{-1}), early spectroscopic evolution into nebular phase (3 months) and nebular spectra dominated by Calcium emission. The nature of this class remains mysterious due to contradictory lines of evidence. While the halo location and no evidence of in situ star formation to deep limits suggests a white dwarf origin, the presence of hydrogen emission at late-time suggests a massive star. There are two possible resolutions. One possibility is that the white dwarf explosion shockfront ran into a previously ejected hydrogen-rich shell of a nova-like eruption. Another possibility is that the fates of massive stars formed in low metallicity environments is entirely different, with a larger fraction undergoing significant fallback onto the core to form black holes. Progress here requires statistics to address whether or not the remote location is the key to explain this class or simply a red herring.

4. *Low Velocity Transients:* Another curious transient in the luminosity gap is SN 2008ha (-14 mag; Foley et al. 2009b; Valenti et al. 2009). In addition to the low velocity and the fast evolution, spectroscopically it is characterized by very low velocities (2000 km s^{-1}). We obtained a nebular spectrum of SN 2008ha which was Calcium-rich and showed trace of Hα emission. Additionally, PTF has found several very low-velocity supernovae, spectroscopically similar to SN 2008ha but spanning a wide range in luminosities (-14 to -19 mag). The R-band light curves in this sample appear to have a similar rise and decline independent of peak luminosity. PTF 09ego, the most luminous member of this class, has a total ejecta mass of 4 M$_\odot$. Therefore, there is plausible evidence for this class having a massive star origin.

5. *Luminous Supernovae:* The class of luminous supernovae is outside the scope of this thesis. However, I discuss them very briefly here for completeness, as it is also a

recently uncovered rare class of explosions (although in the distant universe). Specifically, SN 2007bi (Gal-Yam et al. 2009) has a secure measurement of $> 5\,M_\odot$ of Nickel in the ejecta and likely represents a pair instability explosion of a $150\,M_\odot$ star. The hydrogen-rich variety (SN2006gy-like) explodes with an incredible amount of energy, likely powered by interaction (Ofek et al. 2007). The hydrogen-free variety (SN 2005ap-like) may even be powered by magnetars (Kasen & Bildsten 2010). Regardless of origin, these supernovae are extermely blue and long-lived and can serve as powerful light houses at high redshifts (Quimby et al. 2009).

Additionally, progress was made in understanding extremes in supernovae and novae. The faintest thermonuclear supernova (SN2007ax, Chapter 2) had a Nickel-56 mass of $\approx 0.1\,M_\odot$. A sub-class of Type IIP supernovae are also subluminous, among the faintest are PTF 10vdl (-13.7 mag; Gal-Yam et al. 2011) and PTF 10ehy (-13). Subluminous Type IIP supernovae (Pastorello et al. 2004) have lower energy, lower velocity and lower Nickel-56 mass and at least one member (SN 2005cs; Maund et al. 2005) has a direct detection of a low to moderate mass red supergiant progenitor. P60-FasTING (Chapter 3) uncovered a population of faint and fast classical novae. They appear to be well explained as hotter white dwarfs or binaries with higher mass transfer rates. Attempts to parametrize novae simply by the mass of the white dwarf, and hence, use them as distance indicators are not fruitful. Nova physics is diverse and spans at least a four dimensional parameter space of white dwarf mass, composition, accretion rate and temperature.

8.2 The Way Forward

We are at the brink of a new paradigm in understanding cosmic explosions. Systematic searches have started to uncover a plethora of stellar outcomes that have given us much work to do ahead. Searches such as the Palomar Transient Factory and the upcoming La Silla Quest[2] are well suited to probe the 2–10 day regime of phase space.

With the promise of advanced gravitational wave interferometers coming online in the second half of this decade, the detection of neutron star binary coalescence once every month is expected to become routine. The electromagnetic counterpart would reveal distance, en-

[2] http://hepwww.physics.yale.edu/lasillaquest/

ergetics, kinematics and composition and be invaluable in probing the astrophysical nature of the gravitational wave event.

However, the electromagnetic signal is theoretically predicted to be very low luminosity (-13 to -16 mag) and very short lived (1 hour to 1 day). Given the advanced LIGO[3] (a-LIGO) sensitivity limit of 200 Mpc, we need to search to a depth of 24 mag. Furthermore, the localization of low frequency gravitational waves by triangulating the GW signal by exploiting three baselines between a-LIGO in Hanford, a-LIGO in Louisiana and VIRGO in Italy is inherently poor. Optimistic simulations (Wen & Chen 2010) of triple coincidence detections suggest 50% of GW coalescence events will be localized within 23 deg^2 and 90% within 320 deg^2.

A single 23 deg^2 snapshot of the dynamic optical sky to a flux limit of 24 mag would be swamped with false positives: ≈ 210 background supernovae in galaxies more distant than the local horizon and ≈ 60 foreground flare stars and cataclysmic variables in our own Milky Way. Spectroscopic follow-up to classify each of these within one day would push the limits of even 30-m class telescopes. We can make this intractable search feasible by leveraging a-LIGO's sensitivity limitation. By focussing our follow-up resources only on transients spatially coincident with galaxies known to be in the local Universe, we can reduce the false positive rate by three orders of magnitude. However, as discussed in Chapter 4, our existing catalog of galaxies is missing $\approx 50\%$ of the starlight at 200 Mpc. We are now undertaking a 3π narrow-band survey (using four filters centered on redshifted Hα) on the Palomar 48-inch to bring the completeness of this census to $\approx 90\%$.

We need a wider, deeper and faster cadence search than the current state of the art. With an "A+" report card from the decadal survey, the astronomical community is optimistic about the Large Synoptic Survey Telescope (LSST)[4] coming online at the end of the decade. The LSST will satisfy the wide (10 deg^2) and deep (24 mag) but at a slow 3 day cadence. To fill the important niche of ephemeral transients, the coals are in the fire for the Next Generation Transient Facility on Palomar mountain (NGTF; PI Shri Kulkarni). NGTF will satisfy the wide (35 deg^2) and fast (minute to hour cadence) but only go down to 21 mag.

There will be two major bottlenecks to leveraging synoptic surveys: rapid identification of rare transients and prompt spectroscopic follow-up. To drink from the firehose of LSST,

[3] http://www.ligo.org

[4] http://www.lsst.org

clever methods will need to be devised to identify rare transients worthy of further follow-up. At the point of discovery, the only information in hand is the brightness, amplitude, rise-time, color and location. Location can be further exploited to look for a quiescent counterpart and historic evidence for variability in pre-explosion imaging. If located in a galaxy with a known redshift, we can immediately derive a luminosity which can serve as an effective unambiguous filter. This is yet another reason to complete the census of galaxies in the local Universe.

If a transient class is dominated by specific line emission, wide-field narrow-band imaging can serve as a filter. However, spectroscopy would be the critical follow-up step. Therefore, NGTF is working on robotic, very low-resolution, integral field unit spectrographs (The SED Machine[5]; PI Nick Konidaris). Efforts are also underway to multiplex spectrographs with integral field units (HETDEX[6]) or programmable fibers (LAMOST[7], BigBOSS[8]).

The holy grail of discovering the light associated with the sound is within reach. Here is to an explosively fun decade ahead.

[5]http://sites.google.com/site/nickkonidaris/sed-machine
[6]http://hetdex.org/
[7]http://www.lamost.org/website/en/
[8]http://bigboss.lbl.gov/

Appendix A

Understanding Extreme Timescales: GRB 070610⋆

M. M. Kasliwal[1], S. B. Cenko[2], S. R. Kulkarni[1], P. B. Cameron[1], E. Nakar[1], E. O. Ofek[1], A. Rau[1], A. M. Soderberg[1], S. Campana[3], J. S. Bloom[4], D. A. Perley[4], L. K. Pollack[17], S. Barthelmy[5], J. Cummings[5], N. Gehrels[5], H. A. Krimm[6,16], C. B. Markwardt[6,7], G. Sato[5], P. Chandra[8], D. Frail[9], D. B. Fox[10], P. A. Price[11], E. Berger[12,13], S. A. Grebenev[14], R. A. Krivonos[14,15] & R. A. Sunyaev[14,15]

[1] Division of Physics, Mathematics and Astronomy, California Institute of Technology, MS 105-24, Pasadena, CA 91125, USA

[2] Space Radiation Laboratory, California Institute of Technology, MS 220-47, Pasadena, CA 91125, USA

[3] INAF, Osservatorio Astronomica di Brera, via E. Bianchi 46, I-23807 Merate (LC), Italy

[4] Department of Astronomy, University of California, Berkeley, CA 94720, USA

[5] NASA Goddard Space Flight Center, Greenbelt, MD 20771, USA

[6] CRESST and Astroparticle Physics Laboratory, NASA/GSFC, Greenbelt, MD 20771, USA

[7] Department of Astronomy, University of Maryland, College Park, MD 20742, USA

[8] University of Virginia, P.O. Box 400325, Charlottesville, VA 22903, USA

[9] National Radio Astronomy Observatory, Socorro, NM 87801, USA

[10] Department of Astronomy & Astrophysics, 525 Davey Laboratory, Pennsylvania State University, University Park, PA 16802, USA

[11] Institute for Astronomy, University of Hawaii, 2680 Woodlawn Drive, Honolulu, HI 96822, USA

[12] Observatories of the Carnegie Institute of Washington, Pasadena, CA 91101, USA

[13] Princeton University Observatory, Princeton, NJ 08544, USA

[14] Space Research Institute, Profsoyuznaya 84/32, 117997 Moscow, Russia

[15] Max-Plank-Institut fuer Astrophysik, Karl-Schwarzschild-Str. 1, D-85741 Garching, Germany

[16] Universities Space Research Association, 10211 Wincopin Circle, Suite 500, Columbia, MD 21044

[17] Department of Astronomy and Astrophysics, University of California, Santa Cruz, CA 95064

Abstract

GRB 070610 is a typical high-energy event with a duration of 5 s. Yet within the burst localization we detect a highly unusual X-ray and optical transient, *Swift* J195509.6+261406. We see high amplitude X-ray and optical variability on very short time scales even at late times. Using near-infrared imaging assisted by a laser guide star and adaptive optics, we identified the counterpart of *Swift* J195509.6+261406. Late-time optical and near-infrared imaging constrain the spectral type of the counterpart to be fainter than a K-dwarf assuming it is of Galactic origin. It is possible that GRB 070610 and *Swift* J195509.6+261406 are unrelated sources. However, the absence of a typical X-ray afterglow from GRB 070610 in conjunction with the spatial and temporal coincidence of the two motivate us to suggest that the sources are related. The closest (imperfect) analog to *Swift* J195509.6+261406 is V4641 Sgr, an unusual black hole binary. We suggest that *Swift* J195509.6+261406 along with V4641 Sgr, define a sub-class of stellar black hole binaries — the fast X-ray novae. We further suggest that fast X-ray novae are associated with bursts of gamma-rays. If so, GRB 070610 defines a new class of celestial gamma-ray bursts and these bursts dominate the long-duration GRB demographics.

*A version of this chapter is published with the title "GRB 070610: A Curious Galactic Transient" in the *The Astrophysical Journal Letters*, 2008, vol. 678, issue 2, pp. 1127-1135, and is reproduced by permission of the AAS.

A.1 Discovery of GRB 070610

Launched in November 2004, the *Swift* Gamma-Ray Burst Explorer (Gehrels et al. 2004) was designed to localize γ-ray bursts (GRBs) and undertake rapid and sustained X-ray and Ultra-Violet observations of the resulting afterglow. With over two hundred events now localized and studied, *Swift* has made fundamental contributions to both long-duration soft bursts (LSBs) and short-duration hard bursts (SHBs). LSBs appear to trace cosmological massive-star formation rate with one event at a redshift of 6.3. SHBs have been seen at typical redshifts of ~ 0.5 in both elliptical and star-forming galaxies. There is now some circumstantial evidence for SHBs being the result of coalescence of compact objects.

At 20:52:26 UT on 2007 June 10 the Burst Alert Telescope (BAT; Barthelmy et al. 2005) aboard *Swift* triggered on GRB 070610. The high-energy prompt emission had a duration (T_{90}) of 4.6 s (Pagani et al. 2007b). Over the range 15–150 keV the burst could be fitted with a power law with photon index $\Gamma = 1.76 \pm 0.25$, resulting in a fluence of $(2.4 \pm 0.4) \times 10^{-7}\,\mathrm{erg\,cm^{-2}}$ (Tueller et al. 2007). A blackbody model is inconsistent with this emission (reduced χ^2 =1.7).

The burst profile consisted of a single symmetric peak (Figure A.1). Fitting the profile (Norris et al. 1996), we calculate a rise time (i.e. half width at half maximum) of 1.68 ± 0.55 s. As can be seen from Figure A.2, the duration and the hardness ratio of *Swift* J195509.6+261406 are both consistent with the broader population of extragalactic long-duration GRBs observed by *Swift*.

The BAT localized GRB 070610 to $\alpha = 19^{\mathrm{h}}55^{\mathrm{m}}13\overset{\mathrm{s}}{.}1$, $\delta = +26^{\circ}15'20''$ (J2000.0) and a 90%-containment radius of $1.8'$. As can be seen in Figure A.3 the field is dense, which is not surprising given the Galactic location ($l = 63.3^{\circ}$ and $b = -1.0^{\circ}$).

Here we report the discovery of an unusual X-ray transient (hereafter referred to as *Swift* J195509.6+261406) in the error circle of GRB 070610 and followup optical, near-infrared (NIR) and radio observations.

A.2 *Swift* J195509.6+261406: A Transient X-ray Source

The X-ray Telescope (XRT; Burrows et al. 2005b) began observing the field of GRB 070610 3.2 ks after the initial BAT trigger (prompt slewing was disabled due to an Earth limb con-

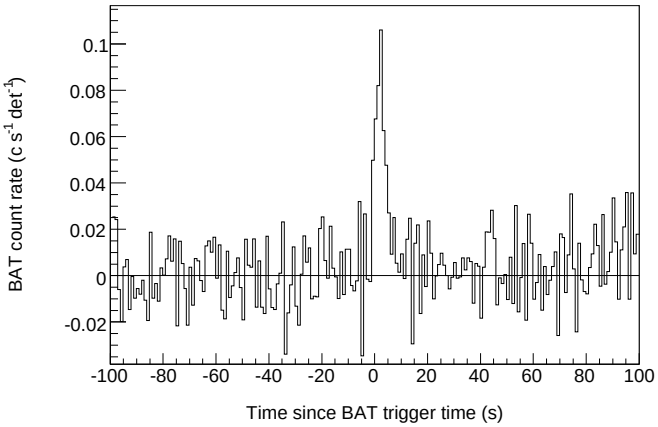

Figure A.1 15-150 keV *Swift*-BAT light curve of GRB 070610, with 1-s time resolution. The conversion factor to translate the ordinate to cgs flux units is 5.6×10^{-7} erg cm^{-2} c^{-1} det (1 det = 0.16 cm^2).

straint). The XRT detected a single uncatalogued variable source in the BAT error circle at $\alpha = 19^{\rm h}55^{\rm m}9\farcs6$, $\delta = +26°14'6\farcs7$ (90% confidence error circle of $4\farcs3$ radius; Pagani et al. 2007a). This position was further refined to $\alpha = 19^{\rm h}55^{\rm m}9\farcs66$, $\delta = +26°14'5\farcs2$ (90% confidence error circle of $1\farcs2$ radius [1]).

The XRT continued to monitor *Swift* J195509.6+261406 over the course of the next month until the source was no longer detected.

The XRT data were processed with `xrtpipeline (v0.10.6)`. All data were obtained in photon counting mode. In this mode the entire CCD is read and the time resolution is limited to 2.5 s. We extracted grade 0–12 events (Burrows et al. 2005b) from a 15 pixel radius circular region centered on the source. To account for the background, we extracted events within a 40 pixel radius circular region in the vicinity of the transient but not encompassing any other source in the field. We adaptively extracted the light curve binning the data in order to have 10 counts per bin. The light curve was corrected for the extraction region losses and for CCD defects as well as for vignetting by using the task `xrtlccorr (v0.1.9)`, which generates an orbit-by-orbit correction based on the instrument map.

The X-ray light curve of *Swift* J195509.6+261406 is shown in Figure A.4 and com-

[1] http://astro.berkeley.edu/∼nat/swift/xrt_pos.html

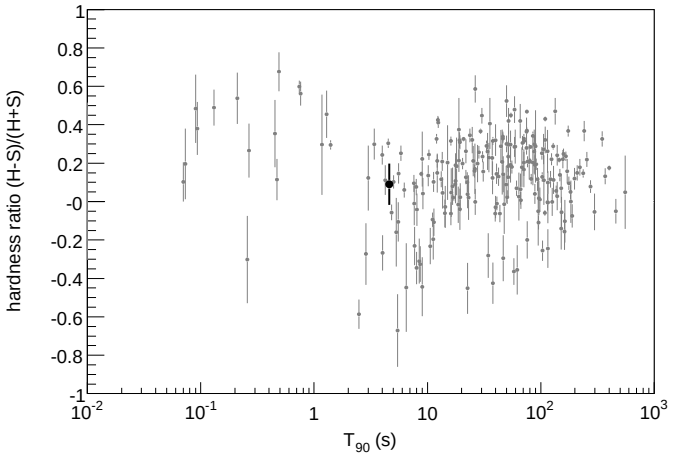

Figure A.2 Plot of duration (T_{90}) and hardness ratio (HR) of 226 *Swift* bursts from GRB 041217 to GRB 070616. We define hardness ratio as $(H - S)/(H + S)$, where S and H are energy fluences in 15–50 keV and 50–150 keV, respectively. The values of T_{90} and hardness ratio for GRB 070610 (marked by a large filled black circle) are 4.6 ± 0.4 s and 0.09 ± 0.11 (90% confidence level), respectively.

pared to a small sample of long-duration GRB afterglows in Figure A.5. Kann et al. 2007 were the first to suggest that this GRB was likely to be of Galactic origin. Clearly, *Swift* J195509.6+261406 differs from typical GRB X-ray afterglows in two fundamental respects. First, it does not exhibit the strong (overall) secular decrease in flux over timescales of hours (Nousek et al. 2006; Zhang et al. 2006). While the decay index in long-duration GRBs can vary markedly from one phase to another, *Swift* J195509.6+261406 shows no significant decline until very late times ($\sim 10^6$ s).

Secondly, the XRT light curve of *Swift* J195509.6+261406 consists of spikes — never seen before in any afterglow. In particular we draw the attention of the reader to a dramatic flare at $t \sim 7.86 \times 10^4$ s, jumping by a factor of $\Delta f/f \sim 100$ in flux over a time scale of $\Delta t/t \sim 10^{-4}$ (see Figure A.4, inset). None of the sixty nine XRT flares described in Chincarini et al. (2007) exhibit a comparable amplitude spike at late time. While a strong X-ray flare has been seen in GRB 050502B (Falcone et al. 2006) (see Figure A.5) the fractional duration, $\Delta t/t$ is much larger (~ 0.5). Less significant variability is present throughout the duration of observations of *Swift* J195509.6+261406 .

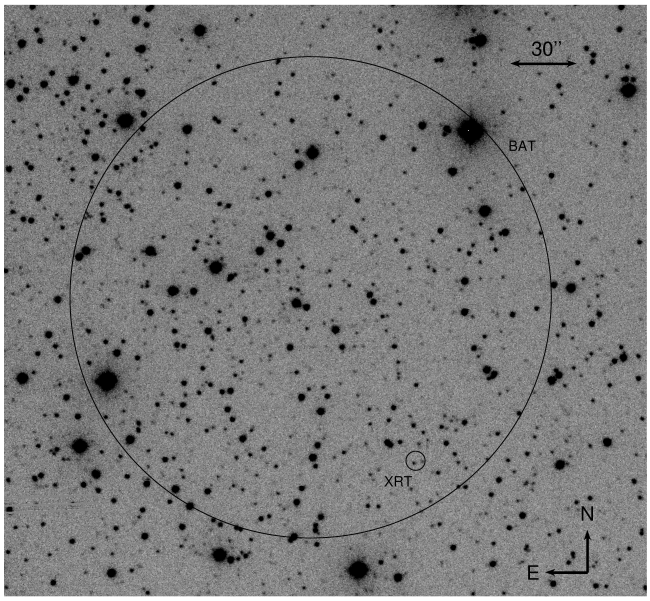

Figure A.3 Optical image (i'-band) of the field of GRB 070610 obtained by the automated Palomar 60-inch telescope on UT 2007 June 12. The BAT localization of GRB 070610 has a radius of $1.8'$, while the XRT localization of *Swift* J195509.6+261406 has a radius of $4.3''$; both are indicated with black circles. The bright source in the XRT circle is *Swift* J195509.6+261406 .

We searched the XRT flare for pulsations. 521 photons were extracted within $60''$of the source position and corrected to the solar system barycenter with the task `barycorr`. To search for pulsations we constructed the Z_1^2 power spectrum to a maximum frequency of 0.2 Hz (Buccheri et al. 1983). The largest observed value of Z_1^2 was 25.2 at a frequency of 0.1446 Hz. Since Z_n^2 is distributed as χ^2 with $2n$ degrees of freedom, this value corresponds to a single trial detection significance of 4.8σ in equivalent Gaussian units. Given that we have performed 350 trials, the significance of this detection is 3.4σ, and thus we do not consider this result to be conclusive evidence of periodicity.

For spectral analysis the ancillary response files were generated with the task `xrtmkarf`. We used the latest spectral redistribution matrices (v009). Data were extracted from single or consecutive orbits in order to have at least 100 counts per spectrum. Spectra were binned to a minimum of 15 counts per energy bin. The resulting spectra were inconsistent with a blackbody (reduced χ^2 =1.9) and consistent with a power law model (task `phabs`). The best fit column density ($N_{\rm H}$) and photon index (Γ) for each epoch are summarized

Table A.1. XRT Spectral Analysis

Epoch Start (MJD)	Total Exposure (s)	$N_{\rm H}$ (10^{22} cm^{-2})	Γ
54261.907	4811	$0.30^{+0.29}_{-0.23}$	1.43 ± 0.37
54262.641	7912	$0.76^{+0.24}_{-0.18}$	1.93 ± 0.18
54263.268, 54264.004	2947, 10500	$0.59^{+0.31}_{-0.23}$	1.11 ± 0.22
54265.387	6026	$0.61^{+0.53}_{-0.33}$	1.33 ± 0.40
Flare	...	$0.92^{+0.91}_{-0.57}$	1.74 ± 0.48
All but flare	...	$0.72^{+0.14}_{-0.12}$	1.71 ± 0.11

Note. — We have fit the XRT data to a power-law model of the form $N(E) \propto E^{-\Gamma}$, leaving the line-of-sight $N_{\rm H}$ as a free parameter.

in Table A.1. Overall, we find that the inferred flux conversion is approximately 1 count s$^{-1} \approx 1.3 \times 10^{-10}$ erg cm^{-2} s^{-1} in the 0.3–10 keV band.

We extrapolate the XRT flare spectrum to BAT (15–50 keV) and predict a flux of 1.8×10^{-9} erg cm^{-2}s^{-1}. This corresponds to a BAT count rate of 0.0032 counts s $^{-1}$ det^{-1}. This is consistent with a 2-σ upper limit from two 64s intervals of BAT data straddling the XRT flare — 0.0038 counts s $^{-1}$ det^{-1} (at 78499.8 s) and 0.012 counts s $^{-1}$ det^{-1}(at 78563.8 s).

The inferred interstellar extinction along this low Galactic latitude is quite high and thus uncertain: $N_{\rm H}$ of 1.1×10^{22} cm^{-2} (Dickey & Lockman 1990); 0.8×10^{22} cm^{-2} (Kalberla et al. 2005); and 1.56-1.89$\times 10^{22}$ cm^{-2} (Schlegel et al. 1998b). The former two estimates are based on H I data whereas the latter on diffuse infrared emission. Given the uncertainty in the inferred $N_{\rm H}$ the XRT spectrum cannot be used to determine the distance to *Swift* J195509.6+261406.

A.3 A Flickering Optical Variable

Rapid observations in response to the BAT trigger, in particular by the *OPTIMA-Burst* team (Stefanescu et al. 2007a), revealed a rapidly variable (time scales as low as tens of seconds) optical transient inside the XRT error circle of *Swift* J195509.6+261406. As-

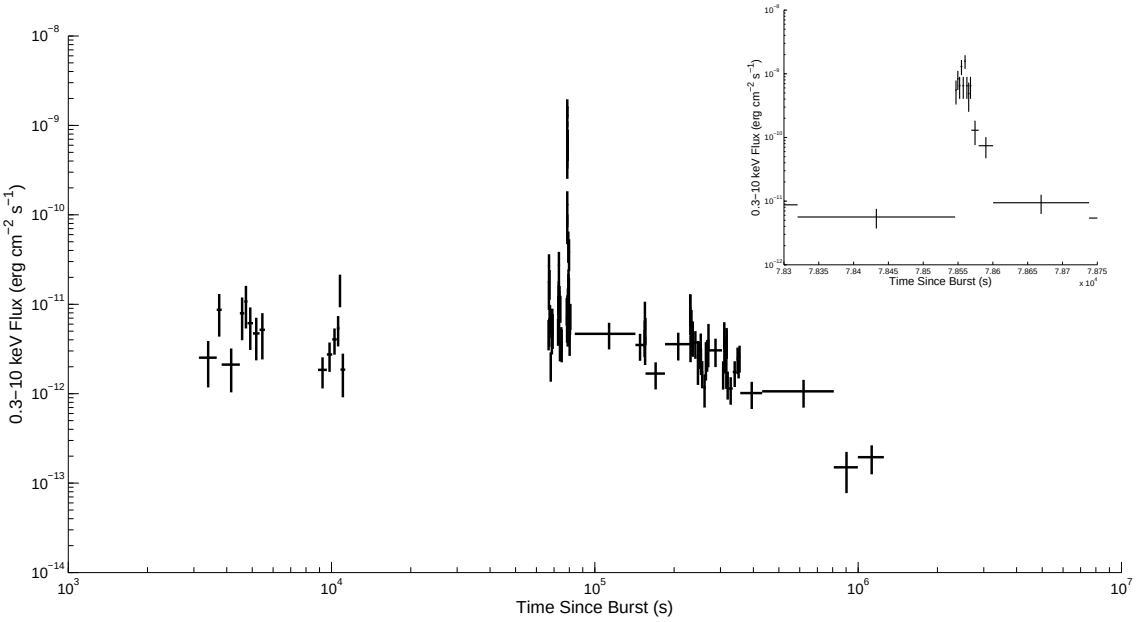

Figure A.4 XRT light curve of *Swift* J195509.6+261406 in the energy band 0.3–10 keV. The dramatic X-ray flare at $t \sim 7.86 \times 10^4$ s is shown in the inset.

tronomers using other facilities — including the OSN 1.5-m telescope (Postigo et al. 2007), the 2-m Schmidt telescope of the Thüringer Landessternwarte (Kann et al. 2007), the 25-cm *TAROT* facility (Klotz et al. 2007), and the 40-cm *Watcher* telescope (French et al. 2007) — confirmed the detection of this variable source. Detections and upper limits reported to the GRB Coordinates Network (GCN[2]) are shown in Figure A.6.

Drawn by the excitement of these discoveries, we began monitoring the field of *Swift* J195509.6+261406 in the i' filter with the automated Palomar 60-inch telescope (P60; Cenko et al. 2006b) starting at 5:47 UT 2007 June 12 and continued over the next several nights. In addition, we imaged the field in *R*-, *I*- and *g*- bands with the *Low Resolution Imaging Spectrograph* (LRIS; Oke et al. 1995) mounted at the Cassegrain focus of the Keck I 10-m telescope. All images were reduced using standard IRAF[3] routines.

The light curve obtained from our observations is also summarized in Figure A.6. The P60 and the Keck photometry can be found in Table A.5 and Table A.2 respectively.

[2]http://gcn.gsfc.nasa.gov/gcn3_archive.html

[3]IRAF is distributed by the National Optical Astronomy Observatory, which is operated by the Association for Research in Astronomy, Inc., under cooperative agreement with the National Science Foundation.

Table A.2. Optical Observations of *Swift* J195509.6+261406 at Keck and Palomar

Mean Epoch (2007 UT)	Facility	Filter	Exposure (s)	Magnitude (s)
Jun 13.570	LRIS	I	120×3	> 24.0
Jun 15.517	LRIS	I	200×3	24.37 ± 0.21
Jun 15.524	LRIS	R	180×1	22.25 ± 0.06
Jun 15.527	LRIS	R	180×1	24.21 ± 0.13
Jun 15.531	LRIS	R	180×1	23.28 ± 0.07
Jun 15.534	LRIS	R	180×1	24.09 ± 0.11
Jun 15.594	LRIS	R	45×8	> 25.0
Aug 13.336	LRIS	R	300×4	> 26.0
Sep 13.362	LFC	i'	360×26	> 24.5

Note. — Zeropoints computed in the Vega system. Errors quoted are 1-σ photometric and instrumental errors summed in quadrature. Upper limits quoted are 3-σ. No correction has been made for the large line-of-sight extinction.

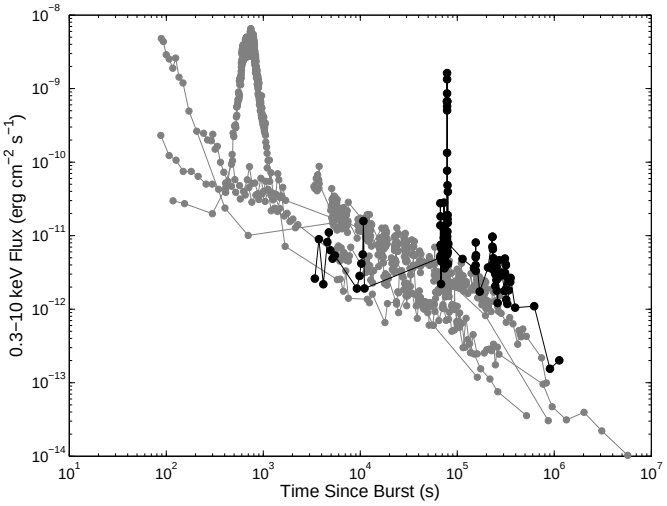

Figure A.5 XRT light curves of a small sample of extragalactic long-duration GRBs (GRBs 050315, 050318, 050319, 050416A, and 050502B) are shown in grey. Data are from Evans et al. 2007. All show the approximately power-law decay typical of GRB afterglows. GRB 050502B exhibits a bright flare around $t \sim 10^3$ s (see Falcone et al. 2006). However, the rise time of this flare is much longer than the spike seen in *Swift* J195509.6+261406 (shown in black).

The P60 light curve is dominated by flickering and magnificent flares on the night of UT 2007 June 12 (see Figure A.7). We observed over eleven flares with amplitudes greater than one magnitude in only three hours. The brightest of these flares rose and dropped by more than 3.5 magnitudes within 6 minutes. The amplitude of the flares is a lower limit because the P60 images are not deep enough to detect the quiescent counterpart (see below). The timescale is also an upper limit because it is entirely possible that variability is more rapid than our sampling rate (~ 60 s). If we define duty-cycle as the fraction of time for which the *Swift* J195509.6+261406 was brighter than $i' < 20$, then the duty cycle based on the first night of data is 18.6%. Given that there was no detection on subsequent ten nights, the duty cycle reduces to 5.8%.

We see a dramatic flare in the *LRIS* data five days (UT 2007 June 15) after the high-energy emission, even though the peak magnitude is much fainter. The brightest observed flare in R-band was 2 magnitudes in three minutes (see Figure A.8). Much like the behavior

seen in X-rays (§A.2), such dramatic optical variability at late times is unlike anything seen before from an extragalactic GRB optical afterglow. Unfortunately none of our optical data directly overlap the XRT light curve, making a direct correlation between the two impossible.

Two months after the burst, the optical counterpart faded in R-band to fainter than 26.0 and three months after the burst, faded in i'-band to fainter than 24.5 (see Table A.2).

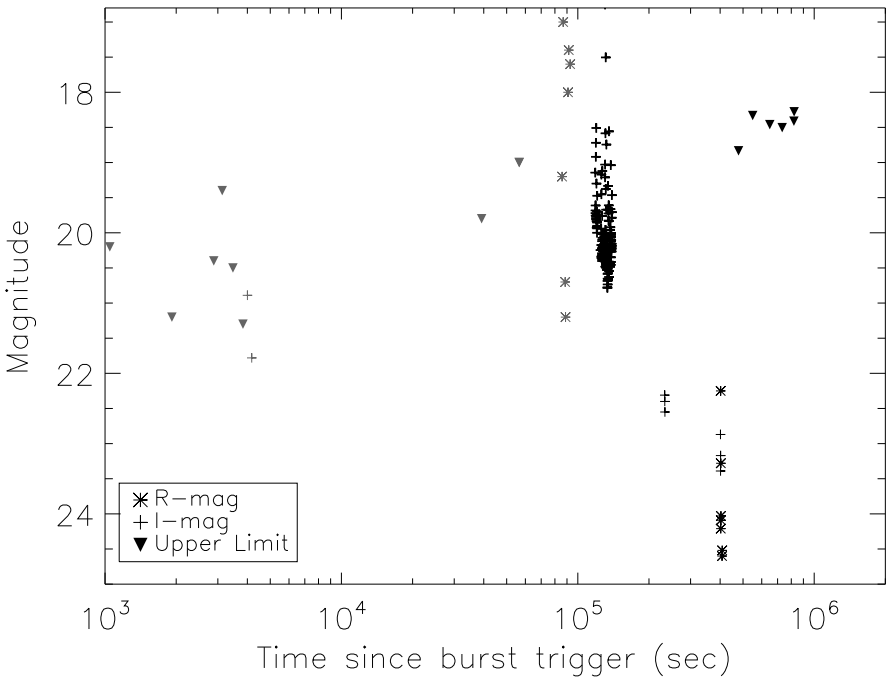

Figure A.6 Optical light curve of *Swift* J195509.6+261406, including data from P60 (black), Keck/LRIS (black), and the literature (grey). (French et al. 2007; Postigo et al. 2007; Kann et al. 2007; Updike et al. 2007a; Stefanescu et al. 2007b; Yoshida et al. 2007; Klotz et al. 2007; Stefanescu et al. 2007c; Updike et al. 2007b).

A.4 A Near Infrared Counterpart

Given the large line-of-sight extinction, we undertook late-time NIR imaging at a variety of facilities to search for a quiescent counterpart to *Swift* J195509.6+261406. The results of our campaign are summarized in Table A.3.

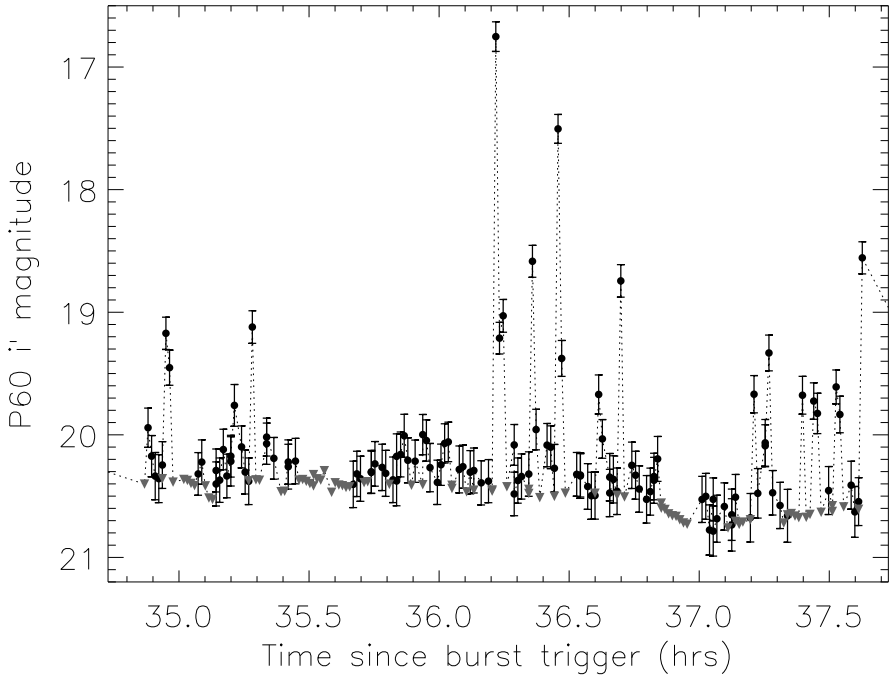

Figure A.7 P60 i'-band light curve from the night of 2007 June 12. Upper limits are indicated by grey inverted triangles. The rapid variability (time scales less than 60 s, our sampling rate) at late times is unlike any previous long-duration GRB optical afterglow.

In detail, we observed the field of *Swift* J195509.6+261406 with the Near InfraRed Imager and spectrograph (NIRI; Hodapp et al. 2003) mounted on the 8-m Gemini North telescope on two occasions. On 2007 June 19 we obtained 18×60 s images in the K-band under exquisite seeing ($\sim 0.4''$) and photometric conditions. The observations on UT 2007 July 15 suffered from poor seeing and clouds.

On UT 2007 June 21, starting 13:10, we observed the transient with Laser Guide Star Adaptive Optics (LGS-AO; Wizinowich et al. 2006; van Dam et al. 2006) on the Keck II telescope and the Near-Infrared Camera 2 (NIRC2). A total of 17 images were obtained, each consisting of three 20s co-added integrations, in the K' filter using the wide-angle camera. We also obtained further late-time observations on UT 2007 Sep 21 and UT 2007 Sep 30.

Finally, J- and H-band images were obtained with the Wide-Field Infrared Camera (WIRC; Wilson et al. 2003) mounted on the Palomar Hale 200-inch (P200) telescope. Thirty

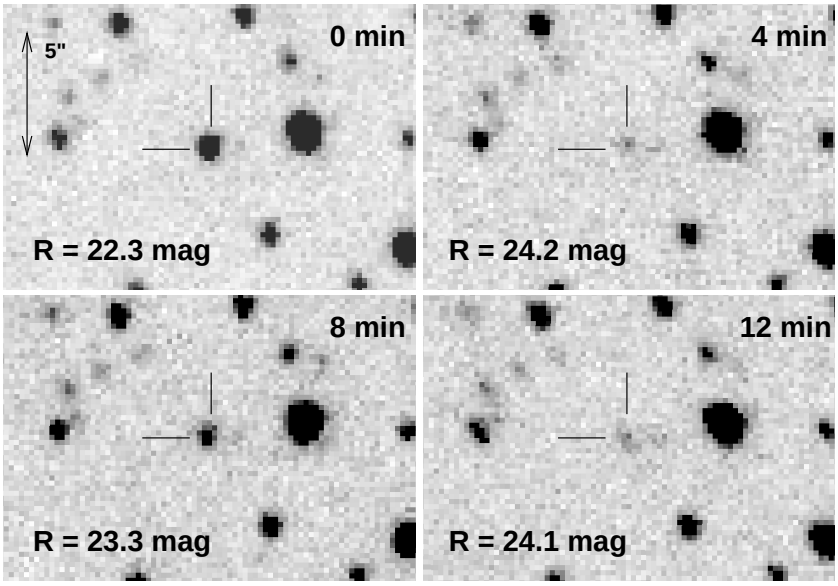

Figure A.8 Close up view of the optical field of the *Swift* J195509.6+261406 optical transient using the *LRIS* instrument on the Keck I 10-m telescope; 2007 June 15 starting at 12:33 UT. All four images were taken in the R-band with a 180 s exposure in sequence. The transient brightens by over two magnitudes in only three minutes about five days after the burst trigger. Such rapid variability at late times is unprecedented from an extragalactic GRB optical afterglow.

four images each with integration time of 30 s were taken in each filter on the night of UT 21 June 2007.

All but the LGS data were processed with standard IRAF routines. Custom routines in *Python* and *IDL* (written by JSB and LP) were used for the LGS-AO reductions; a custom distortion correction (obtained by PBC [4]) was applied to the LGS-AO imaging. We created an astrometric solution using our Gemini/NIRI K-band image from the night of June 19 relative to about fifty point sources from the 2-μm All-Sky Survey(2MASS; Skrutskie et al. 2006). The resulting RMS positional uncertainty was $0.125''$ in right ascension and $0.098''$ in declination. This NIRI K-band image was then used to create a catalog of about one hundred point sources for astrometric matching with all other images. The NIRI K-band image was chosen because of the excellent seeing conditions ($\sim 0.4''$) and the larger field of view in comparison to NIRC2. Typical RMS positional uncertainties relative to the reference

[4]http://www2.keck.hawaii.edu/inst/n2TopLev/post_observing/dewarp/

Table A.3. NIR Observations of *Swift* J195509.6+261406

Epoch (2007 UT)	Facility	Filter	Magnitude
Jun 19.549	Gemini-N/NIRI	K	19.30 ± 0.23
Jun 21.220	Keck II/LGS-AO+NIRC2	K'	19.83 ± 0.15
Jul 15.309	Gemini-N/NIRI	K	> 19.5
Jun 21.352	P200/WIRC	J	> 20.5
Jun 21.400	P200/WIRC	H	> 19.5
Sep 21.632	Keck II/LGS-AO+NIRC2	K'	> 20.3
Sep 30.264	Keck II/LGS-AO+NIRC2	K'	> 21.5

Note. — Errors quoted are 1-σ photometric and instrumental errors summed in quadrature. Upper limits quoted are 3-σ. No correction has been made for the large line-of-sight extinction.

image were $\approx 0.07''$ in each coordinate. Using these astrometric solutions, we determine a position for the optical transient in the Keck R-band flares of $\alpha = 19^{\rm h}55^{\rm m}09\farcs646, \delta = +26^\circ14'05\farcs62$ (J2000.0).

Despite the presence of two nearby objects (A and B), our astrometric accuracy is sufficient to unambiguously identify th K-band counterpart to *Swift* J195509.6+261406 (X in Figure A.9). Using the LGS-AO/NIRC2 image, we find that the location of this NIR counterpart is $\alpha = 19^{\rm h}55^{\rm m}9\farcs649$, $\delta = +26^\circ14'5\farcs65$ (J2000.0), with an uncertainty of 100 mas in each direction.

Due to the crowded field, PSF-matched photometry was performed on all images using the IRAF `DAOPHOT` package. We summarize our NIR observations in Table A.3. For reference, the $RIJHK_{\rm s}$ magnitudes of two extremely nearby objects A and B are provided in Table A.4. Our late-time data, over three and a half months after the burst, constrains the quiescent counterpart to be fainter than $K' > 21.5$ (see Figure A.9).

Table A.4. Photometry of Nearby Contaminating Sources A and B

Epoch (2007 UT)	Facility	Filter	Magnitude Source A	Magnitude Source B
Jun 15.594	Keck I/LRIS	R	> 25.0	> 25.0
Aug 13.336	Keck I/LRIS	R	> 26.0	> 26.0
Jun 15.517	Keck I/LRIS	I	24.83 ± 0.21	24.93 ± 0.22
Jun 21.352	P200/WIRC	J	> 20.5	> 20.5
Jun 21.400	P200/WIRC	H	> 19.5	> 19.5
Jun 21.220	Keck II/LGS	K'	20.30 ± 0.16	19.44 ± 0.14

Note. — Source B is 471 ± 22 mas West and 670 ± 22 mas South of *Swift* J195509.6+261406 . In images with poorer angular resolution, stars A and B may contaminate the photometry of the transient (i.e. our NIRI imaging).

A.5 Search for a Radio Counterpart

On 2007 June 15 we undertook Very Large Array (VLA)[5] observations of *Swift* J195509.6+261406. The observations were obtained in 2×50 MHz bands around 8.46 GHz and lasted about an hour.

We observed 1956+283 (a phase calibrator) for 0.8 minutes and then switched to *Swift* J195509.6+261406 for 4.8 minutes. The sequence ended with a 6 minute observation of 0137+331 (3C48; flux calibrator).

Data were analyzed using the Astronomical Image Processing System (AIPS) software of National Radio Astronomy Observatory (NRAO). VLA antennas N16, W64, E72 and W48 and baseline combinations EVLA antennas E16, W24, N64, W40, E56, W48 and N40 were flagged. In total, flagging resulted in a loss of about 100 baselines.

Owing to the VLA being in the "A" configuration, we obtained excellent image resolution of $0.42'' \times 0.21''$. However, *Swift* J195509.6+261406 was not detected and we get an upper limit of $7.3 \pm 31.5\,\mu$Jy.

[5]The National Radio Astronomy Observatory is a facility of the National Science Foundation operated under cooperative agreement by Associated Universities, Inc.

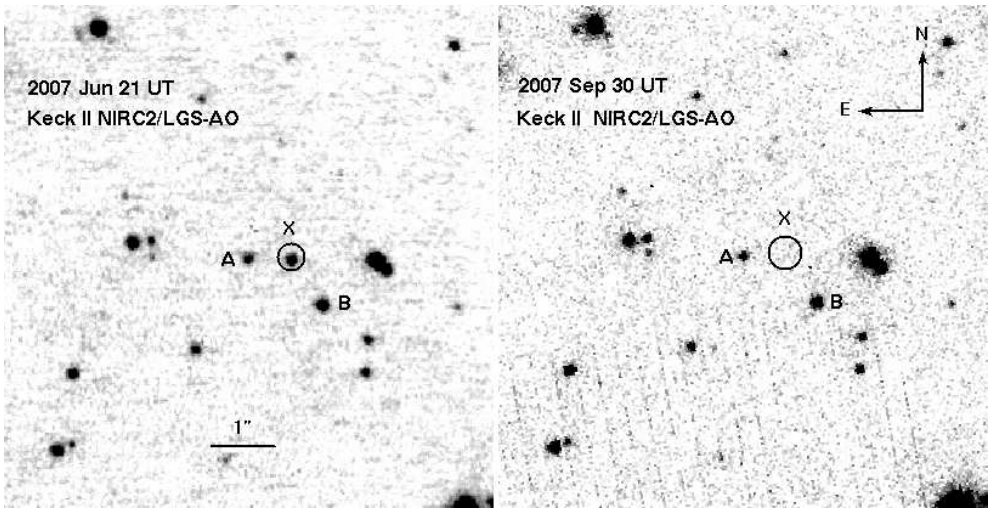

Figure A.9 A K-band image of the field of *Swift* J195509.6+261406 obtained with NIRC-2 imager behind the Keck II Laser Guide Star (LGS) system on 2007 June 21 (left) and 2007 Sep 30 (right). The 2-σ error circle of the optical transient (taken from our *LRIS* imaging) is shown as a black circle overlaid on the LGS image. Clearly we can identify the object marked as 'X' as the NIR counterpart of *Swift* J195509.6+261406.

A.6 Archival Observations

A query of the *Simbad* database reveals no catalogued object within the BAT localization. The *INTEGRAL* observatory conducts regular scans of the Galactic plane and, in addition, performed several long pointed observations of the field around *Swift* J195509.6+261406. Over the past four years, this field has been observed with the IBIS instrument to total 1.5 Ms being within its fully-coded field-of-view (FCFOV, $9^\circ \times 9^\circ$) and up to 2.5 Ms being within the partially coded field-of-view ($29^\circ \times 29^\circ$). The efficiency of observations within the FCFOV falls to zero at the field's edge. The coverage of these 4 years by observations was non-uniform with the maximum exposure reached in the fall of 2006 (for FCFOV).

There is no reported source close to the transient's position in the recent IBIS/ISGRI soft gamma-ray catalogs (Krivonos et al. 2007; Bird et al. 2007). We have also reanalyzed the archival data of *INTEGRAL* and failed to detect the source. A 4-σ limit of 0.9 mCrab in the 18–45 keV band (or 0.8 mCrab in the 17–60 keV band) has been received (flux of 1 mCrab corresponds to 1.1 and 1.4×10^{-11} erg cm^{-2} s^{-1} in these bands respectively for a source with Crab-like spectrum). There was also no source detected on a time scale of one

individual pointing (2.0–3.6 ksec). We derive a 4-σ limit of $\sim$20 mCrab.

Spitzer observed the position of *Swift* J195509.6+261406 during the Galactic Legacy Infrared Mid-Plane Survey Extraordinaire (GLIMPSE) on 2004 Oct 31st. Conservative upper limits for a source at the K-band position are 280, 350, 1700 and 6350 μJy at 3.6, 4.5, 5.8 and 8.0μm respectively.

A.7 Basic Considerations: Distance, Energetics and Radius

The fluence, the hardness and the duration of GRB 070610 are not atypical of GRBs. However, *Swift* J195509.6+261406 is an atypical afterglow in the X-ray band (§A.2). The optical counterpart is also atypical. Correcting for the total interstellar extinction along the line of sight, the apparent i'-band magnitude of the optical transient is as bright as ~ 13 mag more than a day after the burst trigger — there is no other optical extragalactic afterglow as bright at such late times.

The issue that faces us is quite simple: is GRB 070610 related to *Swift* J195509.6+261406? For extragalactic long-duration GRBs that the *Swift*-XRT was able to observe within an hour of the burst trigger, the overwhelming majority have a detected X-ray afterglow.

We therefore consider it unlikely that GRB 070610 arises from a background (i.e. extragalactic) event. The spatial and temporal coincidence of GRB 070610 and *Swift* J195509.6+261406 suggest that these are strongly related. If so, the event is of Galactic origin. Accepting this association we turn our attention to the fundamental parameters characterizing *Swift* J195509.6+261406.

The extinction estimate based on the full X-ray spectrum excluding the flare (see Table A.1) corresponds to $E(B-V) = 1.0$–1.5 mag (Based on optical spectral classification of nearby stars, we find $E(B-V) \sim 1.1$). Assuming $R = 3.1$, this corresponds to $A_K = 0.4$–0.5 mag. The infrared K'-band magnitude of the NIR counterpart *Swift* J195509.6+261406 is no brighter than $\sim$ 21.5 (Table A.3). From late-time optical observations, we also know that R $>$ 26.0 (Table A.2). Since the farthest distance for a star in the disk of our galaxy is 30 kpc, we get extinction-corrected absolute magnitude of $M_K > 3.6$ and $M_R > 4.8$. This clearly rules out the luminosity class of giants and supergiants (Cox 2000a). This also constrains the spectral type to be cooler than G8 (Kraus & Hillenbrand 2007b). If we assume a distance of 10 kpc, we can further constrain it to a spectral type cooler than M3.

The prompt γ-ray burst peak flux is 5×10^{-8} erg cm^{-2}s^{-1}, the peak X-ray flare flux is twice as faint and the mean flux over the first week is approximately a factor of 10^4 fainter than the burst peak flux. These translate to the following isotropic luminosities: $6 \times 10^{38}\ d_{10}^2$ erg s^{-1}, $3 \times 10^{38}\ d_{10}^2$ erg s^{-1} and $5 \times 10^{34}\ d_{10}^2$ erg s^{-1}.

The prompt gamma-rays can constrain the radius of the emission. The BAT burst duration of several seconds (see Figure A.1) puts an upper limit on the size of the emitting region (along the line of sight) to be smaller than $\sim 10^{11}\beta_c$ cm, where β_c is the causal speed in units of the light speed (i.e, the speed in which information, such as sound, travels). Since we expect $\beta_c \ll 1$ in non-compact objects (e.g., main sequence stars) the source of the prompt gamma-rays is a black hole, a neutron star or a white dwarf (the sound crossing time of the latter is seconds).

On the other hand, the non-thermal gamma-rays can be used to put a lower limit on the emission radius. If the gamma-ray spectrum continues to high energy ($E > m_e c^2$) then pair production opacity starts playing a role. Using the formulation of Lejeune & Schaerer (2001) and assuming a non-relativistic source we find that the size of the emitting region has to be $\gtrsim L\sigma_T/(0.1\pi m_e c^3) \approx 10^9 d_{10}^2$ cm, where the approximated numerical factor (taken here as 0.1π) depends on the radiation spectrum and the geometry of the source (Svensson 1987). This radius implies that if the engine of the burst is a neutron star or a black hole then the observed gamma-rays are produced far from the engine by (possibly relativistic) ejecta.

A.8 A Curious Galactic Transient

With a compact object (§ A.7) and a fainter than K-dwarf companion, *Swift* J195509.6+261406 is likely a binary system. We now turn our attention to investigate the mechanism powering the unusual emission, with an emphasis on identifying analogous systems in our Galaxy.

At first blush, soft γ-ray repeater (SGR) flares appear to be a viable model for *Swift* J195509.6+261406. SGR exhibits hard X-ray flares with durations ranging from 0.1 s to 10 s and isotropic luminosities of 10^{46} erg (Aptekar et al. 2001; Hurley et al. 2005). Furthermore, variable X-ray afterglows have been detected after several SGR outbursts (see e.g., Woods & Thompson 2006).

However, this interpretation has several problems. First, SGR flares lasting longer than

1 s, dubbed "intermediate" SGR flares, have an energy release $\approx 10^{41}$ erg, two orders of magnitude larger than our upper limit for *Swift* J195509.6+261406 (Woods & Thompson 2006). Second, pulsations are typically observed in SGR flare X-ray afterglows at the neutron star spin rate. We see no evidence for pulsations from *Swift* J195509.6+261406 (though constrained by the 2.5 s sampling interval). Finally, no known SGR has a companion. If *Swift* J195509.6+261406 were caused by an SGR flare, a cooler than K-dwarf companion would make *Swift* J195509.6+261406 the first binary magnetar.

Unlike SGR flares, the remaining possibilities are ultimately powered by accretion instead of magnetic activity (Arefiev et al. 2003 provide a comprehensive review of such transients in the hard X-ray sky). Cygnus X-1, a black hole binary with a supergiant companion, exhibits hard x-ray outbursts (Stern et al. 2001; Golenetskii et al. 2003). The *INTEGRAL* mission has identified a class of bright hard X-ray transients, the so-called Supergiant Fast X-ray Transients (SFXT; Negueruela et al. 2007). However, these events are relatively soft, and have timescales of 10^3 s or longer. Furthermore, the super-giant donor is an essential part of the SFXT story — the X-ray flares arise from accretion of "blobs" in the wind of the supergiant star. The faintness of the quiescent counterpart convincingly rules out the giant and supergiant scenarios.

The high peak luminosity strongly suggests an event like CI Cam (see Belloni et al. 1999). However, this too is a questionable analog for the reasons of the lack of a bright optical/NIR counterpart and also the short flare duration. For the same reasons, the analogy to A0538−66 (the well known Be-pulsar X-ray binary in the LMC) can also be ruled out.

The bursting pulsar GRO J1744−28 shares some properties with those from GRB 070610. From 1995–1997, thousands of bursts were detected by *BATSE* out to > 60 keV (Kouveliotou et al. 1996; Woods et al. 1999). The spectrum of the bursts in *BATSE* and *RXTE* was adequately modeled by a thermal bremsstrahlung model having $kT \sim 10$ keV; burst durations were approximately 10 s. GRO J1744−28 consists of a neutron star in an 11.8 d orbit with a low mass companion (Finger et al. 1996). However, unlike *Swift* J195509.6+261406, there is no evidence for a highly variable optical emission associated with these bursts. Also the high-energy bursts from GRO J1744−28 are highly repetitive. Searches for other episodes of emission from GRB 070610 did not yield any obvious candidates either in the BAT data or in the extensive *INTEGRAL* survey (§ A.6) and the Interplanetary Network (§ A.9).

The best analog to the X-ray and optical emission from *Swift* J195509.6+261406 is V4641 Sgr (Markwardt et al. 2007) — a transient which has been recognized by several authors as being one of the fastest transients in the hard X-ray (in't Zand et al. 2000; Uemura et al. 2002; Arefiev et al. 2003). V4641 Sgr came to the attention of astronomers through a major outburst in 1999 (see in't Zand et al. 2000). We now infer that this object is a binary consisting of a B9 III star orbiting a $9\,M_{\odot}$ black hole (Orosz et al. 2001). The system exhibited strong and fast X-ray and optical variability — similar to what we see in *Swift* J195509.6+261406.

Rapid ($< 100\,$s) and intense (modulation index, $S = \langle f \rangle / \Delta(f) \gtrsim 10$; here f is the X-ray flux and Δf is the variability in f) variability but with mean X-ray luminosity $\langle L \rangle$ that is well below Eddington flux mark V4641 Sgr from the other black hole binaries (Revnivtsev et al. 2002). The classical black hole LMXBs such as A0620−00 exhibit X-ray novae with peak super-Eddington flux and a decline over a month (see reviews by Tanaka & Shibazaki 1996; Remillard & McClintock 2006). Micro-quasars such as GRS 1915+10 exhibit intense variations (with S approaching ten) but only when $\langle L \rangle$ is extremely high, $\langle L \rangle \sim 10^{39}$ erg s^{-1} (e.g. Belloni et al. 1997; Muno et al. 1999).

The first difference between *Swift* J195509.6+261406 and V4641 Sgr is the donor star: *Swift* J195509.6+261406 has a cool dwarf donor, while V4641 Sgr has a B9 giant donor. We suggest that the distinctive variability of V4641 Sgr arises from the black hole companion and has less to do with the nature of the donor star. This conjecture would allow us to infer that the compact object in *Swift* J195509.6+261406 is also a black hole. While V4641 Sgr seems to be the closest event we have to *Swift* J195509.6+261406, it is clear that no perfect analog to *Swift* J195509.6+261406 exists. In particular, there has been no report of a burst of gamma-rays from V4641 Sgr. However, the absence could be due to the short duration duty cycle of the gamma-ray bursts.

With two similar objects in hand—V4641 Sgr and GRB 070610—we now have the luxury of defining a new class of transients: fast X-ray novae which, in addition to the rapid X-ray and optical variability but at sub-Eddington luminosities, are also (apparently) marked by GRB-like bursts.

What differentiates fast X-ray novae from the regular X-ray novae? Regular X-ray novae are essentially black hole binaries undergoing the equivalent of dwarf novae i.e. instabilities

in the disk. During the major burst of 1999, V4641 Sgr exhibited radio emission and relativistic motion (Hjellming et al. 2000). The radio flux of V4641 Sgr declined very steeply initially; from 360 mJy at 8.3 GHz to 30 mJy at 8.46 GHz in one day (Hjellming et al. 2000). According to Orosz et al. 2001, the distance to V4641 Sgr is 7.4–12.3 kpc and the apparent expansion velocity is $> 9.5c$ (assuming the lowest proper motion estimate from Hjellming et al. 2000) — making V4641 Sgr the most relativistic of Galactic sources. This suggests that perhaps the key difference between fast X-ray novae and the regular X-ray novae is the speed at which the ejecta is emitted. Unfortunately, neither was GRB070610 as bright as V4641 Sgr in the optical and X-ray immediately after the flare nor were our radio observations undertaken promptly after the detection of GRB 070610 to verify this hypothesis.

A.9 Implications: Galactic GRBs

Spurred by the connection between *Swift* J195509.6+261406 with a Galactic transient we investigated whether this source or its analog V4641 Sgr emitted bursts of gamma-rays in the past. We have constructed a list of 1211 GRBs detected by the IPN (Hurley et al. 1999), whose position is constrained by at least one annulus with semi-width smaller than 0.5 deg. This catalog contains events observed from 1990 November 12, to 2005 October 31 (see Ofek 2007 for more details). We did not find any IPN GRB that coincides with either of these positions.

We also searched for *Swift*-BAT sub-threshold events which are consistent with the positions of V4641 Sgr and *Swift* J195509.6+261406. There is no BAT sub-threshold event within $5'$ from the location of V4641 Sgr. But, we find an event at a signal-to-noise ratio (SNR) of 5.0 located at RA=298.77°, Dec=+26.221° ($1.8'$ from the position of GRB 070610) and occurring on UT 2006 Nov 17.7812. However, adjusted for the approximate number of times this field has been observed, the significance drops below 2-σ. We consider it likely this sub-threshold event is nothing more than a statistical fluctuation.

V4641 Sgr has been undergoing major bursts approximately every two years (see Uemura et al. 2004). The absence of a detection of a gamma-ray burst could simply be due to lack of coverage or that not all such bursting activity are preceded by a burst of gamma-rays.

Another possible member of this class of fast X-ray novae is XTEJ1901+014 (Karasev et al.

2007) which is potentially associated with GRB020406 (Remillard & Smith 2002).

Nonetheless, it is reasonable to speculate that a burst similar to *Swift* J195509.6+261406 occurs in our Galaxy, say, every decade. This alone immediately makes *Swift* J195509.6+261406 and related events as the most common of long-duration gamma-ray bursts. (The mean time between cosmological GRBs in our Galaxy is no smaller than $10^5\,\mathrm{yr}$).

Several hundred years ago, optical astronomers put all new apparitions of stars as *novae stella.* Over the past century astronomers have shown that *novae stella* split into three distinctly different phenomena: novae, supernovae of type Ia and core collapse supernovae. The novae, in turn, are divided into five families which arise from instabilities in the accretion disk feeding a white dwarf, neutron star or a black hole and on the surfaces of white dwarfs and neutron stars.

History is repeating itself. Only thirty years ago, astronomers referred to all bursts of gamma-ray radiation as GRBs. Over the last decade astronomers have established SHBs and LSBs to be of cosmological origin (Metzger et al. 1997; Gehrels et al. 2005; Bloom et al. 2006b; Fox et al. 2005) and reasonably established their origin: coalescence of compact objects and deaths of massive stars respectively.

However, fissures are already developing. Recently, hypergiant flares from magnetars in our own Galaxy and nearby galaxies have been found to contaminate the SHB sample. The Galactic rate of the hypergiant flares is likely $10^{-3}\,\mathrm{yr}^{-1}$ (Ofek 2007) much larger than the estimated Galactic SHB rate of $10^{-6}\,\mathrm{yr}^{-1}$ (Nakar et al. 2006; Guetta & Piran 2006).

Our galaxy has at least two fast X-ray novae systems (V4641 Sgr and *Swift* J195509.6+261406). The rate of GRB 070610-like events (with no assumption about beaming) is likely to be about $3.5^{+8.0}_{-2.9}\,\mathrm{yr}^{-1}$ which is five orders of magnitude larger than the estimated cosmological GRBs rate. However, these events are yet unobservable outside our galaxy with the current limitation in sensitivity of high energy detectors. As usual the meekest events dominate the demography.

We thank M. van Kerkwijk for help with Keck observations and discussions. We thank J. Cohen, J. Simon, A. Kraus, M. Muno, E. S. Phinney and R. Narayan for valuable discussions. We also acknowledge D. Law, T. Treu and P. Marshall. As always we are grateful to the selfless librarians and astronomers who maintain the *Simbad* database. M. M. K. thanks the Gordon and Betty Moore Foundation for support with the George Ellory Hale Fellow-

ship. S. B. C. and A. M. S. are supported by a NASA Graduate Student Research Fellowship. JSB is a Sloan Research Fellow and is partially supported by a Hellman Faculty Award. P. C. S. is supported by a Jansky Fellowship. E. B. is supported by a Hubble fellowship. GRB research at Caltech is supported in part by grants from NSF (AST program) and NASA (Swift and HST mission).

Table A.5: Optical Observations of *Swift* J195509.6+261406 with the Palomar 60-inch

Epoch (2007 UT)	**Facility**	**Filter**	**Phase (hr)**	**Exposure (s)**	**Magnitude**
June 12.2416	P60	i'	32.92	30.0 × 1	19.1 ± 0.14
June 12.2422	P60	i'	32.94	30.0 × 1	>19.8
June 12.2433	P60	i'	32.96	30.0 × 3	>19.8
June 12.2444	P60	i'	32.99	30.0 × 5	19.7 ± 0.16
June 12.2450	P60	i'	33.00	30.0 × 5	19.6 ± 0.15
June 12.2456	P60	i'	33.02	30.0 × 5	19.6 ± 0.15
June 12.2462	P60	i'	33.03	30.0 × 5	19.7 ± 0.15
June 12.2467	P60	i'	33.05	30.0 × 5	>19.8
June 12.2473	P60	i'	33.06	30.0 × 5	>19.8
June 12.2479	P60	i'	33.07	30.0 × 5	>19.8
June 12.2484	P60	i'	33.09	30.0 × 1	>19.8
June 12.2484	P60	i'	33.09	30.0 × 5	>19.8
June 12.2490	P60	i'	33.10	30.0 × 1	18.9 ± 0.13
June 12.2496	P60	i'	33.11	30.0 × 1	18.7 ± 0.12
June 12.2501	P60	i'	33.13	30.0 × 1	>19.8
June 12.2513	P60	i'	33.15	30.0 × 5	>19.8
June 12.2518	P60	i'	33.17	30.0 × 3	19.8 ± 0.18
June 12.2518	P60	i'	33.17	30.0 × 5	19.7 ± 0.17
June 12.2524	P60	i'	33.18	30.0 × 3	19.7 ± 0.16
June 12.2529	P60	i'	33.19	30.0 × 3	19.7 ± 0.16

Continued on Next Page...

Table A.5 – Continued

Epoch (2007 UT)	Facility	Filter	Phase (hr)	Exposure (s)	Magnitude
June 12.2541	P60	i'	33.22	30.0 × 5	>19.9
June 12.2547	P60	i'	33.23	30.0 × 1	>19.8
June 12.2547	P60	i'	33.23	30.0 × 5	>19.9
June 12.2552	P60	i'	33.25	30.0 × 1	18.5 ± 0.14
June 12.2558	P60	i'	33.26	30.0 × 1	>19.8
June 12.2569	P60	i'	33.29	30.0 × 1	>19.9
June 12.2569	P60	i'	33.29	30.0 × 3	>19.9
June 12.2569	P60	i'	33.29	30.0 × 5	>19.9
June 12.2575	P60	i'	33.30	30.0 × 1	19.2 ± 0.15
June 12.2581	P60	i'	33.32	30.0 × 1	19.8 ± 0.17
June 12.2598	P60	i'	33.36	30.0 × 5	19.9 ± 0.16
June 12.2604	P60	i'	33.37	30.0 × 5	>19.9
June 12.2610	P60	i'	33.39	30.0 × 5	>19.9
June 12.2615	P60	i'	33.40	30.0 × 5	>19.9
June 12.2621	P60	i'	33.41	30.0 × 5	>20.0
June 12.2626	P60	i'	33.43	30.0 × 5	>20.0
June 12.2632	P60	i'	33.44	30.0 × 3	19.9 ± 0.16
June 12.2632	P60	i'	33.44	30.0 × 5	>20.0
June 12.2638	P60	i'	33.45	30.0 × 3	19.7 ± 0.16
June 12.2644	P60	i'	33.47	30.0 × 3	19.6 ± 0.15
June 12.2649	P60	i'	33.48	30.0 × 3	19.8 ± 0.16
June 12.2655	P60	i'	33.50	30.0 × 3	19.9 ± 0.17
June 12.2666	P60	i'	33.52	30.0 × 3	>20.0
June 12.2666	P60	i'	33.52	30.0 × 5	19.8 ± 0.16
June 12.2678	P60	i'	33.55	30.0 × 1	19.4 ± 0.14
June 12.2678	P60	i'	33.55	30.0 × 3	>20.0
June 12.2678	P60	i'	33.55	30.0 × 5	19.9 ± 0.16

Continued on Next Page...

Table A.5 – Continued

Epoch (2007 UT)	Facility	Filter	Phase (hr)	Exposure (s)	Magnitude
June 12.2689	P60	i'	33.58	30.0 × 3	19.9 ± 0.17
June 12.3132	P60	i'	34.64	30.0 × 3	20.2 ± 0.19
June 12.3225	P60	i'	34.86	30.0 × 3	>20.4
June 12.3230	P60	i'	34.88	30.0 × 3	19.9 ± 0.16
June 12.3236	P60	i'	34.89	30.0 × 3	20.1 ± 0.16
June 12.3242	P60	i'	34.90	30.0 × 3	20.3 ± 0.19
June 12.3247	P60	i'	34.92	30.0 × 3	20.3 ± 0.19
June 12.3253	P60	i'	34.93	30.0 × 1	>20.3
June 12.3253	P60	i'	34.93	30.0 × 3	20.2 ± 0.19
June 12.3259	P60	i'	34.94	30.0 × 1	19.1 ± 0.13
June 12.3265	P60	i'	34.96	30.0 × 1	19.4 ± 0.14
June 12.3270	P60	i'	34.97	30.0 × 1	>20.3
June 12.3288	P60	i'	35.01	30.0 × 5	>20.3
June 12.3293	P60	i'	35.03	30.0 × 5	>20.3
June 12.3299	P60	i'	35.04	30.0 × 5	>20.3
June 12.3305	P60	i'	35.05	30.0 × 5	>20.4
June 12.3311	P60	i'	35.07	30.0 × 5	20.3 ± 0.17
June 12.3316	P60	i'	35.08	30.0 × 5	20.2 ± 0.18
June 12.3322	P60	i'	35.10	30.0 × 5	>20.4
June 12.3328	P60	i'	35.11	30.0 × 5	>20.5
June 12.3334	P60	i'	35.12	30.0 × 5	>20.5
June 12.3339	P60	i'	35.14	30.0 × 3	20.4 ± 0.17
June 12.3339	P60	i'	35.14	30.0 × 5	20.2 ± 0.17
June 12.3345	P60	i'	35.15	30.0 × 3	20.3 ± 0.18
June 12.3351	P60	i'	35.17	30.0 × 3	20.1 ± 0.16
June 12.3357	P60	i'	35.18	30.0 × 3	20.3 ± 0.17
June 12.3363	P60	i'	35.19	30.0 × 1	20.2 ± 0.20

Continued on Next Page...

Table A.5 – Continued

Epoch (2007 UT)	Facility	Filter	Phase (hr)	Exposure (s)	Magnitude
June 12.3363	P60	i'	35.19	30.0 × 3	20.1 ± 0.17
June 12.3369	P60	i'	35.21	30.0 × 1	19.7 ± 0.17
June 12.3380	P60	i'	35.24	30.0 × 3	20.0 ± 0.17
June 12.3386	P60	i'	35.25	30.0 × 3	20.3 ± 0.17
June 12.3392	P60	i'	35.26	30.0 × 1	>20.3
June 12.3392	P60	i'	35.26	30.0 × 3	20.3 ± 0.19
June 12.3397	P60	i'	35.28	30.0 × 1	19.1 ± 0.13
June 12.3403	P60	i'	35.29	30.0 × 1	>20.3
June 12.3409	P60	i'	35.30	30.0 × 1	>20.3
June 12.3420	P60	i'	35.33	30.0 × 1	20.0 ± 0.16
June 12.3420	P60	i'	35.33	30.0 × 3	20.0 ± 0.15
June 12.3432	P60	i'	35.36	30.0 × 3	20.1 ± 0.17
June 12.3443	P60	i'	35.39	30.0 × 5	>20.4
June 12.3449	P60	i'	35.40	30.0 × 5	>20.4
June 12.3455	P60	i'	35.42	30.0 × 3	20.2 ± 0.18
June 12.3455	P60	i'	35.42	30.0 × 5	20.2 ± 0.18
June 12.3466	P60	i'	35.44	30.0 × 5	20.2 ± 0.18
June 12.3472	P60	i'	35.46	30.0 × 5	>20.3
June 12.3478	P60	i'	35.47	30.0 × 5	>20.3
June 12.3484	P60	i'	35.48	30.0 × 5	>20.3
June 12.3490	P60	i'	35.50	30.0 × 5	>20.3
June 12.3495	P60	i'	35.51	30.0 × 1	>20.3
June 12.3495	P60	i'	35.51	30.0 × 5	>20.4
June 12.3501	P60	i'	35.53	30.0 × 1	>20.3
June 12.3507	P60	i'	35.54	30.0 × 1	>20.3
June 12.3513	P60	i'	35.55	30.0 × 1	>20.2
June 12.3524	P60	i'	35.58	30.0 × 5	>20.4

Continued on Next Page...

Table A.5 – Continued

Epoch (2007 UT)	Facility	Filter	Phase (hr)	Exposure (s)	Magnitude
June 12.3530	P60	i'	35.60	30.0 × 5	>20.3
June 12.3536	P60	i'	35.61	30.0 × 5	>20.4
June 12.3542	P60	i'	35.62	30.0 × 5	>20.4
June 12.3547	P60	i'	35.64	30.0 × 5	>20.4
June 12.3553	P60	i'	35.65	30.0 × 5	>20.4
June 12.3559	P60	i'	35.66	30.0 × 5	20.4 ± 0.18
June 12.3565	P60	i'	35.68	30.0 × 5	20.3 ± 0.18
June 12.3571	P60	i'	35.69	30.0 × 5	20.3 ± 0.18
June 12.3576	P60	i'	35.71	30.0 × 5	>20.3
June 12.3582	P60	i'	35.72	30.0 × 5	>20.3
June 12.3588	P60	i'	35.73	30.0 × 3	20.3 ± 0.17
June 12.3588	P60	i'	35.73	30.0 × 5	20.3 ± 0.17
June 12.3594	P60	i'	35.75	30.0 × 3	20.2 ± 0.18
June 12.3605	P60	i'	35.78	30.0 × 5	20.2 ± 0.18
June 12.3611	P60	i'	35.79	30.0 × 5	20.3 ± 0.18
June 12.3617	P60	i'	35.80	30.0 × 5	>20.4
June 12.3623	P60	i'	35.82	30.0 × 5	20.3 ± 0.18
June 12.3628	P60	i'	35.83	30.0 × 3	20.3 ± 0.20
June 12.3628	P60	i'	35.83	30.0 × 5	20.1 ± 0.18
June 12.3635	P60	i'	35.85	30.0 × 3	20.1 ± 0.18
June 12.3641	P60	i'	35.86	30.0 × 3	20.0 ± 0.17
June 12.3646	P60	i'	35.87	30.0 × 3	20.2 ± 0.18
June 12.3652	P60	i'	35.89	30.0 × 3	>20.4
June 12.3658	P60	i'	35.90	30.0 × 3	20.2 ± 0.17
June 12.3670	P60	i'	35.93	30.0 × 1	>20.4
June 12.3670	P60	i'	35.93	30.0 × 3	19.9 ± 0.16
June 12.3676	P60	i'	35.95	30.0 × 1	20.0 ± 0.16

Continued on Next Page...

Table A.5 – Continued

Epoch (2007 UT)	Facility	Filter	Phase (hr)	Exposure (s)	Magnitude
June 12.3682	P60	i'	35.96	30.0 × 1	20.2 ± 0.19
June 12.3694	P60	i'	35.99	30.0 × 3	20.3 ± 0.18
June 12.3700	P60	i'	36.00	30.0 × 3	20.2 ± 0.16
June 12.3705	P60	i'	36.02	30.0 × 3	20.0 ± 0.16
June 12.3711	P60	i'	36.03	30.0 × 3	20.0 ± 0.16
June 12.3717	P60	i'	36.04	30.0 × 1	>20.4
June 12.3717	P60	i'	36.04	30.0 × 3	>20.4
June 12.3729	P60	i'	36.07	30.0 × 3	20.2 ± 0.19
June 12.3735	P60	i'	36.09	30.0 × 3	20.2 ± 0.17
June 12.3740	P60	i'	36.10	30.0 × 3	>20.4
June 12.3746	P60	i'	36.11	30.0 × 3	20.3 ± 0.17
June 12.3752	P60	i'	36.13	30.0 × 1	>20.4
June 12.3752	P60	i'	36.13	30.0 × 3	20.2 ± 0.18
June 12.3764	P60	i'	36.16	30.0 × 3	20.3 ± 0.18
June 12.3776	P60	i'	36.18	30.0 × 5	20.3 ± 0.17
June 12.3782	P60	i'	36.20	30.0 × 1	>20.4
June 12.3782	P60	i'	36.20	30.0 × 5	>20.4
June 12.3787	P60	i'	36.21	30.0 × 1	16.7 ± 0.12
June 12.3793	P60	i'	36.23	30.0 × 1	19.2 ± 0.12
June 12.3799	P60	i'	36.24	30.0 × 1	19.0 ± 0.13
June 12.3805	P60	i'	36.26	30.0 × 1	>20.4
June 12.3817	P60	i'	36.28	30.0 × 3	20.0 ± 0.16
June 12.3817	P60	i'	36.28	30.0 × 5	20.4 ± 0.17
June 12.3823	P60	i'	36.30	30.0 × 3	20.3 ± 0.18
June 12.3829	P60	i'	36.31	30.0 × 3	20.3 ± 0.18
June 12.3840	P60	i'	36.34	30.0 × 1	>20.4
June 12.3840	P60	i'	36.34	30.0 × 3	>20.4

Continued on Next Page...

Table A.5 – Continued

Epoch (2007 UT)	Facility	Filter	Phase (hr)	Exposure (s)	Magnitude
June 12.3840	P60	i'	36.34	30.0 × 5	20.3 ± 0.18
June 12.3846	P60	i'	36.35	30.0 × 1	18.5 ± 0.13
June 12.3852	P60	i'	36.37	30.0 × 1	19.9 ± 0.16
June 12.3858	P60	i'	36.38	30.0 × 1	>20.5
June 12.3869	P60	i'	36.41	30.0 × 3	20.0 ± 0.17
June 12.3875	P60	i'	36.42	30.0 × 3	20.1 ± 0.17
June 12.3881	P60	i'	36.44	30.0 × 1	>20.5
June 12.3881	P60	i'	36.44	30.0 × 3	20.2 ± 0.19
June 12.3887	P60	i'	36.45	30.0 × 1	17.5 ± 0.11
June 12.3893	P60	i'	36.47	30.0 × 1	19.3 ± 0.14
June 12.3899	P60	i'	36.48	30.0 × 1	>20.4
June 12.3917	P60	i'	36.52	30.0 × 5	20.3 ± 0.17
June 12.3923	P60	i'	36.54	30.0 × 3	20.3 ± 0.18
June 12.3923	P60	i'	36.54	30.0 × 5	20.3 ± 0.17
June 12.3935	P60	i'	36.57	30.0 × 5	20.4 ± 0.18
June 12.3940	P60	i'	36.58	30.0 × 5	20.4 ± 0.19
June 12.3946	P60	i'	36.59	30.0 × 1	>20.4
June 12.3946	P60	i'	36.59	30.0 × 5	20.4 ± 0.19
June 12.3952	P60	i'	36.61	30.0 × 1	19.6 ± 0.15
June 12.3958	P60	i'	36.62	30.0 × 1	20.0 ± 0.15
June 12.3970	P60	i'	36.65	30.0 × 3	20.3 ± 0.19
June 12.3970	P60	i'	36.65	30.0 × 5	20.4 ± 0.19
June 12.3976	P60	i'	36.67	30.0 × 3	20.3 ± 0.19
June 12.3982	P60	i'	36.68	30.0 × 1	>20.4
June 12.3982	P60	i'	36.68	30.0 × 3	20.4 ± 0.18
June 12.3988	P60	i'	36.69	30.0 × 1	18.7 ± 0.13
June 12.3993	P60	i'	36.71	30.0 × 1	>20.5

Continued on Next Page...

Table A.5 – Continued

Epoch (2007 UT)	Facility	Filter	Phase (hr)	Exposure (s)	Magnitude
June 12.4005	P60	i'	36.74	30.0 × 3	20.2 ± 0.18
June 12.4011	P60	i'	36.75	30.0 × 3	20.3 ± 0.19
June 12.4017	P60	i'	36.76	30.0 × 3	20.4 ± 0.18
June 12.4029	P60	i'	36.79	30.0 × 5	20.5 ± 0.19
June 12.4035	P60	i'	36.81	30.0 × 5	20.4 ± 0.19
June 12.4041	P60	i'	36.82	30.0 × 3	20.3 ± 0.18
June 12.4041	P60	i'	36.82	30.0 × 5	20.3 ± 0.18
June 12.4047	P60	i'	36.84	30.0 × 3	20.1 ± 0.18
June 12.4052	P60	i'	36.85	30.0 × 1	>20.5
June 12.4052	P60	i'	36.85	30.0 × 3	>20.5
June 12.4058	P60	i'	36.86	30.0 × 1	>20.6
June 12.4064	P60	i'	36.88	30.0 × 1	>20.6
June 12.4070	P60	i'	36.89	30.0 × 1	>20.6
June 12.4076	P60	i'	36.91	30.0 × 1	>20.6
June 12.4082	P60	i'	36.92	30.0 × 1	>20.6
June 12.4088	P60	i'	36.93	30.0 × 1	>20.7
June 12.4094	P60	i'	36.95	30.0 × 1	>20.7
June 12.4118	P60	i'	37.01	30.0 × 5	20.5 ± 0.18
June 12.4124	P60	i'	37.02	30.0 × 5	20.5 ± 0.18
June 12.4130	P60	i'	37.03	30.0 × 5	20.7 ± 0.20
June 12.4136	P60	i'	37.05	30.0 × 3	20.5 ± 0.17
June 12.4136	P60	i'	37.05	30.0 × 5	20.7 ± 0.20
June 12.4142	P60	i'	37.06	30.0 × 3	20.6 ± 0.19
June 12.4153	P60	i'	37.09	30.0 × 5	20.5 ± 0.19
June 12.4159	P60	i'	37.11	30.0 × 5	>20.7
June 12.4165	P60	i'	37.12	30.0 × 3	20.6 ± 0.20
June 12.4165	P60	i'	37.12	30.0 × 5	20.7 ± 0.21

Continued on Next Page...

Table A.5 – Continued

Epoch (2007 UT)	Facility	Filter	Phase (hr)	Exposure (s)	Magnitude
June 12.4171	P60	i'	37.13	30.0 × 1	>20.7
June 12.4171	P60	i'	37.13	30.0 × 3	20.5 ± 0.18
June 12.4177	P60	i'	37.15	30.0 × 1	>20.7
June 12.4183	P60	i'	37.16	30.0 × 1	>20.7
June 12.4195	P60	i'	37.19	30.0 × 1	>20.6
June 12.4195	P60	i'	37.19	30.0 × 3	20.6 ± 0.19
June 12.4201	P60	i'	37.21	30.0 × 1	19.6 ± 0.15
June 12.4207	P60	i'	37.22	30.0 × 1	20.4 ± 0.20
June 12.4219	P60	i'	37.25	30.0 × 1	20.0 ± 0.19
June 12.4219	P60	i'	37.25	30.0 × 3	20.0 ± 0.17
June 12.4225	P60	i'	37.26	30.0 × 1	19.3 ± 0.14
June 12.4231	P60	i'	37.28	30.0 × 1	20.4 ± 0.18
June 12.4243	P60	i'	37.31	30.0 × 3	20.5 ± 0.18
June 12.4249	P60	i'	37.32	30.0 × 3	>20.7
June 12.4255	P60	i'	37.33	30.0 × 1	>20.6
June 12.4255	P60	i'	37.33	30.0 × 3	20.6 ± 0.21
June 12.4261	P60	i'	37.35	30.0 × 1	>20.6
June 12.4267	P60	i'	37.36	30.0 × 1	>20.6
June 12.4273	P60	i'	37.38	30.0 × 1	>20.6
June 12.4279	P60	i'	37.39	30.0 × 1	19.6 ± 0.15
June 12.4285	P60	i'	37.41	30.0 × 1	>20.6
June 12.4291	P60	i'	37.42	30.0 × 1	>20.6
June 12.4297	P60	i'	37.44	30.0 × 1	19.7 ± 0.14
June 12.4303	P60	i'	37.45	30.0 × 1	19.8 ± 0.16
June 12.4309	P60	i'	37.46	30.0 × 1	>20.6
June 12.4321	P60	i'	37.49	30.0 × 3	20.4 ± 0.19
June 12.4327	P60	i'	37.51	30.0 × 1	>20.5

Continued on Next Page...

Table A.5 – Continued

Epoch (2007 UT)	Facility	Filter	Phase (hr)	Exposure (s)	Magnitude
June 12.4327	P60	i'	37.51	30.0 × 3	>20.6
June 12.4333	P60	i'	37.52	30.0 × 1	19.6 ± 0.13
June 12.4339	P60	i'	37.54	30.0 × 1	19.8 ± 0.14
June 12.4345	P60	i'	37.55	30.0 × 1	>20.5
June 12.4357	P60	i'	37.58	30.0 × 3	20.4 ± 0.19
June 12.4363	P60	i'	37.59	30.0 × 3	20.6 ± 0.20
June 12.4368	P60	i'	37.61	30.0 × 1	>20.6
June 12.4368	P60	i'	37.61	30.0 × 3	20.5 ± 0.19
June 12.4374	P60	i'	37.62	30.0 × 1	18.5 ± 0.13
June 12.4540	P60	i'	38.02	30.0 × 1	20.1 ± 0.18
June 12.4552	P60	i'	38.05	30.0 × 3	20.4 ± 0.18
June 12.4557	P60	i'	38.06	30.0 × 3	20.4 ± 0.18
June 12.4563	P60	i'	38.08	30.0 × 1	20.2 ± 0.19
June 12.4563	P60	i'	38.08	30.0 × 3	20.2 ± 0.17
June 12.4570	P60	i'	38.09	30.0 × 1	19.9 ± 0.18
June 12.4576	P60	i'	38.10	30.0 × 1	20.4 ± 0.18
June 12.4582	P60	i'	38.12	30.0 × 1	20.1 ± 0.20
June 12.4588	P60	i'	38.13	30.0 × 1	>20.4
June 12.4594	P60	i'	38.15	30.0 × 1	19.9 ± 0.17
June 12.4600	P60	i'	38.16	30.0 × 1	19.6 ± 0.15
June 12.4606	P60	i'	38.18	30.0 × 1	>20.4
June 12.4618	P60	i'	38.21	30.0 × 3	20.0 ± 0.17
June 12.4624	P60	i'	38.22	30.0 × 3	20.2 ± 0.17
June 12.4630	P60	i'	38.24	30.0 × 3	20.4 ± 0.18
June 12.4636	P60	i'	38.25	30.0 × 3	20.2 ± 0.16
June 12.4642	P60	i'	38.26	30.0 × 1	>20.4
June 12.4642	P60	i'	38.26	30.0 × 3	20.0 ± 0.15

Continued on Next Page...

Table A.5 – Continued

Epoch (2007 UT)	Facility	Filter	Phase (hr)	Exposure (s)	Magnitude
June 12.4648	P60	i'	38.28	30.0 × 1	20.4 ± 0.20
June 12.4654	P60	i'	38.29	30.0 × 1	19.0 ± 0.13
June 12.4660	P60	i'	38.31	30.0 × 1	20.1 ± 0.16
June 12.4666	P60	i'	38.32	30.0 × 1	20.3 ± 0.18
June 12.4679	P60	i'	38.35	30.0 × 3	20.1 ± 0.17
June 12.4685	P60	i'	38.37	30.0 × 3	20.2 ± 0.18
June 12.4691	P60	i'	38.38	30.0 × 1	>20.4
June 12.4691	P60	i'	38.38	30.0 × 3	20.1 ± 0.17
June 12.4703	P60	i'	38.41	30.0 × 3	20.0 ± 0.16
June 12.4709	P60	i'	38.43	30.0 × 3	20.0 ± 0.17
June 12.4715	P60	i'	38.44	30.0 × 3	>20.4
June 12.4721	P60	i'	38.45	30.0 × 3	20.2 ± 0.18
June 12.4727	P60	i'	38.47	30.0 × 3	20.0 ± 0.15
June 12.4733	P60	i'	38.48	30.0 × 3	20.0 ± 0.15
June 12.4739	P60	i'	38.50	30.0 × 3	20.1 ± 0.16
June 12.4748	P60	i'	38.52	30.0 × 3	20.2 ± 0.17
June 12.4754	P60	i'	38.53	30.0 × 3	20.2 ± 0.18
June 12.4766	P60	i'	38.56	30.0 × 5	20.1 ± 0.18
June 12.4772	P60	i'	38.58	30.0 × 5	20.2 ± 0.18
June 12.4778	P60	i'	38.59	30.0 × 3	20.1 ± 0.17
June 12.4778	P60	i'	38.59	30.0 × 5	20.2 ± 0.17
June 12.4784	P60	i'	38.61	30.0 × 3	20.1 ± 0.17
June 12.4790	P60	i'	38.62	30.0 × 3	19.7 ± 0.15
June 12.4796	P60	i'	38.63	30.0 × 1	>20.0
June 12.4796	P60	i'	38.63	30.0 × 3	>20.1
June 12.4816	P60	i'	38.68	30.0 × 5	>19.8
June 12.4822	P60	i'	38.70	30.0 × 1	19.4 ± 0.15

Continued on Next Page...

Table A.5 – Continued

Epoch (2007 UT)	**Facility**	**Filter**	**Phase (hr)**	**Exposure (s)**	**Magnitude**
June 12.4822	P60	i'	38.70	30.0 × 5	19.7 ± 0.16
June 13.2392	P60	i'	56.86	60.0 × 1	>20.2
June 13.2484	P60	i'	57.08	60.0 × 5	>20.0
June 14.4137	P60	i'	85.05	180. × 1	>18.4
June 15.2329	P60	i'	104.7	180. × 1	>18.3
June 16.4076	P60	i'	132.9	180. × 1	>18.8
June 17.2273	P60	i'	152.5	180. × 1	>18.3
June 18.3801	P60	i'	180.2	180. × 1	>18.4
June 19.3444	P60	i'	203.3	180. × 1	>18.5
June 20.3703	P60	i'	228.0	180. × 1	>18.4
June 20.3889	P60	i'	228.4	180. × 1	>18.2

Appendix B

List of Journal Publications

1. M. M. Kasliwal, S. R. Kulkarni, A. Gal-Yam, O. Yaron, R. M. Quimby, E. O. Ofek, P. Nugent, D. Poznanski, J. Jacobsen, A. Sternberg, I. Arcavi, D. A. Howell, M. Sullivan, D. J. Rich, P. F. Burke, J. Brimacombe, D. Milisavljevic, R. Fesen, L. Bildsten, K. Shen, S. B. Cenko, J. S. Bloom, E. Hsiao, N. M. Law, N. Gehrels, S. Immler, R. Dekany, G. Rahmer, D. Hale, R. Smith, J. Zolkower, V. Velur, R. Walters, J. Henning, K. Bui, and D. McKenna, *"Rapidly Decaying Supernova 2010X: A Candidate ".Ia" Explosion,"* *ApJ* **723** (Nov., 2010) L98–L102, `arXiv:1009.0960 [astro-ph.HE]`.

2. M. M. Kasliwal, S. R. Kulkarni, R. M. Quimby, E. O. Ofek, P. Nugent, J. Jacobsen, A. Gal-Yam, Y. Green, I. Arcavi, O. Yaron, J. L. Howell, D. B. Fox, S. B. Cenko, I. Kleiser, J. S. Bloom, A. Miller, D. Poznanski, W. Li, A. V. Filippenko, D. Starr, N. M. Law, G. Helou, D. A. Frail, J. D. Neill, K. Forster, D. C. Martin, S. P. Tendulkar, N. Gehrels, J. Kennea, M. Sullivan, R. Dekany, G. Rahmer, D. Hale, R. Smith, J. Zolkower, V. Velur, R. Walters, J. Henning, K. Bui, D. McKenna, and C. Blake, *"PTF10fqs: A Luminous Red Nova in the Spiral Galaxy Messier 99,"* *ApJ* **730** (Apr., 2011) 134, `arXiv:1005.1455 [astro-ph.SR]`.

3. M. M. Kasliwal, S. B. Cenko, S. R. Kulkarni, E. O. Ofek, R. Quimby, and A. Rau, *"Discovery of a new photometric sub-class of faint and fast classical novae,"* *ApJ* **734** (Jun., 2011), `arXiv:1003.1720 [astro-ph.SR]`.

4. M. M. Kasliwal, R. Massey, R. S. Ellis, S. Miyazaki, and J. Rhodes, *"A Comparison of Weak-Lensing Measurements from Ground- and Space-Based Facilities,"* *ApJ* **684** (Sept., 2008) 34–45, `arXiv:0710.3588`.

5. M. M. Kasliwal, E. O. Ofek, A. Gal-Yam, A. Rau, P. J. Brown, S. B. Cenko, P. B. Cameron, R. Quimby, S. R. Kulkarni, L. Bildsten, P. Milne, and G. Bryngelson, *"SN 2007ax: An Extremely Faint Type Ia Supernova,"* *ApJ* **683** (Aug., 2008) L29–L32, arXiv:0807.0660.

6. M. M. Kasliwal, S. B. Cenko, S. R. Kulkarni, P. B. Cameron, E. Nakar, E. O. Ofek, A. Rau, A. M. Soderberg, S. Campana, J. S. Bloom, D. A. Perley, L. K. Pollack, S. Barthelmy, J. Cummings, N. Gehrels, H. A. Krimm, C. B. Markwardt, G. Sato, P. Chandra, D. Frail, D. B. Fox, P. A. Price, E. Berger, S. A. Grebenev, R. A. Krivonos, and R. A. Sunyaev, *"GRB 070610: A Curious Galactic Transient,"* *ApJ* **678** (May, 2008) 1127–1135, arXiv:0708.0226.

7. M. M. Kasliwal, V. Charmandaris, D. Weedman, J. R. Houck, E. Le Floc'h, S. J. U. Higdon, L. Armus, and H. I. Teplitz, *"Identifying Silicate-absorbed ULIRGs at z ˜ 1-2 in the Bootes Field Using the Spitzer IRS,"* *ApJ* **634** (Nov., 2005) L1–L4, arXiv:astro-ph/0509607.

8. M. M. Kasliwal, R. V. E. Lovelace, and J. R. Houck, *"Confinement of Supernova Explosions in a Collapsing Cloud,"* *ApJ* **630** (Sept., 2005) 875–878, arXiv:astro-ph/0505298.

9. M. Sullivan, M. M. Kasliwal, P. E. Nugent, D. A. Howell, R. C. Thomas, E. O. Ofek, I. Arcavi, S. Blake, J. Cooke, A. Gal-Yam, I. M. Hook, P. Mazzali, P. Podsiadlowski, R. Quimby, L. Bildsten, J. S. Bloom, S. B. Cenko, S. R. Kulkarni, N. Law, and D. Poznanski, *"The Subluminous and Peculiar Type Ia Supernova PTF09dav,"* *ArXiv e-prints* (Mar., 2011) , arXiv:1103.1797 [astro-ph.CO].

10. S. B. Cenko, J. S. Bloom, S. R. Kulkarni, L. E. Strubbe, A. A. Miller, N. R. Butler, R. M. Quimby, A. Gal-Yam, E. O. Ofek, E. Quataert, L. Bildsten, D. Poznanski, D. A. Perley, A. N. Morgan, A. V. Filippenko, I. Arcavi, S. Ben-Ami, A. Cucchiara, C. D. Fassnacht, Y. Green, I. M. Hook, D. A. Howell, D. J. Lagattuta, N. M. Law, M. M. Kasliwal, P. E. Nugent, J. M. Silverman, M. Sullivan, S. P. Tendulkar, and O. Yaron, *"PTF10iya: A short-lived, luminous flare from the nuclear region of a star-forming galaxy,"* *ArXiv e-prints* (Mar., 2011) , arXiv:1103.0779 [astro-ph.HE].

11. A. Corsi, E. O. Ofek, D. A. Frail, D. Poznanski, I. Arcavi, A. Gal-Yam, S. R. Kulkarni, K. Hurley, P. A. Mazzali, D. A. Howell, M. M. Kasliwal, Y. Green, D. Murray,

D. Xu, S. Ben-ami, J. S. Bloom, B. Cenko, N. M. Law, P. Nugent, R. M. Quimby, V. Pal'shin, J. Cummings, V. Connaughton, K. Yamaoka, A. Rau, W. Boynton, I. Mitrofanov, and J. Goldsten, *"PTF 10bzf (SN 2010ah): a broad-line Ic supernova discovered by the Palomar Transient Factory," ArXiv e-prints* (Jan., 2011) , arXiv:1101.4208 [astro-ph.CO].

12. 2011arXiv1103.3010O E. O. Ofek, D. A. Frail, B. Breslauer, S. R. Kulkarni, P. Chandra, A. Gal-Yam, M. M. Kasliwal, and N. Gehrels, *"A VLA search for 5 GHz radio transients and variables at low Galactic latitudes," ArXiv e-prints* (Mar., 2011) , arXiv:1103.3010 [astro-ph.HE].

13. J. Cooke, R. S. Ellis, M. Sullivan, P. Nugent, D. A. Howell, A. Gal-Yam, C. Lidman, J. S. Bloom, S. B. Cenko, M. M. Kasliwal, S. R. Kulkarni, N. M. Law, E. O. Ofek, and R. M. Quimby, *"Hubble Space Telescope Studies of Nearby Type Ia Supernovae: The Mean Maximum Light Ultraviolet Spectrum and its Dispersion," ArXiv e-prints* (Oct., 2010) , arXiv:1010.2211 [astro-ph.CO].

14. K. Sheth, M. Regan, J. L. Hinz, A. Gil de Paz, K. Menéndez-Delmestre, J. Muñoz-Mateos, M. Seibert, T. Kim, E. Laurikainen, H. Salo, D. A. Gadotti, J. Laine, T. Mizusawa, L. Armus, E. Athanassoula, A. Bosma, R. J. Buta, P. Capak, T. H. Jarrett, D. M. Elmegreen, B. G. Elmegreen, J. H. Knapen, J. Koda, G. Helou, L. C. Ho, B. F. Madore, K. L. Masters, B. Mobasher, P. Ogle, C. Y. Peng, E. Schinnerer, J. A. Surace, D. Zaritsky, S. Comerón, B. de Swardt, S. E. Meidt, M. Kasliwal, and M. Aravena, *"The Spitzer Survey of Stellar Structure in Galaxies (S^4G)," ArXiv e-prints* (Oct., 2010) , arXiv:1010.1592 [astro-ph.CO].

15. A. M. Smith, S. Lynn, M. Sullivan, C. J. Lintott, P. E. Nugent, J. Botyanszki, M. Kasliwal, R. Quimby, S. P. Bamford, L. F. Fortson, K. Schawinski, I. Hook, S. Blake, P. Podsiadlowski, J. Joensson, A. Gal-Yam, I. Arcavi, D. A. Howell, J. S. Bloom, J. Jacobsen, S. R. Kulkarni, N. M. Law, E. O. Ofek, and R. Walters, *"Galaxy Zoo Supernovae," ArXiv e-prints* (Nov., 2010) , arXiv:1011.2199 [astro-ph.IM].

16. K. R. Covey, L. A. Hillenbrand, A. A. Miller, D. Poznanski, S. B. Cenko, J. M. Silverman, J. S. Bloom, M. M. Kasliwal, W. Fischer, J. Rayner, L. M. Rebull,

N. R. Butler, A. V. Filippenko, N. M. Law, E. O. Ofek, M. Agüeros, R. G. Dekany, G. Rahmer, D. Hale, R. Smith, R. M. Quimby, P. Nugent, J. Jacobsen, J. Zolkower, V. Velur, R. Walters, J. Henning, K. Bui, D. McKenna, S. R. Kulkarni, and C. Klein, *"PTF10nvg: An Outbursting Class I Protostar in the Pelican/North American Nebula,"* *AJ* **141** (Feb., 2011) 40–+, arXiv:1011.2565 [astro-ph.SR].

17. A. A. Miller, L. A. Hillenbrand, K. R. Covey, D. Poznanski, J. M. Silverman, I. K. W. Kleiser, B. Rojas-Ayala, P. S. Muirhead, S. B. Cenko, J. S. Bloom, M. M. Kasliwal, A. V. Filippenko, N. M. Law, E. O. Ofek, R. G. Dekany, G. Rahmer, D. Hale, R. Smith, R. M. Quimby, P. Nugent, J. Jacobsen, J. Zolkower, V. Velur, R. Walters, J. Henning, K. Bui, D. McKenna, S. R. Kulkarni, and C. R. Klein, *"Evidence for an FU Orionis Outburst from a Classical T Tauri Star,"* *ArXiv e-prints* (Nov., 2010) , arXiv:1011.2063 [astro-ph.SR].

18. E. O. Ofek, I. Rabinak, J. D. Neill, I. Arcavi, S. B. Cenko, E. Waxman, S. R. Kulkarni, A. Gal Yam, P. E. Nugent, L. Bildsten, J. S. Bloom, A. V. Filippenko, K. Forster, D. A. Howell, J. Jacobsen, M. M. Kasliwal, N. Law, C. Martin, D. Poznanski, R. M. Quimby, K. J. Shen, M. Sullivan, R. Dekany, G. Rahmer, D. Hale, R. Smith, J. Zolkower, V. Velur, R. Walters, J. Henning, K. Bui, and D. McKenna, *"Supernova PTF 09uj: A possible shock breakout from a dense circumstellar wind,"* *ArXiv e-prints* (Sept., 2010) , arXiv:1009.5378 [astro-ph.HE].

19. S. B. Cenko, D. A. Frail, F. A. Harrison, J. B. Haislip, D. E. Reichart, N. R. Butler, B. E. Cobb, A. Cucchiara, E. Berger, J. S. Bloom, P. Chandra, D. B. Fox, D. A. Perley, J. X. Prochaska, A. V. Filippenko, K. Glazebrook, K. M. Ivarsen, M. M. Kasliwal, S. R. Kulkarni, A. P. LaCluyze, S. Lopez, A. N. Morgan, M. Pettini, and V. R. Rana, *"Afterglow Observations of Fermi-LAT Gamma-Ray Bursts and the Emerging Class of Hyper-Energetic Events,"* *ArXiv e-prints* (Apr., 2010) , arXiv:1004.2900 [astro-ph.HE].

20. R. M. Quimby, S. R. Kulkarni, M. M. Kasliwal, A. Gal-Yam, I. Arcavi, M. Sullivan, P. Nugent, R. Thomas, D. A. Howell, L. Bildsten, J. S. Bloom, C. Theissen, N. Law, R. Dekany, G. Rahmer, D. Hale, R. Smith, E. O. Ofek, J. Zolkower, V. Velur, R. Walters, J. Henning, K. Bui, D. McKenna, D. Poznanski, S. B. Cenko, and D. Levitan,

"Mysterious transients unmasked as the bright blue death throes of massive stars," *ArXiv e-prints* (Sept., 2009) , arXiv:0910.0059 [astro-ph.CO].

21. I. Arcavi, A. Gal-Yam, M. M. Kasliwal, R. M. Quimby, E. O. Ofek, S. R. Kulkarni, P. E. Nugent, S. B. Cenko, J. S. Bloom, M. Sullivan, D. A. Howell, D. Poznanski, A. V. Filippenko, N. Law, I. Hook, J. Jönsson, S. Blake, J. Cooke, R. Dekany, G. Rahmer, D. Hale, R. Smith, J. Zolkower, V. Velur, R. Walters, J. Henning, K. Bui, D. McKenna, and J. Jacobsen, *"Core-collapse Supernovae from the Palomar Transient Factory: Indications for a Different Population in Dwarf Galaxies,"* *ApJ* **721** (Sept., 2010) 777–784, arXiv:1004.0615 [astro-ph.CO].

22. V. B. Bhalerao, M. H. van Kerkwijk, F. A. Harrison, M. M. Kasliwal, S. R. Kulkarni, and V. R. Rana, *"The Polar Catalysmic Variable 1RXS J173006.4+033813,"* *ApJ* **721** (Sept., 2010) 412–423, arXiv:1008.2002 [astro-ph.SR].

23. N. Elias-Rosa, S. D. Van Dyk, W. Li, A. A. Miller, J. M. Silverman, M. Ganeshalingam, A. F. Boden, M. M. Kasliwal, J. Vinkó, J. Cuillandre, A. V. Filippenko, T. N. Steele, J. S. Bloom, C. V. Griffith, I. K. W. Kleiser, and R. J. Foley, *"The Massive Progenitor of the Type II-linear Supernova 2009kr,"* *ApJ* **714** (May, 2010) L254–L259, arXiv:0912.2880 [astro-ph.SR].

24. R. A. Scalzo, G. Aldering, P. Antilogus, C. Aragon, S. Bailey, C. Baltay, S. Bongard, C. Buton, M. Childress, N. Chotard, Y. Copin, H. K. Fakhouri, A. Gal-Yam, E. Gangler, S. Hoyer, M. Kasliwal, S. Loken, P. Nugent, R. Pain, E. Pécontal, R. Pereira, S. Perlmutter, D. Rabinowitz, A. Rau, G. Rigaudier, K. Runge, G. Smadja, C. Tao, R. C. Thomas, B. Weaver, and C. Wu, *"Nearby Supernova Factory Observations of SN 2007if: First Total Mass Measurement of a Super-Chandrasekhar-Mass Progenitor,"* *ApJ* **713** (Apr., 2010) 1073–1094, arXiv:1003.2217 [astro-ph.CO].

25. P. Chandra, D. A. Frail, D. Fox, S. Kulkarni, E. Berger, S. B. Cenko, D. Bock, F. Harrsion, and M. Kasliwal, *"Discovery of Radio Afterglow from the Most Distant Cosmic Explosion,"* *ApJ* **712** (Mar., 2010) L31–L35, arXiv:0910.4367 [astro-ph.CO].

26. S. B. Cenko, D. A. Frail, F. A. Harrison, S. R. Kulkarni, E. Nakar, P. C. Chandra, N. R. Butler, D. B. Fox, A. Gal-Yam, M. M. Kasliwal, J. Kelemen, D. Moon, E. O.

Ofek, P. A. Price, A. Rau, A. M. Soderberg, H. I. Teplitz, M. W. Werner, D. Bock, J. S. Bloom, D. A. Starr, A. V. Filippenko, R. A. Chevalier, N. Gehrels, J. N. Nousek, and T. Piran, *"The Collimation and Energetics of the Brightest Swift Gamma-ray Bursts," ApJ* **711** (Mar., 2010) 641–654, arXiv:0905.0690 [astro-ph.HE].

27. E. O. Ofek, B. Breslauer, A. Gal-Yam, D. Frail, M. M. Kasliwal, S. R. Kulkarni, and E. Waxman, *"Long-duration Radio Transients Lacking Optical Counterparts are Possibly Galactic Neutron Stars," ApJ* **711** (Mar., 2010) 517–531, arXiv:0910.3676 [astro-ph.HE].

28. A. Rau, G. H. A. Roelofs, P. J. Groot, T. R. Marsh, G. Nelemans, D. Steeghs, M. Salvato, and M. M. Kasliwal, *"A Census of AM CVn Stars: Three New Candidates and One Confirmed 48.3-Minute Binary," ApJ* **708** (Jan., 2010) 456–461, arXiv:0909.4542 [astro-ph.

29. N. M. Law, S. R. Kulkarni, R. G. Dekany, E. O. Ofek, R. M. Quimby, P. E. Nugent, J. Surace, C. C. Grillmair, J. S. Bloom, M. M. Kasliwal, L. Bildsten, T. Brown, S. B. Cenko, D. Ciardi, E. Croner, S. G. Djorgovski, J. van Eyken, A. V. Filippenko, D. B. Fox, A. Gal-Yam, D. Hale, N. Hamam, G. Helou, J. Henning, D. A. Howell, J. Jacobsen, R. Laher, S. Mattingly, D. McKenna, A. Pickles, D. Poznanski, G. Rahmer, A. Rau, W. Rosing, M. Shara, R. Smith, D. Starr, M. Sullivan, V. Velur, R. Walters, and J. Zolkower, *"The Palomar Transient Factory: System Overview, Performance, and First Results," PASP* **121** (Dec., 2009) 1395–1408, arXiv:0906.5350 [astro-ph.IM].

30. A. Rau, S. R. Kulkarni, N. M. Law, J. S. Bloom, D. Ciardi, G. S. Djorgovski, D. B. Fox, A. Gal-Yam, C. C. Grillmair, M. M. Kasliwal, P. E. Nugent, E. O. Ofek, R. M. Quimby, W. T. Reach, M. Shara, L. Bildsten, S. B. Cenko, A. J. Drake, A. V. Filippenko, D. J. Helfand, G. Helou, D. A. Howell, D. Poznanski, and M. Sullivan, *"Exploring the Optical Transient Sky with the Palomar Transient Factory," PASP* **121** (Dec., 2009) 1334–1351, arXiv:0906.5355 [astro-ph.CO].

31. A. Gal-Yam, P. Mazzali, E. O. Ofek, P. E. Nugent, S. R. Kulkarni, M. M. Kasliwal, R. M. Quimby, A. V. Filippenko, S. B. Cenko, R. Chornock, R. Waldman, D. Kasen, M. Sullivan, E. C. Beshore, A. J. Drake, R. C. Thomas, J. S. Bloom, D. Poznanski, A. A. Miller, R. J. Foley, J. M. Silverman, I. Arcavi, R. S. Ellis, and J. Deng, *"Supernova 2007bi as a pair-instability explosion," Nature* **462** (Dec., 2009) 624–627,

arXiv:1001.1156 [astro-ph.CO].

32. D. A. Perley, S. B. Cenko, J. S. Bloom, H. Chen, N. R. Butler, D. Kocevski, J. X. Prochaska, M. Brodwin, K. Glazebrook, M. M. Kasliwal, S. R. Kulkarni, S. Lopez, E. O. Ofek, M. Pettini, A. M. Soderberg, and D. Starr, *"The Host Galaxies of Swift Dark Gamma-ray Bursts: Observational Constraints on Highly Obscured and Very High Redshift GRBs,"* *AJ* **138** (Dec., 2009) 1690–1708, arXiv:0905.0001 [astro-ph.HE].

33. S. B. Cenko, J. Kelemen, F. A. Harrison, D. B. Fox, S. R. Kulkarni, M. M. Kasliwal, E. O. Ofek, A. Rau, A. Gal-Yam, D. A. Frail, and D. Moon, *"Dark Bursts in the Swift Era: The Palomar 60 Inch-Swift Early Optical Afterglow Catalog,"* *ApJ* **693** (Mar., 2009) 1484–1493, arXiv:0808.3983.

34. A. W. Shafter, A. Rau, R. M. Quimby, M. M. Kasliwal, M. F. Bode, M. J. Darnley, and K. A. Misselt, *"M31N 2007-11d: A Slowly Rising, Luminous Nova in M31,"* *ApJ* **690** (Jan., 2009) 1148–1157, arXiv:0809.1388.

35. R. M. Crockett, J. J. Eldridge, S. J. Smartt, A. Pastorello, A. Gal-Yam, D. B. Fox, D. C. Leonard, M. M. Kasliwal, S. Mattila, J. R. Maund, A. W. Stephens, and I. J. Danziger, *"The type IIb SN 2008ax: the nature of the progenitor,"* *MNRAS* **391** (Nov., 2008) L5–L9, arXiv:0805.1913.

36. A. Pastorello, M. M. Kasliwal, R. M. Crockett, S. Valenti, R. Arbour, K. Itagaki, S. Kaspi, A. Gal-Yam, S. J. Smartt, R. Griffith, K. Maguire, E. O. Ofek, N. Seymour, D. Stern, and W. Wiethoff, *"The Type IIb SN 2008ax: spectral and light curve evolution,"* *MNRAS* **389** (Sept., 2008) 955–966, arXiv:0805.1914.

37. P. Chandra, S. B. Cenko, D. A. Frail, R. A. Chevalier, J. Macquart, S. R. Kulkarni, D. Bock, F. Bertoldi, M. Kasliwal, D. B. Fox, P. A. Price, E. Berger, A. M. Soderberg, F. A. Harrison, A. Gal-Yam, E. O. Ofek, A. Rau, B. P. Schmidt, P. B. Cameron, L. L. Cowie, A. Cowie, K. C. Roth, M. Dopita, B. Peterson, and B. E. Penprase, *"A Comprehensive Study of GRB 070125, A Most Energetic Gamma-Ray Burst,"* *ApJ* **683** (Aug., 2008) 924–942, arXiv:0802.2748.

38. A. M. Soderberg, E. Berger, K. L. Page, P. Schady, J. Parrent, D. Pooley, X. Wang, E. O. Ofek, A. Cucchiara, A. Rau, E. Waxman, J. D. Simon, D. Bock, P. A. Milne,

M. J. Page, J. C. Barentine, S. D. Barthelmy, A. P. Beardmore, M. F. Bietenholz, P. Brown, A. Burrows, D. N. Burrows, G. Bryngelson, S. B. Cenko, P. Chandra, J. R. Cummings, D. B. Fox, A. Gal-Yam, N. Gehrels, S. Immler, M. Kasliwal, A. K. H. Kong, H. A. Krimm, S. R. Kulkarni, T. J. Maccarone, P. Mészáros, E. Nakar, P. T. O'Brien, R. A. Overzier, M. de Pasquale, J. Racusin, N. Rea, and D. G. York, *"Erratum: An extremely luminous X-ray outburst at the birth of a supernova,"* *Nature* **454** (July, 2008) 246–+.

39. E. O. Ofek, M. Muno, R. Quimby, S. R. Kulkarni, H. Stiele, W. Pietsch, E. Nakar, A. Gal-Yam, A. Rau, P. B. Cameron, S. B. Cenko, M. M. Kasliwal, D. B. Fox, P. Chandra, A. K. H. Kong, and R. Barnard, *"GRB 070201: A Possible Soft Gamma-Ray Repeater in M31,"* *ApJ* **681** (July, 2008) 1464–1469, `arXiv:0712.3585`.

40. A. M. Soderberg, E. Berger, K. L. Page, P. Schady, J. Parrent, D. Pooley, X. Wang, E. O. Ofek, A. Cucchiara, A. Rau, E. Waxman, J. D. Simon, D. Bock, P. A. Milne, M. J. Page, J. C. Barentine, S. D. Barthelmy, A. P. Beardmore, M. F. Bietenholz, P. Brown, A. Burrows, D. N. Burrows, G. Byrngelson, S. B. Cenko, P. Chandra, J. R. Cummings, D. B. Fox, A. Gal-Yam, N. Gehrels, S. Immler, M. Kasliwal, A. K. H. Kong, H. A. Krimm, S. R. Kulkarni, T. J. Maccarone, P. Mészáros, E. Nakar, P. T. O'Brien, R. A. Overzier, M. de Pasquale, J. Racusin, N. Rea, and D. G. York, *"An extremely luminous X-ray outburst at the birth of a supernova,"* *Nature* **453** (May, 2008) 469–474, `arXiv:0802.1712`.

41. S. B. Cenko, D. B. Fox, B. E. Penprase, A. Cucchiara, P. A. Price, E. Berger, S. R. Kulkarni, F. A. Harrison, A. Gal-Yam, E. O. Ofek, A. Rau, P. Chandra, D. A. Frail, M. M. Kasliwal, B. P. Schmidt, A. M. Soderberg, P. B. Cameron, and K. C. Roth, *"GRB 070125: The First Long-Duration Gamma-Ray Burst in a Halo Environment,"* *ApJ* **677** (Apr., 2008) 441–447, `arXiv:0712.2828`.

42. L. Guzzo, P. Cassata, A. Finoguenov, R. Massey, N. Z. Scoville, P. Capak, R. S. Ellis, B. Mobasher, Y. Taniguchi, D. Thompson, M. Ajiki, H. Aussel, H. Böhringer, M. Brusa, D. Calzetti, A. Comastri, A. Franceschini, G. Hasinger, M. M. Kasliwal, M. G. Kitzbichler, J. Kneib, A. Koekemoer, A. Leauthaud, H. J. McCracken, T. Murayama, T. Nagao, J. Rhodes, D. B. Sanders, S. Sasaki, Y. Shioya, L. Tasca,

and J. E. Taylor, *"The Cosmic Evolution Survey (COSMOS): A Large-Scale Structure at z=0.73 and the Relation of Galaxy Morphologies to Local Environment," ApJS* **172** (Sept., 2007) 254–269, arXiv:astro-ph/0701482.

43. A. Rau, R. Schwarz, S. R. Kulkarni, E. O. Ofek, M. M. Kasliwal, C. Brinkworth, S. B. Cenko, Y. Lipkin, and A. M. Soderberg, *"The Incidence of Dwarf Novae in Large Area Transient Searches," ApJ* **664** (July, 2007) 474–480, arXiv:astro-ph/0611933.

44. E. O. Ofek, P. B. Cameron, M. M. Kasliwal, A. Gal-Yam, A. Rau, S. R. Kulkarni, D. A. Frail, P. Chandra, S. B. Cenko, A. M. Soderberg, and S. Immler, *"SN 2006gy: An Extremely Luminous Supernova in the Galaxy NGC 1260," ApJ* **659** (Apr., 2007) L13–L16, arXiv:astro-ph/0612408.

45. S. B. Cenko, M. Kasliwal, F. A. Harrison, V. Pal'shin, D. A. Frail, P. B. Cameron, E. Berger, D. B. Fox, A. Gal-Yam, S. R. Kulkarni, D. Moon, E. Nakar, E. O. Ofek, B. E. Penprase, P. A. Price, R. Sari, B. P. Schmidt, A. M. Soderberg, R. Aptekar, D. Frederiks, S. Golenetskii, D. N. Burrows, R. A. Chevalier, N. Gehrels, P. J. McCarthy, J. A. Nousek, and T. Piran, *"Multiwavelength Observations of GRB 050820A: An Exceptionally Energetic Event Followed from Start to Finish," ApJ* **652** (Nov., 2006) 490–506, arXiv:astro-ph/0608183.

46. A. M. Soderberg, E. Berger, M. Kasliwal, D. A. Frail, P. A. Price, B. P. Schmidt, S. R. Kulkarni, D. B. Fox, S. B. Cenko, A. Gal-Yam, E. Nakar, and K. C. Roth, *"The Afterglow, Energetics, and Host Galaxy of the Short-Hard Gamma-Ray Burst 051221a," ApJ* **650** (Oct., 2006) 261–271, arXiv:astro-ph/0601455.

47. A. M. Soderberg, S. R. Kulkarni, E. Nakar, E. Berger, P. B. Cameron, D. B. Fox, D. Frail, A. Gal-Yam, R. Sari, S. B. Cenko, M. Kasliwal, R. A. Chevalier, T. Piran, P. A. Price, B. P. Schmidt, G. Pooley, D. Moon, B. E. Penprase, E. Ofek, A. Rau, N. Gehrels, J. A. Nousek, D. N. Burrows, S. E. Persson, and P. J. McCarthy, *"Relativistic ejecta from X-ray flash XRF 060218 and the rate of cosmic explosions," Nature* **442** (Aug., 2006) 1014–1017, arXiv:astro-ph/0604389.

48. D. A. Frail, P. B. Cameron, M. Kasliwal, E. Nakar, P. A. Price, E. Berger, A. Gal-Yam, S. R. Kulkarni, D. B. Fox, A. M. Soderberg, B. P. Schmidt, E. Ofek, and S. B. Cenko,

"An Energetic Afterglow from a Distant Stellar Explosion," ApJ **646** (Aug., 2006) L99–L102, arXiv:astro-ph/0604580.

49. B. E. Penprase, E. Berger, D. B. Fox, S. R. Kulkarni, S. Kadish, L. Kerber, E. Ofek, M. Kasliwal, G. Hill, B. Schaefer, and M. Reed, *"Spectroscopy of GRB 051111 at z = 1.54948: Kinematics and Elemental Abundances of the GRB Environment and Host Galaxy," ApJ* **646** (July, 2006) 358–368, arXiv:astro-ph/0512340.

50. J. B. Haislip, M. C. Nysewander, D. E. Reichart, A. Levan, N. Tanvir, S. B. Cenko, D. B. Fox, P. A. Price, A. J. Castro-Tirado, J. Gorosabel, C. R. Evans, E. Figueredo, C. L. MacLeod, J. R. Kirschbrown, M. Jelinek, S. Guziy, A. D. U. Postigo, E. S. Cypriano, A. Lacluyze, J. Graham, R. Priddey, R. Chapman, J. Rhoads, A. S. Fruchter, D. Q. Lamb, C. Kouveliotou, R. A. M. J. Wijers, M. B. Bayliss, B. P. Schmidt, A. M. Soderberg, S. R. Kulkarni, F. A. Harrison, D. S. Moon, A. Gal-Yam, M. M. Kasliwal, R. Hudec, S. Vitek, P. Kubanek, J. A. Crain, A. C. Foster, J. C. Clemens, J. W. Bartelme, R. Canterna, D. H. Hartmann, A. A. Henden, S. Klose, H. Park, G. G. Williams, E. Rol, P. O'Brien, D. Bersier, F. Prada, S. Pizarro, D. Maturana, P. Ugarte, A. Alvarez, A. J. M. Fernandez, M. J. Jarvis, M. Moles, E. Alfaro, K. M. Ivarsen, N. D. Kumar, C. E. Mack, C. M. Zdarowicz, N. Gehrels, S. Barthelmy, and D. N. Burrows, *"A photometric redshift of z = 6.39 plusmn 0.12 for GRB 050904," Nature* **440** (Mar., 2006) 181–183, arXiv:astro-ph/0509660.

51. E. Berger, P. A. Price, S. B. Cenko, A. Gal-Yam, A. M. Soderberg, M. Kasliwal, D. C. Leonard, P. B. Cameron, D. A. Frail, S. R. Kulkarni, D. C. Murphy, W. Krzeminski, T. Piran, B. L. Lee, K. C. Roth, D. Moon, D. B. Fox, F. A. Harrison, S. E. Persson, B. P. Schmidt, B. E. Penprase, J. Rich, B. A. Peterson, and L. L. Cowie, *"The afterglow and elliptical host galaxy of the short γ-ray burst GRB 050724," Nature* **438** (Dec., 2005) 988–990, arXiv:astro-ph/0508115.

52. D. B. Fox, D. A. Frail, P. A. Price, S. R. Kulkarni, E. Berger, T. Piran, A. M. Soderberg, S. B. Cenko, P. B. Cameron, A. Gal-Yam, M. M. Kasliwal, D. Moon, F. A. Harrison, E. Nakar, B. P. Schmidt, B. Penprase, R. A. Chevalier, P. Kumar, K. Roth, D. Watson, B. L. Lee, S. Shectman, M. M. Phillips, M. Roth, P. J. McCarthy, M. Rauch, L. Cowie, B. A. Peterson, J. Rich, N. Kawai, K. Aoki, G. Kosugi,

T. Totani, H. Park, A. MacFadyen, and K. C. Hurley, *"The afterglow of GRB 050709 and the nature of the short-hard γ-ray bursts," Nature* **437** (Oct., 2005) 845–850, arXiv:astro-ph/0510110.

Appendix C

Quotable Quotes by SRK

- *Mansi has thrown a party at Cahill patio. Yummy food.*

  Date: Tue, 26 Apr 2011 17:05:34 -0700

- *The committee UNANIMOUSLY suggested "Go into a cave and contemplate all the puzzles you have unearthed. Novae may not be fashionable but you have unearthed a great puzzle. Deep contemplation is a necessary arsenal of a great scientist.*

  Date: Tue, 26 Apr 2011 17:05:34 -0700

- *PTF is a bit of a loose federation.*

  Date: Wed, 4 May 2011 14:59:18 -0700

- *Palomar Observatory: Present & Future; The talk is based on the idea that Less is More and defy the general idea prevailing in Astronomy such of More is Less (XXXX and other projects; some even local)*

  Date: Sun, 24 Apr 2011 21:37:44 -0700 (PDT)

- *This is of direct benefit to the students. I have no desire to negotiate. We went through this last time and I am done. Rarely, I am so definitive.*

  Date: Thu, 12 May 2011 10:03:52 -0700

- *Subject: Drinks with famous astronomer*

  Date: Mon, 09 May 2011 15:54:42 -0700

- *According to Mail Today of New Delhi I am the SRK of Space*

  Date: Sat, 16 Apr 2011 17:29:01 -0700

- *Subject: drinks today*

  I had a full day of TAC. I am TACed out.

  Date: Wed, 13 Apr 2011 15:48:37 -0700

- *Subject: Re: PTF11bij is also a gap transient*

  Hi Mansi: Congratulations. You will soon be the Queen of the 2005E hill and hopefully also 2002bj.

  Date: Fri, 08 Apr 2011 08:33:51 -0700

- *Subject: Exciting Monday Lunch*

  Smart theorists could even finish a paper by the time the discussion is over.

  Date: Mon, 4 Apr 2011 08:49:11 -0700 (PDT)

- *Subject: IJL Monday*

  Reminder: Tomorrow is Monday ("It is Just Lunch" for busy astronomers)

  Date: Sun, 20 Mar 2011 09:12:17 -0700 (PDT)

- *The Eddington Lectures were a hit with the Brits. The humor was sizzling and the PTF results simply stunned the audience. Thanks for all of you. The even better news is that I think I can even try 60b60.*

  Date: Fri, 11 Mar 2011 22:54:28 +0000

- *I fully appreciate that sequencing the beast is like managing olive-oil coated pasta (spaghetti, vermicelli, capellini, pici, gomito, fusilli, rigatoni and others) with a chop stick.*

  Date: Tue, 08 Mar 2011 07:13:11 -0800

- *I am glad that you are helping your junior colleague. Remember that one good turn always generates another good turn etc.*

  Date: Fri, 04 Mar 2011 06:39:35 -0800

- *Subject: Re: Good News on Pappalardo*

  ha! raking in those fellowships.

  Date: Fri, 07 Jan 2011 06:53:58 +0530

- *I am thinking of having an entire afternoon for a new festival ABSOLUT NERD This is nominally to be held in the vicinity of the winter solstice. we will focus on crystal ball gazing of Astronomy in the period 2011 through 2019.*

  Date: Tue, 21 Dec 2010 16:43:38 -0800

- *I did get the note but not digested it yet. No point discussing until a bit more of digestion and maturity.*

  Date: Wed, 01 Dec 2010 11:59:35 +0900

- *This is short notice and nonetheless I am asking if you and Setu would be free for dinner either today or tomorrow. The purpose is to celebrate the end of letters for Mansi.*

  Date: Fri, 26 Nov 2010 14:35:20 -0500

- *In life there (frequently) comes a time when one has to choose. Sometimes these are big opportunities (e.g. job, marriage, choosing the right rabbit at the pound etc). but the same yes/no decision event occurs routinely. Most people punt on it by not taking a decision and letting a natural flow figure out the answer.*

  Date: Thu, 04 Nov 2010 07:32:32 -0700

- *I am puzzled why people like to speak so much (and lose their audience). There must be a primal urge to proselytize (perhaps this is the fundamental origin of religion).*

  Date: Wed, 27 Oct 2010 09:55:48 +0800

- *Subject: Fwd: [IITDBatch1978] 4 jokes for the CWG event*
  India and Indians have lots of problems but quality of jokes has steadilyimproved over the past two decades.

  Date: Wed, 20 Oct 2010 06:12:45 -0700

- *Subject: Re: 4-m run*
  WE NEED QUALITY FRESH CANDIDATES. EVERYONE; PLEASE SCAN, SCAN, SCAN

  Date: Sat, 09 Oct 2010 14:09:53 -0700

- *When I woke up in the morning I realized that I had made a mistake in my writeup of 10vdl. Apparently, Eran realized that last night as well (though I was more efficient*

since I combined this activity with sleep!). In any case please see the corrected version at the Twiki site.

Date: Thu, 07 Oct 2010 10:45:59 -0700

- *Subject: AAS Meeting*

  Mansi ... you should register for a thesis talk;

  Robert ... good time to network

  Shriharsh and Kunal: Mainly for cultural experience and also to appreciate the kind of research peers are doing and the start of networking

  Branimir, Assaf: No rush but you are welcome to attend

  Eran: You can now rest given that you have a good job.

  Date: Thu, 16 Sep 2010 11:14:16 +0530

- *The ratio of classified events to papers now stand at 200:1. [I realize that there are some papers in prep but prep time of many months is not helpful].*

  Date: Sun, 29 Aug 2010 17:43:15 -0700

- *Subject: Skype when you are rested*

  Date: Wed, 18 Aug 2010 14:31:49 +0800

- *I regret to inform you that XXX died a truly fiery death (and that too in a footnote, not even a regular paragraph). All decadal committees are allowed to make at least one mistake.*

  Date: Fri, 13 Aug 2010 13:31:21 -0700

- *Subject: Either Sucker Transient or Nobel-Prize time for Cenko*

  Date: Sat, 07 Aug 2010 19:41:26 -1000

- *Subject: srk back in action*

  i am back in action starting Wednesday. Undergoing a root canal operation today, a lobotomy tomorrow followed by being tarred in Canadian Maple Syrup (i.e. XXX Board Meetings) let us get a few papers out over the next two weeks

  Date: Mon, 12 Jul 2010 09:27:45 -0700

- *Subject: 10 nights of KPNO 4-m time*

  Good job, everyone. Maybe the tide is turning or simply we are experiencing random positive fluctuations.

  Date: Tue, 15 Jun 2010 21:51:15 -0700

- *Subject: Some limelight on PTF*

  Dear TILU+CC gang: Here is an excerpt of a letter from the Director of IOA, Cambridge University, UK: "It is with immense pleasure that I write to invite you to visit the UK next year as the 2011 Eddington Lecturer... We would be especially keen to hear you talk about the Palomar Transient Factory and the wonderful science that is coming out of PTF."

  All of you are the real heros (and heroines – Mansi gets a special nod) of this recognition.

  Date: Thu, 27 May 2010 19:09:03 -0700

- *Subject: Theorists (General Advice)*

  In my mind, all observers should -severely- attempt to do the theory on their own. They should read the papers but calling in 1-800-THEORIST is not a good idea.

  Date: Sat, 15 May 2010 13:20:55 -0700

- *Subject: NGTF (Welcome inputs from Young Turks)*

  Lessons I learnt from PTF are as follows: a. develop and stick to a clear goal (not several goals) b. recognize the value of human capital c. never, never, underestimate software (cost& complexity) d. followup is king e. assume that NSF will not fund exceptional projects.

  Date: Sun, 09 May 2010 14:52:31 -0700

- *Subject: M99 (steps, questions)*

  First of all congratulations on finding the long awaited messenger. (V838 Mon is Moses, M85OT was Jesus and M99 OT is Mohamed). With three objects the religion is now complete (which means that there is nothing more to be learnt from these objects in the future).

  Date: Sun, 18 Apr 2010 12:59:43 -0700

- *We are now behind the fire, the smoke, the snow and the rain. The good season is now upon us (March through October is our best time). This should be our great year (hopefully not the greatest).*

  Date: Fri, 26 Mar 2010 09:46:16 -0700

- *Subject: Future*

  Any scientist who works without "unfair advantage" is a fool and deserves the fate of fools.

  Date: Wed, 17 Mar 2010 19:42:42 -0700

- *Subject: Re: Please send out ATELS*

  "On behalf of PTF, Bloom, Bust and Bang report the following

  PTF10xxx was identified as a transient by Bluff, an undergraduate student and spectroscopic observations were undertaken at the Big Bang Observatory on 1-April-2010 (observers: Bounty and Beautiful). Spectroscopic identification was done by Bravo Bravado.

  Herein we report the following additional observations. Beu Beauty and Binary Bunt undertook radio observations at the Boundless Observatory and find the source to be a Billion Janskys...

  Date: Wed, 10 Mar 2010 16:44:05 -0600

- *Subject: [Following the Oscar awards] Our Own Robert Quimby wins the ....*

  I am very happy to inform you that our own Robert Quimby wins the Astronomical Society of the Pacific Trumpler Award for 2010

  This is the best part of getting to be old (the other part is getting wiser ...) You get to shine in both types of radiation: reflected (increasingly) and your own light (decreasingly).

  Date: Mon, 08 Mar 2010 20:55:40 -0600

- *Subject: Re: PTF10bt!*

  You are a superwoman. Rest well.

  Date: Sat, 09 Jan 2010 21:08:10 +0530

- *Subject: Maxi transient*

  We had a PTF telecon today (Mansi is relentless)

  Date: Wed, 30 Dec 2009 22:28:53 +0200

- *Subject: Xmas at B'lekem (Bethlehem)*

  I touched the Silver Star where JC was reportedly born (down in the grotto of the Church of Nativity) – my Arab guide insisted that I do this.

  Date: Fri, 25 Dec 2009 21:40:25 +0530

- *Only by being diligent we can make discoveries.*

  Date: Mon, 23 Nov 2009 09:44:49 -0700

- *Please remember the Golden rule: Figures tell the story. The text is merely to show that you have done some work.*

  Date: Mon, 9 Nov 2009 10:56:24 -0800

- *Subject: Cornell After Dinner Talk (Pictures)*

  Can you please send two pictures of each: picture when you entered Cornell (designed to make you look cute and innocent) current picture (designed to make you look like a power person)

  Date: Sat, 10 Oct 2009 09:47:58 -0400

- *Subject: Someone stole my idea of a pet restaurant (SRK at Cornell)*

  Date: Thu, 08 Oct 2009 23:12:12 -0400

- *Subject: not to panic*

  Words were simply not coming out given the high pace of activity for the past few days. But now that I relaxed I am fine.

  Date: Thu, 1 Oct 2009 09:10:44 -0700

- *The more rules you make the less you will achieve. You also do not need to consult me anymore. Be respond but more than anything else respond rapidly. Fortune favors the brave but bravery requires response.*

  Date: Wed, 02 Sep 2009 09:03:38 +0200

- *Subject: Got Bored and here is the product*

  The vacation is going well. I do not know how people can spend a day at the beach.

  Date: Sat, 01 Aug 2009 17:54:04 -1000

- *Subject: Re: couldn't cancel ddt*

  not to worry. life in the fast lane is rarely smooth.

  Date: Wed, 8 Jul 2009 13:28:47 -1000

- *Subject: VLA Workshop*

  Mansi and I agreed we will drive to Socorro (saves $ and gives a chance to talk about astronomy, life, girls, boys, economics).

  Date: Thu, 30 Apr 2009 07:44:50 -0700

- *Subject: SRK's Gordon Lecture (NAIC)*

  The talk was uniformly agreed to be entertaining, "provocative" (many) and "brilliant" (a few).

  Date: Tue, 21 Apr 2009 08:38:43 -0700 (PDT)

- *Subject: Solved all of our funding problems (Middle East Madness)*

  I have solved all of our funding problems. I bought a bunch of sewing machines and I am prepared to sell it for the "ballotechnic mercury" these machines contain. (references Samuel Cohen, Saddam Hussein).

  Date: Tue, 14 Apr 2009 23:06:29 -0700

- *Subject: First Transient and Hopefully More to Come*

  I am glad to inform you that over the weekend the weather Gods cooperated. [We have been having a very late wet season in Southern California]. Somewhat ahead of our planned schedule PTF has found a genuine transient: a Ia supernovae.

  Date: Mon, 9 Mar 2009 16:08:11 -0700

- *Subject: Re: PTF Successful First Light*

  ...Enough of this high school humor. What else should I say. CONGRATULATIONS!! YOU GUYS ARE THE BEST. The Project went from concept to execution in less than 2 years! That is why I say that Palomar is still the best (if not the biggest).

As PI I am simply thrilled and hope we can deliver some stunning science (e.g. a new star of Bethlehem).

Date: Sat, 13 Dec 2008 17:29:15 +0200

- *Subject: good to see*

  young people talking to each other on the new transient and mapping out various strategies (spitzer, lgs, etc). keep up. now i can get run over by a truck without changing the time line for the world.

  director shri (wasting my time in directing)

  Date: Fri, 16 May 2008 11:20:05 -0700 (PDT)

- *Subject: elocution*

  Remember that high speed talking in paragraph units is not effective communication!

  Date: Thu, 3 Apr 2008 01:48:28 -0700

- *Subject: Party today at my house?*

  Today is Mansi's exam. Mansi insisted on an exam on a holiday since she is keen to go to India and ride on an elephant while fiance rides on horse etc.

  You are invited to a party at 5 pm regardless of the outcome of the exam!

  Date: Mon, 21 Jan 2008 07:41:07 -0800 (PST)

- *Subject: Re: nirspec ideas*

  *The optical interferometry idea is *excellent*. I commend you for that. A wide and innocent look at new phenomena is a strength of the young mind. Focusing and getting the job done is what old hands conclude is the real business. You should maintain a wide and innocent look (10/10 points on that) but also balance real accomplishments*

  Date: Sun, 21 Oct 2007 20:06:54 -0700

- *I had a good time today. I met Dr. Buzz Aldrin, Ms. Eileen Collins ... Moral: Unless your name is Enrico (F) or Albert (E) you should cultivate the art of giving at least moderately humorous talk.*

  Date: Mon, 9 Apr 2007 21:16:50 -0700 (PDT)

- *Hopefully your grandparents will not suggest a 2-in-1 deal and get you married at the*

same time!

Date: Fri, 2 Feb 2007 19:52:41 -0800

- *Subject: SRK at 50*

  As befitting a micro celebrity I have been asked to write a piece about myself, state of Indian science etc for various magazines and newspapers in India. It has the usual story of how I trudged through 6 feet of snow and used abacus for calculations etc.

  Date: Wed, 15 Nov 2006 08:20:27 -0800

- *RSVP including whehter you are bringing swimming trunks or not.*

  Date: Sat, 2 Dec 2006 08:32:27 -0800 (PST)

- *I am of the opinion that students must learn hard technical skills. I take it for granted that they will figure out IRAF and data analysis. As I have said before I am not terribly concerned about the number of papers a student writes (since it is not difficult to do so). But they must do some practical work and develop confidence to solve problems.*

  Date: Tue, 22 Nov 2005 14:17:50 -0800 (PST)

Bibliography

Abazajian, K. N., et al. 2009, ApJS, 182, 543

Adelman-McCarthy, J. K., et al. 2007, ApJS, 172, 634

Afşar, M., & Bond, H. E. 2007, AJ, 133, 387

Alard, C., & Lupton, R. H. 1998, ApJ, 503, 325

Anderson, J. P., & James, P. A. 2009, MNRAS, 399, 559

Aptekar, R. L., Frederiks, D. D., Golenetskii, S. V., Il'inskii, V. N., Mazets, E. P., Pal'shin, V. D., Butterworth, P. S., & Cline, T. L. 2001, ApJS, 137, 227

Arbour, R. 2007, Central Bureau Electronic Telegrams, 904, 1

Arcavi, I., et al. 2010, ApJ, 721, 777

Arefiev, V. A., Priedhorsky, W. C., & Borozdin, K. N. 2003, ApJ, 586, 1238

Arnett, D. 1996, Supernovae and nucleosynthesis. an investigation of the history of matter, from the Big Bang to the present, ed. Arnett, D.

Arnett, D., & Bazan, G. 1997, Science, 276, 1359

Arnett, W. D. 1968, Nature, 219, 1344

—. 1982, ApJ, 253, 785

Arnett, W. D., Branch, D., & Wheeler, J. C. 1985, Nature, 314, 337

Arp, H. C. 1956, AJ, 61, 15

Astier, P., et al. 2006, A&A, 447, 31

Barbon, R., Ciatti, F., & Rosino, L. 1973, A&A, 29, 57

Barsukova, E., Fabrika, S., Hornoch, K., Sholukhova, O., & Valeev, A. 2008, The Astronomer's Telegram, 1871, 1

Barsukova, E., Valeev, A., Sholukhova, O., Fabrika, S., Burwitz, V., & Pietsch, W. 2007, The Astronomer's Telegram, 1314, 1

Barthelmy, S. D., et al. 2005, Space Science Reviews, 120, 143

Belloni, T., Mendez, M., King, A. R., van der Klis, M., & van Paradijs, J. 1997, ApJ, 488, L109+

Belloni, T., et al. 1999, ApJ, 527, 345

Benetti, S., et al. 2005, ApJ, 623, 1011

Berger, E., Kulkarni, S. R., & Chevalier, R. A. 2002, ApJ, 577, L5

Berger, E., et al. 2009, ApJ, 699, 1850

Beswick, R. J., Muxlow, T. W. B., Argo, M. K., Pedlar, A., Marcaide, J. M., & Wills, K. A. 2005, ApJ, 623, L21

Bildsten, L., Shen, K. J., Weinberg, N. N., & Nelemans, G. 2007a, ApJ, 662, L95

—. 2007b, ApJ, 662, L95

Bird, A. J., et al. 2007, ApJS, 170, 175

Blondin, S., Modjaz, M., Kirshner, R., Challis, P., Matheson, T., & Calkins, M. 2007, Central Bureau Electronic Telegrams, 907, 1

Blondin, S., & Tonry, J. L. 2007, ApJ, 666, 1024

Bloom, J. S., Starr, D. L., Blake, C. H., Skrutskie, M. F., & Falco, E. E. 2006a, in Astronomical Society of the Pacific Conference Series, Vol. 351, Astronomical Data Analysis Software and Systems XV, ed. C. Gabriel, C. Arviset, D. Ponz, & S. Enrique, 751

Bloom, J. S., et al. 2006b, ApJ, 638, 354

Bodaghee, A., et al. 2007, A&A, 467, 585

Bode, M. F., Darnley, M. J., Shafter, A. W., Page, K. L., Smirnova, O., Anupama, G. C., & Hilton, T. 2009, ApJ, 705, 1056

Boissier, S., & Prantzos, N. 2009, A&A, 503, 137

Bond, H. E., Bedin, L. R., Bonanos, A. Z., Humphreys, R. M., Monard, L. A. G. B., Prieto, J. L., & Walter, F. M. 2009, ApJ, 695, L154

Bond, H. E., & Siegel, M. H. 2006, AJ, 131, 984

Bond, H. E., White, R. L., Becker, R. H., & O'Brien, M. S. 2002, PASP, 114, 1359

Boschi, F., & Munari, U. 2004, A&A, 418, 869

Botticella, M. T., et al. 2009, MNRAS, 398, 1041

Branch, D. 2003, in IAU Symposium, Vol. 212, A Massive Star Odyssey: From Main Sequence to Supernova, ed. K. van der Hucht, A. Herrero, & C. Esteban, 346–+

Brown, P. J., et al. 2005, ApJ, 635, 1192

Brown, W. R., Kilic, M., Allende Prieto, C., & Kenyon, S. J. 2011, MNRAS, 411, L31

Buccheri, R., et al. 1983, A&A, 128, 245

Burrows, D. N., et al. 2005a, Science, 309, 1833

—. 2005b, Space Science Reviews, 120, 165

Burwitz, V., Pietsch, W., Henze, M., Updike, A., Milne, P., Williams, G., & Hartmann, D. H. 2007, The Astronomer's Telegram, 1275, 1

Cameron, P. B., et al. 2005, Nature, 434, 1112

Cappellaro, E., Mazzali, P. A., Benetti, S., Danziger, I. J., Turatto, M., della Valle, M., & Patat, F. 1997, A&A, 328, 203

Cardelli, J. A., Clayton, G. C., & Mathis, J. S. 1989, ApJ, 345, 245

Castro-Tirado, A. J., Brandt, S., Lund, N., & Sunyaev, R. 1999, A&A, 347, 927

Cenko, S. B., et al. 2006a, PASP, 118, 1396

—. 2006b, PASP, 118, 1396

Chevalier, R. A., Fransson, C., & Nymark, T. K. 2006, ApJ, 641, 1029

Chincarini, G., et al. 2007, ArXiv Astrophysics e-prints

Chochol, D., et al. 2006, Chinese Journal of Astronomy and Astrophysics Supplement, 6, 010000

Ciardullo, R., Ford, H. C., Neill, J. D., Jacoby, G. H., & Shafter, A. W. 1987, ApJ, 318, 520

Ciroi, S., Di Mille, F., Rafanelli, P., & Temporin, S. 2007, The Astronomer's Telegram, 1292, 1

Coelho, E. A., Shafter, A. W., & Misselt, K. A. 2008, ApJ, 686, 1261

Cohen, M., Wheaton, W. A., & Megeath, S. T. 2003, AJ, 126, 1090

Cox, A. N. 2000a, Allen's astrophysical quantities (Allen's astrophysical quantities, 4th ed. Publisher: New York: AIP Press; Springer, 2000. Editedy by Arthur N. Cox. ISBN: 0387987460)

—. 2000b, Allen's Astrophysical Quantities, ed. Cox, A. N.

Crockett, R. M., et al. 2008, MNRAS, 391, L5

Cutri, R. M., et al. 2011, The Astronomer's Telegram, 3099, 1

Dale, D. A., et al. 2009, ApJ, 703, 517

Darbha, S., Metzger, B. D., Quataert, E., Kasen, D., Nugent, P., & Thomas, R. 2010, MNRAS, 409, 846

Darnley, M. J., et al. 2004, MNRAS, 353, 571

—. 2006, MNRAS, 369, 257

della Valle, M., & Livio, M. 1995, ApJ, 452, 704

Di Mille, F., Ciroi, S., Orio, M., Rafanelli, P., Bianchini, A., Nelson, T., & Andreuzzi, G. 2008, The Astronomer's Telegram, 1818, 1

Dickey, J. M., & Lockman, F. J. 1990, ARAA, 28, 215

Dilday, B., et al. 2010, ApJ, 713, 1026

Downes, R. A., & Duerbeck, H. W. 2000, AJ, 120, 2007

Drake, S. A., & Ulrich, R. K. 1980, ApJS, 42, 351

Epelstain, N., Yaron, O., Kovetz, A., & Prialnik, D. 2007, MNRAS, 374, 1449

Evans, P. A., et al. 2007, A&A, 469, 379

Fairall, A. P. 1972, Monthly Notes of the Astronomical Society of South Africa, 31, 23

Falcone, A. D., et al. 2006, ApJ, 641, 1010

Fenimore, E. E., Madras, C. D., & Nayakshin, S. 1996, ApJ, 473, 998

Ferland, G. J., & Persson, S. E. 1989, ApJ, 347, 656

Ferrarese, L., Côté, P., & Jordán, A. 2003, ApJ, 599, 1302

Filippenko, A. V., Li, W. D., Treffers, R. R., & Modjaz, M. 2001, in Astronomical Society of the Pacific Conference Series, Vol. 246, IAU Colloq. 183: Small Telescope Astronomy on Global Scales, ed. B. Paczynski, W.-P. Chen, & C. Lemme, 121–+

Filippenko, A. V., et al. 1992, AJ, 104, 1543

Finger, M. H., Koh, D. T., Nelson, R. W., Prince, T. A., Vaughan, B. A., & Wilson, R. B. 1996, Nature, 381, 291

Foley, R. J., Brown, P. J., Rest, A., Challis, P. J., Kirshner, R. P., & Wood-Vasey, W. M. 2009a, ArXiv e-prints

—. 2010, ApJ, 708, L61

Foley, R. J., et al. 2009b, AJ, 138, 376

Fox, D. B., et al. 2005, Nature, 437, 845

French, J., Melady, G., Kubanek, P., & Jelinek, M. 2007, GCN Circular 6500

Fryer, C. L. 1999, ApJ, 522, 413

Fryer, C. L., et al. 2009, ApJ, 707, 193

Gaensler, B. M., et al. 2005, Nature, 434, 1104

Gal-Yam, A., & Leonard, D. C. 2009, Nature, 458, 865

Gal-Yam, A., Maoz, D., Guhathakurta, P., & Filippenko, A. V. 2003, AJ, 125, 1087

—. 2008, ApJ, 680, 550

Gal-Yam, A., Ofek, E. O., & Shemmer, O. 2002, MNRAS, 332, L73

Gal-Yam, A., & Quimby, R. 2007, The Astronomer's Telegram, 1236, 1

Gal-Yam, A., et al. 2004, ApJ, 609, L59

—. 2009, Nature, 462, 624

Garnavich, P. M., et al. 2004, ApJ, 613, 1120

Gehrels, N., et al. 2004, ApJ, 611, 1005

—. 2005, Nature, 437, 851

Gogarten, S. M., et al. 2010, ApJ, 712, 858

Golenetskii, S., Aptekar, R., Frederiks, D., Mazets, E., Palshin, V., Hurley, K., Cline, T., & Stern, B. 2003, ApJ, 596, 1113

Guetta, D., & Piran, T. 2006, A&A, 453, 823

Hajduk, M., et al. 2007, MNRAS, 378, 1298

Hakobyan, A. A. 2008, Astrophysics, 51, 69

Hakobyan, A. A., Mamon, G. A., Petrosian, A. R., Kunth, D., & Turatto, M. 2009, A&A, 508, 1259

Hamuy, M., Phillips, M. M., Suntzeff, N. B., Schommer, R. A., Maza, J., Smith, R. C., Lira, P., & Aviles, R. 1996, AJ, 112, 2438

Harrison, F. A., et al. 2010, ArXiv e-prints

Hayden, B. T., et al. 2010, ApJ, 712, 350

Heger, A., Fryer, C. L., Woosley, S. E., Langer, N., & Hartmann, D. H. 2003, ApJ, 591, 288

Henze, M., Pietsch, W., Burwitz, V., Hatzidimitriou, D., Reig, P., Primak, N., & Papamastorakis, G. 2008, The Astronomer's Telegram, 1790, 1

Hill, G. J., Nicklas, H. E., MacQueen, P. J., Mitsch, W., Wellem, W., Altmann, W., Wesley, G. L., & Ray, F. B. 1998, in Society of Photo-Optical Instrumentation Engineers (SPIE) Conference Series, Vol. 3355, Society of Photo-Optical Instrumentation Engineers (SPIE) Conference Series, ed. S. D'Odorico, 433–443

Hjellming, R. M., et al. 2000, ApJ, 544, 977

Hodapp, K. W., et al. 2003, PASP, 115, 1388

Hoeflich, P., & Khokhlov, A. 1996, ApJ, 457, 500

Hoffman, D., et al. 2011, The Astronomer's Telegram, 3160, 1

Holtzman, J. A., Burrows, C. J., Casertano, S., Hester, J. J., Trauger, J. T., Watson, A. M., & Worthey, G. 1995, PASP, 107, 1065

Hook, I. M., Jørgensen, I., Allington-Smith, J. R., Davies, R. L., Metcalfe, N., Murowinski, R. G., & Crampton, D. 2004, PASP, 116, 425

Hornoch, K., Scheirich, P., Garnavich, P. M., Hameed, S., & Thilker, D. A. 2008, A&A, 492, 301

Howell, D. A. 2001, ApJ, 554, L193

Howell, D. A., et al. 2005, ApJ, 634, 1190

Hubble, E. P. 1929, ApJ, 69, 103

Hurley, K., Briggs, M. S., Kippen, R. M., Kouveliotou, C., Meegan, C., Fishman, G., Cline, T., & Boer, M. 1999, ApJS, 120, 399

Hurley, K., et al. 2005, Nature, 434, 1098

Immler, S., et al. 2006, ApJ, 648, L119

in't Zand, J. J. M., et al. 2000, A&A, 357, 520

Isern, J., Canal, R., & Labay, J. 1991, ApJ, 372, L83

Ivezic, Z., Tyson, J. A., Allsman, R., Andrew, J., Angel, R., & for the LSST Collaboration. 2008, ArXiv e-prints

Jeffery, D. J., & Branch, D. 1990, in Supernovae, Jerusalem Winter School for Theoretical Physics, ed. J. C. Wheeler, T. Piran, & S. Weinberg, 149

Jha, S., et al. 2006, AJ, 131, 527

Johnston, H. M., Kulkarni, S. R., & Oke, J. B. 1989, ApJ, 345, 492

Jordi, K., Grebel, E. K., & Ammon, K. 2006, A&A, 460, 339

Jose, J., & Hernanz, M. 1998, ApJ, 494, 680

Kalberla, P. M. W., Burton, W. B., Hartmann, D., Arnal, E. M., Bajaja, E., Morras, R., & Pöppel, W. G. L. 2005, A&A, 440, 775

Kann, D. A., Wilson, A. C., Schulze, S., Klose, S., Henze, M., Ludwig, F., Laux, U., & Greiner, J. 2007, GCN Circular 6505

Kantharia, N. G., Anupama, G. C., Prabhu, T. P., Ramya, S., Bode, M. F., Eyres, S. P. S., & O'Brien, T. J. 2007, ApJ, 667, L171

Karachentsev, I. D., & Kutkin, A. M. 2005, Astronomy Letters, 31, 299

Karasev, D. I., Lutovinov, A. A., & Grebenev, S. A. 2007, Astronomy Letters, 33, 159

Kasen, D., & Bildsten, L. 2010, ApJ, 717, 245

Kasliwal, M. M., Cenko, S. B., Ofek, E. O., Quimby, R., Rau, A., & Caltech, S. R., K. 2009a, The Astronomer's Telegram, 1984, 1

Kasliwal, M. M., Cenko, S. B., Ofek, E. O., Quimby, R., Rau, A., & Kulkarni, S. R. 2009b, The Astronomer's Telegram, 1934, 1

Kasliwal, M. M., Cenko, S. B., Quimby, R., Rau, A., Ofek, E. O., & Kulkarni, S. R. 2008a, The Astronomer's Telegram, 1880, 1

Kasliwal, M. M., Cenko, S. B., Rau, A., Ofek, E. O., Quimby, R., & Kulkarni, S. R. 2008b, The Astronomer's Telegram, 1854, 1

—. 2008c, The Astronomer's Telegram, 1663, 1

—. 2008d, The Astronomer's Telegram, 1627, 1

—. 2008e, The Astronomer's Telegram, 1717, 1

—. 2008f, The Astronomer's Telegram, 1719, 1

—. 2008g, The Astronomer's Telegram, 1826, 1

Kasliwal, M. M., & Kulkarni, S. R. 2010, The Astronomer's Telegram, 2590, 1

Kasliwal, M. M., Ofek, E. O., Rau, A., Cenko, S. B., Quimby, R., & Kulkarni, S. R. 2008h, The Astronomer's Telegram, 1646, 1

Kasliwal, M. M., Quimby, R., Cenko, S. B., Rau, A., Ofek, E. O., & Kulkarni, S. R. 2008i, The Astronomer's Telegram, 1764, 1

Kasliwal, M. M., Quimby, R., Rau, A., Ofek, E., Cenko, B., & Kulkarni, S. 2007, The Astronomer's Telegram, 1330, 1

Kasliwal, M. M., Rau, A., Salvato, M., Cenko, S. B., Ofek, E. O., Quimby, R., & Kulkarni, S. R. 2009c, The Astronomer's Telegram, 1886, 1

Kasliwal, M. M., et al. 2008j, ApJ, 683, L29

—. 2010, The Astronomer's Telegram, 3094, 1

Kawabata, K. S., et al. 2010, Nature, 465, 326

Kawai, N., et al. 2006, Nature, 440, 184

Kennicutt, Jr., R. C., et al. 2003, PASP, 115, 928

Khan, R., Stanek, K. Z., Prieto, J. L., Kochanek, C. S., Thompson, T. A., & Beacom, J. F. 2010, ArXiv e-prints

Kilic, M., Brown, W. R., Allende Prieto, C., Agüeros, M. A., Heinke, C., & Kenyon, S. J. 2011a, ApJ, 727, 3

Kilic, M., et al. 2011b, MNRAS, L233+

Kitaura, F. S., Janka, H., & Hillebrandt, W. 2006, A&A, 450, 345

Kleiser, I. K. W., et al. 2011, ArXiv e-prints

Klotz, K. A., Boer, B. M., Atteia, A. J. L., & Gendre, G. B. 2007, GCN Circular 6513

Kochanek, C. S., et al. 2001, ApJ, 560, 566

Kogure, T. 1961, PASJ, 13, 335

Kouveliotou, C., Meegan, C. A., Fishman, G. J., Bhat, N. P., Briggs, M. S., Koshut, T. M., Paciesas, W. S., & Pendleton, G. N. 1993, ApJ, 413, L101

Kouveliotou, C., van Paradijs, J., Fishman, G. J., Briggs, M. S., Kommers, J., Harmon, B. A., Meegan, C. A., & Lewin, W. H. G. 1996, Nature, 379, 799

Kraus, A. L., & Hillenbrand, L. A. 2007a, AJ, 134, 2340

—. 2007b, ArXiv e-prints, 708

Krivonos, R., Revnivtsev, M., Lutovinov, A., Sazonov, S., Churazov, E., & Sunyaev, R. 2007, ArXiv Astrophysics e-prints

Kulkarni, S., & Kasliwal, M. M. 2009a, in Astrophysics with All-Sky X-Ray Observations, ed. N. Kawai, T. Mihara, M. Kohama, & M. Suzuki, 312

Kulkarni, S. R. 2005, ArXiv Astrophysics e-prints

Kulkarni, S. R., & Kasliwal, M. M. 2009b, in Astronomy, Vol. 2010, astro2010: The Astronomy and Astrophysics Decadal Survey, 165–+

Kulkarni, S. R., et al. 2007, 447, 458

Law, N. M., et al. 2009, PASP, 121, 1395

Lee, C., Ries, C., Riffeser, A., & Seitz, S. 2007, The Astronomer's Telegram, 1324, 1

Leibundgut, B., et al. 1993, AJ, 105, 301

Lejeune, T., & Schaerer, D. 2001, A&A, 366, 538

Li, L., & Paczyński, B. 1998, ApJ, 507, L59

Li, W., Chornock, R., Leaman, J., Filippenko, A. V., Poznanski, D., Wang, X., Ganeshalingam, M., & Mannucci, F. 2011, MNRAS, 412, 1473

Li, W., Filippenko, A. V., Treffers, R. R., Riess, A. G., Hu, J., & Qiu, Y. 2001, ApJ, 546, 734

Li, W. D., et al. 2000, in American Institute of Physics Conference Series, Vol. 522, American Institute of Physics Conference Series, ed. S. S. Holt & W. W. Zhang, 103

Livio, M. 1992, ApJ, 393, 516

Livne, E. 1990, ApJ, 354, L53

Mannucci, F., Della Valle, M., Panagia, N., Cappellaro, E., Cresci, G., Maiolino, R., Petrosian, A., & Turatto, M. 2005, A&A, 433, 807

Markwardt, C. B., Pagani, C., Evans, P., Gavriil, F. P., Kennea, J. A., Krimm, H. A., Landsman, W., & Marshall, F. E. 2007, The Astronomer's Telegram, 1102, 1

Martin, D. C., et al. 2005, ApJ, 619, L1

Martini, P., Wagner, R. M., Tomaney, A., Rich, R. M., della Valle, M., & Hauschildt, P. H. 1999, AJ, 118, 1034

Maund, J. R., Smartt, S. J., & Danziger, I. J. 2005, MNRAS, 364, L33

Mazzali, P. A., Chugai, N., Turatto, M., Lucy, L. B., Danziger, I. J., Cappellaro, E., della Valle, M., & Benetti, S. 1997, MNRAS, 284, 151

Mazzali, P. A., Röpke, F. K., Benetti, S., & Hillebrandt, W. 2007, Science, 315, 825

McClintock, J. E., Narayan, R., Garcia, M. R., Orosz, J. A., Remillard, R. A., & Murray, S. S. 2003, ApJ, 593, 435

McClintock, J. E., & Remillard, R. A. 1986, ApJ, 308, 110

McLaughlin, D. B. 1960, in Stellar Atmospheres, ed. J. L. Greenstein, 585–+

Metzger, B. D., Piro, A. L., Quataert, E., & Thompson, T. A. 2009, ArXiv e-prints

Metzger, B. D., et al. 2010, MNRAS, 406, 2650

Metzger, M. R., Djorgovski, S. G., Kulkarni, S. R., Steidel, C. C., Adelberger, K. L., Frail, D. A., Costa, E., & Frontera, F. 1997, Nature, 387, 878

Mihos, J. C., Harding, P., Feldmeier, J., & Morrison, H. 2005, ApJ, 631, L41

Milisavljevic, D., & Fesen, R. 2010, Central Bureau Electronic Telegrams, 2167, 1

Modjaz, M., Li, W., Filippenko, A. V., King, J. Y., Leonard, D. C., Matheson, T., Treffers, R. R., & Riess, A. G. 2001, PASP, 113, 308

Moriya, T., Tominaga, N., Tanaka, M., Nomoto, K., Sauer, D. N., Mazzali, P. A., Maeda, K., & Suzuki, T. 2010, ApJ, 719, 1445

Morrell, N., & Folatelli, G. 2007, Central Bureau Electronic Telegrams, 908, 1

Morrissey, P., et al. 2007, ApJS, 173, 682

Mullan, B., et al. 2011, ArXiv e-prints

Munari, U., Sordo, R., Castelli, F., & Zwitter, T. 2005, A&A, 442, 1127

Muno, M. P., Morgan, E. H., & Remillard, R. A. 1999, ApJ, 527, 321

Muno, M. P., et al. 2006, ApJ, 636, L41

Myers, A. T., Krumholz, M. R., Klein, R. I., & McKee, C. F. 2011, ArXiv e-prints

Nakar, E., Gal-Yam, A., & Fox, D. B. 2006, ApJ, 650, 281

Negueruela, I., Smith, D. M., Torrejon, J. M., & Reig, P. 2007, ArXiv e-prints, 704

Nelemans, G., Portegies Zwart, S. F., Verbunt, F., & Yungelson, L. R. 2001, A&A, 368, 939

Nomoto, K., & Iben, Jr., I. 1985, ApJ, 297, 531

Nordhaus, J., Burrows, A., Almgren, A., & Bell, J. 2010, ApJ, 720, 694

Norris, J. P., Nemiroff, R. J., Bonnell, J. T., Scargle, J. D., Kouveliotou, C., Paciesas, W. S., Meegan, C. A., & Fishman, G. J. 1996, ApJ, 459, 393

Nousek, J. A., et al. 2006, ApJ, 642, 389

Nugent, P., Kim, A., & Perlmutter, S. 2002, PASP, 114, 803

Nugent, P., Phillips, M., Baron, E., Branch, D., & Hauschildt, P. 1995, ApJ, 455, L147+

Nugent, P. E. 2009, in Bulletin of the American Astronomical Society, Vol. 41, Bulletin of the American Astronomical Society, 419

O'Connor, E., & Ott, C. D. 2011, ApJ, 730, 70

Ofek, E. O. 2007, ApJ, 659, 339

Ofek, E. O., et al. 2007, ApJ, 659, L13

—. 2008, ApJ, 674, 447

Ogley, R. N., Chaty, S., Crocker, M., Eyres, S. P. S., Kenworthy, M. A., Richards, A. M. S., Rodríguez, L. F., & Stirling, A. M. 2002, MNRAS, 330, 772

Oke, J. B., & Gunn, J. E. 1982, PASP, 94, 586

Oke, J. B., et al. 1995, PASP, 107, 375

Orosz, J. A., et al. 2001, ApJ, 555, 489

—. 2002, ApJ, 568, 845

Osten, R. A., Drake, S., Tueller, J., Cummings, J., Perri, M., Moretti, A., & Covino, S. 2007, ApJ, 654, 1052

Ovcharov, E., Valcheva, A., Kostov, A., Nikolov, Y., Georgiev, T., & Nedialkov, P. 2007, The Astronomer's Telegram, 1312, 1

Padmanabhan, T. 2001, Theoretical Astrophysics, Volume 2: Stars and Stellar Systems, ed. Padmanabhan, T.

Pagani, C., Racusin, J. L., & Kennea, J. A. 2007a, GCN Circular 6506

Pagani, C., et al. 2007b, GCN Circular 6489

Pastorello, A., et al. 2004, MNRAS, 347, 74

—. 2007, Nature, 447, 829

—. 2008, MNRAS, 389, 113

Patat, F., Maund, J. R., Benetti, S., Botticella, M. T., Cappellaro, E., Harutyunyan, A., & Turatto, M. 2010, A&A, 510, A108+

Payne-Gaposchkin, C. 1964, The galactic novae, ed. Gaposchkin, C. H. P.

Peng, C. Y., Ho, L. C., Impey, C. D., & Rix, H. 2002, AJ, 124, 266

Penhallow, W. S., Wenzel, W., Jager, A., Kirshner, R., Wilson, I., Horine, E., & Peters, J. 1986, IAUC, 4225, 2

Pennypacker, C. R., et al. 1989, AJ, 97, 186

Perets, H. B., Badenes, C., Arcavi, I., Simon, J. D., & Gal-yam, A. 2010a, ArXiv e-prints

—. 2011a, ApJ, 730, 89

Perets, H. B., Gal-yam, A., Crockett, R. M., Anderson, J. P., James, P. A., Sullivan, M., Neill, J. D., & Leonard, D. C. 2011b, ApJ, 728, L36+

Perets, H. B., et al. 2010b, Nature, 465, 322

Phillips, M. M. 1993, ApJ, 413, L105

Pietsch, W., Burwitz, V., Stoss, R., Updike, A., Hartmann, D., Milne, P., & Williams, G. 2007, The Astronomer's Telegram, 1230, 1

Poole, T. S., et al. 2008, MNRAS, 383, 627

Postigo, A. d. U., Castro-Tirado, A. J., & Aceituno, F. 2007, GCN Circular 6501

Poznanski, D., et al. 2010, Science, 327, 58

Prieto, J. L., Stanek, K. Z., & Beacom, J. F. 2008a, ApJ, 673, 999

Prieto, J. L., et al. 2008b, ApJ, 681, L9

Pskovskii, Y. P. 1984, SOVAST, 28, 658

Pumo, M. L., et al. 2009, ApJ, 705, L138

Quimby, R., et al. 2007, The Astronomer's Telegram, 1118, 1

Quimby, R. M. 2006, PhD thesis, The University of Texas at Austin

Quimby, R. M., et al. 2009, ArXiv e-prints

Rahmer, G., Smith, R., Velur, V., Hale, D., Law, N., Bui, K., Petrie, H., & Dekany, R. 2008, in Presented at the Society of Photo-Optical Instrumentation Engineers (SPIE) Conference, Vol. 7014, Society of Photo-Optical Instrumentation Engineers (SPIE) Conference Series

Rau, A., Kasliwal, M. M., & Salvato, M. 2009a, The Astronomer's Telegram, 1887, 1

Rau, A., Kulkarni, S. R., Ofek, E. O., & Yan, L. 2007, ApJ, 659, 1536

Rau, A., et al. 2009b, PASP, 121, 1334

Remillard, R. A., & McClintock, J. E. 2006, ARAA, 44, 49

Remillard, R. A., & Smith, D. 2002, Atel 88

Retter, A., & Marom, A. 2003, MNRAS, 345, L25

Revnivtsev, M., Gilfanov, M., Churazov, E., & Sunyaev, R. 2002, A&A, 391, 1013

Rich, D., & Burke, P. 2010, Central Bureau Electronic Telegrams, 2166, 1

Rich, R. M., Mould, J., Picard, A., Frogel, J. A., & Davies, R. 1989, ApJ, 341, L51

Richmond, M. W., et al. 1996, AJ, 111, 327

Roelofs, G. H. A., Nelemans, G., & Groot, P. J. 2007, MNRAS, 382, 685

Russell, D. G. 2002, ApJ, 565, 681

Sahu, D. K., Anupama, G. C., Srividya, S., & Muneer, S. 2006, MNRAS, 372, 1315

Sahu, D. K., Gurugubelli, U. K., Anupama, G. C., & Nomoto, K. 2011, ArXiv e-prints

Sand, D. J., et al. 2011, ApJ, 729, 142

Scannapieco, E., & Bildsten, L. 2005, ApJ, 629, L85

Schlegel, D. J., Finkbeiner, D. P., & Davis, M. 1998a, ApJ, 500, 525

—. 1998b, ApJ, 500, 525

Scott, A. D. 2000, MNRAS, 313, 775

Sguera, V., et al. 2006, ApJ, 646, 452

Shafter, A. W., Ciardullo, R., Bode, M. F., Darnley, M. J., & Misselt, K. A. 2008, The Astronomer's Telegram, 1832, 1

Shafter, A. W., & Irby, B. K. 2001, ApJ, 563, 749

Shafter, A. W., Rau, A., Quimby, R. M., Kasliwal, M. M., Bode, M. F., Darnley, M. J., & Misselt, K. A. 2009, ApJ, 690, 1148

Shafter, A. W., et al. 2011, ArXiv e-prints

Shara, M. M. 1981, ApJ, 243, 926

Shen, K. J., & Bildsten, L. 2009, ApJ, 692, 324

Shen, K. J., Kasen, D., Weinberg, N. N., Bildsten, L., & Scannapieco, E. 2010, ApJ, 715, 767

Sheth, K., et al. 2010, ArXiv e-prints

Skrutskie, M. F., et al. 2006, AJ, 131, 1163

Smartt, S. J. 2009, ARAA, 47, 63

Smartt, S. J., Eldridge, J. J., Crockett, R. M., & Maund, J. R. 2009, MNRAS, 395, 1409

Smith, N., et al. 2009, ApJ, 697, L49

—. 2010, AJ, 139, 1451

Soker, N., & Tylenda, R. 2003, ApJ, 582, L105

Sollerman, J., et al. 2002, A&A, 386, 944

Sparks, W. B., et al. 2008, AJ, 135, 605

Stefanescu, A., Slowikowska, A., Kanbach, G., Duscha, S., Schrey, F., Steinle, H., & Ioannou, Z. 2007a, GCN Circular 6492

Stefanescu, A., Slowikowska, A., Kanbach, G., et al. 2007b, GCN Circular 6508

—. 2007c, GCN Circular 6532

Stern, B. E., Beloborodov, A. M., & Poutanen, J. 2001, ApJ, 555, 829

Sullivan, M., et al. 2011, ArXiv e-prints

Svensson, R. 1987, MNRAS, 227, 403

Tanaka, Y., & Shibazaki, N. 1996, ARAA, 34, 607

Taubenberger, S., et al. 2008, MNRAS, 385, 75

—. 2009, MNRAS, 397, 677

Thompson, T. A., Prieto, J. L., Stanek, K. Z., Kistler, M. D., Beacom, J. F., & Kochanek, C. S. 2009, ApJ, 705, 1364

Townsley, D. M., & Bildsten, L. 2004, ApJ, 600, 390

Tueller, J., et al. 2007, GCN Circular 6491

Turatto, M., Benetti, S., & Cappellaro, E. 2003, in From Twilight to Highlight: The Physics of Supernovae, ed. W. Hillebrandt & B. Leibundgut, 200–+

Tylenda, R., et al. 2011, A&A, 528, A114+

Uemura, M., Kato, T., Watanabe, T., Stubbings, R., Monard, B., & Kawai, N. 2002, PASJ, 54, 95

Uemura, M., et al. 2004, PASJ, 56, 823

Uomoto, A. 1986, ApJ, 310, L35

Updike, A. C., Hartmann, D. H., Henson, G., et al. 2007a, GCN Circular 6507

Updike, A. C., Milne, P. A., Williams, G. G., et al. 2007b, GCN Circular 6536

Valcheva, A., Ovcharov, E., Latev, G., Kostov, A., Nikolov, Y., Georgiev, T., & Nedialkov, P. 2008, The Astronomer's Telegram, 1687, 1

Valenti, S., et al. 2009, Nature, 459, 674

van Dam, M. A., et al. 2006, PASP, 118, 310

van den Bergh, S. 1997, AJ, 113, 197

van den Bergh, S., & Younger, P. F. 1987, A&AS, 70, 125

van Dokkum, P. G. 2001, PASP, 113, 1420

Waldman, R., Sauer, D., Livne, E., Perets, H., Glasner, A., Mazzali, P., Truran, J. W., & Gal-Yam, A. 2010, ArXiv e-prints

Warner, B. 2006, Journal of the American Association of Variable Star Observers (JAAVSO), 35, 98

Wen, L., & Chen, Y. 2010, Phys. Rev. D, 81, 082001

Werk, J. K., Putman, M. E., Meurer, G. R., Oey, M. S., Ryan-Weber, E. V., Kennicutt, Jr., R. C., & Freeman, K. C. 2008, ApJ, 678, 888

Werk, J. K., Putman, M. E., Meurer, G. R., Thilker, D. A., Allen, R. J., Bland-Hawthorn, J., Kravtsov, A., & Freeman, K. 2010a, ApJ, 715, 656

Werk, J. K., et al. 2010b, AJ, 139, 279

Williams, B. F., et al. 2007, ApJ, 656, 756

Williams, R. E. 1992, AJ, 104, 725

Williams, R. E., Phillips, M. M., & Hamuy, M. 1994, ApJS, 90, 297

Wilson, J. C., et al. 2003, in Presented at the Society of Photo-Optical Instrumentation Engineers (SPIE) Conference, Vol. 4841, Instrument Design and Performance for Optical/Infrared Ground-based Telescopes. Edited by Iye, Masanori; Moorwood, Alan F. M. Proceedings of the SPIE, Volume 4841, pp. 451-458 (2003)., ed. M. Iye & A. F. M. Moorwood, 451–458

Wizinowich, P. L., et al. 2006, in Presented at the Society of Photo-Optical Instrumentation Engineers (SPIE) Conference, Vol. 6272, Advances in Adaptive Optics II. Edited by Ellerbroek, Brent L.; Bonaccini Calia, Domenico. Proceedings of t he SPIE, Volume 6272, pp. 627209 (2006).

Woods, P. M., & Thompson, C. 2006, Soft gamma repeaters and anomalous X-ray pulsars: magnetar candidates (Compact stellar X-ray sources), 547–586

Woods, P. M., et al. 1999, ApJ, 517, 431

Woosley, S. E., & Weaver, T. A. 1980, ApJ, 238, 1017

—. 1994, ApJ, 423, 371

—. 1995, ApJS, 101, 181

Wright, E. L., et al. 2010, AJ, 140, 1868

Yaron, O., Prialnik, D., Shara, M. M., & Kovetz, A. 2005, ApJ, 623, 398

Yoshida, M., Yanagisawa, K., Shimizu, Y., et al. 2007, GCN Circular 6512

Zhang, B., Fan, Y. Z., Dyks, J., Kobayashi, S., Mészáros, P., Burrows, D. N., Nousek, J. A., & Gehrels, N. 2006, ApJ, 642, 354

Zwicky, F. 1936, PASP, 48, 191